

UNIVERSITY OF GAZIANTEP
GRADUATE
SCHOOL OF NATURAL&APPLIED SCIENCES

**THERMODYNAMIC AND THERMOECONOMIC
ANALYSIS AND OPTIMIZATION OF BIOGAS USAGE IN
ELECTRICITY AND HYDROGEN PRODUCTIONS FROM
WASTEWATER TREATMENT SYSTEMS**

M.Sc THESIS
IN
MECHANICAL ENGINEERING

SİNAN DEMİR

JUNE 2012

**Thermodynamic and Thermo-economic Analysis and
Optimization of Biogas Usage in Electricity and Hydrogen
Productions from Wastewater Treatment Systems**

M.Sc. Thesis

In

Mechanical Engineering

University of Gaziantep

Supervisor

Asst. Prof. Dr. Ayşegül Abuşoğlu

By

Sinan Demir

June 2012

T.C.
UNIVERSITY OF GAZIANTEP
GRADUATE SCHOOL OF
NATURAL & APPLIED SCIENCES

Name of thesis: Thermodynamic and Thermoeconomic Analysis and Optimization of Biogas Usage in Electricity and Hydrogen Productions from Wastewater Treatment Systems

Name of the student: Sinan Demir

Exam date: 18 June 2012

Approval of the Graduate School of Natural and Applied Sciences


Prof. Dr. Ramazan KOÇ

Director

I certify that this thesis satisfies all the requirements as a thesis for the degree of Master of Science.

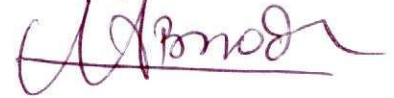

Prof. Dr. Canan DÜLGER

Head of Department

This is to certify that we have read this thesis and that in our consensus opinion it is fully adequate, in scope and quality, as a thesis for the degree of Master Science.

Asst. Prof. Dr. Ayşegül ABUŞOĞLU

Supervisor



Examining Committee Members:

Prof. Dr. M. Sait SÖYLEMEZ

Prof. Dr. Zuhal OKTAY

Asst. Prof. Dr. Ayşegül ABUŞOĞLU

Signature




ABSTRACT

THERMODYNAMIC AND THERMOECONOMIC ANALYSIS AND OPTIMIZATION OF BIOGAS USAGE IN ELECTRICITY AND HYDROGEN PRODUCTIONS FROM WASTEWATER TREATMENT SYSTEMS

DEMİR, Sinan

M.Sc. in Mechanical Engineering

Supervisor: Assist. Prof. Dr. Ayşegül ABUŞOĞLU

June 2012, 225 pages

In this thesis, we perform thermodynamic and thermoeconomic analysis and optimization of biogas usage in electricity and hydrogen productions from wastewater treatment systems. The procedure and formulations of the analyses are provided and applied to an actual municipal wastewater treatment plant and a biogas engine powered cogeneration system located in Gaziantep, Turkey [GASKI] using actual operational and cost data. The plant treats nearly 222,000 m³/day of domestic wastewater and as a result of the sludge stabilization in the plant, daily biogas generation is 10,000-18,000 m³. The annual electricity production of the cogeneration is 8760 GWh and the total annual biogas consumption is 3,400,000 m³. The overall exergetic efficiency of GASKI WWTP including BEPC system is found to be 46.2%. The specific unit exergetic costs for the treated wastewater and electricity produced are obtained to be 3.804 ¢/m³ and 25 \$/GJ, respectively. Seven hydrogen production models for the present municipal wastewater treatment plant are developed and thermodynamic and economic analyses of these models are performed using the actual data obtained from GASKI WWTP and BEPC.

Key words: Wastewater treatment, Cogeneration, Thermodynamic, Thermoeconomic, Optimization, Hydrogen production.

ÖZET

ATIK SU ARITMA SİSTEMLERİNDE ÜRETİLEN BİYOGAZIN ELEKTRİK VE HİDROJEN ÜRETİMİNDE KULLANIMININ TERMODİNAMİK VE TERMOEKONOMİK ANALİZ VE OPTİMİZASYONU

DEMİR, Sinan

Yüksek Lisans Tezi, Makine Mühendisliği Bölümü

Tez Yöneticisi: Y. Doç. Dr. Ayşegül ABUŞOĞLU

Haziran 2012, 225 sayfa

Bu çalışmada, atık su arıtma sistemlerinde üretilen biyogazın elektrik ve hidrojen üretiminde kullanımının termodinamik ve termoeconomik analiz ve optimizasyonu gerçekleştirilmiştir. Termodinamik ve termoeconomik analizler için geliştirilen prosedür ve formüller Gaziantep’te bulunan gerçek bir kentsel atık su arıtma tesisine ve biyogaz motor tahrikli gerçek bir kojenerasyon sistemine [GASKI] uygulanmıştır. Mevcut atık su arıtma tesisi günde 222.000 m³ atık suyu arıtmaktadır ve tesisteki çamur şartlandırma işlemi sonucu günde ortalama 10.000–18.000 m³ biyogaz üretilmektedir. Kojenerasyon sisteminde bulunan biyogaz motoru yıllık 8760 GWh elektrik üretmektedir ve bunun için toplam yıllık biyogaz tüketimi 3.400.000 m³’ tür. GASKI atık su arıtma sistemi ve biyogaz motor tahrikli kojenerasyon sisteminin toplam ekserji verimi ise %46.2 olarak bulunmuştur. Yapılan termoeconomik analiz neticesinde, arıtılmış atık suyun ve üretilen elektriğin birim ekserji maliyetleri sırasıyla 3.804 º/m³ ve 25 \$/GJ olarak hesaplanmıştır. Bu tezde, kentsel atık su arıtma sistemleri için yedi ayrı hidrojen üretim modeli geliştirilmiştir ve bu modellerin termodinamik ve ekonomik analizleri tez çalışmasında verilen gerçek işletme ve maliyet değerleri kullanılarak gerçekleştirilmiştir.

Anahtar kelimeler: Atık su arıtma sistemi, Kojenerasyon, Termodinamik, Termoeconomik, Optimizasyon, Hidrojen üretimi.

“I believe that water will one day be employed as fuel, that hydrogen and oxygen which constitute it, used singly or together, will furnish an inexhaustible source of heat and light, of an intensity of which coal is not capable.”

Jules Verne, The Mysterious Island (1874)

ACKNOWLEDGEMENTS

First of all, I would like to thank the creator of whole universe since nothing is ever possible without him including this study.

I would like to thank my supervisor Asst. Prof. Dr. Ayşegül Abuşoğlu for giving me the opportunity to do my dissertation in the all our study areas. Without her tireless interest and continuous guidance, the completion of this thesis would not have been possible. She gave me a strong foundation for my future studies with this study.

I would also like to thank Prof. Dr. Zuhale Oktay and Prof. Dr. M. Sait Söylemez for serving in my thesis committee and providing valuable contributions and recommendations.

I would like to thanks to Plant Managers and workers of GASKI Wastewater Treatment Facility, especially Environmental Engineer Eyüp Anlatıcı for helping me with actual plant data and comprehensive technical information about wastewater treatment systems.

This study is sponsored by The scientific and Technological Research Council of Turkey (Tübitak) under the project 110M053. I would like to thanks for their financial support.

I would like to thanks to all my classmates and my best friends, Ökkeş Ramazan Aslan, in Gaziantep.

I would like to thank peoples who could not remember their names. Please forgive me.

I could not forget to thank my family, my elder sister Dr. Sibel Demir, for their presence, care, attention and support. My family is the biggest supporter for me materially and morally. I will carry you forever in my heart.

Finally, I would like to thank myself.

CONTENTS

ABSTRACT	i
ÖZET	ii
DEDICATION	iii
ACKNOWLEDGEMENTS	iv
CONTENTS	v
LIST OF FIGURES	x
LIST OF TABLES	xiii
LIST OF SYMBOLS	xvii
CHAPTER 1: INTRODUCTION	1
1.1 Background.....	1
1.2 Scope and Outline of the Study.....	3
CHAPTER 2: LITERATURE SURVEY	5
2.1 Introduction.....	5
2.2 Biogas and Electricity Productions from Wastewater Treatment Plants....	6
2.3 Sewage Sludge Evaluation Methods.....	9
2.4 Hydrogen Production Methods in Wastewater Treatment Plants.....	13
2.5 Thermodynamic and Thermoeconomic Analyses and Optimization of Wastewater Treatment Plants.....	15
2.6 Thermodynamic and Thermoeconomic Analyses and Optimization of Biogas Engine Powered Cogeneration System.....	17
2.7 Thermodynamic and Thermoeconomic Analyses and Optimization of Hydrogen Production from Renewable Energy Sources.....	19
2.8 Conclusions.....	25
CHAPTER 3: ENERGY RECOVERY FROM MUNICIPAL WASTEWATER TREATMENT PLANTS IN TURKEY...	27
3.1 Introduction.....	27
3.2 Biogas and Electricity Productions Potential of Municipal Wastewater Treatment Plants.....	28

3.3 Energy Recovery from Sewage Sludge of Municipal Wastewater Treatment Plants.....	31
3.4 Conclusions.....	35
CHAPTER 4: THERMODYNAMIC ANALYSIS.....	36
4.1 Introduction.....	36
4.2 Energy Analysis.....	37
4.2.1 Mass Balance.....	37
4.2.2 Energy Balance.....	38
4.3 Exergy Analysis.....	39
4.3.1 Reference Environment and Exergy Components.....	39
4.3.2 Exergy Balance, Exergy Destruction, and Exergy Loss.....	44
4.3.3 Exergetic Efficiency.....	46
4.3.4 Exergy Destruction Ratio and Exergy Loss Ratio.....	46
4.4 Performance Assessment Parameters in Cogeneration Systems.....	47
4.5 Thermodynamic Analysis of Hydrogen Production Models.....	49
4.6 Conclusions.....	50
CHAPTER 5: THERMOECONOMIC ANALYSIS.....	51
5.1 Introduction.....	51
5.2 Economic Analysis.....	53
5.2.1 Time Value of Money.....	53
5.2.2 Inflation, Escalation, and Levelization.....	57
5.2.3 Time Assumptions.....	60
5.2.4 Depreciation.....	60
5.2.5 Financing and Required Returns on Capital.....	61
5.2.6 Fuel, Operating, and Maintenance Costs.....	62
5.2.7 Taxes and Insurance.....	63
5.3 Thermo-economic Analysis.....	64
5.3.1 Exergy Costing.....	64
5.3.2 Aggregation Level for Applying Exergy Costing.....	67
5.4 Thermo-economic Variables for Component Evaluation.....	67
5.4.1 Cost of Exergy Destruction.....	68
5.4.2 Relative Cost Difference.....	69
5.4.3 Exergoeconomic Factor.....	70
5.5 The Specific Exergy Costing (SPECOC) Method.....	70

5.5.1 The \dot{F} and \dot{P} principles.....	72
5.6 Conclusions.....	73
CHAPTER 6: THERMOECONOMIC OPTIMIZATION.....	74
6.1 Introduction.....	74
6.2 Thermo-economic Optimization Approaches.....	75
6.3 Cost Optimal Exergetic Efficiency for An Isolated System Component.....	77
6.4 Thermo-economic Optimization Methodology of Existing Complex Systems.....	82
6.5 Conclusions.....	83
CHAPTER 7: GASKI WASTEWATER TREATMENT PLANT.....	84
7.1 Introduction.....	84
7.2 Municipal Wastewater Treatment Plants Overview.....	84
7.3 GASKI Wastewater Treatment Plant.....	86
7.3.1 Primary Treatment System.....	87
7.3.2 Secondary Treatment System.....	90
7.3.3 Sludge Flootation and Thickening System.....	92
7.3.4 Anaerobic Sludge Digestion System.....	93
7.4 GASKI Biogas Engine Powered Cogeneration System.....	96
7.5 Conclusions.....	98
CHAPTER 8: HYDROGEN PRODUCTION MODELS FOR WASTEWATER TREATMENT PLANTS.....	99
8.1 Introduction.....	99
8.2 Hydrogen Production by Electrolysis.....	101
8.2.1 Alkaline Electrolysis.....	104
8.2.2 Proton Exchange Membrane (PEM) Electrolysis.....	86
8.2.3 High Temperature Steam Electrolysis (SOEC).....	107
8.3 Bio-hydrogen Production from Sewage Sludge.....	108
8.4 Hydrogen Production Models Developed for GASKI Municipal WWTP.....	111
8.5 Hydrogen Storage.....	117
8.6 Conclusion.....	119
CHAPTER 9: RESULTS AND DISCUSSIONS.....	120
9.1 Introduction.....	120

9.2 Description of GASKI Wastewater Treatment Plant.....	121
9.2.1 Primary Treatment System.....	122
9.2.2 Secondary Treatment System.....	122
9.2.3 Sludge Flootation and Thickening System.....	124
9.2.4 Anaerobic Sludge Digestion System.....	127
9.3 Description of Biogas Engine Powered Cogeneration System.....	129
9.4 Gas Engine Operating and Performance Characteristics.....	130
9.5 Energy and Exergy Relations.....	137
9.5.1 GASKI Wastewater Treatment Plant.....	138
9.5.2 Biogas Engine Powered Cogeneration System.....	140
9.6 Results and Discussion for Energy and Exergy Analysis.....	142
9.6.1 Energy and Exergy Analysis of Primary Treatment System (PTS).....	142
9.6.2 Energy and Exergy Analysis of Secondary Treatment System (STS).....	144
9.6.3 Energy and Exergy Analysis of Flotation and Thickening System (FTS).....	148
9.6.4 Energy and Exergy Analysis of Anaerobic Digestion System (ADS).....	151
9.6.5 Energy and Exergy Analysis of Biogas Engine Powered Cogeneration.....	156
9.7 Economic Analysis.....	159
9.7.1 GASKI WWTP: Primary Economic Control Volume.....	160
9.7.2 GASKI BEPC: Secondary Economic Control Volume.....	163
9.8 Thermo-economic Analysis.....	164
9.8.1 GASKI WWTP: Primary Economic Control Volume.....	165
9.8.2 GASKI BEPC: Secondary Economic Control Volume.....	170
9.9 Thermo-economic Optimization of GASKI WWTP.....	178
9.10 Accuracy of Measurements in GASKI WWTP and BEPC System.....	182
9.11 Thermodynamic and Economic Analyses of Developed Hydrogen	

Production Models for Wastewater Treatment Plants.....	182
9.12Conclusions.....	191
CHAPTER 11: CONCLUSIONS.....	192
REFERENCES.....	205

LIST OF FIGURES

	Page
Figure 3.1: Sludge, biogas and electricity production potential of Turkey.....	32
Figure 5.1: Logical chain of thermoeconomic concepts.....	52
Figure 7.1: Satellite view of the GASKI Wastewater Treatment Plant.....	87
Figure 7.2: Coarse and fine screens of the GASKI WWTP.....	89
Figure 7.3: Grit and grease removal tanks of the GASKI WWTP.....	89
Figure 7.4: Primary sedimentation tanks of the GASKI WWTP.....	90
Figure 7.5: Aeration tanks of the GASKI WWTP.....	91
Figure 7.6: Flotation tanks of the GASKI WWTP.....	92
Figure 7.7: Thickening tanks of the GASKI WWTP.....	93
Figure 7.8: Anaerobic digestion tanks of the GASKI WWTP.....	95
Figure 7.9: The views of the biogas store tanks in GASKI WWTP.....	95
Figure 7.10: A view of the DeSO _x unit in GASKI WWTP.....	96
Figure 7.11: GASKI Biogas Engine Powered Cogeneration System.....	96
Figure 7.12: DEUTZ gas engine actuated generator sets in GASKI cogeneration GASKI cogeneration.....	97
Figure 8.1: Some feedstocks and process alternatives.....	100
Figure 8.2: Thermal contributions in electrolysis and fuelcell modes of operation.....	102
Figure 8.3: A simple water electrolyzer.....	103
Figure 8.4: A graphical indication of the state of development of the different types of electrolyzers.....	103
Figure 8.5: Alkaline water electrolyzer.....	105
Figure 8.6: PEM water electrolyzer.....	106
Figure 8.7: SOEC steam electrolyzer.....	108
Figure 8.8: Hydrogen production model-1.....	111
Figure 8.9: Hydrogen production model-2.....	112
Figure 8.10: Hydrogen production model-3.....	113

Figure 8.11:	Hydrogen production model-4.....	114
Figure 8.12:	Hydrogen production model-5.....	115
Figure 8.13:	Hydrogen production model-6.....	116
Figure 8.14:	Hydrogen production model-7.....	116
Figure 8.15:	Schematic of a typical compressed H ₂ gas composite tank.....	118
Figure 8.16:	Schematic of a Precooled Linde–Hampson liquefaction cycle.....	119
Figure 9.1:	A simple flow schematic of GASKI WWTP.....	121
Figure 9.2:	Schematic of Primary Treatment Process of GASKI WWTP.....	123
Figure 9.3:	Schematic of Secondary Treatment Process of GASKI WWTP.....	125
Figure 9.4:	Schematic of Thickening and Flotation Process of GASKI WWTP.....	126
Figure 9.5:	Schematic of Anaerobic Digestion Process of GASKI WWTP.....	128
Figure 9.6:	Biogas Engine Powered Cogeneration Unit of GASKI WWTP.....	131
Figure 9.7:	Exergy Assessment of the Four Subsystems in GASKI WWTP.....	155
Figure 9.8:	Overall Exergy Assessment of GASKI WWTP and BEPC (or CP).....	160
Figure 9.9:	A Simplified Schematic of GASKI WWTP: Primary Economic Control Volume.....	161
Figure 9.10:	Schematic of GASKI BEPC: Secondary Economic Control Volume.....	163
Figure 9.11:	Variation of exergoeconomic factors for the subcomponents of WWTP with respect to corresponding cost rate of exergy destructions.....	171
Figure 9.12:	Variation of exergetic efficiency and exergy destruction cost rates with respect to (a) the pressure ratio of air-biogas mixture for the Compressor (b) the pressure ratio of exhaust gas for the Turbine.....	174
Figure 9.13:	Variation of exergetic efficiency and exergy destruction cost rates with respect to (a) the exit temperature of hot (process) water for EGHE (b) the exit temperature of lubrication oil for LOHE.....	175
Figure 9.14:	Variation of exergetic efficiency and exergy destruction cost rates with respect to (a) the pressure ratio of P12 (b) the pressure ratio of P13.....	177

Figure 9.15: Variation of the product cost of the partially treated wastewater at the exit of primary treatment system with respect to different COD values and corresponding exergetic efficiencies.....	179
Figure 9.16: Variation of the product cost of the treated wastewater at the exit of secondary treatment system with respect to different COD values and corresponding exergetic efficiencies.....	179
Figure 9.17: Variation of the product cost of the sewage sludge at the exit of thickening and flotation system with respect to different dry matter contents and corresponding exergetic efficiencies.....	180
Figure 9.18: Comparison of hydrogen production rates of the models developed for GASKI WWTP.....	188
Figure 9.19: Comparison of electricity consumption rates of the models developed for GASKI WWTP.....	189
Figure 9.20: Comparison of hydrogen production costs of the models developed for GASKI WWTP.....	191

LIST OF TABLES

	Page
Table 3.1: Primary production of biogas and electricity production from biogas in selected EU-countries in 2009.....	29
Table 3.2: The main wastewater indicators of municipalities in Turkey between 2001-2010.....	30
Table 5.1: Summary of selected tax depreciation methods.....	62
Table 7.1: Main design data of the GASKI WWTP.....	88
Table 7.2: Main design data of the GASKI WWTP screens.....	88
Table 7.3: Main design data of the GASKI WWTP grit and grease removal tanks.....	89
Table 7.4: Main design data of the GASKI WWTP primary sedimentation tanks.....	90
Table 7.5: Main design data of the GASKI WWTP aeration tanks.....	91
Table 7.6: Main design data of the GASKI WWTP secondary sedimentation tanks.....	92
Table 7.7: Main design data of the GASKI WWTP flotation tanks.....	92
Table 7.8: Main design data of the GASKI WWTP thickening tanks.....	93
Table 7.9: Main design data of the GASKI WWTP anaerobic digestion tanks.....	94
Table 7.10: Main engine characteristic data of TCG 2020 12V and TCG2020 16V.....	98
Table 8.1: Properties of hydrogen as a fuel.....	100
Table 8.2: Characteristics of existing and advanced electrolyzers.....	104
Table 8.3: An overview of known biological hydrogen production.....	109
Table 8.4: Comparison of various hydrogen production processes.....	110
Table 9.1: Wastewater inlet and exit conditions for GASKI WWTP.....	124
Table 9.2: The produced biogas composition in GASKI WWTP.....	129
Table 9.3: Calculated engine operating and performance characteristics.....	138

Table 9.4:	Primary Treatment System data, thermodynamic properties, energy and exergy rates in the plant with respect to state points in Figure 9.2.....	143
Table 9.5:	Energy and exergy analysis results for the components in the Primary Treatment System (PTS). State numbers refer to Figure 9.2 and Table 9.4.....	145
Table 9.6:	The digested dry sludge composition in a municipal wastewater treatment plant.....	145
Table 9.7:	Secondary Treatment System data, thermodynamic properties, energy and exergy rates in the plant with respect to state points in Figure 9.4.....	146
Table 9.8:	Energy and exergy analyses results for the components in the Secondary Treatment System (STS). State numbers refer to Figure 9.3 and Table 9.7.....	147
Table 9.9:	Flotation and Thickening System data, thermodynamic properties, energy and exergy rates in the plant with respect to state points in Figure 9. 4.....	148
Table 9.10:	Energetic and exergetic analyses results for the subsystems in Flotation and Thickening System (FTS). State numbers refer to Figure 9.4 and Table 9.9.....	150
Table 9.11:	Anaerobic Digestion System data, thermodynamic properties, and energy and exergy rates in the plant with respect to state points in Figure 9.5.....	153
Table 9.12:	Energetic and exergetic analyses results for the subsystems in the Anaerobic Digestion System (ADS). State numbers refer to Figure 9.5 and Table 9.11.....	155
Table 9.13:	Biogas Engine Powered Cogeneration data, thermodynamic properties, energy and exergy rates in the plant with respect to state points in Figure 9.6.....	156
Table 9.14:	Energy and exergy analyses results for the subsystems in the Biogas Engine Powered Cogeneration (BEPC). State numbers refer to Figure 9.6 schematized in the first part of the study and Table 9.13.....	159

Table 9.15:	The cost rates associated with first capital investment and OM costs for the subcomponents of the GASKI WWTP (Primary Economic Control Volume).....	162
Table 9.16:	The cost rates associated with first capital investment and OM costs for the subcomponents of the Biogas Engine Powered Cogeneration (Second economic control volume).....	164
Table 9.17:	Exergetic cost rate balances and corresponding auxiliary equations for each subsystem of first economic control volume (GASKI WWTP). State numbers refer to Figure 9.9.....	165
Table 9.18:	Exergy flow rates, cost flow rates and the unit exergy costs associated with the main streams and components of the first economic control volume (GASKI WWTP). States are referred to Figure 9.9.....	167
Table 9.19:	The unit exergetic costs of fuels and products, cost rate of exergy destruction, operation and maintenance cost rate, and exergoeconomic factor for the first economic control volume (GASKI WWTP) components.....	169
Table 9.20:	Exergetic cost rate balances and corresponding auxiliary equations for each subsystem of second economic control volume (BEPC). State numbers refer to Figure 9.10.....	171
Table 9.21:	Exergy flow rates, cost flow rates and the unit exergy costs associated with the main streams and components of the second economic control volume (BEPC). States are referred to Figure 9.10.....	172
Table 9.22:	The unit exergetic costs of fuels and products, cost rate of exergy destruction, operation and maintenance cost rate, and exergoeconomic factor for the second economic control volume (BEPC) components.....	176
Table 9.23:	The costs obtained through thermoeconomic analysis (base case) and thermoeconomic optimization (cost optimal case) for the municipal WWTP.....	181
Table 9.24:	Uncertainty of the measured quantities in GASKI WWTP.....	182

Table 9.25:	Thermodynamic data and results of the energy and economic analyses of model-1 with respect to the state points in Figure 8.8.....	183
Table 9.26:	Thermodynamic data and results of the energy and economic analyses of model-2 with respect to the state points in Figure 8.9.....	184
Table 9.27:	Thermodynamic data and results of the energy and economic analyses of model-3 with respect to the state points in Figure 8.10.....	184
Table 9.28:	Thermodynamic data and results of the energy and economic analyses of model-4 with respect to the state points in Figure 8.11.....	185
Table 9.29:	Thermodynamic data and results of the energy and economic analyses of model-5 with respect to the state points in Figure 8.12.....	186
Table 9.30:	Thermodynamic data and results of the energy and economic analyses of model-6 with respect to the state points in Figure 8.13.....	187
Table 9.31:	Thermodynamic data and results of the energy and economic analyses of model-7 with respect to the state points in Figure 8.14.....	188
Table 9.32:	Economic analysis results of hydrogen production models developed.....	190
Table 9.33:	Hydrogen liquefaction cost of models developed for GASKI WWTP.....	191

LIST OF SYMBOLS

c	cost per unit of exergy (\$/GJ)
\dot{C}	cost rate associated with exergy (\$/h)
C	payment (\$)
E	the amount of emission based on energy content (g/kWh)
$\dot{E}x$	exergy rate (kW)
$\dot{E}x_{\text{heat}}$	rate of exergy transfer by heat (kW)
h	enthalpy (kJ/kg)
i	rate of return (%)
\dot{m}	mass flow rate (kg/s)
P	present value of the payment (\$)
\dot{Q}	rate of heat transfer (kW)
s	entropy (kJ/kg K)
T	temperature (K)
T_0	environment temperature (K)
w	specific work (kJ/kg)
\dot{W}	power (kW)
X	the amount of emission based on exergy content (g/kWh)
$y_{\text{dest},k}$	component exergy destruction over total exergy input
$y_{\text{dest},k}^*$	component exergy destruction over total exergy destruction
\dot{Z}	cost rate associated with the sum of capital investment and O&M (\$/h)
\dot{Z}^{CI}	cost rate associated with capital investment (\$/h)
\dot{Z}^{OM}	cost rate associated with O&M (\$/h)

Abbreviations

ADRHE	Anaerobic Digestion Recirculation Heat Exchanger
ADS	Anaerobic Digestion System
BEPC	Biogas Engine Powered Cogeneration
CC	Carrying Charges
CRF	Capital Recovery Factor
DeSO _x	Desulphurization
DEUTZ	Engine Company and Supplier
EGHE	Exhaust Gas Heat Exchanger
FTS	Flotation and Thickening System
ICE	Internal Combustion Engine
IEA	International Energy Agency
LHV	Lower Heating Value, kJ/ kg
LOHE	Lubrication Oil Heat Exchanger
OMC	Operating and Maintenance Costs
PEC	Purchased Equipment Cost
PTS	Primary Treatment System
STS	Secondary Treatment System
TEDAŞ	Turkish Electricity Distribution Co.
WWTP	Wastewater Treatment Plant

Subscripts

eff	effective
L	levelized
k	any component
m	year
dest	destruction

Greek Letters

η	energy efficiency
η_{turb}	turbine isentropic efficiency
η_{comp}	compressor isentropic efficiency
ε	exergy efficiency
ψ	specific flow exergy (kJ/kg)
ψ^{CH}	chemical specific flow exergy (kJ/kg)
ψ^{PH}	physical specific flow exergy (kJ/kg)
ψ^{T}	total specific flow exergy (kJ/kg)
τ	total annual operating hours of system at full load (h)

CHAPTER 1

INTRODUCTION

1.1 Background

Effects of the utilization of fossil fuels, such as global climate change, world energy conflicts and energy source shortages, have increasingly threatened world stability. Most of the researchers show their reliance on renewable energy technologies for sustainable development and long lasting life on this planet for their daily energy needs through waste-to-energy routes, which do not cause negative societal impacts. Renewable energy creates multiple public benefits such as environmental improvement due to the reduction of power plant greenhouse emissions, thermal pollution, and increased fuel diversity, reduction of energy price volatility effects on the economy, national economic security, and increase of economic productivity through more efficient production processes [1-2].

Water that has been used by people and disposed into a receiving water body with altered physical and chemical parameters is defined as wastewater. Wastewater collection systems and centralized and decentralized treatment systems are designed and managed primarily to protect human and environmental health. Wastewaters are usually classified as industrial wastewater or municipal wastewater. Many industrial wastewaters require pretreatment to remove non-compatible substances prior to discharge into the municipal system. Water collected in municipal wastewater systems, having been put to a wide variety of uses, contains a wide variety of contaminants. If the water has been contaminated with soluble or insoluble organic or inorganic material, a combination of mechanical, chemical and/or biological purification procedures may be required to protect the environment from periodic or

permanent pollution or damage. For this reason, legislation in industrialized and in many developing countries has reinforced environmental laws that regulate the maximum allowed residual concentrations of carbon, nitrogen, and phosphorous compounds in purified wastewater, before it is disposed into a river or into any other receiving water body [3-5].

Sludge is by far the largest in volume amongst the byproducts of wastewater treatment plants, and its utilization and disposal is perhaps one of the most complex environmental problems of the engineers. A sludge processing intended to reduce smell, reduce the quantity of the organic solids, eliminate disease causing bacteria, improve the dewatering characteristics of sludge, and reduce the water content so that the end product can be treated further or disposed of with handling problems and environmental consequences. These can be achieved through sludge stabilization, conditioning and dewatering [6]. Among the sludge stabilization methods, anaerobic digestion is one of the most well-known methods. Digestion process is a series of processes in which microorganisms break down biodegradable material either in the absence of (anaerobic) or presence of oxygen (aerobic). Biogas is produced by anaerobic process in wastewater treatment plants and can be converted economically viable combined heat and power projects.

Hydrogen is an attractive second energy sources when considering the use of renewable energy for hydrogen production [7]. Electrolysis is one of the most well-known hydrogen production methods. During the electrolysis, electricity required is supplied from renewable energies. Hydrogen production via electricity could be applicable in practice only if a significant part of the electricity was produced from renewable energy sources such as biomass, biogas, wind, sun etc. [8].

Hydrogen also can be produced through biological processes and produced hydrogen called as biohydrogen. These processes can use a variety of feed stocks and also waste materials. Sewage sludge contains high levels of organic matter (for example carbohydrates and proteins) and these are a potential substrate for producing hydrogen. Biohydrogen production by using sewage sludge has several advantages. Sewage sludge is available in wastewater treatment plants and can be obtained little or without paying money.

The purpose of this study is to analyze and assess of an actual wastewater treatment plant and a biogas engine powered cogeneration system operation parameters thermodynamically and to optimize costs of the components thermoeconomically by the means of the exergetic cost accounting methodology which have clearly easy to follow procedure and accuracy of results as compared to pure mathematical optimization methods which may end with a complex and unsolvable problem in the case of the existing wastewater treatment plant and a cogeneration system improvement.

1.2 Scope and Outline of the Study

In this thesis, firstly we analyze and optimize of an existing wastewater treatment plant thermodynamically and thermoeconomically by means of the exergy and exergetic cost accounting method. The procedure and formulations of such a comprehensive analysis are provided and they are applied to an actual wastewater treatment system located in Gaziantep, Turkey. (GASKI Wastewater Treatment Plant). Secondly hydrogen production models are improved and adapted to GASKI Wastewater Treatment Plant and thermodynamic and economic analyses are performed. The outline of the study with respect to chapters is as follows:

In Chapter 2, a comprehensive literature survey on wastewater treatment plants is presented. The survey is presented under six titles: biogas and electricity productions from wastewater treatment plants, sewage sludge evaluation methods, hydrogen production methods in waste wastewater treatment plants, thermodynamic and thermoeconomic analyses and optimization of wastewater treatment plants, thermoeconomic analyses and optimization of biogas engine powered cogeneration system, and thermodynamic and thermoeconomic analyses and optimization of hydrogen production from renewable energy sources

In Chapter 3, an overview of energy recovery from municipal wastewater treatment plants of the Turkey is presented. The content of this chapter includes biogas and electricity productions potential and energy recovery from sewage sludge of municipal wastewater treatment plants. In this chapter; sludge, biogas and electricity

production potential of Turkey is shown on the Turkey's map and, difference energy recovery methods of sewage sludge are discussed.

In Chapter 4, general formulations of thermodynamic analysis including both energy and exergy methods are given.

In Chapter 5, general principles, terminology, and formulation of thermoeconomic analysis, which is also called exergoeconomic analysis are presented. The formulations in Chapter 4 and 5 are in general format and are applicable to various energy conversion systems including cogeneration and wastewater treatment plants.

In Chapter 6, general principles and formulations of thermoeconomic optimization are provided. These methods use a primary optimization performance measure: minimizing the total levelized cost of the system products that includes the cost of external fuel resources, capital investment and operating and maintenance cost.

In Chapter 7, the short overview of municipal wastewater treatment plants concept are provided. The detailed description of GASKI Wastewater Treatment Plant including main and auxiliary system components and Biogas Engine Powered Cogeneration System is presented.

In Chapter 8, the hydrogen production methods including electrolysis and biological processes and hydrogen storage processes are presented and seven different hydrogen production models are improved for the GASKI Wastewater Treatment Plant.

In Chapter 9, Thermodynamic and thermoeconomic analysis and optimization procedures developed in previous chapters are applied to the GASKI wastewater treatment plant and biogas engine powered cogeneration system. Thermodynamic and economic analyses are applied to the hydrogen production models developed, and finally hydrogen liquefaction electricity consumption and electricity consumption cost of the models are presented.

In Chapter 10, conclusions drawn from the study are pointed out and certain recommendations are provided.

CHAPTER 2

LITERATURE SURVEY

2.1 Introduction

In modern societies proper management of wastewater is a necessity, not an option. Historically, the practice of collecting and treating wastewater prior to disposal is a relatively recent undertaking. Although remains of sewers have been found in ancient cities, the extent of their use for wastewater carriage is not known.

The first ‘modern’ sewerage systems for wastewater carriage was built in Hamburg, Germany, in 1842 by an innovative English engineer named Lindley [9]. Lindley’s system included many of the principles that are still in use today. Most of the improvements in wastewater collection systems over the last 100 years have consisted of improved materials and the inclusion of manholes, pumping stations and other appurtenances.

Various treatment processes were tried in the late 1800s and early 1900s, and by the 1920s, wastewater treatment had evolved to those processes in common use today. Design of wastewater treatment facilities remained empirical, however, until midcentury. In the last 30 to 40 year, great advances have been made in understanding wastewater treatment, and the original processes have been formulated and quantified. The science of wastewater treatment is far from static, however. Advanced wastewater- treatment processes are currently being developed that will produce potable water from domestic wastewater. Problems associated with wastewater reuse will no doubt challenge the imagination of engineers for many years to come [5].

In this chapter, a comprehensive literature survey on thermodynamic and thermoeconomic analyses and optimization of biogas usage in electricity and hydrogen productions from wastewater treatment systems is presented. The survey is presented under six titles: biogas and electricity productions from wastewater treatment plants, sewage sludge evaluation methods, hydrogen production methods in wastewater treatment plants, and thermodynamic and thermoeconomic analyses and optimizations of wastewater treatment plant, biogas engine powered cogeneration plant and hydrogen production from renewable energy sources. The survey provides a historical view and various methodology developed over the years. The advantageous and disadvantageous of different methods and their practical implications are discussed in reference to mentioned literature.

2.2 Biogas and Electricity Productions from Wastewater Treatment Plants

Biogas is a gas combustible mixture produced during the organic matter anaerobic digestion, sludge, in the sewage treatment. The amount of each gas in the mixture depends on many factors as the type of digester and the kind of organic matter. In any way this mixture is basically made of methane (CH_4) and carbon dioxide (CO_2), and its heating value is straightly linked to the methane content [10].

The pressure has been increased on the conventional source of energy due to continue requirement of energy that increased the importance of renewable & non-conventional source of energy. On the other hand due to burning of fossil fuel chances of “Global Warming” is also increased by which most of the countries attract towards the importance of non-conventional source of energy. Bioenergy production based on decomposition of sludge material definitely is helpful in solving the problem of energy crisis in the house hold of staff at site and to remove some pressure from the conventional sources of energy [11].

Kalloum et al., [12] presented biogas production from the sludge of the municipal WWTP of Adrar city (southwest of Algeria). The quantity of biogas produced was 280.31 ml with a yield of 30 ml of biogas/mg of COD removed. This study presented an important energetic opportunity by producing 30,950 kWh.

Bodik et al., [13] presented a contribution review for the actual status of biogas production in the European countries with a focus on the Slovak municipal WWTPs. In 49 monitored Slovak WWTPs, the anaerobic digestion with biogas production was operated. In this study total volume of digestion tanks is about 195,000 m³ but the total daily biogas production is only approximately 55,000 m³ d⁻¹. The contribution described the actual load parameters of digestion tanks, specific biogas production, electrical power capacity, and production on the Slovak WWTP obtained on the basis of a questionnaire from Slovak Water Companies.

Francioso et al., [14] presented the chemical characterization of municipal wastewater sludge produced by two-phase anaerobic digestion for biogas production. In the presented study, the chemical features of municipal wastewater sludges treated in two-phase separate digesters, one for acetogenesis and the other one for methanogenesis, were characterized by using chemical analysis, stable carbon isotope ratios and a special spectroscopy method.

Yadvika et al., [15] presented a review study about enhancement of biogas production from solid substrates using different techniques. Researchers have tried different techniques to enhance gas production.

Asam et al., [16] investigated an improvement of biogas production per unit of feedstock in biogas plants. This research carried out in laboratory scale batch digesters assessed the biogas potential of energy crops and solid manure fractions from manure separation units. Luostarinen et al., [17] studied feasibility of co-digesting grease trap sludge from a meat-processing plant and sewage sludge in batch and reactor experiments at 35 °C.

Tsagarakis [18] presented a technoeconomic analysis has been undertaken considering the optimum number of energy producing generators using biogas coming from anaerobic digestion. Inputs for this analysis originate from available data on the first generator for energy production from biogas, installed in Greece at the wastewater treatment facility of Iraklio city.

Stern et al., [19] presented performance of a bench-scale membrane pilot plant for the upgrading of biogas in a wastewater treatment plant. The methane concentration in biogas produced at a municipal wastewater treatment plant could be enhanced from 62±63 mol% to as much as 97 mol% in a bench-scale membrane pilot plant operating under the conditions of this study. Therefore, the energy content of the biogas was significantly enhanced.

Tsagarakis and Papadogiannis [20] presented a technical–economic evaluation with the available data of 5.5 years of operation from the wastewater treatment facility of Iraklio city with 120,000 inhabitants. It was concluded that the cost per kWh produced is 0.072€, while it was purchased at 0.07€, a highly subsidized price, since the cost of the primary material for producing 1 kWh is 0.085€. It was shown that energy produced is covering 15.9% of the total electricity needs of the facility. This percentage is really low since, according to the analysis pursued in this paper, it could go up to 39% if the recorded problems were successfully solved. The ultimate objective of this paper was to provide a methodology for accessing the electricity produced from other such facilities by tracking and analyzing the problems reported in the examined plant.

Solyom et al. [21] presented a microwave treatment as a way to accelerate the hydrolysis in anaerobic digestion of municipal wastewater sludge. The influence of the absorbed energy, power and a thermal microwave effect on organic matter solubilization and biogas production has been studied. In addition, a novel method that considers the absorbed energy in the microwave system was proposed, in order to obtain comparable experimental results. The absorbed energy was calculated from an energy balance.

Villela and Silveira [22] in their study proposed the use of biogas generated in the Wastewater Treatment Plant of a dairy industry. The objective was to apply a thermoeconomic analysis to the supplementary cold water production of an absorption refrigeration system ($\text{NH}_3 + \text{H}_2\text{O}$) by the burning of such gas. As a conclusion, the absorption refrigeration system was found better than that of compression refrigeration system, when the biogas cost was not considered.

Rasi et al., [23] studied biogas composition and variation in three different biogas production plants to provide information pertaining to its potential use as biofuel. Methane, carbon dioxide, oxygen, nitrogen, volatile organic compounds (VOCs) and sulphur compounds were measured in samples of biogases from a landfill, sewage treatment plant sludge digester and farm biogas plant.

2.3 Sewage Sludge Evaluation Methods

Sludge is by far the largest in volume amongst the by-products of wastewater treatments, and its processing and disposal one of the most complex environmental problems facing the engineers in this field. This is because the sludge resulting from the wastewater treatment operations and processes is usually in the form of a very dilute suspension, which typically contains from 0.25 to 12% solids, depending on the operation and process used [6]. Besides, sludge is composed largely of the substances responsible for the offensive, pathogenic and toxic characteristics of the untreated wastewater [24].

Sewage sludge has been used in agriculture over a long time. Since 1986 the utilization of sewage sludge has been subject to provisions stipulated in the EU Directive (86/278/EEC) [25]. The Directive sets out requirements with respect to the quality of sludge, the soil on which it is to be used, the loading rate, and the crops that may be grown on treated land.

Strategic environmental assessment (SEA) of sewage sludge management in a Danish municipality in Aalborg, with 160,000 inhabitants, using alternative methods for aggregation of environmental impacts was performed by Poulsen and Hansen [26]. The purpose is was to demonstrate the use of SEA in relation to sludge management and to improve SEA methodology. Six different scenarios for management of sewage sludge within the Aalborg municipality involving thermal treatment, composting and landfilling of sludge were evaluated. Environmental impact categories considered were global warming, non-renewable resources and land use. Thermal sludge treatment with energy utilization was shown to be a promising option for sewage sludge management in Aalborg. Sensitivity of the relative environmental impacts with respect to calculation methodology and input parameter values were evaluated to identify important parameters and calculation

methods. The analysis showed that aggregation procedures, sludge biogas potential and sludge production were very important whereas sludge transport was not.

A mathematical model was produced by Andrews et. al., [27] in order to examine the impact of sewage sludge and fertilizer application to arable land and the effect of different crop regimes on the amount of nitrate leached to chalk groundwater. The model enables examination of the relationship between the arable/hydrogeological systems and the environmental implications of sludge application and of different arable regimes. Results are of use in developing strategies for arable farming and sludge application in areas sensitive to nitrate leaching.

Land application of sewage sludge in China was thoroughly reviewed by Wang [28]. He informed that most sewage sludge has not been treated and disposed of properly, resulting in environmental pollution and potential exposure to humans. His study pointed out to promote land application of sewage sludge in China, a statewide survey of sewage sludge production and harmful components in sewage sludge should be carried out.

In another study of Wang et al., [29], field experiments were conducted to study the effect of sewage sludge application on the heavy metal content in soils and grasses. The experimental results showed that nutrient content of the soil, especially organic matter, was increased after sewage sludge application. The grass biomass was increased and the grass growing season was longer. Therefore, it was suggested that the sewage sludge produced from the wastewater treatment plant should not be applied to farmland, for which B grade soil or better is required. The sludge is suitable for application to forestry and grasslands or nurseries where food chain contamination with cadmium is not a concern.

Bengtsson and Tillman [30] presented the Swedish debate on the sustainability of using sewage sludge as fertilizer in agriculture. The study investigated how actors define problems and interpret the risks and benefits of sludge use. Specifically, the study concentrated on the role of science in the sludge controversy.

Ahmed et al., [31] presented a study of sewage sludge use in agriculture and its effect on plant and soil. The plant macro and micro nutrients as well as organic matter

make sludge disposal in soil an attractive option. Nitrogen has received most attention and it is normally the most abundant sludge nutrient. One of the best alternatives to waste disposal is through the soil-plant system as a fertilizer. Based on properties different wastes can be co-recycled in order to take simultaneously the best profit and minimize environmental pollution.

Werther and Ogada [6] discussed various issues related to the combustion of sewage sludge. The four sludge disposal methods which have been currently used, recycling in agriculture, landfilling, dumping into sea and incineration, were examined, and the future trend presented showing the increasing role of sludge incineration. They classified sewage sludge combustion possibilities into three groups: Mono-combustion, co-combustion and alternative processes. Various mono-combustion incinerators, including multiple hearth, fluidized bed and smelting furnaces were briefly discussed, whereas for co-combustion, attention has been given to co-combustion with coals in pulverized and fluidized bed coal combustors, as well as co-incineration with municipal solid wastes in various furnaces.

A new type of sewage sludge incinerator that combines a pressurized fluidized bed combustor and a turbocharger driven by flue gas was proposed by Murakami et al. [32]. He claimed that, with his proposed design, an energy savings of approximately 50% could be achieved as compared to a conventional plant.

Stasta et al., [33] presented the current situation in sludge disposal in the Czech Republic and some other European countries.

Houdkova et al., [34] focused on the heat and economic aspects of selected sludge management options. This paper compared the three alternative technologies of sludge management where sludge is has been used to produce energy. Heat and economic balances were performed on the basis of the pilot tests of sludge dewatering at a big waste water treatment plant with the aim to use credible data for all the analyses. Therefore results of their work provided the information of practical value.

Nadal et al., [35] presented a cost-benefit analysis after substituting classical fuel for sewage sludge as an alternative fuel in a clinker kiln in Catalonia, Spain. The economic benefits resulting in the reduction of CO₂ emissions were compared with the changes in human health risks.

Zabaniotou and Theofilou [36] presented the results of a study concerning the utilization of sewage sludge as an alternative fuel at cement kilns, covering all process, health and safety and environmental matters.

Fytili and Zabaniotou [37] reviewed the past and future trends in sludge handling, focusing mainly at thermal processes, e.g. pyrolysis, wet oxidation, gasification, and the utilization of sewage sludge in cement manufacture as a co-fuel.

Varga and Bokanyi [38] discussed the different methods for the utilization of the sewage sludge. They found that the utilization of the municipal sewage sludge as a fertilizer is has been limited by the environmental problems due to the presence of toxicants. These toxic compounds can be removed by chemical or bio leaching, but the former is costly because of the chemicals and requires further cleaning operations. The latter process needs more studies using genetically manipulated microorganisms in order to improve the rate of the leaching.

Galvez et al. [39] studied the effect of the interaction of exhaust from the combustion of sewage sludge and cement raw material in a laboratory furnace. The experiments were performed at 300°C, close to the temperature at the cyclones in cement. The results showed that the presence of cement raw material at the outlet of the combustion gases is beneficial for the decrease of pollutant emissions.

Nadziakiewicz and Koziol [40] considered co-combustion of sludge with coal. The results of the experiments performed with an experimental boiler were presented. The effects of the following parameters were considered: composition and thermal parameters of the sludge and their change during the year, emissions of SO₂, NO_x, CO and dust from the experimental boiler for various compositions of the fuel. As a result of the analysis, the parameters limiting the amount of sludge in a mixture with coal were identified.

Kim and Parker [41] presented an evaluation of the production of oil from primary waste activated and digested sludges. The pyrolysis was performed in a laboratory-scale horizontal batch reactor. The maximum oil yield was achieved with primary sludge at 500 °C.

Candel et al., [42] designed an experiment aimed to reproduce the behavior of different compounds and heavy metals in the soil as a part of the non-saturated zone. They found high concentrations of nitrates and ammonium in leachates, which imply an important environmental risk.

Kalderis et al., [43] examined four essentially different and widely established methods for the treatment of sewage sludge and determines the applicability of each one of them in the economical, geographical and environmental settings of the island of Crete in Greece. The judgment criteria and the economical parameters were used for the evaluation of the methods may be a useful tool for other wastewater treatment plants in various Mediterranean islands.

Fonts et al. [44] reviewed the state of the art of sewage sludge pyrolysis for liquid production, which is has been under study for recent years.

Tanczuk and Ulbricht [45] presented an algorithm for the evaluation of energetic potential of sewage biomass for Opole city in Poland. Technical biomass potential was showed with reference to heat demand of the rural district of Opole.

2.4 Hydrogen Production Methods in Wastewater Treatment Plants

Hydrogen is often referred to as the energy carrier of the future because it can be used to store intermittent renewable energy sources such as solar, wind, biomass energy [46]. Hydrogen can be produced from wastewater treatment plants by various methods such as electrolysis, biological, thermo-chemical.

Coskun et al., [8] performed an energy analysis of hydrogen production with biogas-based electricity. In their study, a facility generating its own electricity from biogas obtained from wastewater treatment plant was considered for investigation. Hydrogen production process conducted using biogas-based electricity was

examined by three methods of electrolysis. The results of this study indicated that outdoor temperature greatly affects biogas and hydrogen production. The cities with high-temperate climate may achieve higher overall system energy efficiency.

Shiga et al., [47] reviewed various steps involving hydrogen production from biogas, its storage and transportation, and its marketing as a commodity. Various scenarios were studied, and design and cost relationships were developed for feasible alternatives.

Martini [48] studied the hydrogen production from biogas. He developed a model to simulate the different operational conditions of a plant and to explore alternative configurations.

Pandu and Joseph [49] reviewed the biohydrogen production processes in their paper. In their review, the major biological processes discussed for hydrogen production were bio-photolysis of water by algae, dark fermentation, photo-fermentation of organic materials and the sequential dark and photo-fermentation processes.

Kapdan and Kargi [50] presented the biohydrogen production from some waste materials. Types of potential waste materials, bio-processing strategies, microbial cultures to be used, bio-processing conditions and the recent developments were discussed with their relative advantages.

Genc [51] reviewed the biohydrogen production from waste sludge in her paper. She emphasized the importance of sludge pretreatment due to low sludge yield of fermentative hydrogen production methods.

Ni et al., [52] overviewed the alternative thermochemical (pyrolysis and gasification) and biological (biophotolysis, water-gas shift reaction and fermentation) processes for hydrogen production from biomass. The future development also was addressed.

Ntaikou et al., [53] presented a review paper in which he aimed to summarize the microbiological and technological background of the dark fermentation processes for

hydrogen generation, emphasising on the exploitation of biomass and wastes as potential feedstocks.

Levin et al., [54] compared the hydrogen production rates of various biohydrogen systems by standardizing the units of hydrogen production and then by calculating the size of biohydrogen systems that would be required to power proton exchange membrane (PEM) fuel cells of various sizes.

Sen et al., [55] analyzed the yields, reaction rates and reactor designs, and compared effectiveness of different substrate microorganism combinations. This paper identified gaps and possible directions for the future development of biological hydrogen production.

Biagini et al., [56] studied the different thermochemical configurations for producing hydrogen from biomass fuels. Their aim was to provide data for the production unit and the following optimization of the 'hydrogen chain' (from energy source selection to hydrogen utilization) in the frame of the Italian project 'Filiera Idrogeno'. Different options and conditions were studied by developing process models with uniform hypothesis to compare the results.

Gasafi et al., [57] presented an economic analysis of sewage sludge gasification in supercritical water for hydrogen production. The costs of hydrogen production and revenues obtained from the disposal of sewage sludge were determined using the method of the total annual revenue requirement.

Petrov et al. [58] presented an assessment of electrolytic production from H₂S in Black Sea waters and also in wastewater treatment plants.

2.5 Thermodynamic and Thermo-economic Analyses and Optimization of Wastewater Treatment Plants

There is an increasing demand for more sustainable wastewater treatment systems. However, the criteria needed to characterize such a system are not fully developed.

One important tool in the analysis of the sustainability of a wastewater treatment system is the exergy analysis [59].

Armando et al., [60] analyzed the degradation of the water of a river in terms of its exergy while passing through the urban zone of a city. This paper compared the degradation process of the river from point to point and they aimed to unify all the water quality measurements into the same exergy units.

Mora and Oliveira [59] evaluated the environmental impact of wastewater treatment plants based on data generated by the exergy analysis, calculating and applying environmental impact indexes for two wastewater treatment plants located in the Metropolitan Area of São Paulo. The environmental impact of the waste water treatment plants was performed by means of evaluating two environmental impact exergy based indexes: the environmental exergy efficiency and the total pollution rate. The analysis of the results showed that this method can be used to quantify and also optimize the environmental performance of wastewater treatment plants.

Ptasinski et al., [61] presented a new method of sewage sludge treatment that contributes to the sustainable technology more than traditional methods by achieving a higher rational efficiency of sludge processing. This was obtained by preserving the chemical exergy present in the sludge and transforming it into a chemical one-methanol.

Abusoglu et al., [62] considered an actual wastewater treatment plant in the city of Gaziantep, Turkey. This paper proposed a methodology based on energy and exergy criteria to evaluate and quantify the efficient energy use together with the environmental impact of energy conversion process that take part in WWTPs.

Lamas et al., [63] described a methodology developed for determination of costs associated to products generated in a small wastewater treatment station for sanitary wastewater from a university campus. This methodology was applied to a hypothetical system and presented consistent results when compared to expected values based on previous exergetic expertise [64].

Kadar and Siboni [65] presented an optimization of energy economy in the design and operation of wastewater treatment plants. This study evaluated the reduction of energy cost in a typical extended aeration process flow configuration.

2.6 Thermodynamic and Thermo-economic Analyses and Optimization of Biogas Engine Powered Cogeneration System

Coble and Contreras [66] compared two technologies for using biogas as an energy source: cogeneration using either motor-generators or phosphoric acid fuel cells. The comparison was made from the energetic, exergetic, thermo-economic and environmental points of view, internalizing all the costs involved in each case. They used data supplied by an urban wastewater treatment plant at the City of Madrid, Spain.

Hessami [67] described three electricity and/or heat generation applications fuelled by biogas or landfill gas produced from organic waste material and noted that cogeneration is currently the most suitable energy management strategy for applications requiring both heat and power simultaneously.

Dong et al., [68] carried out a review on the development of small and micro-scale biomass-fuelled combined heat and power systems concentrating on the current application of organic Rankine cycle (ORC) in small- and micro-scale biomass-fuelled CHP systems and compared ORC with other technologies such as biomass gasification and micro-turbine based biomass-fuelled CHP systems.

Pellegrini et al. [69] presented a comparative thermo-economic study of biomass integrated gasification combined cycle systems for sugarcane mills. The configurations studied were based on real systems that could be adapted to biomass use. Different steam consumptions in the process were considered, in order to better integrate these configurations in the mill.

Raj et al., [70] reviewed the present day cogeneration technologies based on renewable sources of energy. Study of novel methods, existing designs, theoretical and experimental analyses, modeling and simulation, environmental issues and economics and related energy policies were discussed in this paper.

Basrawi et al., [71] investigated the appropriate electricity output capacity of micro gas turbine cogeneration systems depending on scale of the sewage treatment plant. Performance under three typical ambient temperature conditions was investigated. Considering operation under various loads and efficiency under a partial load condition, the optimal combination with different sizes was also proposed. It was found that the micro gas turbine cogeneration system that has approximately the same fuel energy input under full load as the biogas energy produced in the plant has the highest efficiency. However, in the case of heat demand of the plant varying throughout the year such as the operation in a cold region, partial load operation will be frequent and efficiency will decrease.

Caceres et al., [72] developed the thermodynamic equilibrium analysis of grape pomace anaerobic digestion based on the equilibrium constants for predicting the potential production of biogas and its composition. In addition, a dynamic model of a biogas-fuelled microturbine system for distributed generation applications was derived.

Bruno et al., [73] analyzed various integrated configurations of several types of commercially available absorption cooling chillers and micro gas turbine cogeneration systems driven by biogas. In this paper they conducted a case study for an existing sewage treatment plant. Chilled water was used to reduce humidity in the biogas pre-treatment process and cool the combustion air of the micro gas turbine. They identified the most interesting integrated configurations for trigeneration systems that use biogas and micro gas turbines. They analyzed these configurations and compared them with conventional configurations using operational data from an existing sewage treatment plant.

Farhad et al., [74] studied three configurations of solid oxide fuel cell (SOFC) micro-combined heat and power (micro-CHP) systems with a particular emphasis on the application for single-family detached dwellings. Biogas was considered to be the primary fuel for the systems studied. In each system, a different method was used for processing the biogas fuel to prevent carbon deposition over the anode of the cells used in the SOFC stack. The results predicted through computer simulation of these

systems confirm that the net AC electrical efficiency of around 42.4%, 41.7% and 33.9% are attainable for systems I–III, respectively.

Kang et al., [75] investigated the influence of firing biogas on the performance and operating characteristics of gas turbines. Combined heat and power systems based on two different gas turbines (simple and recuperative cycle engines) in a similar power class were simulated. A full off-design analysis was performed to predict the variations in operations due to firing biogas instead of natural gas.

Abusoglu et al., [76] presented the thermoeconomic analysis of a biogas engine powered cogeneration system. Operation of an existing cogeneration system was described in detail and a methodology based on exergoeconomic relations and SPECO method was provided to allocate cost flows through subcomponents of the plant.

Henham and Makkar [77] presented combustion of simulated biogas in a dual-fuel diesel engine. This study examined the engine performance using simulated biogas of varying quality representing the range of methane: carbon dioxide composition which may be encountered in gas from different sources.

2.7 Thermodynamic and Thermoeconomic Analyses and Optimization of Hydrogen Production from Renewable Energy Sources

One of the most interesting developments of energy systems based on the utilization of hydrogen is their integration with renewable sources of energy. In fact, hydrogen can operate as a storage and carrying medium of these primary sources. The design and operation of the system could change noticeably, depending on the type and availability of the primary source [78].

Santarelli et al., [78] aimed to design and analysis of stand-alone energy systems serving the electricity needs during a complete year of operation, of an isolated residential building situated in a selected site. In this paper, three types of renewable sources of energy were considered: solar radiation, hydraulic power and wind

energy. The purpose of the analysis was to highlight the differences between the systems using the three different types of renewable energy sources.

Deshmukh and Boehm [79] presented a detailed review of renewably driven hydrogen systems and modeling approaches applicable to these systems. Several renewable energy technologies, including solar photovoltaic, wind, and hydro, were considered as the power source. This paper particularly emphasized the aspects of modeling of the various components for the renewable hydrogen system.

Bartels et al., [80] summarized the economics of producing hydrogen from the conventional and alternative energy resources such as natural gas, coal, atoms, sunlight, wind, and biomass; and gave an overview of the energy resource for each feedstock.

Fabiano and Perego [81] investigated the influence of pH and temperature on hydrogen bio-production. An optimum value of temperature corresponding to 40°C was experimentally determined by means of batch fermentation runs carried out at different operative temperatures.

Burgess and Velasco [82] estimated the energy content, the operational energy inputs, and the net energy ratio of an industrial tubular photobioreactor used for the photosynthetic production of H₂ by microalgae. The calculated H₂ output of the photobioreactor was based on a range of algal photosynthetic H₂ generation efficiencies, and on the application of standard theory for tubular solar collectors. The results showed that photobiological hydrogen could be a viable H₂ generation technology, if tight constraints on energy inputs are met.

Kalinci et al., [83] reviewed various processes for conversion of biomass into hydrogen gas in terms of two main groups, namely (i) thermo-chemical processes (pyrolysis, conventional gasification, supercritical water gasification), and (ii) biological conversions (fermentative hydrogen production, photosynthesis, biological water gas shift reactions). Biomass-based hydrogen production systems were discussed in terms of their energetic and exergetic aspects.

Modarresi et al., [84] applied an exergy analysis to a novel process for biological production of hydrogen from biomass employing thermophilic and photo-heterotrophic bacteria. The exergy content of the process streams was calculated using a MS-Excel spreadsheet. The efficiency based on chemical exergy of biomass feed and produced pure hydrogen refers to 36–45% depending on the configuration of the overall process.

Perera et al., [85] compiled to evaluate the benefit of higher fermentation temperatures in terms of net energy gain. This evaluation showed that the improvement in hydrogen yield at higher temperatures is not justified as the net energy gain not only declined with increase of temperature, but also was mostly negative when the fermentation temperature exceeded 25 °C.

Cohce et al., [86] investigated a novel biomass-based hydrogen production plant. The main plant processes are biomass gasification, steam methane reforming and shift reaction. The modeling of the gasifier uses the Gibbs free energy minimization approach and chemical equilibrium considerations. The plant, with modifications, was simulated and analyzed thermodynamically using the Aspen Plus process simulation code. Exergy analysis was used throughout the investigation, in addition to energy analysis.

Siddiqui et al., [87] compared the total energy produced from co-digested food waste and sewage sludge for single phase mesophilic anaerobic digestion producing methane and two-phase hydrogen production followed by methane production.

Nath and Das [88] studied on modeling and optimization of fermentative hydrogen production. Biohydrogen production depends on a number of variables, including pH, temperature, substrate concentration and nutrient availability, among others. Mathematical modeling of several distinct processes such as kinetics of microbial growth and products formation, steady state behavior of organic substrate along with its utilization and inhibition were presented.

Tock and Marechal [89] analyzed the thermochemical production of hydrogen from lignocellulosic biomass which was systematically analyzed by developing thermo-

environomic models combining thermodynamics with economic analysis, process integration techniques and optimization strategies for the conceptual process design. The trade-off between H₂ and electricity co-production and H₂ or electricity only generation was assessed with regard to energy, economic and environmental considerations.

Balta et al., [90] presented a thermodynamic assessment of geothermal energy use in hydrogen production. A high-temperature electrolysis process coupled with and powered by a geothermal source was considered for a case study, and its thermodynamic analysis through energy and exergy was conducted for performance evaluation purposes.

Kanoglu et al., [91] developed models for the use of geothermal energy for hydrogen production. The effect of geothermal water temperature on the amount of hydrogen production per unit mass of geothermal water was investigated for all four models, and the results were compared. The results show that as the temperature of geothermal water increases the amount of hydrogen production increases.

Ratlamwala et al., [92] proposed a novel integrated geothermal absorption system for hydrogen liquefaction, power and cooling productions. The effect of geothermal, ambient temperature and concentration of ammonia-water vapor on the system outputs and efficiencies were studied through energy and exergy analyses. It was found that both energetic and exergetic coefficient of performances, and amounts of hydrogen gas pre-cooled and liquefied decrease with increase in the mass flow rate of geothermal water.

Yilmaz et al., [93] considered seven models for the production and liquefaction of hydrogen by geothermal energy. In these models, they used electrolysis and high-temperature steam electrolysis processes for hydrogen production, a binary power plant for geothermal power production, and a pre-cooled Linde-Hampson cycle for hydrogen liquefaction. Also, an absorption cooling system was used for the pre-cooling of hydrogen before the liquefaction process. A methodology was developed for the economic analysis of the models. The results showed that the cost of hydrogen production and liquefaction decreases as the geothermal water temperature

increases. Also, capital costs for the models involving hydrogen liquefaction were greater than those for the models involving hydrogen production only.

Balta et al., [7] conducted an exergy, cost, energy and mass analysis of a copper-chlorine thermochemical water splitting cycle driven by geothermal energy for hydrogen production. They investigated and illustrated the relations between thermodynamic losses and capital costs. The results showed that hydrogen cost was closely and directly related to the plant capacity and also exergy efficiency. Increasing economic viability and reducing the hydrogen production costs would help these cycles play a more critical role in switching to hydrogen economy.

Kanoglu et al., [94] developed an exergoeconomic procedure based on the exergy flows and cost formation within a high temperature steam electrolysis system. The cost accounting procedure was based on the specific exergy costing (SPECO) methodology. Exergy based cost-balance equations are obtained by fuel and product approach. Cost allocations in the system were obtained and effect of the second-law efficiency on exergetic cost parameters was investigated.

Joshi et al., [95] assessed and compared various solar-based hydrogen production processes such as solar thermal photovoltaic, photoelectrolysis, biophotolysis etc. for their merits and demerits in terms of exergy efficiency and sustainability factor. For a case study the exergy efficiency of hydrogen production process and the hydrogen system was discussed in terms of sustainability.

Zhang et al., [96] presented solar energy powered thermodynamic cycle using supercritical carbon dioxide as working fluid for the combined production of hydrogen and thermal energy. The proposed system consists of evacuated solar collectors, power generating turbine, water electrolysis, heat recovery system, and feed pump. In the presented study, an experimental prototype was designed and constructed. The performance of the cycle was tested experimentally under different weather conditions.

Joshi et al., [97] presented a comparative performance assessment study of solar thermal and photovoltaic hydrogen production methods. It was found that the solar

thermal hydrogen production via electricity production is an environmentally benign method and possesses higher exergy efficiency than photovoltaic hydrogen production.

Paola et al., [98] presented an optimization of hydrogen production by electrolysis using renewable energy resources. The simulation program, called “Ren Hydrogen”, provided a qualitative calculation of the hydrogen production during the whole year, comparing different technological options and leading to the techno-economic optimization of the photovoltaic electrolysis system.

Esmaili et al., [99] analyzed a low-temperature electrolysis hydrogen production system using molybdenum-oxo catalysts in the cathode and a platinum based anode. A thermodynamic model was developed for the electrolysis process in order to predict and analyze the energy and exergy efficiencies.

Sherif et al., [100] presented a review of hydrogen energy technologies, namely technologies for hydrogen production, storage, distribution, and utilization. They discussed possibilities for utilization of wind energy to generate hydrogen in parallel with possibilities to use hydrogen to enhance wind power competitiveness.

Bechrakis et al., [101] presented a case study with respect to the current trends in hydrogen technology and market developments. Their main goal was to design an autonomous, environmentally sustainable and zero emission power system using commercially available equipment. In order to achieve the optimum cost effective solution, its limitations were defined by simulating its performance over a year. A scenario was chosen which is representative of an area with significant wind potential, where the grid connection is relatively long or the construction of the line itself would irretrievably harm the environment.

Mathur et al., [102] presented an economic analysis of one of the most promising hydrogen production methods—using wind energy for producing hydrogen through electrolysis of seawater—with a concentration on the Indian transport sector. The analysis provided insights about several questions such as the advantages of offshore

plants over coastal installations, economics of large wind-machine clusters, and comparison of cost of producing hydrogen with competing gasoline.

Khan and Iqbal [103] presented a detailed modeling, simulation, and analysis of an isolated wind-hydrogen hybrid energy system. Dynamic nonlinear models of all the major subsystems were developed based on sets of empirical and physical relationships.

Calderon et al., [104] presented the results of an exergy analysis conducted during the operation of a test-bed hybrid wind/solar generator with hydrogen support, designed and constructed at the Industrial Engineering School of the University of Extremadura, Badajoz (Spain). An exergy analysis was made of the different components of the system, calculating their exergy efficiencies and exergy losses, and proposing future improvements to increase the efficiency of the use of the surplus energy produced by the wind/solar generator.

Kalinci et al., [105] presented an exergoeconomic analysis of hydrogen production from plasma gasification of sewage sludge using specific exergy cost method. They also determined exergy destructions and exergy destruction costs. They calculated that the pressure swing adsorption has the largest exergy destruction rates followed by the plasma gasification components. They also determined exergy efficiencies for these components.

2.8 Conclusions

The extended overview provided in this chapter indicates that there are a few number studies on thermodynamic and thermoeconomic analyses and optimization of biogas usage in electricity and hydrogen productions from wastewater treatment systems in literature. Some studies consider conceptual hydrogen production methods with alternative systems and assumed operating conditions. This thesis differs from the previously conducted studies as follows:

a) The presented study is on the thermodynamic and thermoeconomic analyses and optimization of biogas usage in electricity and hydrogen productions from

wastewater treatment systems. The thesis is original in this scope and content and there is no such study in the open literature, to the best of the author's knowledge and it is the main motivation behind this study.

b) In literature, a small number of studies consider thermodynamic and thermoeconomic analyses of biogas engine powered cogeneration systems and the analysis in these studies are mostly limited to conventional energy analysis and economic considerations.

c) The thesis provides theoretical foundation including procedure and formulation for conventional energy and economic analysis and exergoeconomic analysis and optimization of biogas and hydrogen production from a municipal wastewater treatment system as well as applications on an actual system.

CHAPTER 3

ENERGY RECOVERY FROM MUNICIPAL WASTE WATER TREATMENT PLANTS IN TURKEY

3.1 Introduction

Wastewater treatment plants (WWTPs) present one of the important portions of the comprehensive connection between energy and water. Collecting, treating, and discharging municipal wastewater to acceptable permit standards requires energy, mostly as electricity, but also as fuels [106]. In order to utilize the produced biogas there is one efficient option that is to burn the methane to generate electricity and then recover and use the waste heat to meet digester and space heating loads in WWTP facility. By making use of the waste heat from onsite electricity production, combined heat and power (CHP) production increases fuel efficiency and decreases energy costs.

Sewage sludge is the byproduct of wastewater treatment processes. More than half of its composition is organic, thus it is an important energy source with a considerable economic value [107]. There are many sludge-management options in which production of energy (heat, electricity, or biofuel) is one of the key treatment steps. The most important options are anaerobic digestion, co-digestion, incineration in combination with energy recovery, co-incineration in coal-fired power plants, co-incineration in combination with organic waste focused on energy recovery, use as an energy source in the production of cement or building materials, pyrolysis, gasification, supercritical (wet) oxidation, hydrolysis at high temperature, production of hydrogen, acetone, butanol, or ethanol, and direct generation of electrical energy by means of specific micro-organisms [108].

3.2 Biogas and Electricity Productions Potential of Municipal Wastewater Treatment Plants

Municipal wastewater treatment plant is a facility for removal of mainly organic pollution from wastewaters. Organic pollution is partly transformed into sludge that, with the use of up-to-date technologies, represents an important energy source. Municipal WWTPs generate sludge as a by-product of physical, chemical and biological processes applied during wastewater treatment.

The energy present in sludge can be utilized in anaerobic digestion (AD). Digestion leads to the formation of biogas, rich in methane, which can be recovered, and used as an energy source, making it a great energy saver. There are four main biogas utilization applications: i) production of heat and steam; ii) electricity generation by using cogeneration systems; iii) use as fuel in a vehicle; and iv) production of chemicals. Biogas is mainly used in combined heat and power (CHP) applications all around the world, whereas various EU countries have embarked on programmes to achieve a growing share of biogas in the transport sector for the vehicles [13].

Anaerobic digestion processes are used in European countries for sludge treatment. At the end of the 1970s, the produced biogas was not evaluated economically by the WWTPs. Produced biogas was burning in biogas a flare. However, whenever energy crisis come in view on the World, energy market attempts were made to exploit this energy source.

Biogas production in municipal WWTPs represents a significant contribution to total biogas production. Primary production of biogas and electricity production from biogas in selected EU-countries is presented in Table 3.1.

Table 3.1: Primary production of biogas and electricity production from biogas in selected EU-countries in 2009 [13]

Biogas Production					
Country	Landfills	WWTPs	BGP	Electricity production	
	GWh	GWh	GWh	GWh	MWh/10 ³ cap
Austria	57	220	1642	638	72
Belgium	515	24	909	462	44
Czech Rep.	340	392	779	441	43
Denmark	72	233	854	325	60
France	5144	526	450	847	14
G. Britain	17147	12,902	0	5591	94
Germany	3088	4497	41,417	12,562	152
Greece	538	538,142	2	217	20
Hungary	33	120	204	95	9
Italy	4208	58	901	1739	30
Poland	413	675	52	319	8
Slovakia	9	172	8	21	4
Slovenia	97	35	128	69	34
Spain	1628	116	383	527	13
Sweden	412	698	171	34	4
EU total	34,907	11,671	50,481	25,169	34

The first wastewater treatment plant in Turkey with a capacity of 751,000 m³/year was constructed in 1982. By the end of 1994, the total number of WWTPs with a capacity of 602 Mm³/year was 45. Most of them (41 WWTPs) were biological treatment plants, which have 37.35% of total treated water amount. Between 1994 and 2010, the number of constructed plants was drastically increased, reaching 326. The total capacity of the WWTPs was 5,293 Mm³/year by the end of year 2010 and the amount of wastewater treated by the treatment plants was about 2,719 Mm³/year. Most of them have primary and secondary treatment units (91% of total capacity) while a few have advanced treatment units [109-110]. In Turkey, 52 of its 81

provinces have urban WWTPs and approximately 73% of the country's population being served (see Table 3.2).

Table 3.2: The main wastewater indicators of municipalities in Turkey between 2001-2010 [110]

Years	2001	2002	2003	2004	2006	2008	2010	
Number of municipalities served by sewerage system	2003	2115	2195	2226	2321	2421	2235	
Rate of population served by sewerage system in total population (%)	63	65	67	68	72	73	73	
Amount of wastewater discharged from municipal sewerage to receiving bodies (million m ³ /year)	2301	2498	2861	2923	3367	3261	3582	
Number of wastewater treatment plants	Physical	25	28	31	35	26	29	39
	Biological	98	114	121	133	135	158	199
	Advanced	3	3	4	4	23	32	53
	Natural	-	-	-	-	-	17	35
	Total	126	145	156	172	184	236	326
Total capacity of wastewater treatment plants (million m ³ /year)	Physical	770	771	1046	1385	1329	1538	1839
	Biological	1250	1320	1484	1751	1511	1595	1733
	Advanced	267	267	275	275	808	1001	1709
	Natural	-	-	-	-	-	10	12
	Total	2288	2359	2805	3410	3648	4143	5293
Amount of wastewater treated by wastewater treatment plants (million m ³ /year)	Physical	325	345	482	599	714	736	751
	Biological	663	746	877	1071	927	861	931
	Advanced	206	222	227	231	500	649	1032
	Natural	-	-	-	-	-	6	5
	Total	1194	1312	1587	1901	2140	2252	2719
Number of municipalities served by wastewater treatment plants in total population (%)	27	28	30	36	42	46	52	
Amount of wastewater discharged per capita in municipalities (liters/capita-day)	147	154	173	174	181	173	182	

Depending on the seven geographic regions of Turkey, the amounts of treated wastewater, sludge production, biogas and electricity productions potential of 326 WWTPs in Turkey are presented in Figure 3.1. The total amount of wastewater treated by WWTPs in Turkey is given according to the 2010 data of TSI [110]. Sludge production of each WWTP can be calculated by taking their treated wastewater capacity into consideration as well as in the case of biogas and corresponding electricity productions. For these calculations, the actual data of the existing WWTP presented is taken into account as a starting point. As can be seen from Figure 3.1, annual biogas production potential of all existing WWTPs of Turkey is nearly above 200 million m³. Moreover, biogas production potential may be increased by using newly developed sludge stabilization techniques before the

anaerobic digestion of sludge. If this estimated biogas production potential was totally used for power production, the annual electricity production from sewage sludge based biogas in Turkey would be over 530 GWh which can meet nearly 1% of the total annual energy demand of the country. Considering the digested sludge output as a secondary valuable fuel source for incineration facilities for further power production, this percentage would be increased to 2%, which reveals the fact that WWTPs are practically remarkable renewable energy sources. Besides, energy recovery from a sustainable waste source is not influenced by international prices or political fluctuations as considering Turkey's dependency on foreign sources of energy.

3.3 Energy Recovery from Sewage Sludge of Municipal Wastewater Treatment Plants

Energy recovery from sewage sludge can be achieved by the listed methods: (1) anaerobic digestion process, (2) production of biofuels from sewage sludge, (3) direct production of electricity in microbial fuel cells, (4) incineration with energy recovery, (5) co-incineration in coal-fired power plants, (6) gasification and pyrolysis, (7) use of sludge as an energy and raw material source in the production of Portland cement and building materials, (8) supercritical wet oxidation, and (9) hydrothermal treatment.

Anaerobic Digestion Process:

Anaerobic digestion process is used to stabilize the sewage sludge and to convert part of the volatile compounds into biogas. The biogas can be used as an energy resource at the wastewater treatment plant. Currently, anaerobic digestion of sewage sludge is mainly applied big wastewater treatment plants. However, also, a growing interest is observed in the application of anaerobic treatment in small plants.

Production of Biofuels:

A general process scheme of a microbiological conversion process focused on the production of energy carriers consists of three main steps. The first step consists of a pretreatment that is often necessary to make the substrate accessible to the biological conversion step, and the fermentation step. In general, biomass components, such as

sugar and starch, are easily bioavailable. Possible pretreatment systems are steam treatment, acid or alkaline hydrolysis, treatment using by enzymes, ultrasonic treatment, wet oxidation, high-temperature treatment, solvent extraction, reduction in particle size, extrusion, application of ozone, or a combination of one of these methods.



Figure 3.1: Sludge, biogas and electricity production potential of Turkey

In the fermentation step, the biological conversion takes place. Often, it will be necessary, to obtain optimal process conditions, to split up this step in two treatment steps integrated with each other. After the fermentation step, a post treatment step is always necessary.

Dependent upon the type of microorganisms, energy carriers, such as methane, ethanol, acetone, butanol, or hydrogen, can be produced. Production of ethanol, butanol, or acetone from sewage sludge is less attractive because of the complex separation system that is necessary to separate these components selectively [108].

Direct Production of Electricity in Microbial Fuel Cells:

Microbial fuel cells (MFCs) offer a new source of electricity from waste and other carbohydrate sources. A MFC is a device converts chemical energy to electrical energy by the catalytic reaction of microorganisms. MFCs have been demonstrated by several groups both with and without the use of mediators to facilitate electron transfer to the anode. Micro-organisms that require a mediator do not have electrochemically active surface proteins to transfer electrons to the anode. In MFCs that do not use mediators, metal reducing bacteria such as those of the Geobacteraceae family can reduce many substrates, e.g. [111].

Incineration with Energy Recovery:

Incineration of sewage sludge is intended at a complete oxidation at high temperature of the organic sludge compounds also including the toxic organic compounds. Incineration process can either be applied to mechanically dewatered sludge or dried sludge. Sludge incineration has advantages that are not found in other treatment alternatives, including a large reduction of sludge volume to a small stabilized ash. Disadvantages of the incineration process are potential environmental problems related to sludge incineration are the emissions of pollutants with the exhaust gases to the atmosphere and with the quality of the ashes.

Co-incineration in coal-fired power plants:

To avoid the high costs of a stand-alone incineration plant for sludge and also to improve the energy recovery efficiency, sludge can be evaluated in a coal –fired

power plant. In this case, beneficial use can be made from existing coal combustion installations and existing exhaust gas treatment systems. Because the amount of incinerated sludge is small compared to the amount of coal, the effect of the incineration of the sludge on the air and ash qualities can be neglected. Co-incineration of sewage sludge in a coal-fired power plant is applied in practice [108].

Gasification and Pyrolysis:

Pyrolysis is a form of treatment that chemically decomposes organic materials by heat in the absence of oxygen. Pyrolysis typically occurs under pressure and at operating temperatures above 430 °C. In this process, the sludge is converted into char, ash, pyrolysis oils, water vapor, and trace combustible gases.

In the gasification process, organic or fossil based carbonaceous materials are converted into carbon monoxide, hydrogen and carbon dioxide. Gasification process involves the breakdown of dried sludge or other biomasses in an ash and in combustible gases at high temperatures usually about 1000 °C in an atmosphere with a reduced amount of O₂.

Usage of Sludge as an Energy and Raw Material Source in the Production of Portland Cement and Building Materials:

There are several possibilities to use both the organic and inorganic carbon containing compounds in sewage sludge simultaneously in a beneficial way. A lot of effort has been put into the manufacturing of valuable products by thermal solidification of the inorganic sewage sludge compounds, especially in Japan. The starting point in this production process is either incinerator ash or dried sludge. The solidification process occurs up to 900- 1000 °C. Available temperatures are high enough to destroy the toxic organics.

Another beneficial way to use the inorganic and organic compounds of the sludge is usage of sludge in the production of Portland cement. In this process, either ash or dried sludge can be used and this process is available in practice.

Supercritical Wet Oxidation:

If water is heated and compressed to sufficiently high temperature and pressure, an additional fluid state of water emerges. Water at high temperatures and pressures above 374 °C and 221 bar is a fluid that is neither a gas nor a liquid, it is in its supercritical state. Supercritical water can dissolve oxygen and organic compounds. With supercritical oxidation, the organic compounds are completely oxidized. Nitrogen, available in nitrogen containing compounds, such as ammonia and amino acids, is converted into nitrogen gas. Also toxic organic compounds are completely oxidized.

Hydrothermal Treatment:

Hydrothermal treatment (or thermal hydrolysis) is a process in which the sludge is heated as an aqueous phase to temperatures varying between 120 and about 400 °C. The hydrothermal treatment process aims to disintegrate the sludge and results in a formation and accumulation of dissolved products. This makes it possible to recover and recycle useful resources from the sludge, such as volatile fatty acids, phosphorous compounds, organic compounds for enhanced anaerobic biogas production, and coagulants [108].

3.4 Conclusions

In this chapter, biogas and electricity production potential of municipal wastewater treatment plants are presented and current situation in Turkey is assessed. The energy recovery options of sewage sludge are discussed.

CHAPTER 4

THERMODYNAMIC ANALYSIS

4.1 Introduction

Energy is the most fundamental term in thermodynamics and energy engineering. Energy balances are widely used in the design and analysis of energy conversion systems. Although energy balances can determine energy supply requirements in the form of material streams, heat, and shaft work, they do not provide sufficient information on how efficiently energy is used.

Energy balance focuses on the quantity of energy and fails to account for the quality of energy. The true thermodynamic value (quality) of an energy resource is expressed by its potential to cause a change, that is, “to do something useful”, such as heat a room, compress a gas, or promote an endothermic chemical reaction. Kinetic, potential, mechanical, and electric energy can be fully converted in an ideal process to any other form of energy, whereas the quality of thermal and chemical energy depends on parameters (temperature, pressure, and chemical composition) of the energy carrier and of the environment. Electricity clearly has a greater quality than low-pressure steam or cooling water stream in a power plant. In thermodynamics, the quality of a given quantity of energy is characterized by its exergy [112].

Exergy is the theoretical maximum of useful work (shaft work or electrical work) obtainable from a thermal system as this is brought into thermodynamic equilibrium with the reference environment while heat transfer occurs with this environment only. Alternatively, exergy is the theoretical minimum of work (shaft work or electrical work) required to form a quantity of matter from substances present in the environment and to bring the matter to a specified state. Hence, exergy is a measure

of the departure of the state of the system from the state of the reference environment. The processes in all real energy conversion systems are irreversible and a part of the exergy supplied to the total system is destroyed. Only in a reversible process does the exergy remain constant [113]. The real inefficiencies of a system are exergy destruction, occurring within the system boundaries, and exergy losses, which are exergy transfers out of the system that are not further used in the overall installation. Some of the common causes for exergy destruction include chemical reaction, heat transfer across a finite temperature difference, fluid friction, flow throttling, and mixing of dissimilar fluids.

In this chapter we present general formulations of thermodynamic analysis including energy and exergy methods. The formulations are applicable to energy conversion systems including biogas engine powered cogeneration and wastewater treatment systems.

4.2 Energy Analysis

Energy conservation is expressed by energy balances and together with corresponding mass balances they are widely used in the modeling and analysis of energy conversion systems.

4.2.1 Mass Balance

The conservation of mass principle can be expressed as the net mass transfer to or from a system during a process is equal to the net change (increase or decrease) in the total mass of the system during that process [113]. In the rate form it is expressed as

$$\sum \dot{m}_i - \sum \dot{m}_e = \frac{dm_{\text{system}}}{dt} \quad (4.1)$$

where i and e refer to inlet and exit states of the any control volume, respectively. During a steady flow process, the total amount of mass contained within a control volume does not change with time ($m_{\text{CV}} = \text{constant}$). Then the conservation of mass principle requires that the total amount of mass entering a control volume equal the total amount of mass leaving it. For a general steady-flow system with multiple inlets and exits, the conservation of mass principle can be expressed in the rate form as

$$\sum \dot{m}_i = \sum \dot{m}_e \quad (4.2)$$

4.2.2 Energy Balance

Based on experimental observations, the first law of thermodynamics states that energy can be neither created nor destroyed; it can only change forms. Therefore, every bit of energy should be accounted for during a process [113-115]. The conservation of energy principle may be expressed as follows: The net change (increase or decrease) in the total energy of the system during a process is equal to the difference between the total energy leaving the system during that process. Energy balance for any system undergoing any kind of process can be expressed more compactly in the rate form as [113]

$$\dot{E}_{in} - \dot{E}_{out} = \Delta \dot{E}_{system} \quad (4.3)$$

During a steady-flow process, the total energy content of a control volume remains constant ($E_{CV} = \text{constant}$), and thus the change in the total energy is zero. Therefore, the amount of energy entering a control volume in all forms (by heat, work, and mass) must be equal to the amount of energy leaving it. Then the rate form of the general energy balance reduces for a steady-flow process to

$$\dot{E}_{in} = \dot{E}_{out} \quad (4.4)$$

Noting that energy can be transferred by heat, work, and mass only, the energy balance above for a general steady-flow system can also be written more explicitly as

$$\dot{Q}_{in} + \dot{W}_{in} + \sum \dot{m}_i \left(h_i + \frac{V_i^2}{2} + gz_i \right) = \dot{Q}_{out} + \dot{W}_{out} + \sum \dot{m}_e \left(h_e + \frac{V_e^2}{2} + gz_e \right) \quad (4.5)$$

where h_i , h_e , V_i , V_e , z_i , z_e represent enthalpy, velocity, and elevation of mass entering and leaving the control volume, respectively.

4.3 Exergy Analysis

For the evaluation and improvement of thermal systems, it is essential to understand the sources of thermodynamic inefficiencies and the interactions among system components. All real energy conversion processes are irreversible due to dissipative effects such as chemical reaction, heat transfer through a finite temperature difference, mixing of matter at different compositions or states, unrestrained expansion, and friction. Exergy balances assist in calculating the exergy destruction within system components. Thus, the thermodynamic inefficiencies and the processes that cause them are identified. Only a part of the thermodynamic inefficiencies can be avoided by using the best currently available technology. Improvement efforts should be centered on avoidable inefficiencies. Dimensionless variables can be used for performance evaluations. Appropriately defined exergetic efficiency unambiguously characterizes the performance of a system from the thermodynamic viewpoint.

4.3.1 Reference Environment and Exergy Components

The environment, which appears in the definition of exergy, is a large equilibrium system in which the state variables (T_0, P_0) and the chemical potential of the chemical components contained in it remain constant when in a thermodynamic process heat and materials are exchanged between another system and the environment. This environment is called exergy-reference environment or thermodynamic environment. The temperature T_0 and pressure P_0 of the environment are often taken as standard-state values, such as 298.15 K and 1.013 bar. However, these properties may be specified differently depending on the application. For example, T_0 and P_0 may be taken as the actual or average ambient temperature and pressure, respectively, for the time and location at which the system under consideration operates or is designed to operate. For example, if the system uses air, T_0 would be specified as the average air temperature. If both air and water from the natural surroundings are used, T_0 would usually be specified as the lower of the temperatures for air and water when the installation operates above the ambient temperature [113,115,116].

Although the intensive properties of the environment are assumed to remain constant, the extensive properties can change as a result of interactions with other

systems. It is important that no chemical reactions can take place between the environmental chemical components. The exergy of the environment is equal to zero. The environment is part of the surroundings of any thermal system.

In the absence of nuclear, magnetic, electrical, and surface tension effects, the total exergy of a system (Ex_{sys}) can be divided into four components: Physical exergy, Ex_{sys}^{PH} , kinetic exergy Ex^{KN} , potential exergy, Ex^{PT} , and chemical exergy, Ex^{CH} . Then the total exergy of a system is given by

$$Ex_{sys} = Ex_{sys}^{PH} + Ex^{KN} + Ex^{PT} + Ex^{CH} \quad (4.6)$$

The subscript *sys* distinguishes the total exergy and physical exergy of a system from other exergy quantities, including transfers associated with streams of matter. The total specific exergy on a mass basis ψ_{sys} is

$$\psi_{sys} = \psi_{sys}^{PH} + \psi^{KN} + \psi^{PT} + \psi^{CH} \quad (4.7)$$

The physical exergy associated with a thermodynamic system is given by

$$Ex_{sys}^{PH} = (U - U_0) + p_0(V - V_0) - T_0(S - S_0) \quad (4.8)$$

where U, V and S represent the internal energy, volume and entropy of the system, respectively. The subscript 0 denotes the state of the same system at the temperature T_0 and pressure P_0 of the environment. The rate of physical exergy \dot{Ex}^{PH} associated with a material stream is

$$\dot{Ex}^{PH} = (H - H_0) - T_0(S - S_0) \quad (4.9)$$

where H and S denote the enthalpy and entropy, respectively. The subscript 0 denotes property values at the temperature T_0 and pressure P_0 of the environment. The physical exergy of a system consists of thermal exergy \dot{Ex}^T (due to system temperature) and mechanical exergy \dot{Ex}^M (due to system pressure):

$$\dot{Ex}^{PH} = \dot{Ex}^T + \dot{Ex}^M \quad (4.10)$$

An unambiguous calculation of the specific thermal and specific mechanical exergy is possible only for ideal gases and incompressible liquids:

$$\psi^T = \int_{T_0, P_0}^{T, P} c \left(1 - \frac{T}{T_0} \right) dT \quad (4.11)$$

$$\psi^M = \int_{T_0, P_0}^{T, P} v dP \quad (4.12)$$

where v denotes specific volume. For any fluid, the specific thermal exergy of a stream at temperature T and pressure P is expressed as

$$\psi^T = \psi^{\text{PH}}(T, P) - \psi^{\text{PH}}(T_0, P) \quad (4.13)$$

The mechanical exergy is determined from

$$Ex^M = Ex^{\text{PH}} - Ex^T \quad (4.14)$$

Kinetic and potential exergies are equal to kinetic and potential energies, respectively.

$$Ex^{\text{KN}} = \frac{1}{2} m \vec{v}^2 \quad (4.15)$$

$$Ex^{\text{PT}} = mgz \quad (4.16)$$

Here \vec{v} and z denote velocity and elevation relative to coordinates in the environment ($\vec{v}_0 = 0, z_0 = 0$). Equations 4.15 and 4.16 can be used in conjunction with both systems and material streams. The exergy associated with shaft work, flow of electricity, kinetic energy, or potential energy is equal to the energy amount of each of these quantities.

Chemical exergy is the theoretical maximum useful work obtainable as the system at temperature T and pressure P is brought into chemical equilibrium with the reference environment while heat transfer occurs only with this environment. Thus, for calculating the chemical exergy, not only the temperature T_0 and pressure P_0 but

also the chemical composition of the environment x_i^e have to be specified. By definition, the exergy of the reference environment is equal to zero and there is no possibility of developing work from interactions between parts of the environment.

The standard molar chemical exergy $\psi_{\text{sub}}^{\text{CH}}$ of any substance consisting of its elements can be determined using the change in the specific Gibbs function $\Delta\bar{g}$ for the formation of this substance from the reaction of chemical elements present in the environment:

$$\psi_{\text{sub}}^{\text{CH}}(T_0, P_0) = \bar{g}_{\text{sub}}(T_0, P_0) - \sum_{i=1}^M \nu_i [\psi_i^{\text{CH}}(T_0, P_0) - \bar{g}_i(T_0, P_0)] \quad (4.17)$$

where \bar{g}_i , ν_i and ψ_i^{CH} denote, for the i -th chemical element, the Gibbs function at T_0 and P_0 , the stoichiometric coefficient in the reaction, and the standard chemical exergy, respectively. The chemical exergy of a gas i , having the mole fraction x_i^e in the environmental gas phase is [112,117]

$$\psi_i^{\text{ch}} = -\bar{R}T_0 \ln x_i^e \quad (4.18)$$

The chemical exergy of an ideal mixture of N ideal gases is given by

$$\psi_{\text{M,ig}}^{\text{ch}} = \sum_{i=1}^N x_i \psi_i^{\text{ch}} + \bar{R}T_0 \sum_{i=1}^N x_i \ln x_i \quad (4.19)$$

where T_0 is the environmental temperature, ψ_i^{ch} is the standard molar chemical exergy of the i -th substance and x_i is the mole fraction of the k -th substance in the system at T_0 . For the chemical exergy calculations of liquids, the chemical exergy can be obtained if the activity coefficients γ_k are known such as

$$\psi_{\text{M,l}}^{\text{ch}} = \sum_{i=1}^N x_i \psi_i^{\text{ch}} + \bar{R}T_0 \sum_{i=1}^N x_i \ln(\gamma_k x_i) \quad (4.20)$$

The specific chemical exergy of the sewage at the reference state is related to its COD (chemical oxygen demand) value and may be found from the following relation [118]

$$\psi_{\text{sewage}}^{\text{CH}} = 13.6 \times \text{COD} \quad (4.21)$$

Following Szargut et al. [119] the specific chemical exergy of a technical fuel such as sludge containing a very small amount of ash may be adopted as

$$\psi_{\text{sludge}}^{\text{CH}} = (LHV_{\text{sludge}} + h_{\text{evap}} z_{\text{water}}) \beta + (\psi_{\text{sulfur}}^{\text{CH}} - LHV_{\text{sulfur}}) z_{\text{sulfur}} + \psi_{\text{ash}}^{\text{CH}} z_{\text{ash}} + \psi_{\text{water}}^{\text{CH}} z_{\text{water}} \quad (4.22)$$

where LHV_{sludge} and LHV_{sulfur} are the lower heating values of sludge and sulfur respectively; h_{evap} is the enthalpy of water vaporization; z_{water} , z_{sulfur} , z_{ash} are the mass fractions of water, sulfur and ash respectively; $\psi_{\text{sulfur}}^{\text{CH}}$, $\psi_{\text{ash}}^{\text{CH}}$, and $\psi_{\text{water}}^{\text{CH}}$ are the specific chemical exergies of sulfur, ash, and water respectively. β is a variable ratio which gives the atomic ratios in a mixture and does not depend on environmental parameters. It can be obtained for the sludge including the ratio of oxygen to carbon (O/C) less than 0.5 by the following relation [119]

$$\beta_{\text{sludge}} = 1.0437 + 0.0140 \frac{H}{C} + 0.0968 \frac{O}{C} + 0.0467 \frac{N}{C} \quad (4.23)$$

where H , C , O and N are the percentage values of hydrogen, carbon, oxygen and nitrogen in the sludge, respectively. The specific chemical exergy of the biogas in the reference state must be adjusted relative to its mole fractions, $y_{f,\text{mixt}}$, of the mixture. Thus, the chemical exergy of the biogas mixture at the reference state becomes [120]

$$\psi_{\text{biogas}}^{\text{CH}} = \sum y_{f,\text{mixt}} \psi_{f,\text{mixt}}^{\text{CH}} + R_{f,\text{mixt}} T_0 \sum y_{f,\text{mixt}} \ln y_{f,\text{mixt}} \quad (4.24)$$

where $\psi_{f,\text{mixt}}^{\text{CH}}$ is the specific chemical exergy of any component in the biogas mixture at the reference state.

4.3.2 Exergy Balance, Exergy Destruction, and Exergy Loss

The exergy destruction represents the exergy destroyed $\dot{E}x_D$ due to irreversibilities (entropy generation) within a system. The irreversibilities are caused by chemical reaction, heat transfer through a finite temperature difference, mixing of matter, and unrestrained expansion and friction. The exergy destruction is calculated with the aid of either (a) an exergy balance formulated for the system being considered, or (b) the entropy generation, \dot{S}_{gen} , within the system (calculated from an entropy balance) and the relationship [112,121]

$$\dot{E}x_D = T_0 \dot{S}_{gen} \quad (4.25)$$

The former way is recommended when a comprehensive exergetic evaluation is conducted. The exergy destruction in the overall system is equal to the sum of the exergy destruction in all system components:

$$\dot{E}x_{D,total} = \sum_{k=1}^{n_k} \dot{E}x_{D,k} \quad (4.26)$$

The rate of exergy destruction in the k th component of a system is given by

$$\dot{E}x_{D,k} = \dot{E}x_{F,k} - \dot{E}x_{P,k} - \dot{E}x_{L,k} \quad (4.27)$$

where, $\dot{E}x_{F,k}$ and $\dot{E}x_{P,k}$ are the so-called exergetic fuel and exergetic product, respectively, and $\dot{E}x_{L,k}$ represents the exergy rate loss in the k th component, which is usually zero when the component boundaries are at T_0 . For an overall system, $\dot{E}x_{L,total}$ includes the exergy flow rates of all non-useful streams rejected by this system to the surroundings.

The total exergy destruction value is also obtained from the exergy balance written for the overall system

$$\dot{E}x_{D,total} = \dot{E}x_{F,total} - \dot{E}x_{P,total} - \dot{E}x_{L,total} \quad (4.28)$$

It is apparent that all efforts to improve the thermodynamic efficiency of a component or system should focus on avoidable exergy destruction. An exergy transfer across the boundary of a control volume system can be associated with either a material stream or an energy transfer by work or heat. By taking the positive direction of heat transfer to be to the system and the positive direction of work transfer to be from the system, the general form of the exergy balance for a control volume involving multiple inlet and outlet streams of matter and energy can be expressed as

$$\frac{dEx_{CV}}{dt} = \sum \left(1 - \frac{T_0}{T_k}\right) \dot{Q}_k - \left(\dot{W} - P_0 \frac{dV_{CV}}{dt}\right) + \sum \dot{E}x_i - \sum \dot{E}x_e - \dot{E}x_D \quad (4.29)$$

where $\dot{E}x_i$ and $\dot{E}x_e$ are the total exergy transfer rates at the inlet and outlet, respectively for the total, physical, chemical, kinetic, and potential exergy associated with mass transfers. The term \dot{Q}_k represents the rate of heat transfer at the location on the boundary where the temperature is T_k . The associated rate of exergy transfer $\dot{E}x_{q,k}$ is given by

$$\dot{E}x_{q,k} = \left(1 - \frac{T_0}{T_k}\right) \dot{Q}_k \quad (4.30)$$

For $T_k > T_0$, the exergy rate $\dot{E}x_{q,k}$ associated with heat transfer is always smaller than the heat transfer rate \dot{Q}_k . In applications below the temperature of the environment, $T_k < T_0$, and $\dot{E}x_{q,k}$ and \dot{Q}_k have opposite signs: When energy is supplied to the system, exergy is removed from it and vice versa. For steady-flow systems, $\frac{dEx_{CV}}{dt} = 0$, and Equation 4.29 becomes

$$0 = \sum \left(1 - \frac{T_0}{T_k}\right) \dot{Q}_k - \left(\dot{W} - P_0 \frac{dV_{CV}}{dt}\right) + \sum \dot{E}x_i - \sum \dot{E}x_e - \dot{E}x_D \quad (4.31)$$

4.3.3 Exergetic Efficiency

Dimensionless criteria are used for performance evaluations. Appropriately defined exergetic efficiency unambiguously characterizes the performance of a system or system component from the thermodynamic view point. The exergetic efficiency should also be used to compare the performance of similar components operating under similar conditions. For the comparison of dissimilar components the exergy destruction ratio may be used.

The exergetic efficiency of the k th component ε_k is defined as the ratio between product and fuel. The exergy rates of product $\dot{E}x_{p,k}$ and the fuel $\dot{E}x_{F,k}$ are defined by considering the desired result produced by the component, and the exergetic resources expended to generate this result, respectively:

$$\varepsilon_k = \frac{\dot{E}x_{p,k}}{\dot{E}x_{F,k}} = 1 - \frac{\dot{E}x_{D,k} + \dot{E}x_{L,k}}{\dot{E}x_{F,k}} \quad (4.32)$$

The definition of exergetic efficiency must be meaningful from both the thermodynamic and the economic viewpoints. A distinction between (a) physical and chemical exergy, or (b) thermal, mechanical and chemical exergy, or (c) thermal mechanical, reactive and non-reactive exergy may allow the definitions of more rational exergetic efficiencies for some components.

4.3.4 Exergy Destruction Ratio and Exergy Loss Ratio

In addition to the exergy destruction $\dot{E}x_{D,k}$ and the exergetic efficiencies ε_k , the exergy destruction ratio $y_{D,k}$ is used in the thermodynamic evaluation of a component. This ratio compares the exergy destruction in the k th component with the total fuel exergy supplied $\dot{E}x_{F,\text{total}}$ to the overall system:

$$y_{D,k} = \frac{\dot{E}x_{D,k}}{\dot{E}x_{F,\text{total}}} \quad (4.33)$$

Alternatively, the exergy destruction rate of the k th component can be compared to the total exergy destruction rate $\dot{E}x_{D,\text{total}}$:

$$y_{D,k}^* = \frac{\dot{E}x_{D,k}}{\dot{E}x_{D,\text{total}}} \quad (4.34)$$

The exergy loss ratio is defined similarly to Equation 4.33, by comparing the exergy loss to the total fuel exergy supplied to the overall system

$$y_{L,\text{total}} = \frac{\dot{E}x_{L,\text{total}}}{\dot{E}x_{F,\text{total}}} \quad (4.35)$$

The difference between the exergy destruction ratio and the exergetic efficiency is that in the former the exergy destruction within a component is related to the fuel exergy supplied to the overall system, whereas the latter refers the same exergy destruction to the fuel exergy supplied to the component. The exergy destruction ratio expresses the percentage of the decrease of the exergetic efficiency for the overall system caused by the exergy destruction in the k th system component:

$$\varepsilon_{\text{total}} = \frac{\dot{E}x_{P,\text{total}}}{\dot{E}x_{F,\text{total}}} = 1 - \frac{\dot{E}x_{D,\text{total}} + \dot{E}x_{L,\text{total}}}{\dot{E}x_{F,\text{total}}} = 1 - y_{D,\text{total}} - y_{L,\text{total}} \quad (4.36)$$

Since in almost every case no exergy loss is defined at the component level, the exergy loss ratio is defined only for the overall system.

4.4 Performance Assessment Parameters in Cogeneration Systems

There are several performance assessment parameters of cogeneration systems in literature. Huang [122] describes ten of these parameters: fuel-utilization efficiency, efficiency of power generation, fuel chargeable to power, power-to-heat ratio, energy saving index, fuel energy saving ratio, fuel saving rate, second law efficiency and economic efficiency. Among these parameters, fuel utilization efficiency is the most widely used parameter. However, power to heat ratio and second law efficiency (exergetic efficiency) are stated to be the most useful parameters by Huang.

The concept of fuel utilization efficiency is based on the assumption that the unit energy carried out by the process heat is equally valuable as the unit energy carried out by the produced work or electricity. In other words, any unit amount of energy

transferred for useful application by the system is taken into account with equal value. Fuel utilization efficiency is defined to be the ratio of the energy output rate of the cycle, which is used either as a process heat or electricity, to the energy input rate of the fuel employed by the cogeneration system:

$$\text{FUE} = \frac{(\dot{W}_{\text{el}})_{\text{plant}} + \Delta H_{\text{process}}}{\dot{m}_{\text{fuel}} \cdot \text{LHV}_{\text{fuel}}} \quad (4.37)$$

where $(\dot{W}_{\text{el}})_{\text{plant}}$ is the power produced by cogeneration plant, $\Delta H_{\text{process}}$ is the process heat produced by the same plant and the term in the denominator is the total fuel energy given to the cogeneration plant.

Between the two outputs of a cogeneration system, the value of electricity is higher than that of the process heat. This observation leads us to a simple conclusion: The larger electricity we produce for the same amount of process heat, the better the performance of the cogeneration system is. Hence, the ratio of electricity to the process heat of the cycle provides valuable information for the comparison of different cogeneration system designs. Mathematically power to heat ratio is expressed as

$$\text{PHR} = \frac{(\dot{W}_{\text{el}})_{\text{plant}}}{\Delta H_{\text{process}}} \quad (4.38)$$

Fuel utilization efficiency, which is also called the first law efficiency, has the following weakness: Energy cannot always be exported from a system in the form of work. However, the very foundation of the science of thermodynamics is based on the observation that energy and work are not entirely interchangeable. To remove the weakness of the first law efficiency, a new efficiency needs to be defined for the cogeneration system. This new definition, not only employs the first law of thermodynamics, but also the second law. To define the second law efficiency, the various outputs of the cogeneration system, namely the process heat and the electricity, are measured in terms of their capabilities to produce work. The amount of work that the input fuel can ultimately produce is also evaluated. The ratio of the

output to the input, measured in terms of exergy rate gives the second law efficiency (i.e., exergetic efficiency) as

$$\varepsilon_{\text{PLANT}} = \frac{(\dot{W}_{\text{el}})_{\text{plant}} + \Delta\dot{E}x_{\text{process}}}{\dot{E}x_{\text{fuel}}} \quad (4.39)$$

Where $\Delta\dot{E}x_{\text{process}}$ exergy of the process heat is produced and $\dot{E}x_{\text{fuel}}$ is the total fuel exergy given to the cogeneration plant.

4.5 Thermodynamic Analysis of Hydrogen Production Models

The minimum work needed for 1 kg hydrogen production by the water and hydrogen sulfide electrolysis processes can be calculated by the following equations,

$$w_{\text{rev,elect}} = \frac{\Delta G_{\text{elect,H}_2\text{O}}}{M_{\text{H}_2}} \text{ (kJ/kg)} \quad (4.40)$$

$$w_{\text{rev,elect}} = \frac{\Delta G_{\text{elect,H}_2\text{S}}}{M_{\text{H}_2}} \text{ (kJ/kg)} \quad (4.41)$$

Where $\Delta G_{\text{elect,H}_2\text{O}}$ and $\Delta G_{\text{elect,H}_2\text{S}}$ are the Gibbs free energy (kJ/kmol) of the water and hydrogen sulfide, respectively and M_{H_2} is the molar mass of hydrogen (kg/kmol).

Thus, the actual work demand can be calculated as

$$w_{\text{act,elect}} = \frac{w_{\text{rev,elect}}}{\eta_{\text{th}}} \text{ (kj/kg)} \quad (4.42)$$

Thermal efficiency of the electrolysis unit can be calculated as [123]

$$\eta_{\text{th}} = \frac{\Delta H}{\Delta G + \text{Losses}} = \frac{E_{\Delta H}}{E_{\text{cell}}} \quad (4.43)$$

where ΔH is the enthalpy change of water decomposition reaction as energy input. $E_{\Delta H}$ is the equilibrium voltage and E_{cell} is the cell voltage which is always between 1.8-2.0 V at the current density of 1000-300 Am⁻² for industry water electrolysis [123]. For the alkaline and PEM electrolysis Equation 4.43 can be rewritten in a simple form as,

$$\eta_{th} = \frac{1.48}{E_{cell}} \quad (4.44)$$

4.6 Conclusions

In this chapter, we provided the general formulations for mass, energy, and exergy analyses of energy systems as well as hydrogen production models and also the performance assessment parameters of a cogeneration system. These formulations will be used in thermodynamic analysis of subsystems of GASKI wastewater treatment plant, biogas engine powered cogeneration system and also developed hydrogen production models.

CHAPTER 5

THERMOECONOMIC ANALYSIS

5.1 Introduction

Thermoeconomics (i.e. exergoeconomics) is, in its widest possible sense, the science of natural resources saving that connects physics and economics by means of the second law of thermodynamics. It is the branch of engineering that combines exergy analysis and economic principles to provide system designer or operator with information not available through conventional energy analysis and economic evaluations but crucial to the design and operation of a cost-effective system [112].

Thermoeconomic analysis combines economic and thermodynamic analysis by applying the concept of cost, originally an economic property, to exergy. Most analysts agree that exergy is an adequate thermodynamic property to which we allocate cost because it accounts for the quality of energy [124,125]. The exergy balance accounts for the degradation of the exergy. The input exergy into a process will always be greater than the exergy output:

$$\textit{Exergy Input} - \textit{Exergy Output} = \textit{Irreversibilities} > 0$$

This expression shows that there are irreversibilities during a process. There is an implicit classification of the flows crossing the boundary of the system: the flows that are the production objective, the resources required to carry out the production and those that are residual. This information is not implicit in the second law and is the most important conceptual leap separating and at the same time uniting physics with economics. The following equation

$$\textit{Resources (F)} - \textit{Products (P)} = \textit{Residues (R)} + \textit{Irreversibilities (I)} > 0$$

is of outmost importance because it places “*purpose*” in the heart of thermodynamics. The concept of efficiency defined as

$$\text{Efficiency} = \text{Product} / \text{Resource}$$

is older than thermodynamics and measures the quality of a process. The desire to produce a certain product is external to the system, and must be defined beforehand. Once this has been done, the design of the system and its functional structure will fit the aim of using available resources (capital, raw material, man power). Every definition of efficiency demands a comparison of the product obtained with the resources needed to obtain it. Its inverse value is

$$\text{Unit Consumption} = \text{Resource} / \text{Product}$$

This expression is also a definition of the unit average cost when resources refer to the overall plant instead of individual processes. This concept is the key of thermoeconomics. A logical chain of concepts can be established (see Figure 5.1) which allows connecting physics with economics.

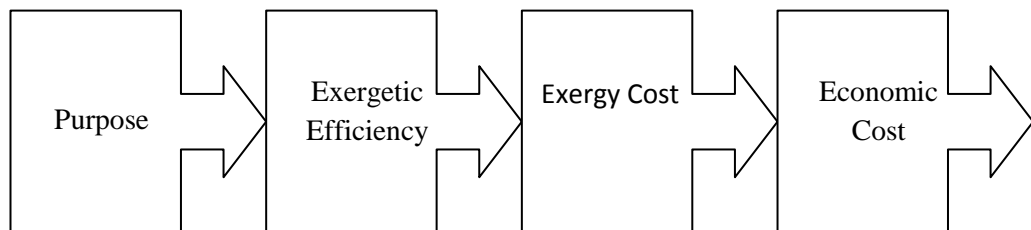


Figure 5.1: Logical chain of thermoeconomic concepts

Thus, thermoeconomics assesses the cost of consumed resources, money and system irreversibilities in terms of the overall production process. They help to point out how resources may be used more effectively in order to save them. Money costs express the economic effect of inefficiencies and are used to improve the cost effectiveness of production processes. Assessing the cost of the flow streams and processes in a plant helps to understand the process of cost formation, from the input resources to the final products.

5.2 Economic Analysis

Good cost estimation is a key factor in successfully completing a design project. Cost estimates should be made during all stages of design to provide a basis for decision making at each stage. Each company has its own preferred approach for conducting an economic analysis and calculating the cost of main products.

5.2.1 Time Value of Money

Decisions about capital expenditures generally require consideration of the earning power of money. A dollar in hand today is worth more than a dollar received one year from now because the dollar in hand now can be invested for the year. Thus, as the cost evaluation of a project requires comparisons of money transactions at various points in time, we need methods that will enable us to account for the value of money over time.

Future Value: If “ P ” dollars (present value) are deposited in an account earning “ i ” percent interest per time period and the interest is compounded at the end of each of “ n ” time periods, the account will grow to a future value, “ F ”

$$F = P(1 + i)^n \quad (5.1)$$

Interest is the compensation paid for the use of borrowed money. The interest rate is usually stated as a percentage; in equations, however, it is expressed as a decimal (e.g., 0.07 instead of 7%). Instead of the term interest rate, we will use the terms rate of return for an investment made and annual cost of money for borrowed capital [126].

Compounding Frequency: In engineering economy, the unit of time is usually taken as the year. If compounding occurs “ p ” times per year ($p \geq 1$) for a total number of “ n ” years ($n \geq 1$), and “ i ” is the annual rate of return, Equation 5.1 becomes

$$F = P \left(1 + \frac{i}{p} \right)^{np} \quad (5.2)$$

Here the product “ np ” is the number of periods and “ i/p ” is the rate of return per period. In this case, the annual rate of return “ i ” is known as the nominal rate of

return. The effective rate of return is the annual rate of return that would yield the same results if compounding were done once a year instead of “ p ” times per year. The effective rate of return, which is higher than the nominal rate of return, is obtained by eliminating F/P from Equations 5.1 and 5.2 as

$$i_{\text{eff}} = \left(1 + \frac{i}{p}\right)^p - 1 \quad (5.3)$$

If continuous compounding of money ($p \rightarrow \infty$) is used, the future value is calculated from

$$F = Pe^{in} \quad (5.4)$$

It is apparent that in the case of continuous compounding the effective rate of return becomes

$$i_{\text{eff}} = e^i - 1 \quad (5.5)$$

In Equations 5.4 and 5.5, “ i ” is the nominal annual rate of return and “ n ” is the total number of years. If the time is less than one year, the simple interest formula can be used to calculate the future value:

$$F = P(1 + ni_{\text{eff}}) \quad (5.6)$$

where “ n ” is now a fraction of a year and “ i_{eff} ” is the annual effective rate of return. Equations 5.2 and 5.4 can be expressed in the same form as Equation 5.1:

$$F = P(1 + i_{\text{eff}})^n \quad (5.7)$$

The term $(1 + i_{\text{eff}})^n$, referred to as the single – payment compound amount factor (SPCAF).

Unless otherwise indicated, the terms interest, rate of return, and annual cost of money refer to their effective values. Also, to simplify calculations, when the cost of money is calculated for one or more years plus a fractional part of a year, Equation 5.7 is applied with a non-integer exponent [127].

Present Value: When evaluating projects, we often need to know the present value of funds that we will spend or receive at some definite periods in the future. The present value (or present worth) of a future amount is the amount that if deposited at a given rate of return and compounded would yield the actual amount received at a future date. From Equation 5.7 we see that a given future amount F has a present value P :

$$P = F \frac{1}{(1 + i_{\text{eff}})^n} \quad (5.8)$$

The term $1/(1 + i_{\text{eff}})^n$, called the single – payment present – worth factor or the single – payment discount factor (SPDF). Since the difference between the future value and the present value is often called discount, in this case the term i_{eff} is called the effective discount rate.

Annuities: An annuity is a series of equal amount money transactions occurring at equal time intervals (periods). Usually, the time period corresponds to one year. Money transactions of this type can be used, for instance to pay off a debt or accumulate a desired amount of capital. Annuities are used in this study to calculate the levelized costs of the final product, fuel, and so forth. An annuity term is the time from the beginning of the first time interval to the end of the last time interval.

If A dollars are deposited at the end of each period in an account earning i_{eff} percent per period (effective rate of return per period), the future sum F (amount of the annuity or future value of the annuity) acquired at the end of the n^{th} period is

$$F = A \frac{(1 + i_{\text{eff}})^n - 1}{i_{\text{eff}}} \quad (5.9)$$

The term $\left[(1 + i_{\text{eff}})^n - 1 \right] / i_{\text{eff}}$ is called the uniform – series compound – amount factor (USCAF), and the reciprocal term of it is called the uniform – series sinking fund factor (USSFF). By combining Equations 5.8 and 5.9, we obtain

$$\frac{P}{A} = \frac{(1 + i_{eff})^n - 1}{i_{eff}(1 + i_{eff})^n} \quad (5.10)$$

The expression on the right side of this equation is called the uniform – series present – worth factor (USPWF). The reciprocal of this factor is the capital recovery factor (CRF):

$$CRF = \frac{A}{P} = \frac{i_{eff}(1 + i_{eff})^n}{(1 + i_{eff})^n - 1} \quad (5.11)$$

The CRF is used to determine the equal amounts A of a series of n money transactions, the present value of which is P .

Capitalized Cost: An asset (e.g., a piece of equipment) of fixed – capital cost C_{FC} will have a finite economic life of n years. The economic life (or book life) of an asset is the best estimate of the length of time that the asset can be used. The salvage value of an asset is the estimated economic worth of the asset at the end of its economic life.

Engineers often want to determine the total cost of an asset under conditions permitting perpetual replacement of the asset without considering inflation. The so-called capitalized cost C_K is defined in engineering economics as the first cost of the asset plus the present value of the indefinite annuity that corresponds to the perpetual replacement of the asset every n year. Assuming that the renewal cost of the asset remains constant (no inflation) at $C_{FC} - S$, and that both the useful life of the asset and the rate of return remain constant, the present value of the indefinite annuity is calculated from Equation 5.8 as [112]

$$(C_K - C_{FC}) = (C_K - S) / (1 + i_{eff})^n \quad (5.12)$$

That is, the capitalized cost C_K is in excess of the fixed – capital cost C_{FC} by an amount which, when compounded at an effective rate of return i_{eff} for n years, will have a future value of C_K minus the salvage value S of the asset. Solving the last equation for C_K , we obtain the capitalized cost as

$$C_K = \left[C_{FC} - \frac{S}{(1 + i_{\text{eff}})^n} \right] \left[\frac{(1 + i_{\text{eff}})^n}{(1 + i_{\text{eff}})^n - 1} \right] \quad (5.13)$$

The second factor in square brackets on the right side of the equation is called the capitalized – cost factor (CCF). The capitalized – cost factor is equal to the capital – recovery factor of an ordinary annuity (Equation 5.11) divided by the effective rate of return.

The use of the term capitalized cost is more meaningful in accounting than in engineering economics where the term merely characterizes a special case of present – value calculation referring to an infinite project life. However, because the term capitalized cost is encountered very often in the literature of both engineering economics and accounting, it is important to be familiar with the different meanings that may be attached to it [112,126].

5.2.2 Inflation, Escalation, and Levelization

Inflation: General price inflation is the rise in price levels associated with an increase in available currency and credit without a proportional increase in available goods and services of equal quality [112]. The consumer price index, which is tabulated by the government, is composite prices index that measures general inflation.

When inflation occurs, costs change every year. Cost changes in past years are considered using appropriate cost indices. For future years a varying annual inflation rate can be used, but such a rate always represents a prediction. For simplicity we assume a constant average annual inflation rate (r_i) for future years.

Escalation: The real escalation rate of expenditure is the annual rate of expenditure change caused by factors such as resource depletion, increased demand, and technological advances [128]. The first two factors lead to a positive real escalation rate whereas the third factor results in a negative rate. The real escalation rate (r_r) is independent and exclusive of inflation.

The nominal (or apparent) escalation rate (r_n) is the total annual rate of change in cost and includes the effects of both real escalation rate and inflation:

$$(1 + r_n) = (1 + r_r)(1 + r_i) \quad (5.14)$$

To simplify calculations, we assume that all costs except fuel costs and the values of by-products change annually with the constant average inflation rate r_i ; that is, we take $r_r = 0$. Since fuel costs are expected over a long period of future years to increase on the average faster than the predicted inflation rate, a positive real escalation rate for fuel costs may be appropriate for the economic analysis of thermal systems.

Levelization: Cost escalation applied to an expenditure (e.g., fuel costs or O&M costs) over n-year period results in a non-uniform cost schedule in which the expenditure at any year is equal to the previous year expenditure multiplied by $(1 + r_n)$, where r_n is the constant rate of change, the nominal escalation rate. The constant – escalation levelization factor (CELF) is used to express the relationship between the value of expenditure at the beginning of the first year (P_0) and an equivalent annuity (A), which is now called a levelized value. The levelization factor depends on both the effective annual cost – of – money rate, or discount rate i_{eff} and the nominal escalation rate r_n :

$$\frac{A}{P_0} = \text{CELF} = \frac{k(1 - k^n)}{1 - k} \text{CRF} \quad (5.15)$$

where

$$k = \frac{1 + r_n}{1 + i_{\text{eff}}} \quad (5.16)$$

and the variables CRF and r_n are determined from Equations 5.11 and 5.14, respectively. Equation 5.15 assumes that all transactions are made at the end of their respective years and (P_0) is the cost at the beginning of the first year.

The concept of levelization is general and is defined as the use of time – value – of – money arithmetic to convert a series of varying quantities to a financially equivalent

constant quantity (annuity) over a specified time interval. We will apply the concept of levelization to calculate the levelized fuel and O&M costs, the levelized total revenue requirements and the levelized total cost of the main product of a thermal system [112].

In the economic analysis of the thermal systems, the annual values of carrying charges, fuel costs, raw water costs, and operating and maintenance (O&M) expenses supplied to the overall system are the necessary input data. However these cost components may vary significantly within the economic life. Therefore, levelized annual values for all cost components should be used in the economic analysis and evaluations of the overall system. The levelized cost is given by [129]

$$A = \text{CRF} \sum_{m=1}^n P_m = \frac{i_{\text{eff}} (1 + i_{\text{eff}})^n}{(1 + i_{\text{eff}})^n - 1} \sum_{m=1}^n P_m \quad (5.17)$$

where

$$P_m = C_m \frac{1}{(1 + i_{\text{eff}})^m} \quad (5.18)$$

The cost rate associated with the capital and O&M expenses for the k th component of a thermal system is

$$\dot{Z}_k = \frac{\text{CC}_L}{\tau} \frac{\text{PEC}_k}{\sum_k \text{PEC}_k} + \frac{\text{OMC}_L}{\tau} \frac{\text{PEC}_k}{\sum_k \text{PEC}_k} \quad (5.19)$$

The first term in the nominator of the right hand side of the equation gives \dot{Z}_k^{CI} , and the second term gives \dot{Z}_k^{OM} . The levelized cost rate of the expenditure (fuel, raw water) supplied to the overall system is

$$\dot{C}_{\text{EX}} = \frac{\text{EXC}_L}{\tau} \quad (5.20)$$

5.2.3 Time Assumptions

In an economic analysis, all available cost numbers (e.g., land costs, total plant facilities investment, other outlays, O&M costs, fuel costs, and by-product values) must be escalated to the date they are expended. In the evaluation of economic analysis, the following assumptions are made:

- Land costs incur at the beginning of the first year of the design and construction period.
- The total capital investment is allocated to the individual years of the design and construction period. The expenditures for each year are incurred in the middle of the year.
- The startup costs are expended in the middle of the last year of design and construction.
- The working capital and the costs of licensing, research, and development are escalated to the end of the last year of design and construction.
- The allowance for funds used during construction (AFUDC) is paid annually during the design and construction period; the sum of AFUDC is calculated at the end of last year of this period.
- The costs of fuel, operation, and maintenance are incurred in the middle of each year of the system economic life.
- The revenues from the sale of products are received in the middle of each year of the system economic life.

For economic analysis of a thermal system, system engineer or plant operator must register the date of reference for each cost number and specify (a) the beginning and length of the design and construction period, (b) the anticipated economic life, and (c) the life for tax purposes. The beginning of commercial operation (beginning of economic-life period) is assumed to coincide with the end of the design and construction period [130].

5.2.4 Depreciation

Depreciation reflects the fact that the value of an asset tends to decrease with age (or use) due to physical deterioration, technological advances, and other factors that

ultimately will lead to the retirement of the asset. In addition, depreciation is a mechanism for repaying the original amount obtained from debt holders if the debt is to be retired. Finally, depreciation is an important accounting concept serving to reduce taxes during plant operation. In that respect, depreciation is not strictly related to the physical or economic lifetime of an asset. The asset life used for tax purposes (as determined by statute) could be shorter than the asset's anticipated economic life.

There are many methods for depreciating the value of an asset. Some of these methods – straight line, sum of the years digits, and declining balance methods – give no consideration to interest costs, whereas others (sinking fund and present worth methods) take into account the interest on investment. Table 5.1 summarizes the mathematical relationships that can be used to calculate the depreciation allocation at the end of a year of the property life, and the cumulative depreciation allocation at the end of a year. The difference between the original cost of a property and the cumulative depreciation at the end of a year is defined as the book value at the end of that year.

5.2.5 Financing and Required Returns on Capital

The money to cover the total capital requirement of an investment can come through the following sources:

- Borrowing capital, for instance by selling bonds (debt financing)
- The sale of common and preferred stock (equity financing)
- Existing fund of the company (self – financing)
- A combination of these

The average cost of money in a project depends on the fractions of the total capital requirement financed through debt, preferred stock, and common stock and on the required return on each type of financing.

Table 5.1 Summary of selected tax depreciation methods [112]

Method	Depreciation Allocation at the End of Year z (DP_z)	Cumulative Depreciation Allocation at the End of Year z $CDP_z = \sum_{i=1}^z DP_i$
Straight line	$\frac{C_0 - S}{n}$	$(C_0 - S) \frac{z}{n}$
Sum of the years digits	$(C_0 - S) \left[\frac{2(n+1-z)}{n(n+1)} \right]$	$(C_0 - S) \left[\frac{z(2n+1-z)}{n(n+1)} \right]$
Double declining balance ($n \geq 3$)	$C_0 \left(\frac{2}{n} \right) \left(\frac{n-2}{n} \right)^{z-1}$	$C_0 \left[1 - \left(\frac{n-2}{n} \right)^z \right]$
125 % declining balance	$C_0 \left(\frac{1.25}{n} \right) \left(\frac{n-1.25}{n} \right)^{z-1}$	$C_0 \left[1 - \left(\frac{n-1.25}{n} \right)^z \right]$
Sinking fund	$(C_0 - S) \left[\frac{i(1+i)^{z-1}}{(1+i)^n - 1} \right]$	$(C_0 - S) \left[\frac{(1+i)^z - 1}{(1+i)^n - 1} \right]$

C_0 = total depreciable investment (TDI) at the beginning of the economic life period (dollars)

S = salvage value of the property at the end of the (tax or economic) life considered in the depreciation (dollars)

n = tax life or economic life considered in the depreciation calculations (years)

i = interest rate (decimal ratio)

z = attained age of the property (years)

The average rate of the cost of money (discount rate) calculated in this way is the before – tax rate. The after – tax discount rate (i_{at}) reflects the effect of the deductibility of debt return on the government income tax calculation for the company, and is calculated from

$$i_{at} = i - f_d i_d t \quad (5.21)$$

where i is the before – tax discount rate, f_d and i_d represent the fraction of the total capital requirement financed through debt, and the corresponding rate of return, respectively, and t is the total income tax rate [112].

5.2.6 Fuel, Operating, and Maintenance Costs

Fuel costs are usually part of the operating and maintenance costs. However, because of the importance of fuel costs in cogeneration systems fuel costs are considered

separately from the O&M costs. The O&M costs can be divided into fixed and variable costs. The fixed O&M costs are composed of costs for operating, labor, maintenance labor, maintenance materials, overhead, administration and support, distribution and marketing, research and development, and so forth. The variable operating costs depend on the average annual system capacity factor, which determines the equivalent average number of hours of system operation per year at full load.

The fuel costs and the variable operating costs can be easily calculated from the flow diagrams. Once we know the flow of a raw material stream or of a utility, we simply multiply the flow by its unit cost and by the average total time of operation per year to obtain the contribution of the flow being considered to the total annual costs.

5.2.7 Taxes and Insurance

Income taxes are calculated by multiplying the income tax rate by the taxable income, which is the difference between total revenue and all tax-deductible expenditures. Income tax rates have varied significantly in recent years [112].

Tax deductible expenditures include fuel costs, O&M charges, return on debt, and investment cost recovery (depreciation calculated for tax purposes). In any year of the economic life of a system, the difference between the income taxes actually paid and the income taxes that would have been paid if a straight-line depreciation had been used is called the deferred income tax.

Depending on the location, the annual property taxes are usually between 1% and 4% of the plant facilities investment [126]. The annual insurance costs are typically between 0.5% and 1.5% of the plant facilities investment. Design engineers can contribute to a reduction in insurance costs by understanding the different types of insurance available, the legal responsibilities of a company with regard to accidents and emergencies, and other factors that must be considered in obtaining adequate insurance.

5.3 Thermo-economic Analysis

Cost accounting in a company is concerned primarily with (a) determining the actual cost of products or services, (b) providing a rational basis for pricing goods and services, (c) providing a means for allocating and controlling expenditures, and (d) providing information on which operating decisions may be based and evaluated [112]. This frequently calls for the use of cost balances. In a conventional economic analysis, a cost balance is usually formulated the overall system operating at steady state

$$\dot{C}_{P,TOT} = \dot{C}_{F,TOT} + \dot{Z}_{TOT}^{CI} + \dot{Z}_{TOT}^{OM} \quad (5.22)$$

The cost balance expresses that the cost rate associated with the product of the system \dot{C}_p equals the total rate of expenditures made to generate the product, namely the fuel cost rate \dot{C}_F and the cost rates associated with capital investment \dot{Z}^{CI} and operating and maintenance \dot{Z}^{OM} . When referring to a single stream associated with a fuel or product, the expression fuel stream or product stream is used. The rates \dot{Z}^{CI} and \dot{Z}^{OM} are calculated by dividing the annual contributions of capital investment and the annual operating and maintenance (O&M) costs, respectively, by the number of time units (usually hours or seconds) of system operation per year. The sum of these two variables is denoted by \dot{Z}

$$\dot{Z} = \dot{Z}^{CI} + \dot{Z}^{OM} \quad (5.23)$$

5.3.1 Exergy Costing

Cost may be defined as the amount of resources needed to obtain a functional product. On one hand, resources take a general meaning. On the other hand, cost is associated with the purpose of production. It is associated neither with price nor with the resources that could be saved if the production process were less efficient or more conventional one [131]. Cost is an emergent property. It cannot be measured as a physical magnitude of a flow stream as temperature or pressure; it depends on the system structure and appears as an outcome of the system analysis. Therefore, it needs precise rules for calculating it from physical data. Cost is a property that cannot be found in the product itself [112,132].

In thermoeconomics, the words history, degradation, exergy, quality, cost, resource, consumption, purpose and causality are related to one another. In the cost formation process, it is essential to analytically search for the locations and physical mechanisms that make up a specific productive flow [133]. The resources are used to provide physico-chemical qualities to the intermediate products until a finished product is obtained. The main problem to be solved using exergy is how to measure and homogenize the accounting of these qualities.

Since exergy measures the true thermodynamic value of the effects associated with heat, work and mass interactions through systems, it is meaningful to use exergy as a basis for assigning costs in thermal systems. Indeed, thermoeconomics rests on the notion that exergy is the only rational basis for assigning costs to the interactions that a thermal system experiences with its surroundings and to the sources of inefficiencies within it. This approach is referred as “exergy costing”.

In exergy costing a cost is associated with each exergy stream. Thus for entering and exiting streams of matter with associated rates of exergy transfer, power and the exergy transfer rate associated with heat transfer may be written, respectively as

$$\dot{C}_i = c_i \dot{E}x_i = c_i (\dot{m}_i \psi_i) \quad (5.24)$$

$$\dot{C}_e = c_e \dot{E}x_e = c_e (\dot{m}_e \psi_e) \quad (5.25)$$

$$\dot{C}_w = c_w \dot{W} \quad (5.26)$$

$$\dot{C}_q = c_q \dot{E}x_q \quad (5.27)$$

where c_i , c_e , c_w , and c_q denote average costs per unit of exergy of material stream at inlet and exit, power and heat respectively and \dot{C}_i , \dot{C}_e , \dot{C}_w and \dot{C}_q are the corresponding cost rates, $\dot{E}x_i$ and $\dot{E}x_e$ are exergy transfers for entering and exiting streams of matter, \dot{W} is power, and $\dot{E}x_q$ is the exergy transfer rate associated with heat transfer. Accordingly, for a component receiving heat transfer and generating power, we may write [112,134,135]

$$\sum_e (c_e \dot{E}x_e)_k + c_{w,k} \dot{W}_k = c_{q,k} \dot{E}x_{q,k} + \sum_i (c_i \dot{E}x_i)_k + \dot{Z}_k \quad (5.28)$$

This equation simply states that the total cost of the exiting exergy streams equals the total expenditure to obtain them: the cost of the entering exergy streams plus the capital and other costs. Note that when a component receives power (as in a compressor or a pump) the second term of the left hand side would move with its positive sign to the right side of this expression. Cost balances are generally written so that all terms are positive.

The exergy rates exiting and entering the k^{th} component are calculated using exergy relations in Chapter 4. The term \dot{Z}_k may be obtained by first calculating the capital investment and operating and maintenance (O&M) costs associated with the k^{th} component and then computing the levelized values of these costs per unit of time (year, hour, or second) of system operation. Based on these costs the general equation for the cost rate (\dot{Z}_i) in \$/s associated with capital investment and the maintenance costs for the k^{th} component is

$$\dot{Z}_k = \frac{Z_k (CRF) \varphi}{(N \times 3600)} \quad (5.29)$$

where Z_k is the purchase cost of the k^{th} component (\$), CRF is the annual capital recovery factor; N is the number of hours of plant operation per year, and φ is the maintenance factor.

When two or more products, by-products and residues are produced simultaneously, how costs can be allocated? Indeed, the main problem of allocating costs has been to find a function that adequately characterizes every one of the internal flows in a system and distributes cost proportionally. This function needs to be universal, sensitive and additive. That is, it needs to have an objective value for every possible material manifestations and it needs to vary when these manifestations do so and each internal flow property needs to be represented additively. There is a wide international consensus that the best function, at least for energy systems, is exergy, which can contain in its own analytical structure of the flow history [132,136].

5.3.2 Aggregation Level for Applying Exergy Costing

For calculating approximate average costs, we can stop our analysis by disaggregating our system at not very detailed level since the level at which the cost balances are formulated affects the results of a thermoeconomic analysis. Cumulative exergy consumption analysis does not go into process details but focuses on the overall exergy consumption.

Accordingly, in thermal design, it is recommended that the lowest possible aggregation level be used [112,133,136]. This level is usually represented by the individual components (compressors, turbines, heat exchangers etc.). Even in cases where the available information is insufficient for applying exergy costing at the component level, it is generally preferable to make appropriate assumptions that enable exergy costing to be applied at the component level than to consider only groups of components [112].

5.4 Thermoeconomic Variables for Component Evaluation

The following quantities, known as thermoeconomic variables, play a central role in the thermoeconomic evaluation and optimization of thermal systems:

- the average unit cost of fuel, $c_{F,k}$ (i.e. $c_{F,k} = \frac{\dot{C}_{F,k}}{\dot{E}x_{F,k}}$)
- the average unit cost of product, $c_{P,k}$ (i.e. $c_{P,k} = \frac{\dot{C}_{P,k}}{\dot{E}x_{P,k}}$)
- the cost rate of exergy destruction, $\dot{C}_{D,k}$
- the relative cost difference, r_k
- the exergoeconomic factor, f_k

In this chapter, three of these variables are discussed: $\dot{C}_{D,k}$, r_k , and f_k while all five thermoeconomic variables are applied to the thermoeconomic analysis and evaluation of the GASKI WWTP and biogas fueled gas engine cogeneration system (see Chapter 9).

5.4.1 Cost of Exergy Destruction

In the cost balance formulas (i.e. Equations 5.22 and 5.28), there is no cost term directly associated with exergy destruction. Accordingly, the cost associated with the exergy destruction in a component or process is a hidden cost, but very important one, that can be revealed only through thermoeconomic analysis. Using the specific exergetic costs associated with fuel, product, and exergy loss for the k th component, the cost rate balance can be written as

$$c_{P,k} \dot{E}x_{P,k} = c_{F,k} \dot{E}x_{F,k} - \dot{C}_{L,k} + \dot{Z}_k \quad (5.30)$$

Using Equation 4.20 from Chapter 4, in order to eliminate $\dot{E}x_{F,k}$, we obtain

$$c_{P,k} \dot{E}x_{P,k} = c_{F,k} \dot{E}x_{P,k} + (c_{F,k} \dot{E}x_{L,k} - \dot{C}_{L,k}) + \dot{Z}_k + c_{F,k} \dot{E}x_{D,k} \quad (5.31)$$

or to eliminate $\dot{E}x_{P,k}$, we obtain

$$c_{P,k} \dot{E}x_{P,k} = c_{F,k} \dot{E}x_{F,k} + (c_{P,k} \dot{E}x_{L,k} - \dot{C}_{L,k}) + \dot{Z}_k + c_{P,k} \dot{E}x_{D,k} \quad (5.32)$$

In both Equations 5.31 and 5.32, the last term on the right hand side involves the rate of exergy destruction. Assuming that the product, $\dot{E}x_{P,k}$ is fixed and that the unit cost of fuel, $c_{F,k}$ of the k th component is independent of the exergy destruction, the cost of exergy destruction can be expressed as

$$\dot{C}_{D,k} = c_{F,k} \dot{E}x_{D,k} \quad (5.33)$$

As the fuel rate $\dot{E}x_{F,k}$ must account for the fixed product rate $\dot{E}x_{P,k}$, and the rate of exergy destruction rate $\dot{E}x_{D,k}$, we may interpret $\dot{C}_{D,k}$ in Equation 5.33 as the cost rate of the additional fuel that must be supplied to the k th component.

Alternatively, assuming that the fuel $\dot{E}x_{F,k}$ is fixed and that the unit cost of product $c_{P,k}$ of the k th component is independent of exergy destruction, we can define the cost of exergy destruction by the last term of Equation 5.32 as

$$\dot{C}_{D,k} = c_{P,k} \dot{E}x_{D,k} \quad (5.34)$$

When exergy of fuel $\dot{E}x_{F,k}$ is fixed, the exergy destruction $\dot{E}x_{D,k}$ reduces to the product of the k th component $\dot{E}x_{P,k}$, and therefore Equation 5.34 can be interpreted as the monetary loss associated with the loss of product.

5.4.2 Relative Cost Difference

The relative cost difference r_k for the k th component is defined as

$$r_k = \frac{c_{P,k} - c_{F,k}}{c_{F,k}} \quad (5.35)$$

The variable expresses the relative increase in the average cost per exergy unit between fuel and product of the component. The relative cost difference is a useful variable for evaluating and optimizing a system component. In an iterative cost optimization of a system, if the cost of fuel of a major component changes from one iteration to the next, the objective of the cost optimization of the component should be to minimize the relative cost difference instead of minimizing the cost per exergy unit of the product with this component.

If Equation 5.35 is rewritten for revealing the real cost sources associated with the k th component, using Equations 5.23 and 5.31 and taking $\dot{C}_{L,k} = 0$, we obtain

$$r_k = \frac{c_{F,k} (\dot{E}x_{D,k} + \dot{E}x_{L,k}) + (\dot{Z}_k^{CI} + \dot{Z}_k^{OM})}{c_{F,k} \dot{E}x_{P,k}} \quad (5.36)$$

Using the exergetic efficiency of the k th component, and using Equation 4.26 from chapter 4, Equation 5.36 may be written as

$$r_k = \frac{1 - \varepsilon_k}{\varepsilon_k} + \frac{\dot{Z}_k^{CI} + \dot{Z}_k^{OM}}{c_{F,k} \dot{E}x_{P,k}} \quad (5.37)$$

5.4.3 Exergoeconomic Factor

As Equations 5.36 and 5.37 indicate, the cost sources in a component may be grouped into two categories. The first consists of non-exergy related costs (capital investment, and operating and maintenance expenses), while the second category consists of exergy destruction and exergy loss. In evaluating the performance of a component, we want to know the relative significance of each category. This is provided by the exergoeconomic factor, f_k defined for the k th component as

$$f_k = \frac{\dot{Z}_k}{\dot{Z}_k + c_{F,k}(\dot{E}_{D,k} + \dot{E}_{L,k})} \quad (5.38)$$

The total cost rate causing the increase in the unit cost from fuel to product is given by the denominator in Equation 5.38. Accordingly, the exergoeconomic factor expresses as a ratio the contribution of the non-exergy related cost to total cost increase. A low value of the exergoeconomic factor calculated for a major component suggests that cost savings in the entire system might be achieved by improving the component efficiency (reducing the exergy destruction) even if the capital investment for this component will increase. On the other hand, a high value of this factor suggests a decrease in the investment costs of this component at the expense of its exergetic efficiency.

5.5 The Specific Exergy Costing (SPECOC) Method

The costs associated with each material and energy stream in a system are calculated with the aid of (a) cost balances written for each system component, and (b) auxiliary costing equations. Assuming that the costs of the exergy streams entering a component known, a cost balance is not sufficient to determine the costs of the exiting exergy streams when the number of exiting streams is larger than one. In this case, auxiliary costing equations must be formulated for the component being considered, the number of these equations being equal to the number of exiting streams minus one [126,134,136].

Different approaches for formulating efficiencies and auxiliary costing equations have been suggested in the literature. These approaches can be divided into two groups: (1) The exergoeconomic accounting methods [112-124,134] aim at the

costing of product streams, the evaluation of components and systems, and the iterative optimization of energy systems; (2) The Lagrangian-based approaches [137-141] aim in optimizing the overall system and the calculation of marginal costs. In literature only total exergy values were used and the auxiliary costing equations were formulated explicitly by using assumptions derived from experience, postulates, or the purpose of the system being analyzed.

A different approach, based on the LIFO (Last In First Out) accounting principle, was presented in refs. [142,143]. In this approach, fuels, products, and costs are defined systematically registering exergy and cost additions and removals from each material and energy stream. In this way, “local average costs” are obtained since the cost per exergy unit of the exergy used in a component is evaluated at the cost at which the removed exergy units were supplied by upstream components. An automatic criterion to generate the auxiliary costing equations based on this principle can be achieved by using computer implementation and an algebraic formulation [144]. In this study, the name SPECO, specific exergy costing method, was given to this approach because of the need of using specific exergies and costs for registering all additions and removals of exergy and cost.

The basic principles of the SPECO approach were then directly applied to exergy streams instead of material and energy streams [136]. It was demonstrated that these principles are sufficient for systematically defining fuel and product of the components and for formulating the auxiliary costing equations used to calculate either average costs (AVCO approach) or local average costs (LIFO approach).

Lagrangian-based approaches, on the other side, employ mathematical techniques to arrive at costs. It can be easily demonstrated that the same cost balances and auxiliary equations used in accounting methods can be obtained through partial derivatives in the Lagrangian-based approaches.

The SPECO method consists of the following three steps:

Step 1- identification of exergy streams: Initially, a decision must be made with respect to whether the analysis of the components should be conducted using total exergy or separate forms of the total exergy of a material stream (e.g. thermal,

mechanical, and chemical exergies). Considering separate exergy forms improves the accuracy of the results. However, this improvement is often marginal and not necessary for extracting the main conclusions from the exergoeconomic evaluation.

Step 2- definition of fuel and product: The product is defined to be equal to the sum of all the exergy values to be considered at the outlet (including the exergy of energy streams generated in the component) plus all the exergy increases between inlet and outlet (i.e. the exergy additions to the respective material streams) that are in accord with the purpose of the component. Similarly, the fuel is defined to be equal to all the exergy values to be considered at the inlet (including the exergy streams supplied to the component) plus all the exergy decreases between inlet and outlet (i.e. the exergy removals from the respective material streams) minus all the exergy increases (between inlet and outlet) that are not in accord with the purpose of the component.

Step 3- cost equations: Exergoeconomics rests on the notion that exergy is the only rational basis for assigning costs to the interactions a thermal system experiences with its surroundings and to the sources of inefficiencies within it [112]. All the equations given in section 5.3 are used throughout the analysis at this step.

5.5.1 The \dot{F} and \dot{P} Principles

The \dot{F} (fuel) principle refers to the removal of exergy from an exergy stream within the component being considered, when for this stream, the exergy difference between inlet and outlet is considered in the definition of the fuel. The \dot{F} principle states that the total cost associated with this removal of exergy must be equal to the cost at which the removed exergy has supplied to the same stream in the upstream components.

The \dot{P} (product) principle refers to the supply of exergy to an exergy stream within the component being considered. The \dot{P} principle states that each exergy unit is supplied to any stream associated with the products at the same average cost c_p . This cost is calculated from the cost balance and the equations obtained by \dot{F} principle. Aggregation level influences accuracy of the results, so it should be set at a lower level [112].

5.6 Conclusions

In this chapter, we provided general principles, terminology, and formulation of thermoeconomic analysis, which is also called exergoeconomic analysis. The procedure and formulation are applicable to all energy systems including GASKI WWTP and biogas fueled gas engine powered cogeneration systems. Detailed formulations considering the operation of the entire systems and components will be provided in Chapter 9.

CHAPTER 6

THERMOECONOMIC OPTIMIZATION

6.1 Introduction

The first step in the definition of optimization problem is to define clearly the boundaries of the system to be optimized. All the subsystems that significantly affect the performance of the system under study should be included in the optimization problem. The selection of criteria on the basis of which the system design will be evaluated and optimized is the key element in formulating an optimization problem. Optimization criteria may be *economic* (total capital investment, total annual levelized costs, annual levelized net profit), *technological* (thermodynamic efficiency, production time, production rate, fuel consumption) and *environmental* (rates of emitted pollutants). An optimized design is characterized by a minimum or maximum value, as appropriate for each selected criterion [112,145].

Another essential element in formulating the optimization problem is the selection of the *design variables* that adequately characterize the possible design options. In selecting these variables, it is necessary to include all the important variables that affect the efficiency and the cost effectiveness of the system. Each component and the system as a whole are defined by a set of quantities. Some of them are fixed by external conditions (e.g. environmental pressure and temperature, fuel price) and are called parameters. The remaining are variables, i.e. their value may change during the optimization procedure. Those variables, the values of which do not depend on another variables or parameters, are called *independent* or *design* variables. The rest can be determined by the solution of a set of *equality* constraints and they are called *dependent* variables.

The mathematical model for an optimization problem consists of:

- An objective function to be minimized
- A set of equality constraints
- A set of inequality constraints

Thermoeconomic optimization methods use a primary optimization performance measure: minimize the total levelized cost of the system products that includes the cost of external fuel resources, capital investment and maintenance cost. Also multicriteria optimization and environmental constraints can be considered.

6.2 Thermoeconomic Optimization Approaches

The balance between thermodynamic measures and capital expenditures is an economic feature, which applies to the thermal system as a whole and to each component individually. The costs of resources usually vary to the opposite direction of the cost of equipment with respect to the design variables. An improvement on the structure or the efficiency of the equipment implies a reduction of the resources consumption but an increase of the capital investment.

The *equality constraints* are provided by appropriate thermodynamic and cost models as well as appropriate boundary conditions. These models must include the flow rate and energy balances for each component, relations associated with the engineering design, such as the local efficiencies of the components. The model adopted by thermoeconomic optimization relates the input (fuels) of each component with its outputs and design variables.

The model can also contain *inequality constraints* that specify the allowable operating ranges, the maximum and minimum performance requirements, and bounds on the availability of resources. When optimum is reached with only equality constraints, we obtain the shadow costs, one for each independent variable. If an inequality constraint is active in the optimum, the cost becomes an opportunity cost for the constrained variable.

There are cost optimization procedures which make no use of the exergy concept. So cost-effectiveness of every change carried out on a plant component must be

assessed in terms of the overall system parameters, e.g. its effect on the consumption of fuel resources. This makes optimization very complex and computer time consuming. With thermoeconomic optimization these difficulties may be overcome. For example, with proper thermoeconomic analysis and under certain conditions, the decomposition is applicable, which facilitates the solution of the problem, because it allows the optimization problem of the whole system to be decomposed into a set of optimization problems of subsystems or components, which are of smaller dimension (i.e. they have fewer independent variables) and can be solved more easily. There was basically, at the beginning, two different thermoeconomic approaches: the *structural* method that use the local unit cost of the irreversibilities and the *autonomous* method introduced by Evans and El-Sayed [146] in 1970 that is the starting point of other state-of-the-art techniques.

There are several approaches to thermoeconomic optimization that were presented in a set of articles in 1993, as a result of the project CGAM [112,117,129,142,143]. *The Exergoeconomic Optimization Approach*, proposed by Tsatsaronis [142] uses an iterative design improvement procedure that does not aim at calculating the global optimum of a predetermined objective function, as the conventional optimization methods do, but tries to find a “good” solution for the overall system design. The basic idea lies in a commonly accepted concept from the cost view point: at constant capacity for a well designed component, group of components, or total system, a higher investment cost should correspond to a more efficient component and vice versa.

The Functional Analysis proposed by Frangopoulos [137-139] and *the Engineering Functional Analysis* proposed by von Spakovsky [141,145] used the method of the Lagrange multipliers and decomposition procedures. Valero and coworkers [168], present a similar approach, but propose to use the unit average exergy costs instead of the Lagrange multipliers.

El- Sayed [146] proposed also, in order to avoid problems with the isolation of the decision variables to divide the decision variables into local variables and global variables, in general the number of global variables is much smaller than the local variables, iterate to find the local optimum of each component respect its local variables and the global optimum respect to the global variables.

The decomposition strategy is based on the *Principle of Thermo-economic Isolation* (TI) introduced by R. Evans in 1980 [141]: A component of a thermal system is thermo-economically isolated from the rest of the system if its production and the unit cost of the resources are known quantities and independent from the rest of the component variables. It is an ideal condition which cannot be fully achieved for most of real systems, but the more the TI conditions are fulfilled the fewer iterations are required to achieve the optimal solution for the whole system. Therefore the thermo-economic model of the system is subdivided or decomposed into subgroups. Each subgroup is optimized in turn, according to a sequential process, iterating around the system until the system's internal economy converges, within prescribed tolerances, to a single set of values. Decomposition may only approach the global optimum since the degree of thermo-economic isolation of the independent variables, the choice of the subgroups and their functions, and the nature of the dependent variables greatly affects how close the approach will be. Nonetheless, the advantages of this strategy facilitates the optimal design of individual units in highly interdependent complex systems, and let the designers to concentrate their efforts on designing the variables of single components, while resting assured that these efforts improve the overall system.

6.3 Cost Optimal Exergetic Efficiency for An Isolated System Component

Several mathematical approaches may be applied to optimize the design of a single system component in isolation from the remaining system components. Some of these approaches can be found in literature [145,147,148]. In this study, the thermo-economic approach that illustrates clearly the connections between thermodynamics and economics are used in the analysis and evaluations of GASKI WWTP and biogas engine powered cogeneration system. With this approach, the cost optimal exergetic efficiency can be obtained for a component isolated from the remaining system components.

The thermo-economic optimization approach is based on following assumptions which are expressed analytically:

Assumption A1: The exergy flow rate of the product $\dot{E}x_{P,k}$, and the unit cost of the fuel $c_{F,k}$ remain constant for the k th component to be optimized:

$$\dot{E}x_{P,k} = \text{constant} \quad (6.1)$$

$$c_{F,k} = \text{constant} \quad (6.2)$$

These equations, which represent constraints of the optimization problem, define mathematically what is meant by isolation in Chapter 9.

Assumption A2: For every system component, we expect the investment costs to increase with increasing capacity and increasing exergetic efficiency of the component. Here, we assume that for the k th component the total capital investment TCI_k can be represented at least approximately by the following relation [143]:

$$\text{TCI}_k = B_k \left(\frac{\varepsilon_k}{1 - \varepsilon_k} \right)^{n_k} \dot{E}x_{P,k}^{m_k} \quad (6.3)$$

where the term $\left(\frac{\varepsilon_k}{1 - \varepsilon_k} \right)^{n_k}$ expresses the effect of efficiency (i.e. thermodynamic performance), while the term $\dot{E}x_{P,k}^{m_k}$ expresses the effect of capacity (i.e. component size) on the value of TCI_k . The parameter B_k is given as constant in the cost equations of the k th component, n_k and m_k are expressed as efficiency and capacity exponents in cost equations respectively. Within a certain range of design options, these three terms are constant [112].

Assumption A3: Usually a part of the operating and maintenance (O&M) costs depends on the total investment costs and another part on the actual production rate. The annual levelized operating and maintenance costs attributed to the k th component are represented as [147]

$$Z_k^{\text{OM}} = \gamma_k (\text{TCI}_k) + \omega_k \tau \dot{E}x_{P,k} + R_k \quad (6.4)$$

In Equation 6.4, γ_k is a coefficient that accounts for the part of the fixed O&M costs depending on the total capital investment associated with the k th component. In large

conventional electric power plants, an average value for the coefficient γ_k of $0.015 \times \text{CELf}$ may be assumed for all plant components where CELf is the constant-escalation levelization factor. For relatively small thermal systems, the coefficient γ_k can be taken as high as 0.10 [143]. ω_k is a constant that accounts for the variable O&M costs associated with the k th component and denotes the O&M cost per unit of product exergy, τ is the average annual time of plant operation at the nominal load; and R_k includes all the remaining O&M costs that are independent of the total capital investment and the exergy of the product.

Assumption A4: The economic analysis of the system being considered is simplified by neglecting the effects of financing, inflation, taxes, insurance, and construction time and by considering the startup costs, working capital, and the costs of licensing, research, and development together with the total capital investment. The annual carrying charge associated with the k th component is then obtained by multiplying the total capital investment for this component TCI_k by the capital recovery factor, β :

$$Z_k^{\text{CI}} = \beta(\text{TCI}_k) \quad (6.5)$$

Assumptions A1 through A4 (Equations 6.1 through 6.5) form the “cost model”. The total annual levelized costs excluding fuel costs associated with the k th component are obtained by combining Equations 6.4 and 6.5

$$Z_k = Z_k^{\text{CI}} + Z_k^{\text{OM}} = (\beta + \gamma_k)(\text{TCI}_k) + \omega_k \tau \dot{E}x_{P,k} \quad (6.6)$$

The corresponding cost rate \dot{Z}_k is obtained by dividing Equation 6.6 by τ ,

$$\dot{Z}_k = \frac{\beta + \gamma_k}{\tau} (\text{TCI}_k) + \omega_k \dot{E}x_{P,k} + \frac{R_k}{\tau} \quad (6.7)$$

From Equation 6.3,

$$\dot{Z}_k = \frac{(\beta + \gamma_k)B_k}{\tau} \left(\frac{\varepsilon_k}{1 - \varepsilon_k} \right)^{n_k} \dot{E}x_{P,k}^{m_k} + \omega_k \dot{E}x_{P,k} + \frac{R_k}{\tau} \quad (6.8)$$

The objective function to be minimized expresses the cost per exergy unit of the product for the k th component. Accordingly, using Equations 5.31 from Chapter 5 and taking $\dot{C}_{L,k} = 0$, we can write

$$\text{Minimize } c_{P,k} = \frac{c_{F,k} \dot{E}x_{F,k} + \dot{Z}_k}{\dot{E}x_{P,k}} \quad (6.9)$$

Using Equation 4.27 from Chapter 4, and Equation 6.8, this objective function may be expressed as

$$\text{Minimize } c_{P,k} = \frac{c_{F,k}}{\dot{E}x_{P,k}} + \frac{(\beta + \gamma_k) B_k}{\tau \dot{E}x_{P,k}^{1-m_k}} \left(\frac{\varepsilon_k}{1 - \varepsilon_k} \right)^{n_k} + \omega_k + \frac{R_k}{\tau \dot{E}x_{P,k}} \quad (6.10)$$

The values of parameters β , γ_k , B_k , τ , ω_k , and R_k remain constant during optimization process, and so $c_{P,k}$ varies only with ε_k [112,143,147]. Thus the optimization problem reduces to the minimization of Equation 6.10 subject to the constraints expressed by Equations 6.1 and 6.2. The minimum cost per exergy unit of product is obtained by differentiating Equation 6.10 and setting the derivative to zero:

$$\frac{dc_{P,k}}{d\varepsilon_k} = 0 \quad (6.11)$$

The resulting cost-optimal exergetic efficiency [147] is

$$\varepsilon_k^{\text{OPT}} = \frac{1}{(1 + F_k)} \quad (6.12)$$

where

$$F_k = \left(\frac{(\beta + \gamma_k) B_k n_k}{\tau c_{F,k} \dot{E}x_{P,k}^{1-m_k}} \right)^{1/(n_k+1)} \quad (6.13)$$

Equations 6.12 and 6.13 show that the cost-optimal exergetic efficiency increases with increasing cost per exergy unit of fuel, $c_{F,k}$, increasing annual number of hours

of system operation τ , decreasing capital recovery factor β , decreasing fixed O&M cost factor γ_k , and decreasing cost exponent n_k . Equation 6.12 may be rewritten as

$$F_k = \frac{1 - \varepsilon_k^{\text{OPT}}}{\varepsilon_k^{\text{OPT}}} \quad (6.14)$$

or using Equation 4.27 from Chapter 4,

$$F_k = \left(\frac{\dot{E}x_{D,k} + \dot{E}x_{L,k}}{\dot{E}x_{P,k}} \right)^{\text{OPT}} \quad (6.15)$$

Since the exergy rate of the product is assumed constant during optimization, the cost-optimal value of the sum $(\dot{E}x_{D,k} + \dot{E}x_{L,k})$ is given by

$$(\dot{E}x_{D,k} + \dot{E}x_{L,k})^{\text{OPT}} = \dot{E}x_{P,k} F_k = \dot{E}x_{P,k} \left(\frac{1 - \varepsilon_k^{\text{OPT}}}{\varepsilon_k^{\text{OPT}}} \right) \quad (6.16)$$

At this point, a simplification of assumption A3 allows some additional results to be obtained: In Equations 6.4 (and in Equations 6.6, 6.7, 6.8 and 6.10) we may neglect the last two terms on the right side referring to a certain portions of the O&M costs since these costs are often small compared with the remaining terms on the same side of the respective equation [143,147]. With this simplification and using Equation 4.26, Equation 6.10 can be expressed in terms of $(\dot{E}x_{D,k} + \dot{E}x_{L,k})$ as

$$\text{Minimize } c_{P,k} = c_{F,k} \left(1 + \frac{\dot{E}x_{D,k} + \dot{E}x_{L,k}}{\dot{E}x_{P,k}} \right) + \frac{(\beta + \gamma_k) B_k}{\tau \dot{E}x_{P,k}^{1-n_k}} \left(\frac{\dot{E}x_{P,k}}{\dot{E}x_{D,k} + \dot{E}x_{L,k}} \right)^{n_k} \quad (6.17)$$

By differentiating Equation 6.17 with respect to $(\dot{E}x_{D,k} + \dot{E}x_{L,k})$ and setting the derivative to zero, we obtain after some manipulation the following relation between the cost-optimal values of the cost rates expressed by $c_{F,k}(\dot{E}x_{D,k} + \dot{E}x_{L,k})$ and \dot{Z}_k :

$$n_k = \frac{c_{F,k} (\dot{E}x_{D,k} + \dot{E}x_{L,k})^{\text{OPT}}}{\dot{Z}_k^{\text{OPT}}} \quad (6.18)$$

Thus, under assumptions A1, A2, A4 and the simplified assumption A3, when the k th component is optimized in isolation, the cost exponent n_k in Equations 6.3, 6.8, 6.10 and 6.15 express the ratio between the cost optimal rate associated with exergy destruction and exergy loss and the cost-optimal rate associated with capital investment.

Using Equations 6.16 and 6.18, we obtain the following expressions for the cost-optimal values of the non-fuel related cost rate \dot{Z}_k , the relative cost difference r_k , Equation 5.37, the exergoeconomic factor f_k , and Equation 5.38, we obtain

$$\dot{Z}_k^{\text{OPT}} = c_{F,k} \dot{E}x_{P,k} \frac{F_k}{n_k} \quad (6.19)$$

$$r_k^{\text{OPT}} = \frac{n_k + 1}{n_k} F_k \quad (6.20)$$

$$f_k^{\text{OPT}} = \frac{1}{1 + n_k} \quad (6.21)$$

The use this optimization approach we must be able to express the total capital investment of a system component as a function of exergetic efficiency and the capacity through a relation similar to Equation 6.3. In Chapter 9, these definitions are given for all components of the GASKI WWTP and biogas engine powered cogeneration system for which meaningful exergetic efficiencies are defined.

6.4 Thermo-economic Optimization Methodology of Existing Complex Systems

The usual approach to the optimization of complex thermal systems is to iteratively optimize subsystems and/or ignore the influence of some structural changes and decision variables. An alternative to this approach is an iterative thermo-economic optimization technique that consists of the following steps:

1. In the first step, the detailed schematics and inputs of the existing system must be evaluated. The use of actual data, vendor's quotations (even contractor's actual operating manuals) can reduce, therefore, the total number of iterations required.

2. A detailed thermoeconomic analysis and evaluations are conducted for the actual system with the data taken in the previous step. In this step, we can easily obtain the decision variables that affect both the exergetic efficiency and the investment costs.
3. If the system has one or two components for which the sum of the cost rates $(\dot{Z}_k + \dot{C}_{D,k})$ is significantly higher than the same sum for the remaining components, the improvements of these components can be modified to approach their corresponding cost-optimal exergetic efficiency, given by Equation 6.12. This is meaningful only for components where each of the terms \dot{Z}_k and $\dot{C}_{D,k}$ has a significant contribution to the costs associated with the respective component.
4. For the remaining components, particularly the ones having a relatively high value of the sum $(\dot{Z}_k + \dot{C}_{D,k})$, the relative deviations of the actual values from the cost-optimal values for the exergetic efficiency and relative cost difference are calculated:

$$\Delta\varepsilon_k = \frac{\varepsilon_k - \varepsilon_k^{\text{OPT}}}{\varepsilon_k^{\text{OPT}}} \times 100 \quad (6.22)$$

$$\Delta r_k = \frac{r_k - r_k^{\text{OPT}}}{r_k^{\text{OPT}}} \times 100 \quad (6.23)$$

5. Finally a parametric study may be conducted to investigate the effect on the optimization results of some parameters and/or assumptions made in the optimization procedure.

6.5 Conclusions

In this chapter, we provided general principles and formulation of thermoeconomic optimization. The detailed formulation for GASKI WWTP and biogas engine powered cogeneration system is provided and applied in Chapter 9.

CHAPTER 7

GASKI WASTEWATER TREATMENT PLANT

7.1 Introduction

Wastewater collected from municipalities and communities must ultimately be returned to receiving waters or to be land or reused. With this aim, wastewater treatment plants are used. The complex question facing the design engineer and public health officer is: what levels of treatment must be achieved in a given application, beyond those prescribed by discharge permits, to ensure protection of public health and the environment? The answer to this question requires detailed analyses of local conditions and needs, application of scientific knowledge and engineering judgment based on the past experience, and consideration of federal, countries, cities, and local regulations. In some cases, a detailed risk assessment may be required [24].

In this chapter, an overview of wastewater treatment is provided firstly, and then the detailed description of GASKI Wastewater Treatment Plant including primary and secondary treatments, sludge flotation and thickening, anaerobic sludge digestion systems and biogas engine powered cogeneration.

7.2 Municipal Wastewater Treatment Plants Overview

Municipal wastewater treatment provides an essential community service that is vital for the protection of public health and the environment. Without affordable water and wastewater services, economic growth and the quality of life are diminished. Most cities, towns and communities in the Turkey provide drinking water and wastewater treatment services. Currently the wastewater treatment industry faces a number of challenges, including urban population growth, the need to treat wet

weather flows, more stringent discharge regulations, and demand for water conservation through wastewater reuse [149].

A wastewater treatment system is comprised of a combination of unit operations and unit processes designed to reduce certain constituents of wastewater to an acceptable level. Many different combinations are possible. Although practically all wastewater treatment systems are unique in some respects, a general grouping of unit operations and unit processes according to target contaminants has evolved over the years [5].

Municipal wastewater treatment systems are usually divided into primary, secondary and sludge stabilization subsystems. The purpose of primary treatment system is to remove solid materials from the incoming wastewater. Large wastes can be removed by screens which are composed of coarse and fine. Inorganic solids are removed in grit and grease tanks, and much of the organic suspended solids are removed through sedimentation process. A typical primary treatment system should remove approximately one-half of the suspended solids in the entering wastewater. The BOD value associated with these solids accounts for about 30 percent of the influent BOD value.

Secondary treatment system usually consists of biological conversion of dissolved and colloidal organics into biomass that can subsequently remove through sedimentation process. Contact between microorganisms and the organics is optimized by suspending the biomass in the wastewater or by passing wastewater over a film of biomass attached to solid surfaces. The most common and well known suspended biomass system is the activated sludge process. Recirculating a portion of the biomass maintains a large number of organisms in contact with the wastewater and speeds up the conversion process [5].

Sludge stabilization process consists of some subsystems. First step of the sludge process is flotation and thickening process. In wastewater treatment, flotation is used to remove suspended matter and to concentrate biosolids. The principal advantages of flotation over sedimentation system are that very small or light particles that settle slowly can be removed more completely and in a shorter time. Once the particles

have been floated to the surface, they can be collected by a skimming operation easily [24].

Sludge thickening system is a process used to increase the dry matter content of sludge by removing a portion of the liquid fraction. To illustrate, if waste activated sludge, which is typically pumped from secondary settling tanks with a content of about 0.8% solids, can be thickened to a content of 4% solids, then a fivefold decrease in the sludge volume is achieved. Thickening is generally accomplished by physical means, including, cosettling, gravity settling, flotation, centrifugation, gravity belt, and rotary drum [24].

The volume reduction obtained by sludge concentration is beneficial to subsequent treatment processes, such as digestion, dewatering drying and incineration from the following standpoints: a) capacity of tanks and equipment required, b) quantity of chemicals required for sludge conditioning, and c) amount of heat required by digesters and amount of auxiliary fuel required for heat drying or incineration, or both [24].

7.3 GASKI Wastewater Treatment Plant

Gaziantep city has an important role its economic, historic and commercial structure in Turkey. Its regional position, the relationship with industrial cities at west of the Turkey and with settlements at the south of Turkey, provides all requirements any kinds of the Southeastern Anatolia Region. Especially after the 1990, population has been increasing rapidly due to the increasing migration and city was obligated to face with infrastructure disabilities. In parallel with the city's economic structure of the economic development, increasing employment opportunities increased regional attractiveness of the city. To prevent these difficulties, it is important that investments should be permanent and long term solution.

The project contract of GASKI Wastewater Treatment Plant (WWTP) was signed by the consortium of Gaziantep Municipality Water and Wastewater Works, Gunal Construction Incorporated Company and Degremont Company (France), in Gaziantep city, in 1990. GASKI WWTP was financed by European Social

Development Bank with the credit of 56 million US Dollars. Wastewater treatment in the plant was started in 1999. The plant has been serving to 1,000,000 equal inhabitants in the Gaziantep city and the total daily capacity of treated wastewater of the plant is 200,000 m³ (see Fig. 7.1). Treated wastewater is discharged to Sacir river for use in irrigation of 80 million m² agricultural land located in the region. Main design data of the GASKI WWTP is presented in Table 7.1.



Figure 7.1: Satellite view of the GASKI Wastewater Treatment Plant

7.3.1 Primary Treatment System

Primary treatment system of the GASKI WWTP consists of coarse and fine screens, grit and grease removal tanks and, primary sedimentation tanks. Screening devices are used to hold coarse solids such as sticks, rags, boards and other large objects from the wastewater. The primary purpose of screens is to protect pumps and other mechanical equipment and to prevent clogging of valves and other appurtenances in

the wastewater plant. Two types of screens, coarse and fine screens are used in preliminary treatment of wastewater: Coarse screens have clear openings ranging from 6 to 150 mm while fine screens have clear openings less than 6 mm. Main design data and the image of the screens in the GASKI WWTP are given in Table 7.2 and Figure 7.2, respectively.

Table 7.1: Main design data of the GASKI WWTP

Total plant area	200,000 m ²	Equivalent population	1,000,000
Wastewater		Pollution load	
Daily flow	200,000 m ³ /day	Maximum BOI ₅ load	60 ton/day
Hourly flow	8333 m ³ /h	Average BOI ₅ concentration	300 mg/liter
Average instantaneous flow	2.3 m ³ /h	PH	5.5<PH<8.5
Dry weather instantaneous flow	3.7 m ³ /h	Temperature	<30°C
Rainy weather instantaneous flow	4.6 m ³ /h	Biogas production	20,000 m ³ /day
Treated wastewater			
Average BOI ₅ concentration		<25 mg/l	
Suspended solid		<35 mg/l	

Table 7.2: Main design data of the GASKI WWTP screens

	Coarse Screen	Fine Screen
Screen range	40 mm	15 mm
Number of screen	3	3

A portion of the suspended solids in municipal wastewater consists of inert inorganic material such as sand, metal fragments, eggshells, etc. This grit is not benefited by secondary treatment or sludge processing techniques and can block conduits and promote excessive wear of mechanical equipment. Removal of grit from wastewater may be accomplished in grit chambers or by the centrifugal separation of solids. Grease is removed to a degree by surface skimming devices in primary sedimentation tanks. Skimming tanks employ baffled subsurface entrance and exit structures which permit floating material to be retained. Retention time is about 15 min or less, and continuous mechanical skimming is usually employed. Main design

data and image of the grit and grease removal tanks in the GASKI WWTP are given in Table 7.3 and Figure 7.3, respectively.



Figure 7.2: Coarse and fine screens of the GASKI WWTP

Table 7.3: Main design data of the GASKI WWTP grit and grease removal tanks

Grit and Grease Removal Tanks	
Tank depth	2.5 m
Unit volume	483 m ³
Retention time	10.4 min
Number of Tank	3



Figure 7.3: Grit and grease removal tanks of the GASKI WWTP

Primary sedimentation process is used as a preliminary step in the further processing of the wastewater. Efficiently designed and operated primary sedimentation tanks should remove from 50-70% of the suspended solids and from 25-40 % of the BOD

(biochemical oxygen demand). Sedimentation tanks have also been used as stormwater retention tanks, which are designed to provide a moderate detention period (10 to 30 min) for overflows from either combined sewers or storm sewers. The purpose of sedimentation is to remove a substantial portion of the organic solids that otherwise would be discharged directly to the receiving waters. The selection of the type of sedimentation unit for a given application is governed by the size of the installation, by rules and regulations of local control authorities, by local site conditions, and by the experience and judgment of the engineer [24]. Main design data and image of the primary sedimentation tanks in the GASKI WWTP are given in Table 7.4 and Figure 7.4, respectively.

Table 7.4: Main design data of the GASKI WWTP's primary sedimentation tanks

Primary Sedimentation Tanks	
Tank depth	3 m
Unit volume	5890 m ³
Diameter	50 m
Retention time	2.1 h
Number of Tank	3



Figure 7.4: Primary sedimentation tanks of the GASKI WWTP

7.3.2 Secondary Treatment System

Secondary treatment system of the GASKI WWTP consists of aeration tanks and secondary sedimentation tanks. Suspended growth processes require reasonably

intense mixing in order to maintain the biological solids in suspension, disperse the waste through the basin, and provide the required oxygen for stabilization in aerobic systems. The process involves air or oxygen being introduced into a mixture of primary treated or screened wastewater combined with organisms to develop a biological flock which reduces the organic content of the sewage. Aeration tanks usually are constructed of reinforced concrete and left open to the atmosphere. Main design data and image of the aeration tanks in the GASKI WWTP are given in Table 7.5 and Figure 7.5, respectively.

Table 7.5: Main design data of the GASKI WWTP aeration tanks

Aeration Tanks	
Tank depth	8 m
Unit volume	14,469 m ³
Diameter	48 m
Retention time	5.2 h
Number of Tank	3



Figure 7.5: Aeration tanks of the GASKI WWTP

Solid separation is the final step in the production of a well clarified, stable effluent low in BOD and suspended solids and, as such, represents a critical link in the operation of an activated sludge treatment process. The following factors must be considered in the design of secondary sedimentation tanks: a) tank types, b) surface and solids loading rates, 3) sidewater depth, 4) flow distribution, 5) inlet design, 6) weir placement and loading rates, and 7) scum removal [24]. Main design data of the secondary sedimentation tanks in the GASKI WWTP are given in Table 7.6.

Table 7.6: Main design data of the GASKI WWTP's secondary sedimentation tanks

Secondary Sedimentation Tanks	
Tank depth	3.6 m
Unit volume	7645 m ³
Diameter	52 m
Retention time	5.5 h
Number of Tank	6

7.3.3 Sludge Flotation and Thickening System

Flotation process is used to remove suspended matter and to concentrate biosolids. The main principal advantages of flotation over sedimentation are that very small or light particles that settle slowly can be removed more completely and in a shorter time. Once the particles have been floated to the surface, they can be collected by a skimming operation [24]. Main design data and image of the flotation tanks in the GASKI WWTP are given in Table 7.7 and Figure 7.6, respectively.

Table 7.7: Main design data of the GASKI WWTP's flotation tanks

Flotation Tanks	
Tank depth	2.4 m
Unit volume	424 m ³
Diameter	15 m
Number of Tank	3



Figure 7.6: Flotation tanks of the GASKI WWTP

Thickening process is used for volume reduction of the sludge. Gravity thickening is one of the most common methods used and is accomplished in a tank similar to a conventional sedimentation tank. Normally, a circular tank is used, and dilute sludge is fed into a center feed well. The feed sludge is allowed to settle and compact, and thickened sludge is withdrawn from the conical tank bottom. Main design data and image of the thickening tanks in the GASKI WWTP are given in Table 7.8 and Figure 7.7, respectively.

Table 7.8: Main design data of the GASKI WWTP's thickening tanks

Thickening Tanks	
Tank depth	4.7 m
Unit volume	804 m ³
Diameter	16 m
Number of Tank	3



Figure 7.7: Thickening tanks of the GASKI WWTP

7.3.4 Anaerobic Sludge Digestion System

Anaerobic digestion is by far the most common process for dealing with wastewater sludge. Anaerobic decomposition produces considerably less biomass than aerobic process. The principal function of anaerobic digestion, therefore, is to convert as much of the sludge as possible to end products such as liquids and gases, while producing as little residual biomass as possible. Furthermore, anaerobic digestion of

sewage sludge produce sufficient biogas to meet most of the energy needs for plant operation.

Two-stage digestion is rarely used in modern digestion design. In two stage digestion, a high rate digester is coupled in series with a second tank. The first tank is used for digestion and is heated and equipped with mixing facilities. The second tank is usually unheated and used principally for storage. Less than 10% of the gas generated comes from the second stage. Main design data and image of the anaerobic digestion tanks in the GASKI WWTP are given in Table 7.9 and Figure 7.8, respectively.

Table 7.9: Main design data of the GASKI WWTP's anaerobic digestion tanks

Primary Anaerobic Digestion Tanks	
Hydraulic depth	13.3 m
Height	18.6 m
Unit volume	8000 m ³
Diameter	26.8 m
Retention time	15 day
Temperature of sludge	35±2 °C
Number of tank	3
Secondary Anaerobic Digestion Tank	
Hydraulic depth	13.3 m
Height	18.6 m
Unit volume	8000 m ³
Diameter	26.8 m
Retention time	5 day
Number of tank	1



Figure 7.8: Anaerobic digestion tanks of the GASKI WWTP

Two biogas tanks with capacity of 800 m³ are used for storage of biogas (see Figure 7.9). The GASKI WWTP has a DeSO_x treatment system in order to get rid of hydrogen sulfide presence in the biogas produced (see Figure 7.10).



Figure 7.9: The views of the biogas store tanks in GASKI WWTP



Figure 7.10: A view of the DeSO_x unit in GASKI WWTP

7.4 GASKI Biogas Engine Powered Cogeneration System

GASKI Biogas engine powered cogeneration system (BEPC) was installed by Gaziantep Municipality Water and Wastewater Works and ILTEKNO Inc. joint venture, and started to produce electricity in 2006. The total installed electricity generation and hot water capacities of the plant is 1.8 MW and 135.11 tons/hr, respectively.



Figure 7.11: GASKI Biogas Engine Powered Cogeneration System

The electricity is generated by two, biogas engine actuated; generator sets (see Figure 7.11). The each engine is four-stroke spark ignition engine in a V configuration, one with 12 cylinders and the other with 16 cylinders. Biogas produced from anaerobic digestion of sludge in GASKI WWTP is used as fuel for engines. The engine – generator sets were imported from DEUTZ AG Engine Company. This company is one of the well known largest international companies at its sector. By considering only one engine with 12 cylinders running currently in the cogeneration plant, the permissible annual electricity production of plant is 14.4 GWh and the annual biogas consumption is nearly 6681.6 tons at designed operating conditions. Plant operation life is to be twenty five years. The total capital investment of plant was about 1.24 million US Dollars.



Figure 7.12: DEUTZ gas engine actuated generator sets in GASKI cogeneration

The system that are mainly installed in plant are engine-generator sets, turbocharger systems, lubrication oil system, compressed air system, cooling system, PLC monitoring control system. The engines used in power house as actuator are named as TCG2020 12V and TCG2020 16V respectively and general view of a TCG2020 is shown in Fig. 7.12. Engines were manufactured by DEUTZ AG Company at the

factories in Cologne, Germany and imported to Turkey. The “12V” represents number of cylinder. The engines is four stroke cycled and turbocharged. The compressed air, as starter, is used to start engine to run. Since engine is turbocharged, there is an inter-cooler system for cooling of charged air before it is sent into the engine cylinders. For engine cooling, an air-water radiator system is chosen. The coolant liquid is water and cycled in a closed loop. The basic data of the engines is listed in Table 7.10.

Table 7.10: Main engine characteristic data of TCG 2020 12V and TCG2020 16V [150]

Engine Type		TCG 2020 V12	TCG 2020 V16
Engine power	kW	1050	1400
Speed	min ⁻¹	1500	1500
Mean effective pressure	bar	15.8	15.8
Exhaust temperature (approx.)	°C	479	479
Exhaust mass flow wet (approx.)	kg/h	5592	7457
Combustion air mass flow (approx.)	kg/h	4993	6657
Combustion air temperature minimum/design	°C	20/25	20/25
Ventilation air flow (approx.)	kg/h	22665	29582
Generator			
Efficiency	%	97.3	97.4
Energy Balance			
Electrical power	kW	1022	1364
Jacket water heat (± 8%)	kW	536	718
Intercooler LT heat (± 8%)	kW	98	130
Exhaust cooled to 150 °C (± 8%)	kW	534	722
Engine radiation heat	kW	45	60
Generator radiation heat	kW	29	36
Fuel consumption (+ 5%)	kW	2489	3329
Electrical efficiency	%	41.0	41.0
Thermal efficiency	%	43.0	42.8
Total efficiency	%	84.0	83.7

7.11 Conclusions

In this chapter, detailed technical information about auxiliary equipments of GASKI WWTP and BEPC system are presented by using vendor quotations and contractor’s guides. Data for the system operation is based on the both plants descriptions will be presented Chapter 9.

CHAPTER 8

HYDROGEN PRODUCTION MODELS FOR WASTEWATER TREATMENT PLANTS

8.1 Introduction

Hydrogen is the most abundant element in the universe. Hydrogen is more and more often mentioned as a solution to the tremendous challenges resulting from the global warming and depletion of oil and gas. However, hydrogen or subsequent synthetic fuels are only energy carriers, i.e. tools to handle the energy. An energy amount equivalent to at least the energy content of the hydrogen must be supplied by energy sources such as wind, sunshine, biomass, geothermal. It can always be discussed which energy sources are primary and which are not, but from a hydrogen energy point of view, the key thing is that energy from other sources is stored as hydrogen for latter conversion [151]. General properties of hydrogen can be seen in Table 8.1.

Hydrogen can be produced from a variety of feedstocks. These include fossil resources, such as natural gas and coal, as well as renewable resources, such as biomass and water with input from renewable energy sources (e.g. sunlight, wind, wave or hydro-power). A variety of process technologies can be used, including chemical, biological, electrolytic, photolytic and thermo-chemical. Each technology is in a different stage of development, and each offers unique opportunities, benefits and challenges. Local availability of feedstock, the maturity of the technology, market applications and demand, policy issues, and costs will all influence the choice and timing of the various options for hydrogen production. An overview of the various feedstocks and process technologies is presented in Figure 8.1 [152].

In this chapter, first, general descriptions of the hydrogen production systems are presented. Three type of electrolysis processes and biohydrogen production methods are discussed with their advantages and disadvantages. Then, hydrogen production models developed for wastewater treatment plants in the frame of GASKI municipal WWTP are presented. Finally hydrogen storage methods are discussed.

Table 8.1: Properties of hydrogen as a fuel [153]

Property	Unit	Value
Density ^a (gas)	kg/m ³	0.0838
HHV and LHV	MJ/kg (liquid)	141.9–119.90
HHV and LHV	MJ/m ³ (volumetric)	11.89–10.05
Boiling point	K	20.41
Freezing point	K	13.97
Density (liquid)	kg/m ³	70.8
Diffusion coefficient in air ^a	cm ² /s	0.61
Specific heat at constant pressure	kJ/kg K	14.89
Ignition limits in air	% (volume)	4–75
Ignition energy in air	Millijoule	0.02
Ignition temperature	K	585
Flame temperature in air	K	2318
Explosion energy	kJ/g TNT	58.823
Flame emissivity	%	17–25
Stoichiometric mixture in air	%	29.53
Stoichiometric air/fuel	kg/kg	34.3/1
Flame velocity	cm/s	2.75
Motivity factor	-	1.0

^a At normal temperature and pressure.

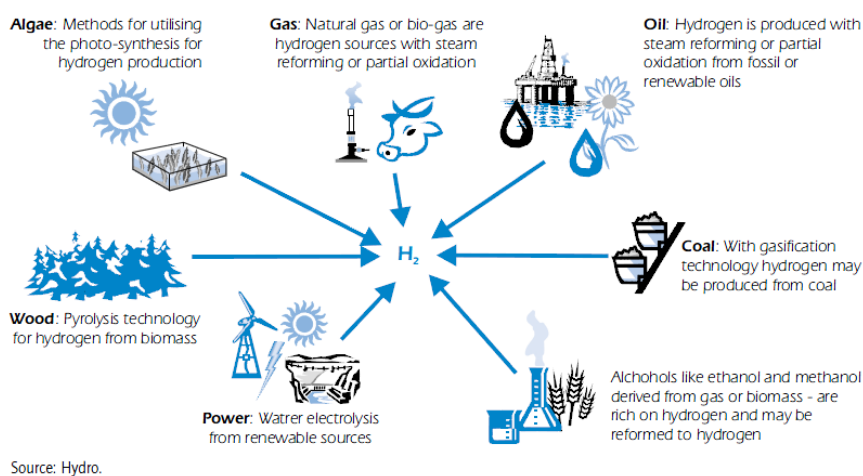


Figure 8.1: Some feedstocks and process alternatives [152]

8.2 Hydrogen Production by Electrolysis

In electrolysis, electricity is used to decompose water into its elemental components: hydrogen and oxygen. Electrolysis is often seen as the most preferred method of hydrogen production as it is the only process that need not rely on fossil fuels. It also has high product purity, and is feasible on small and large scales. Electrolysis can operate over a wide range of electrical energy capacities, for example, taking advantages of more abundant electricity at night [154].

At the heart of electrolysis is an electrolyzer. An electrolyzer is a series of cells each with a positive and negative electrode. The electrodes are immersed in water that has been made electrically conductive, achieved by adding hydrogen or hydroxylions, usually in the form of alkaline potassium hydroxide (KOH) .

For electrolysis, the amount of electrical energy required can be somewhat offset by adding heat energy to the reaction. The minimum amount of voltage required to decompose water is 1.23 V at 77 °F (25 °C). At this voltage, the reaction requires heat energy from the outside to proceed. At 1.47 V (and same temperature) no input heat is required. At greater voltages (and same temperature) heat is released into the surroundings during water decomposition. Operating the electrolyzer at lower voltages with added heat is advantageous, as heat energy is usually cheaper than electricity, and can be recirculated within the process. Thermal contributions in electrolysis and fuelcell modes of operation are shown in Figure 8.2. Furthermore, the efficiency of the electrolysis increases with increased operating temperature [154]. An electrolysis unit as seen in Figure 8.3 works with the following steps [155]:

1. A battery connects the positive terminal (sometimes called the anode) to the negative terminal (or cathode) through an electrolyte. In a simple laboratory experiment, the electrolyte could be pure water. In a real electrolyzer, performance is improved considerably by using a solid polymer membrane as the electrolyte, which allows ions to move through it.
2. When the power is switched on, water (H_2O -shown here as two red blobs joined to one green one) splits into positively charged hydrogen ions

(hydrogen atoms missing electrons, shown in red) and negatively charged oxygen ions (oxygen atoms with extra electrons, shown in green).

3. The positive hydrogen ions are attracted to the negative terminal and recombine in pairs to form hydrogen gas (H_2).
4. Likewise, the negative oxygen ions are drawn to the positive terminal and recombine in pairs there to form oxygen gas (O_2).

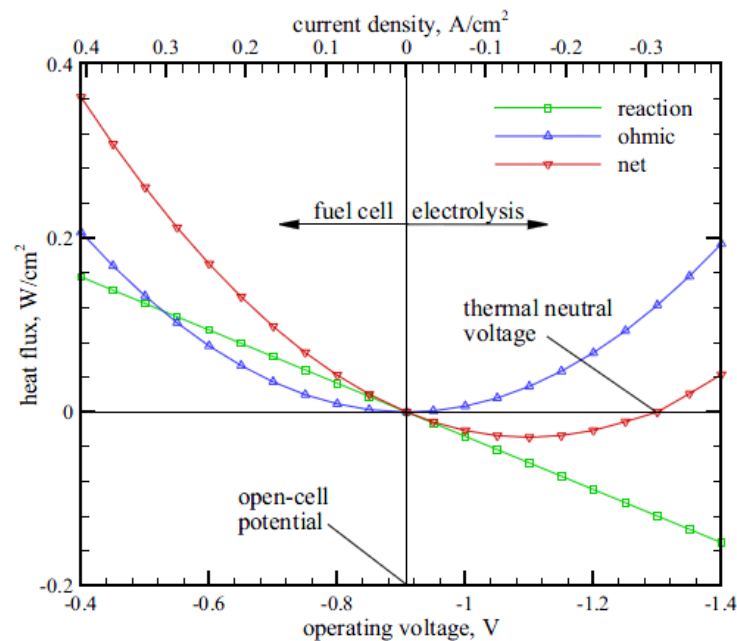


Figure 8.2: Thermal contributions in electrolysis and fuelcell modes of operation [156].

Many different types of electrolysis cells have been proposed and constructed. These are:

- **Alkaline Electrolyzer:** Similar to PEM electrolyzer, these equipment use a alkaline solution as the electrolyte;
- **PEM Electrolyzer:** The Polymer Electrolyte Membrane (PEM) electrolyzer use a solid plastic membrane as electrolyte;
- **Solid Oxide Electrolyzer:** use a solid ceramic material that selectively transmits negative charged oxygen ions at around 500 to 800 °C.

Characteristics of regular and advanced electrolyzer can be seen in Table 8.2.

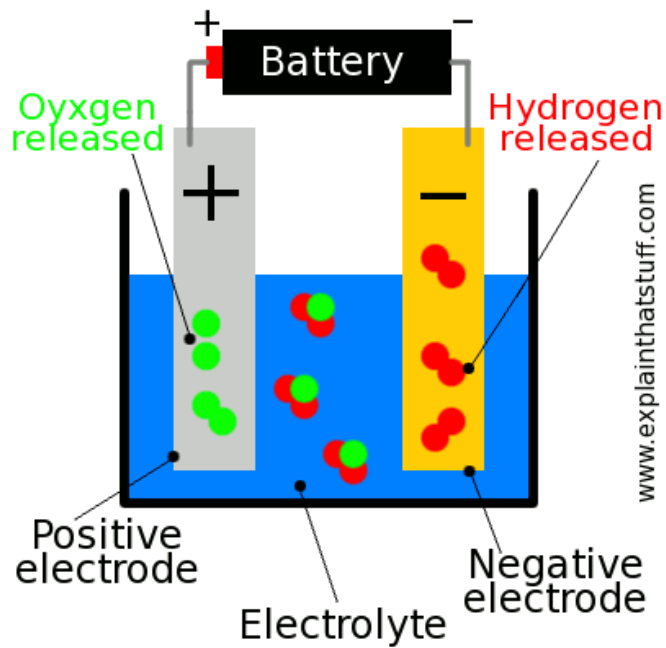


Figure 8.3: A simple water electrolyzer [155]

The technology and size of commercially available electrolyzers vary greatly. In the present survey of commercial electrolyzers focus is only on technology that can be useful to the electrical power grid.

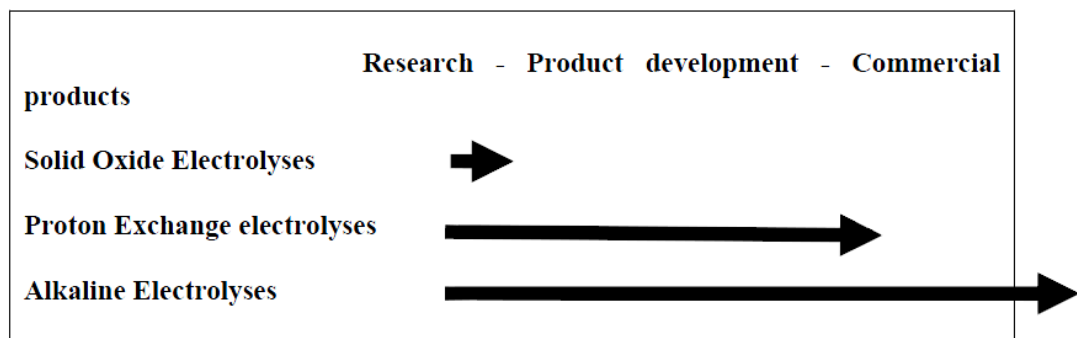


Figure 8.4: A graphical indication of the state of development of the different types of electrolyzers. [151]

Table 8.2: Characteristics of existing and advanced electrolyzers [157]

Technology	Conventional Electrolyser	Advanced Alkaline Electrolyser	Inorganic Membrane Electrolyser	PEM Electrolyser	SOFC High Temperature Steam Electrolyser
Development stage	Commercial large scale units	Prototypes and commercial units	Commercial units	Prototypes and commercial units	Lab stage and commercial units
Cell voltage (V)	1.8-2.2	1.5-2.5	1.6-1.9	1.4-2.0	0.95-1.3
Current density (A/cm ²)	0.13-0.25	0.20-2.0	0.2-1.0	1.0-4.0	0.3-1.0
Temperature (°C)	70-90	80-145	90-120	80-150	800-1000
Pressure (bar)	1.2	Up to 120	Up to 40	Up to 400	Up to 30
Cathode	Stainless steel or Ni	Catalytic or noncatalytic active Ni catalytic	Spinel oxide based on CO	C- fibre and Pt	Ni
Anode	Ni	Catalytic or or noncatalytic active Ni	Spinel oxide based on CO	Porous Ti and proprietary catalyst	Ni-NiO or Perovskite
Gas separator	Asbestos 1.2-1.7 Ohm/cm ²	Asbestos < 100°C; Teflon bonded PBI-K titanate >100°C; 0.5-0.7 Ohm/cm ²	Patented polyantimonic acid membrane 0.2-0.3 Ohm/cm ²	Multilayer expanded metal screens	None
Electrolyte 25-35%	25-40% KOH	14-15% KOH	Perfluorosulfonic KOH	Solid Y ₂ O ₃ acid membrane 10-12 mils thick 0.46 Ohm/cm ²	stabilised ZrO ₃₈₀
Cell efficiency (GJ H ₂ /GJ el)	66-69	69-77	73-81	73-84	81-66
Power need (kWh/Nm ³ H ₂)	4.3-4.9	3.8-4.3	4.8	3.6-4.0	2.5-3.5

8.2.1 Alkaline Electrolysis

Alkaline electrolyte electrolyzers represent a very mature technology that is the current standard for large-scale electrolysis. The anode and cathode materials in these systems are typically made of nickel-plated steel and steel respectively. Electrolyte in these systems is a liquid one based on a highly caustic KOH solution.

The ionic charge carrier is the hydroxylion, OH^- , and a membrane porous to hydroxylions, but not to H_2 and O_2 provides gas separation [151]. Schematic of an alkaline water electrolyzer can be seen in Figure 8.5.

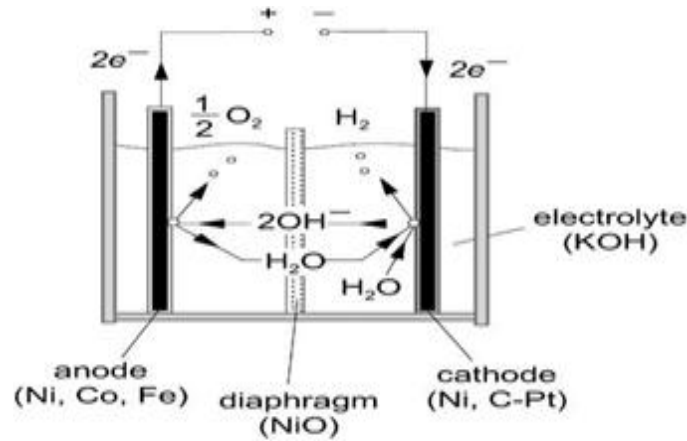


Figure 8.5: Alkaline water electrolyzer [151]

The following reactions take place inside the alkaline electrolysis cell:



The key advantage of this technology includes its maturity and its durability. This technology has low temperature, high purity of the products (>99.8 % H_2). Disadvantages are its use of a highly caustic electrolyte and its inability to produce hydrogen at high pressures. This inability to produce high pressure hydrogen for storage results in the added need for an external compressor which adds cost and complexity to the system [151]. Alkaline electrolyzer also can be used for the electrolysis of hydrogen sulfide. The cathodic process, hydrogen evolution in alkaline solution, is simple and well known. A membrane is necessary to separate the cathodic compartment from polysulfide ions produced at the anode. Sulfur ions can be electrochemically oxidized to elementary sulfur, polysulfides and sulfides, depending on the electrolytic conditions, i.e. overpotential, pH and temperature [158].

8.2.2 Proton Exchange Membrane (PEM) Electrolysis

The PEM water electrolysis cell consists primarily of a PEM on which the anode and cathode are bonded. These electrodes are normally a composite of electrocatalytic particles and electrolyte polymer. Cells that use a solid-polymer electrolyte are usually constructed on the filter press type design. They do not require electrolyte circulation because the electrolyte is immobilized in the form of an ion-exchange resin. The electrodes are either embedded in the surface of the resin sheets or pressed closely against the two opposing faces of the sheet of resin material. A ribbed or corrugated solid metal separator plate is interposed between cells, providing electric continuity between one cell and the next while separating the hydrogen from the oxygen in adjacent cells. This type of cell is usually cooled by circulating water through the cavity between the metal separator and the electrode plate. Hydrogen or oxygen evolved into this cavity is swept out by the coolant stream and is separated from the water outside the cell [151]. A basic schematic of a PEM water electrolysis cell is shown in Figure 8.6.

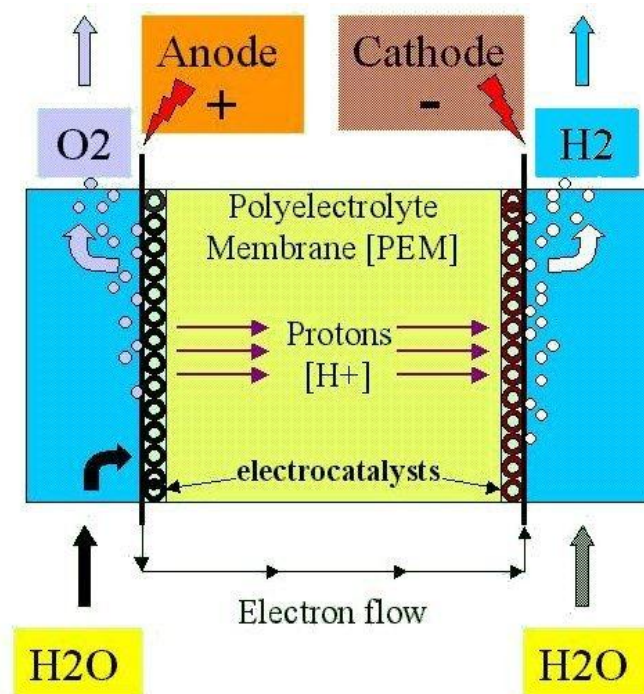


Figure 8.6: PEM water electrolyzer [155]

The principle of PEM electrolysis is presented in Equation (8.4) and (8.5).



PEM electrolyzers require no liquid electrolyte, which simplifies the design significantly. The electrolyte is an acidic polymer membrane. PEM electrolyzers can potentially be designed for operating pressures up to several hundred bar, and are suited for both stationary and mobile applications. The main drawback of this technology is the limited lifetime of the membranes. The major advantages of PEM over alkaline electrolyzers are the higher turndown ratio which means that operating ratio of part load to full load, the increased safety due to the absence of KOH electrolytes, a more compact design due to higher densities, and higher operating pressures. With relatively high cost, low capacity, poor efficiency and short lifetimes, the PEM electrolyzers currently available are not as mature as alkaline electrolyzers. It is expected that the performance of PEM electrolyzers can be improved significantly by additional work in materials development and cell stack design [152].

8.2.3 High Temperature Steam Electrolysis

High-temperature electrolysis is based on technology from high-temperature fuel cells. The electrical energy needed to split water about 800-1000 °C is considerably less than electrolysis at 100 °C. This means that a high-temperature electrolyser can operate at significantly higher overall process efficiencies than regular low-temperature electrolyzers. To achieve high temperature in the process, water is provided as high temperature superheated steam. The necessary electricity input is reduced corresponding to the variation of cell voltage versus temperature.

A typical technology is the solid oxide electrolyser cell (SOEC). This electrolyser is based on the solid oxide fuel cell (SOFC), which normally operates at 700 to 1000 °C. At these temperatures, the electrode reactions are more reversible, and the fuel cell reaction can more easily be reversed to an electrolysis reaction. Attempts are currently underway to develop systems in which some of the electricity consumed by the electrolyser can be replaced with the heat available from geothermal, solar or

natural gas sources, thus reducing the consumption of electricity significantly [152]. A basic schematic of high temperature steam electrolysis is shown in Figure 8.7.

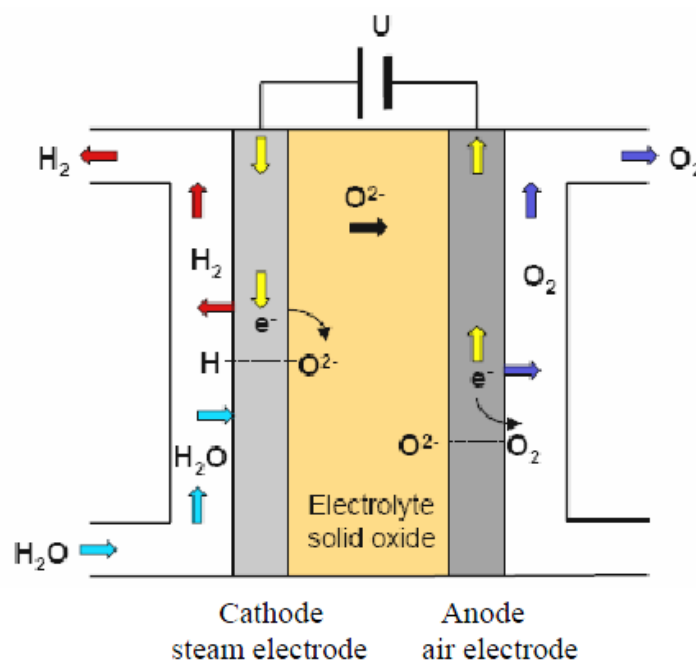


Figure 8.7: SOEC steam electrolyzer [152]

The principle of SOEC electrolysis is presented in Equation (8.6) and (8.7).



The main advantages of SOEC electrolyzer are low overall energy demand, high efficiency increasing with temperature, use of several high temperature steam sources, splitting of CO₂ into CO and O₂ for syngas production and this syngas is used widely in industry for production of a range of chemicals for example synthetic fuels such as SNG (Synthetic Natural Gas).

8.3 Biohydrogen Production

Hydrogen is the element of greatest abundance in the universe; however, its production from renewable resources remains a major challenge. Biohydrogen produced from bio-renewables is a promising alternative for a sustainable energy source. Biohydrogen is a renewable biofuel produced from bio-renewable feedstocks by chemical, thermochemical, biological, biochemical, and biophotolytical methods

[159]. Processes for biological hydrogen production mostly operate at ambient temperatures and pressures, and are expected to be less energy intensive than thermochemical hydrogen production methods. These processes can use a variety of feedstocks as carbon sources. Waste materials can also be used as a carbon source which facilitates waste recycling. [158]. There are several biohydrogen production methods as can be seen in Table 8.3.

Table 8.3: An overview of known biological hydrogen production processes [160]

Process	General reaction	Microorganisms used
1 Direct Biophotolysis	$2 \text{H}_2\text{O} + \text{light} \rightarrow 2 \text{H}_2 + \text{O}_2$	Microalgae
2 Photo-fermentations	$\text{CH}_3\text{COOH} + 2\text{H}_2\text{O} + \text{light} \rightarrow 4\text{H}_2 + 2\text{CO}_2$	Purple bacteria, Microalgae
3 Indirect biophotolysis	(a) $6\text{H}_2\text{O} + 6\text{CO}_2 + \text{light} \rightarrow \text{C}_6\text{H}_{12}\text{O}_6 + 6\text{O}_2$ (b) $\text{C}_6\text{H}_{12}\text{O}_6 + 2\text{H}_2\text{O} \rightarrow 4\text{H}_2 + 2\text{CH}_3\text{COOH} + 2\text{CO}_2$ (c) $\text{C}_6\text{H}_{12}\text{O}_6 + 2\text{H}_2\text{O} \rightarrow 4\text{H}_2 + 2\text{CH}_3\text{COOH} + 2\text{CO}_2$ overall reaction: $12\text{H}_2\text{O} + \text{light} \rightarrow 12\text{H}_2 + 6\text{O}_2$	Microalgae, Cyanobacteria
4 Water Gas Shift Reaction	$\text{CO} + \text{H}_2\text{O} \rightarrow \text{CO}_2 + \text{H}_2$	Fermentative bacteria, Photosynthetic bacteria
5 Two-Phase H_2 + CH_4 Fermentations	(a) $\text{C}_6\text{H}_{12}\text{O}_6 + 2\text{H}_2\text{O} \rightarrow 4\text{H}_2 + 2\text{CH}_3\text{COOH} + 2\text{CO}_2$ (b) $2\text{CH}_3\text{COOH} \rightarrow 2\text{CH}_4 + 2\text{CO}_2$	Fermentative bacteria + Methanogenic bacteria
6 High-yield Dark Fermentations	$\text{C}_6\text{H}_{12}\text{O}_6 + 6\text{H}_2\text{O} \rightarrow 12\text{H}_2 + 6\text{CO}_2$	Fermentative bacteria

Direct biophotolysis is similar to the processes found in plants and algal photosynthesis. In this process solar energy is directly converted to hydrogen via photosynthetic reactions. This is a proper process because of the solar energy is used to convert a readily available substrate, water, to oxygen and hydrogen. The O_2 sensitivity of the hydrogenase enzyme reaction is the main problem of this process. This process must operate at a partial pressure of near one atmosphere of O_2 [158].

In indirect biophotolysis, problems of sensitivity of the hydrogen evolving process are potentially get over by separating temporally and/or spatially oxygen evolution and hydrogen evolution. Thus this process involves separation of the H_2 and O_2 evolution reactions into separate stages, coupled through CO_2 fixation/evolution. Photosynthetic bacteria evolve molecular hydrogen catalyzed by nitrogenase under nitrogen-deficient conditions using light energy and reduced compounds (organic acids) [158].

Hydrogen production via dark fermentation can be achieved mainly by anaerobic or facultative anaerobic bacteria under anaerobic conditions. In contrast to anaerobic methane digestion (in which the intermediate product hydrogen is converted into methane) the final product of the process is hydrogen. An important distinction with anaerobic methane digestion (where methane is produced as a result of co-operative actions of different microorganisms) is that in hydrogen fermentations only hydrogen producing microorganisms are active. Another essential difference is that complex organic compounds in the feedstock are converted to simple molecules not during the digestion process, but rather in a separate process preceding the fermentation. This pretreatment and hydrolysis process is performed by means of physical/chemical methods (e.g. extrusion) and/or treatment with (industrial) enzymes. The resulting organic compounds are converted into hydrogen, acetic acid and CO₂ by microorganisms [160]. Fermentative bacteria producing hydrogen may be cultivated in pure or mixed cultures selected from natural sources such as anaerobically digested sewage sludge or soil [159].

Each biohydrogen production process has own advantage and disadvantage depend on usage. Comparison of these models is listed in Table 8.4 with their advantages and disadvantages.

Table 8.4: Comparison of various hydrogen production processes [49]

Process	Advantages	Disadvantages
Direct bio-photolysis	H ₂ can be produced directly from water and sunlight	Requires high intensity of light, low photochemical efficiency and O ₂ is inhibitory.
Indirect biophotolysis	Blue green algae can produce hydrogen from water. It has the ability to fix N ₂ from atmosphere	Uptake hydrogenates are to be removed.
Photo-fermentation	A wide spectral energy can be used by photosynthetic bacteria.	O ₂ is inhibitory on nitrogenase enzyme and light conversion efficiency is low.
Dark fermentation	It can produce H ₂ without light. No oxygen limitations and can produce several metabolites as by-products. Various substrates can be used in this anaerobic process.	Relatively lower H ₂ yield. At higher H ₂ yield, process becomes thermodynamically unfavorable.
Two-stage fermentation	Can produce relatively higher H ₂ yield. By-products (metabolites) can be efficiently converted to H ₂ .	Requires continuous light source which is difficult for large scale processes.

8.4 Hydrogen Production Models Developed for GASKI Municipal WWTP

In this chapter, hydrogen production models developed for the GASKI municipal wastewater treatment plant are presented.

Model-1:

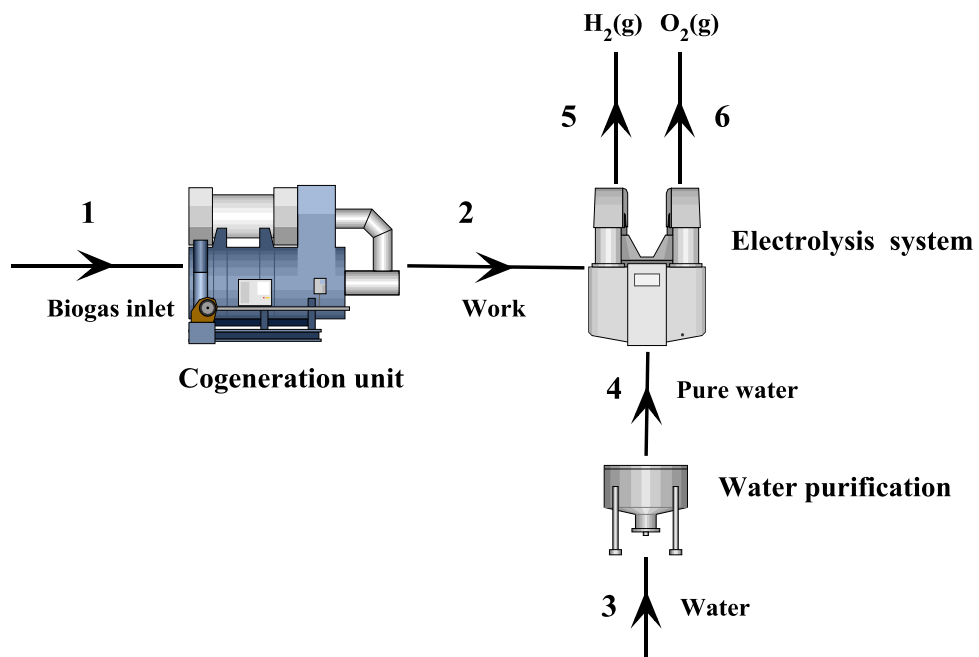


Figure 8.8: Hydrogen production model-1

In the model-1 (see Figure 8.8), a simple alkaline electrolysis process is considered to produce hydrogen. In this model, the work demand for the electrolysis system is provided by the biogas engine powered cogeneration system of GASKI WWTP. The biogas used as fuel in this cogeneration system is produced by a totally renewable process which takes place in the anaerobic digestion reactors of the WWTP. The biogas consumed for 1000 kWh electricity generation in the existing cogeneration system is nearly 61% (0.129 kg/s) of the total biogas produced in the anaerobic digesters, which is 0.212 kg/s. Before the electrolysis processes, the water must be purified through a clean water treatment system. The mass flow rate of the water entering the electrolysis process is taken as 0.06 kg/s. The temperature and pressure of the water are 25°C and 1 bar, respectively.

Model-2:

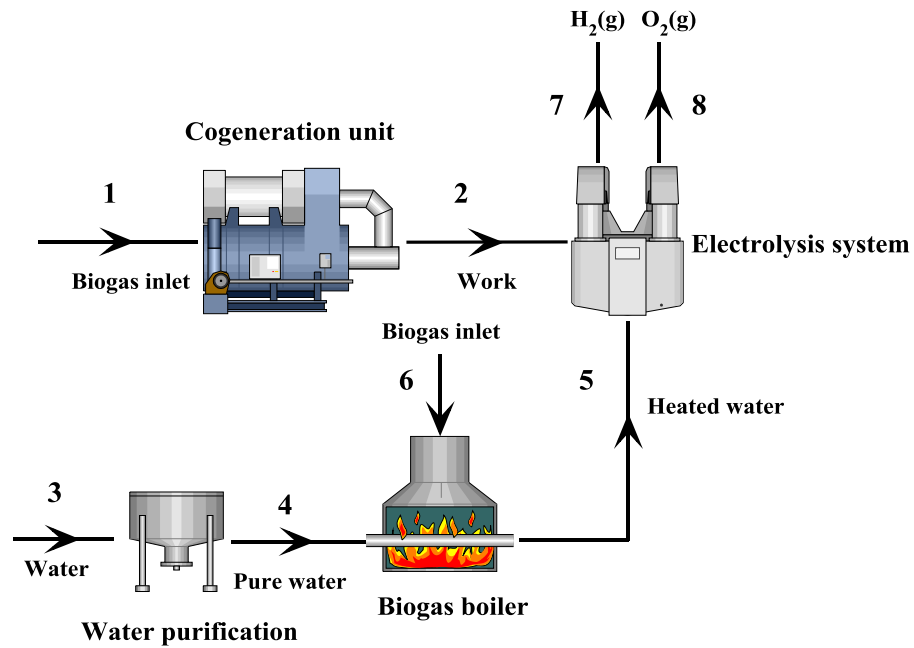


Figure 8.9: Hydrogen production model-2

In the model-2 (see Figure8.9), an alkaline temperature electrolysis process with high temperature steam inlet is considered to produce hydrogen. In this model, the biogas consumed for 1000 kWh electricity generation in the existing cogeneration system is nearly 61% (0.129 kg/s) of the total biogas produced in the anaerobic digesters, which is 0.212 kg/s. A small amount of the remaining part (0.083 kg/s) of the biogas can be used heating of the water in the boiler, which is 0.001 kg/s. The mass flow rate of the water entering the electrolysis process is taken as 0.062 kg/s. The temperature and pressure of the water heated in the boiler are 80°C and 1 bar, respectively.

Model-3:

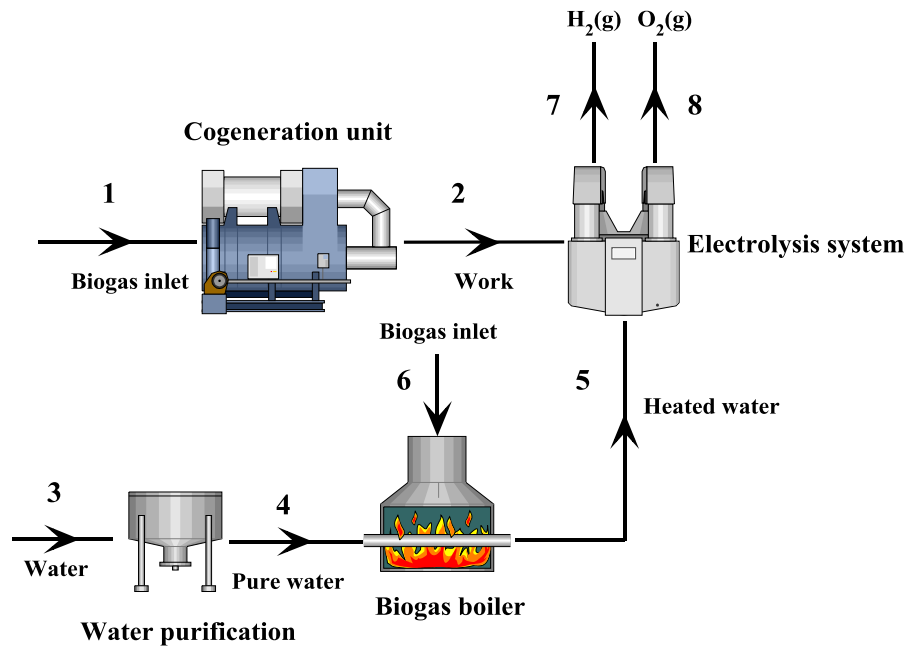


Figure 8.10: Hydrogen production model-3

In the model-3 (see Figure 8.10), a PEM electrolysis process is considered instead of alkaline electrolysis process to produce hydrogen. In this model, the biogas consumed for 1000 kWh electricity generation in the existing cogeneration system is nearly 61% (0.129 kg/s) of the total biogas produced in the anaerobic digesters, which is 0.212 kg/s. A small amount of the remaining part (0.083 kg/s) of the biogas can be used heating of the water in the boiler, which is 0.0011 kg/s. The mass flow rate of the water entering the electrolysis process is taken as 0.065 kg/s. The temperature and pressure of the water heated in the boiler are 80°C and 1 bar, respectively.

Model-4:

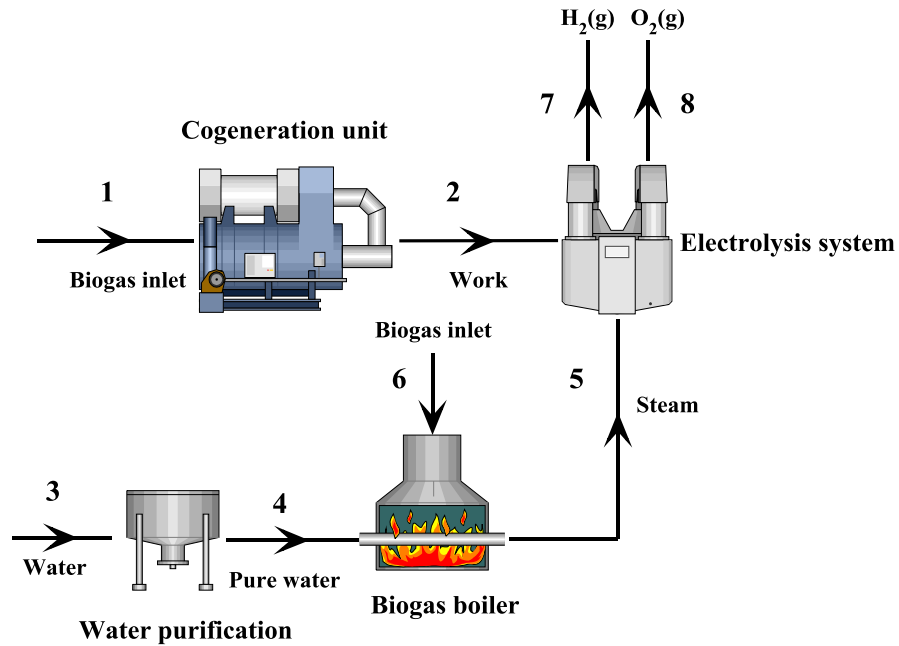


Figure 8.11: Hydrogen production model-4

In the model-4 (see Figure 8.11), a high temperature electrolysis process is considered to produce hydrogen. In this model, the work demand for the electrolysis system is provided by the biogas engine powered cogeneration system of GASKI WWTP. The biogas used as fuel in this cogeneration system is produced by a totally renewable process which takes place in the anaerobic digestion reactors of the WWTP. The biogas consumed for 1000 kWh electricity generation in the existing cogeneration system is nearly 61% (0.129 kg/s) of the total biogas produced in the anaerobic digesters, which is 0.212 kg/s. A small amount of the remaining part (0.083 kg/s) of the biogas can be used to obtain high temperature steam production in the boiler, which is 0.025 kg/s. Before the boiling and electrolysis processes, the water must be purified through a clean water treatment system. The mass flow rate of the water entering the electrolysis process is taken as 0.09 kg/s. The temperature and pressure of the steam produced in the boiler are 800°C and 5 bar, respectively.

Model-5:

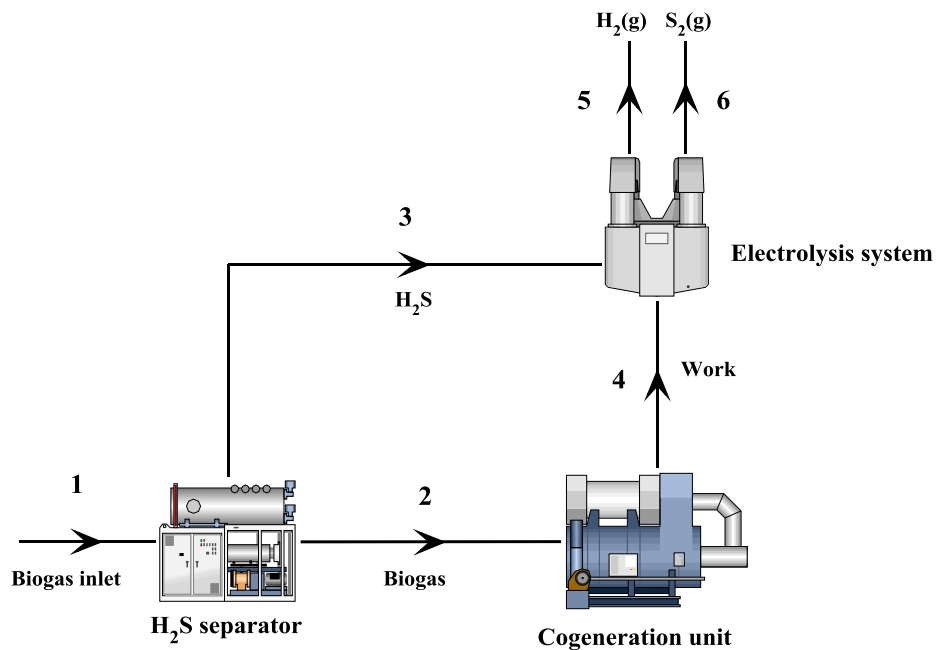


Figure 8.12: Hydrogen production model-5

In the model-5 (see Figure 8.12), a hydrogen sulfide (H_2S) electrolysis process is developed for the hydrogen production. Biogas produced by anaerobic digestion of sludge is mostly methane (up to 60%), the remaining part is mostly acid gases, primarily carbon dioxide, with hydrogen sulfide causing the most problems. When biogas is directly burned as a fuel, engines tend to wear out quickly. To prevent this, H_2S in the biogas is eliminated in a desulfurization unit (DeSO_x) before the combustion process. Although its presence in the biogas may cause lots of system and environmental problems, the energy demand for the electrolysis process of H_2S is lower about 3.25 times than that of the water. In the model-5, biogas produced by the anaerobic digestion of sludge in the WWTP is first passed through a hydrogen sulfide separator and H_2S content of it is collected. Biogas with H_2S free enters the cogeneration unit with the same mass flow rate as in the case of model-1 and 1000 kWh electricity is produced. The mass flow rate of H_2S entering the electrolysis process is 0.0021 kg/s, which can be found theoretically by taking the H_2S content of the biogas produced. In this model, due to the small amount of H_2S collected, the work demand of the electrolysis process is in small quantities (5.83 kWh for GASKI WWTP case).

Model-6:

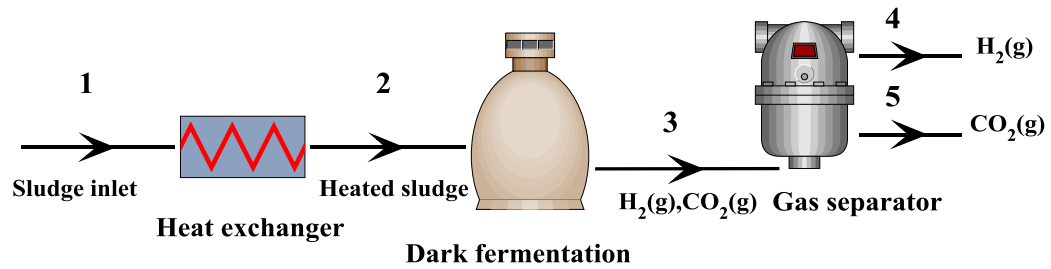


Figure 8.13: Hydrogen production model-6

In the model-6 (see Figure 8.13), a fermentative hydrogen production (biohydrogen) model is considered. In this process digested sewage sludge can be used directly for the hydrogen production in the fermentative conditions. In contrast to anaerobic methane digestion in which the intermediate product hydrogen is converted to methane, the final product of the dark fermentation process is hydrogen. An important distinction with anaerobic methane digestion is that in hydrogen fermentations only hydrogen producing microorganisms are active. The mass flow rate of the sludge before the digestion and fermentation processes in the WWTP is 12.06 kg/s. Since hydrogen produced through dark fermentation is only 60% by volume, it must be purified by using a gas separator.

Model-7:

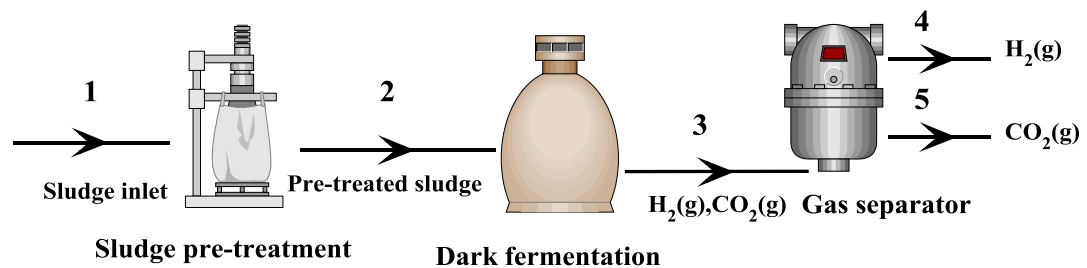


Figure 8.14: Hydrogen production model-7

In the model-7 (see Figure 8.14), a fermentative hydrogen production (biohydrogen) model with sludge pretreatment is considered. This pre-treatment process is performed by means of physical or chemical methods and resulting organic

compounds are converted into hydrogen, acetic acid and carbon dioxide. In the model-7, pre-treatment process is applied to the activated sludge to increase hydrogen production. The mass flow rate of the sludge before the digestion and fermentation processes in the WWTP is 12.06 kg/s.

8.5 Hydrogen Storage

If the greatest challenge in hydrogen use is to extract it, the second greatest challenge is how to store it. Hydrogen has the lowest gas density and the second-lowest boiling point of all known substances, making it a challenge to store as either a gas or a liquid and also as a solid. As a gas, it requires very large storage volumes and pressures. As a liquid, it requires a cryogenic storage system [154].

The most common method to store hydrogen in gaseous form is in steel tanks, although lightweight composite tanks designed to endure higher pressures are also becoming more and more common. Cryogas, gaseous hydrogen cooled to near cryogenic temperatures, is another alternative that can be used to increase the volumetric energy density of gaseous hydrogen. A more novel method to store hydrogen gas at high pressures is to use glass microspheres. The most promising methods to store hydrogen gas under high pressure are composite tanks and glass microspheres [152].

A schematic of a typical high-pressure, C-fibre-wrapped H₂ storage composite tank is shown in Figure 8.15. The advantages composite tanks are their low weight meets key targets, and the tanks are already commercially available, well-engineered and safety-tested, since extensive prototyping experience exists. They also meet codes that are accepted in several countries for pressures in the range of 350-700 bars. Composite tanks require no internal heat exchange and may be usable for cryogas. Their main disadvantages are the large physical volume required, the fact that the ideal cylindrical shape makes it difficult to conform storage to available space, their high cost, and the energy penalties associated with compressing the gas to very high pressures. There are also some safety issues that still have not been resolved, such as the problem of rapid loss of H₂ in an accident [152].

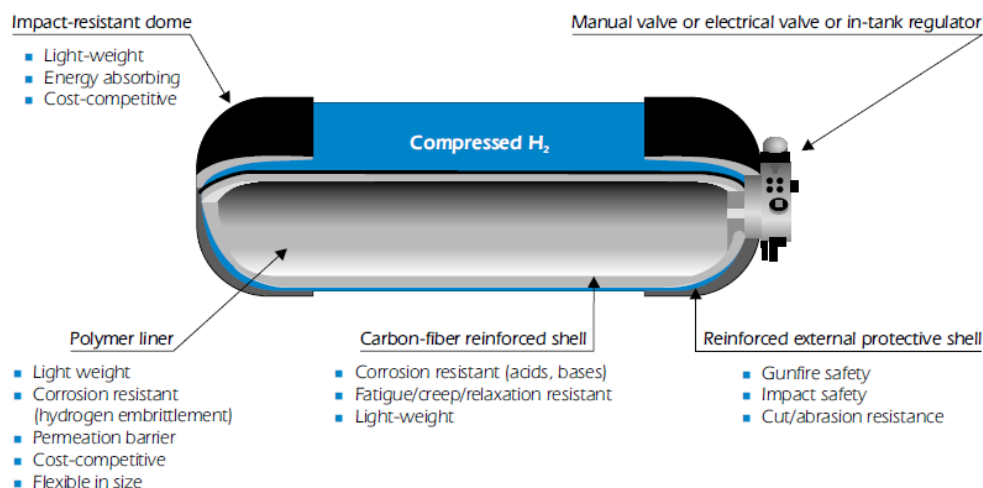


Figure 8.15: Schematic of a typical compressed H₂ gas composite tank [152]

The basic concept for how glass microspheres can be used to store hydrogen gas onboard a vehicle can be described by three steps: charging, filling and discharging. First, hollow glass spheres are filled with H₂ at high pressure (350-700 bar) and high temperature (300°C) by permeation in a high-pressure vessel. Next, the microspheres are cooled down to room temperature and transferred to the low-pressure vehicle tank. Finally, the microspheres are heated to ca. 200-300 °C for controlled release of H₂ to run the vehicle. The main problem with glass microspheres is the inherently low volumetric density that can be achieved and the high pressure required for filling [152].

Liquid hydrogen storage systems overcome many of the weight and size problems associated with high-pressure gas storage systems, albeit at cryogenic temperatures. Liquid hydrogen can be stored just below its normal boiling point of -253 °C (20 K) at or close to ambient pressure in a double walled, super insulating tank. Up to 40% of the energy content in the hydrogen can be lost during the liquefaction operation. The liquid hydrogen storage is very expensive in comparison to other methods. The advantage of liquid hydrogen is its high energy-to-mass ratio, three times that of gasoline. However, it is difficult to store and the insulated tank required may be large and bulky [159]. The precooled Linde–Hampson cycle is a well-known and relatively simple system used for the liquefaction of gases including hydrogen (Figure 8.16).

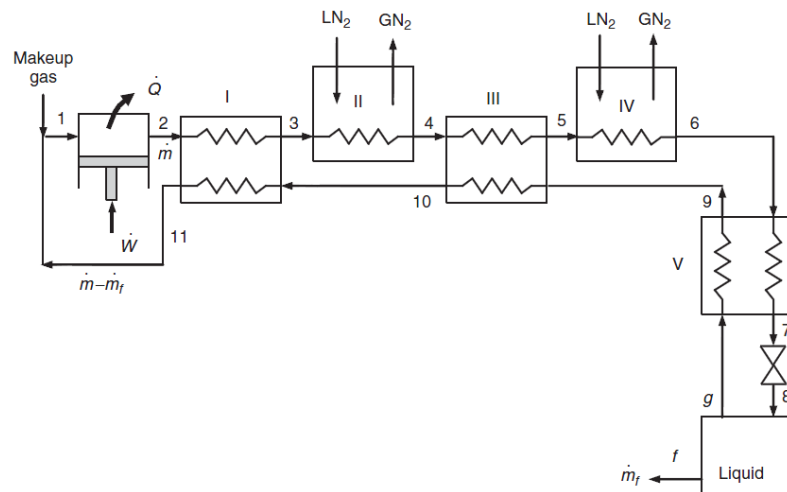


Figure 8.16: Schematic of a Precooled Linde–Hampson liquefaction cycle. [161]

8.6 Conclusion

In this chapter, seven hydrogen production models developed for the GASKI WWTP are presented using the actual operational data which will be given in detail Chapter 9.

CHAPTER 9

RESULTS AND DISCUSSION

9.1 Introduction

In an effectively managed wastewater treatment plant, to develop an adequate cost model to be applied is extremely important because non-stop sewage flowing to the plant has a direct relation with the total value of energy resources to be consumed in the treatment process. Conventional energy and economic valuations of a wastewater treatment system may be used as the tools to understand the characteristics of the costs and benefits of internal flows. However, to understand the real causes and sources of costs which have undeniable impacts on cost structure of the system, we need to develop a more methodological approach that has a fundamental and direct correlation with inefficiencies appeared in the processes and devices of the system. Thermodynamic analysis, using exergy as a basis, can help determine the real costs of producing commodities and in pricing such products. Also, it can help evaluate economic viability and profitability. Energy analysis based on the first law of thermodynamics do not properly describe factors that cause performance to deviate from ideality [162], on the other hand exergy analysis based on the second law of thermodynamics overcomes many of the shortcomings of energy analysis, identifying properly the causes, locations and magnitude of inefficiencies [163].

In this chapter, energy, exergy and exergoeconomic analysis and optimization of GASKI Municipal WWTP and biogas engine powered cogeneration (BEPC) system are conducted using the methodologies described in earlier chapters. The results are obtained and discussed.

9.2 Description of GASKI Wastewater Treatment plant

GASKI Wastewater Treatment Plant (WWTP) is a municipal wastewater treatment facility installed in Gaziantep, Turkey, and the flow schematic of the facility is given in figure 9.1. This plant treats nearly 222,000 m³/day of domestic wastewater using primary, secondary (biological) and tertiary (anaerobic sludge digestion) treatments.

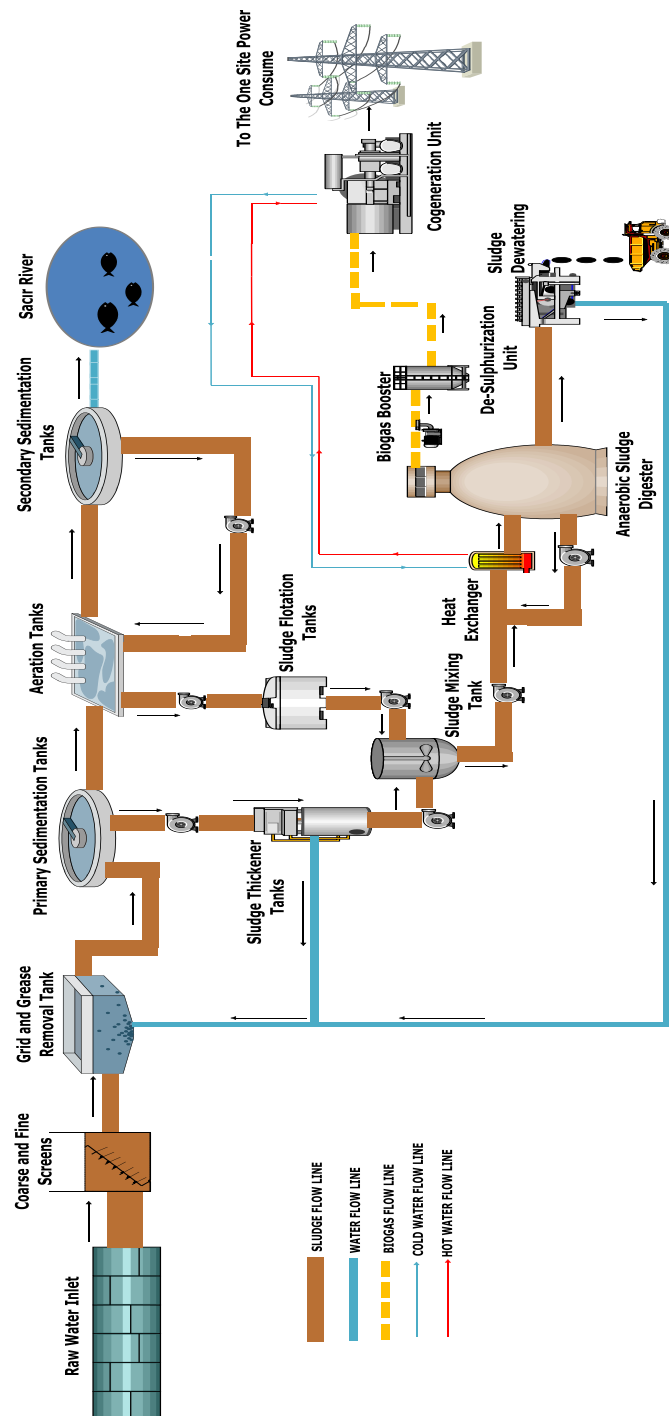


Figure 9.1: A simple flow schematic of GASKI WWTP

9.2.1 Primary Treatment System

The basic wastewater treatment process in GASKI WWTP starts with wastewater flowing into the treatment plant from sewers connected to city's homes and businesses. The incoming wastewater, called influent, passes through screens consisting of upright bars which remove large pieces of trash including rags, sticks, papers, bottles, plastic cups and other similar items. This protects the main sewage pumps and other equipment. The garbage is transported to landfills. The main sewage pumps then lift the wastewater from the screening chamber to the surface level of the plant. Next, the wastewater enters primary settling tanks, also called sedimentation tanks, for one to two hours (see Figure 9.2). The flow of the water is slowed, allowing heavier solids to settle to the bottom of the tank and the lighter materials to float. At the end of the process, the floatable trash, such as grease and small plastic material, rises and is skimmed from the top of the tanks surface. The settled solids, called primary sludge, are then pumped through cyclone degraders, which are devices that use centrifugal force to separate out sand, grit and gravel. This grit is removed, washed and taken to landfills. The degraded primary sludge is pumped to the plant's sludge handling facilities for further processing. The partially treated wastewater from the primary settling tanks then flows to the secondary treatment system. The total mass flow rate of sewage input to GASKI WWTP is 2566.23 kg/s and the non-treated part of the sewage being sent to the outlet chambers in the STP is 86.23 kg/s.

9.2.2 Secondary Treatment System

Secondary treatment is called the activated sludge process (see Figure 9.3). This is because air and sludge from the plant treatment process are added to the wastewater to break it down further. Air pumped into large aeration tanks mixes the wastewater and sludge that stimulates the growth of oxygen-using bacteria and other tiny organisms that are naturally present in the sewage. These beneficial microorganisms consume most of the remaining organic materials that pollute the water and this produces heavier particles that will settle later in the treatment process. Wastewater passes through these bubbling tanks in three to six hours. The aerated wastewater then flows to the final settling tanks. Here the heavy particles and other solids settle to the bottom as secondary sludge.

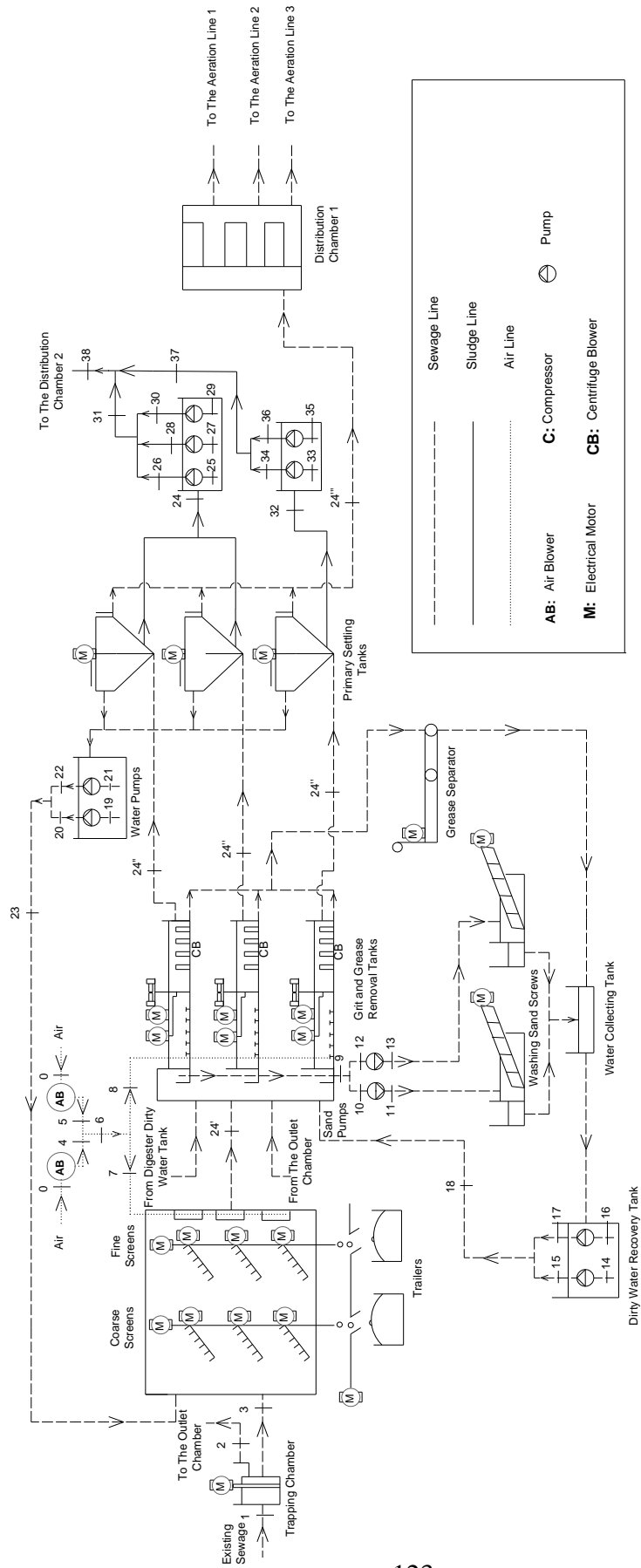


Figure 9.2: Schematic of Primary Treatment Process of GASKI WWTP

Some of this sludge is re-circulated back to the aeration tanks as “seed” to stimulate the activated sludge process. The returned sludge contains millions of microorganisms that help maintain the right mix of bacteria and air in the tank and contribute to the removal of as many pollutants as possible. The remaining secondary sludge is removed from the settling tanks and added to the primary sludge for further processing in the sludge handling facilities. Wastewater passes through the settling tanks in two to three hours and then flows to a disinfection tank.

Even after the primary and secondary treatment, disease-causing organisms may remain in the treated wastewater. To disinfect and kill harmful organisms, the wastewater spends a minimum of 15-20 minutes in chlorine-contact tanks mixing with sodium hypochlorite, the same chemical found in common household bleach. The treated wastewater, or effluent, is then released into the local river. The total mass flow rate of the treated water is 2000.0 kg/s. Disinfection is an essential step because it protects the health of people who use local rivers and enjoy other recreational activities on or near the water. Wastewater (sewage) inlet and exit conditions for the plant are given in Table 9.1.

Table 9.1: Wastewater inlet and exit conditions for GASKI WWTP^a

Parameter	Sewage Inlet (Influent)	Sewage Exit (Effluent)
pH	7.80	7.80
TDS [*] (mg/l)	373.10	16.41
BOD ₅ (mg/l)	372.40	22.01
COD (mg/l)	661.32	64.37

^{*}TDS: Total Dissolved Solids; BOD: Biological Oxygen Demand; COD: Chemical Oxygen Demand

^aThese values are obtained from GASKI WWTP management, which were available in “GASKI WWTP Activity Assessment Report, 2010”, a legal document prepared by the plant management.

9.2.3 Sludge Flotation and Thickening System

The sludge produced by primary and secondary treatment is approximately 99% water and must be concentrated to enable its further processing. Thickening tanks allow the sludge to collect, settle and separate from the water for up to 24 hours (see Figure 9.4). The water is then sent back to the entrance of the plant or to the aeration tanks for additional treatment. The mass flow rate of the sludge is reduced to 12.06 kg/s after the flotation and thickening system.

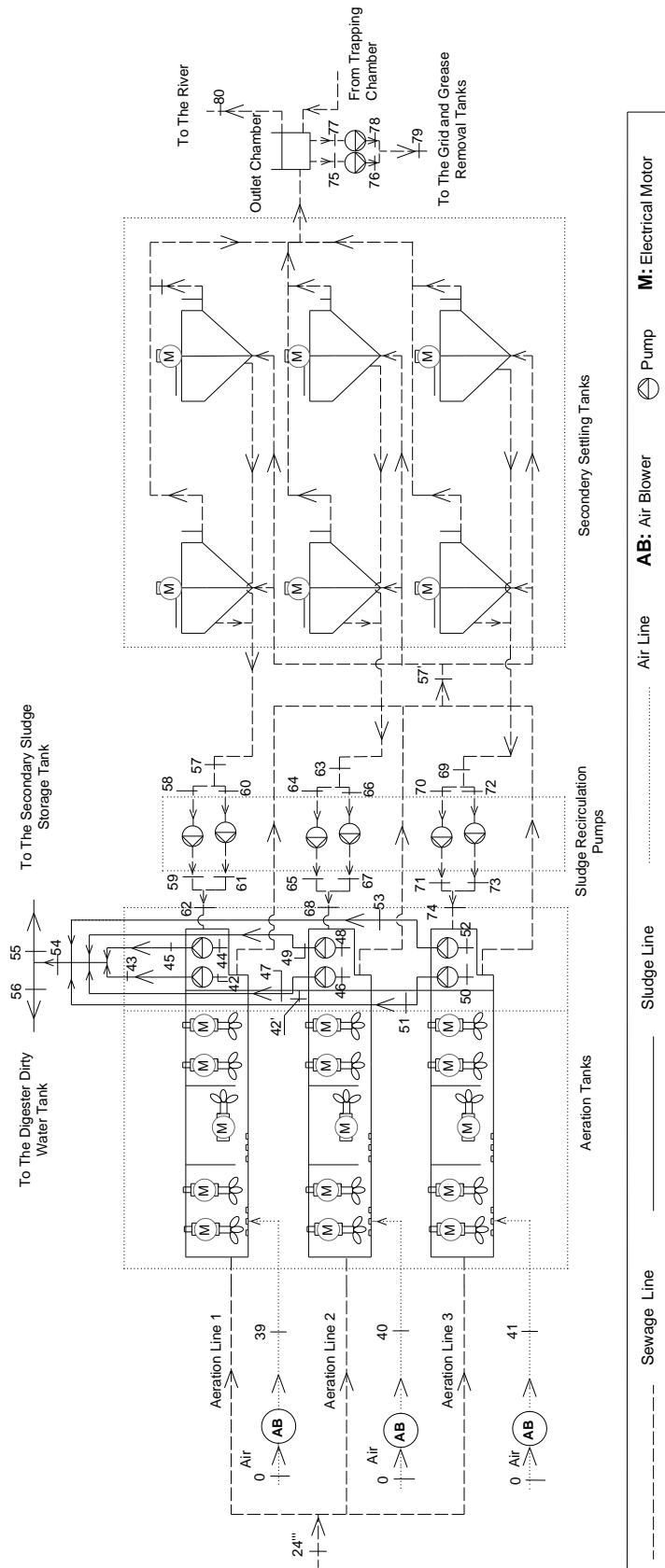


Figure 9.3: Schematic of Secondary Treatment Process of GASKI WWTP

9.2.4 Anaerobic Sludge Digestion System

After thickening and flotation, the sludge is further treated to produce biogas and also to make it safer for the environment. The sludge is placed in oxygen-free tanks, called anaerobic digesters, and heated to 35-40°C for between 15 to 20 days (see Figure 9.5). This stimulates the growth of anaerobic bacteria, which consume organic material in the sludge. Unlike the bacteria in the aeration tanks, these bacteria thrive in an oxygen-free or anaerobic environment. The digestion process stabilizes the thickened sludge by converting much of the material into water, carbon dioxide and methane gas. The black sludge that remains after digestion has the consistency of pea soup and has little odor. This is called digested sludge.

Sludge digestion in the plant achieved by anaerobic high-rate digestion process. Reactors for anaerobic digestion consist of closed tanks with airtight covers. The sludge in the reactors is mechanically mixed to ensure better contact between the organics and the microorganisms, and the units are heated to increase the metabolic rate of the microorganisms, thus speeding up the digestion process. Anaerobic digestion can occur at temperatures as low as 0°C, but the rate of methane production increases with increasing temperature until a relative maximum is reached at 35 to 37°C. In the plant, controlled digestion is performed in mesophilic (30-40°C) temperature conditions. Optimum heating temperature in reactors is around 35°C. The activated sludge loading rate to the reactors is 800-1200 tons per day with the density of 35-55 g/l and the total volume of reactors is 32,000 m³. At the end of the anaerobic sludge digestion process, 10,000-18,000 m³ biogas is generated daily which means approximately 60% of the organic fraction is converted to liquid and gaseous end products after a 15-day period. The higher and lower heating values of biogas containing 55-75% methane ranges between 22-30 MJ/Nm³ and 19-26 MJ/Nm³, respectively [164]. The composition of biogas produced through anaerobic digestion reactors in the plant is given in Table 9.2.

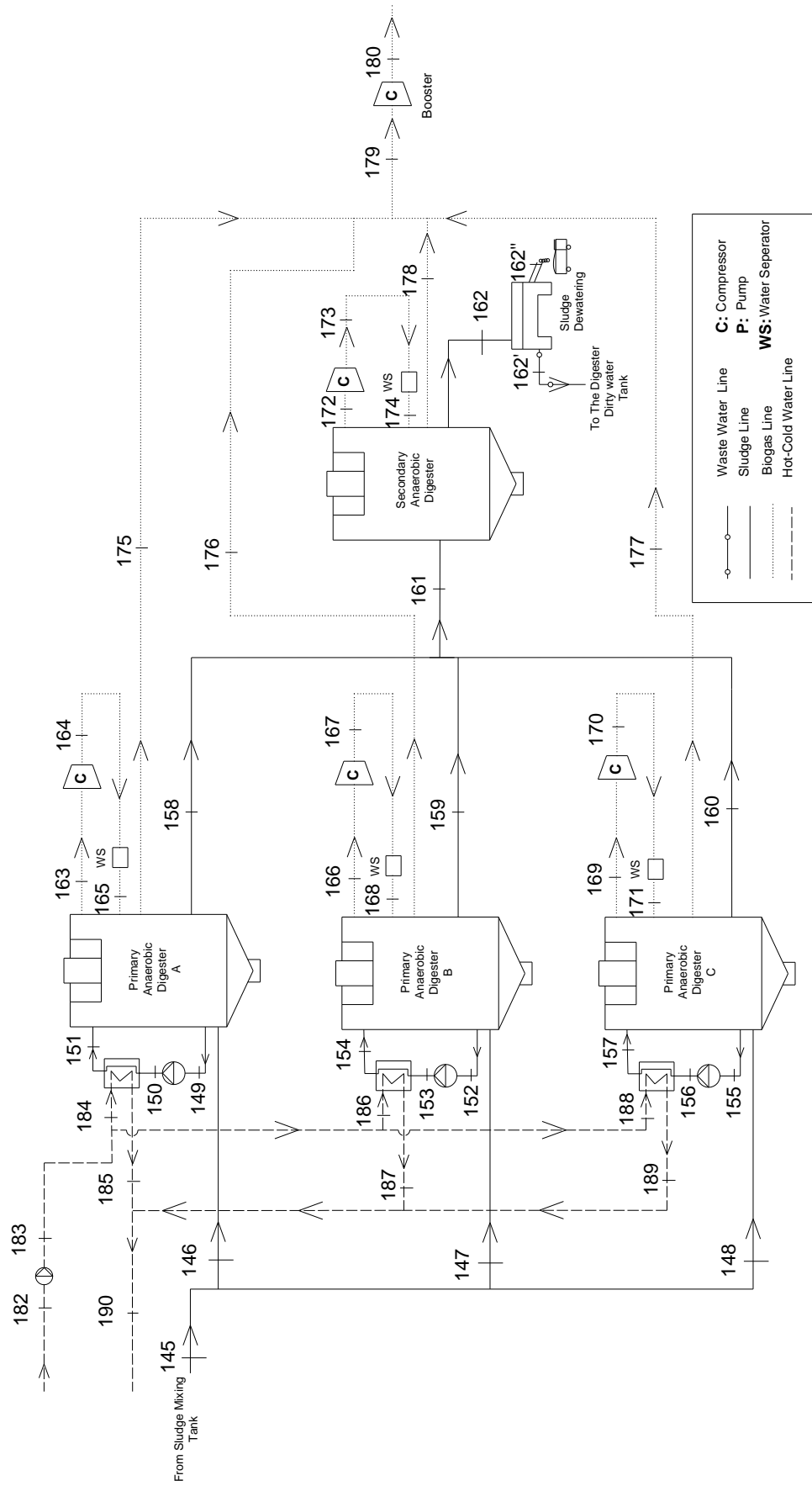


Figure 9.5: Schematic of Anaerobic Digestion Process of GASKI WWTP

Table 9.2: The produced biogas composition in GASKI WWTP^a

Content	Volumetric values (%)
CH ₄	60
CO ₂	35
N ₂	1.5
H ₂	0.3
O ₂	0.5
H ₂ S (2500-3000 ppm)	0.25-0.30
LHV (kJ/kg)	17,892
HHV (kJ/kg)	21,250

^aThese values are obtained from GASKI WWTP management, which were available in “GASKI WWTP Activity Assessment Report, 2010”, a legal document prepared by the plant management.

Digested sludge from anaerobic reactors is collected in a sludge storage tank and is pumped to a dewatering facility. Dewatering reduces the liquid volume of sludge by about 80%. At this process, digested sludge is sent through large centrifuges that operate like the spin cycle of a washing machine. The force from the very fast spinning of the centrifuges separates most of the water from the solids in the sludge, creating a substance known as “biosolid” (i.e. biomass). The water drawn from the spinning process is then returned to the grit and grease removal tanks for reprocessing. Adding a substance called organic polymer improves the consistency of the “sludge cake”, resulting in a firmer, more manageable product. The biosolid cake is approximately 22 percent solid material. The sludge cake is then eliminated in the city’s waste incineration plant.

9.3 Description of Biogas Engine Powered Cogeneration System

Biogas produced through anaerobic sludge digestion process is first transferred to desulphurization ($DeSO_x$) unit for lowering sulphur content to the acceptable legal values and then to a gas engine for electricity production. The total electric produced by the biogas powered gas engine is 1000 kWh, which is used within the wastewater treatment facility. A schematic diagram of the biogas engine powered cogeneration unit of GASKI WWTP with all flow streams is shown in Figure 9.6.

The biogas engine in the GASKI WWTP cogeneration facility is a DEUTZ TCG 2020 V12K gas engine which is a four stroke, spark ignition engine with 12 cylinders in a V configuration. It uses biogas which is produced by anaerobic digestion reactors. The annual electrical energy production is 8.760 GWh, and the annual biogas consumption is nearly 3,400,000 m³ at designed operating conditions, which

means 61% of the biogas produced through anaerobic digesters is consumed by on-site cogeneration system of the plant. In the cogeneration process, the biogas is first mixed with air before flowing through the intake valves of the gas engine. When the engine is started, air-biogas mixture is charged to the compressor of the turbocharger unit. The compressor of the turbocharger is powered by a turbine mounted in the exhaust flow of the engine. The advantage of this is that none of the engine shaft output is used to drive the compressor, and only waste energy in the exhaust is used. The turbocharger is equipped with an intercooler to lower the compressed air-biogas mixture temperature. The exhaust gases leaving the turbine of the turbocharger enter the exhaust gas heat exchanger (EGHE) to transfer heat to the water, which circulates in a closed loop through primary anaerobic digester unit to supply necessary heat for digestion process (see Figure 9.6). The exhaust gas leaving the EGHE is sent to an exhaust filter which captures and thus reduces the CO_2 and CO emissions. The high temperature water flowing through the engine jacket of the gas engine is first used to heat the water from primary digester units (HE-4). It then enters the lubrication oil heat exchanger (LOHE) for the cooling of lubrication oil from the engine. Finally, it returns back to the gas engine after cooling the water (HE-5) which circulates through intercooler in a closed loop. Oil is used for lubrication and cooling purposes of the engine components.

9.4 Gas Engine Operating and Performance Characteristic

For the engine Deutz TCG-2020, the cylinder bore is $B=170$ mm, piston stroke is $S=195$ mm, and the engine speed is $N=1500$ rpm. The other characteristics of the engine and various engine performance parameters are defined below.

The crank offset a is given as

$$a = S/2 \tag{9.1}$$

Average piston speed is

$$U_p = 2SN \tag{9.2}$$

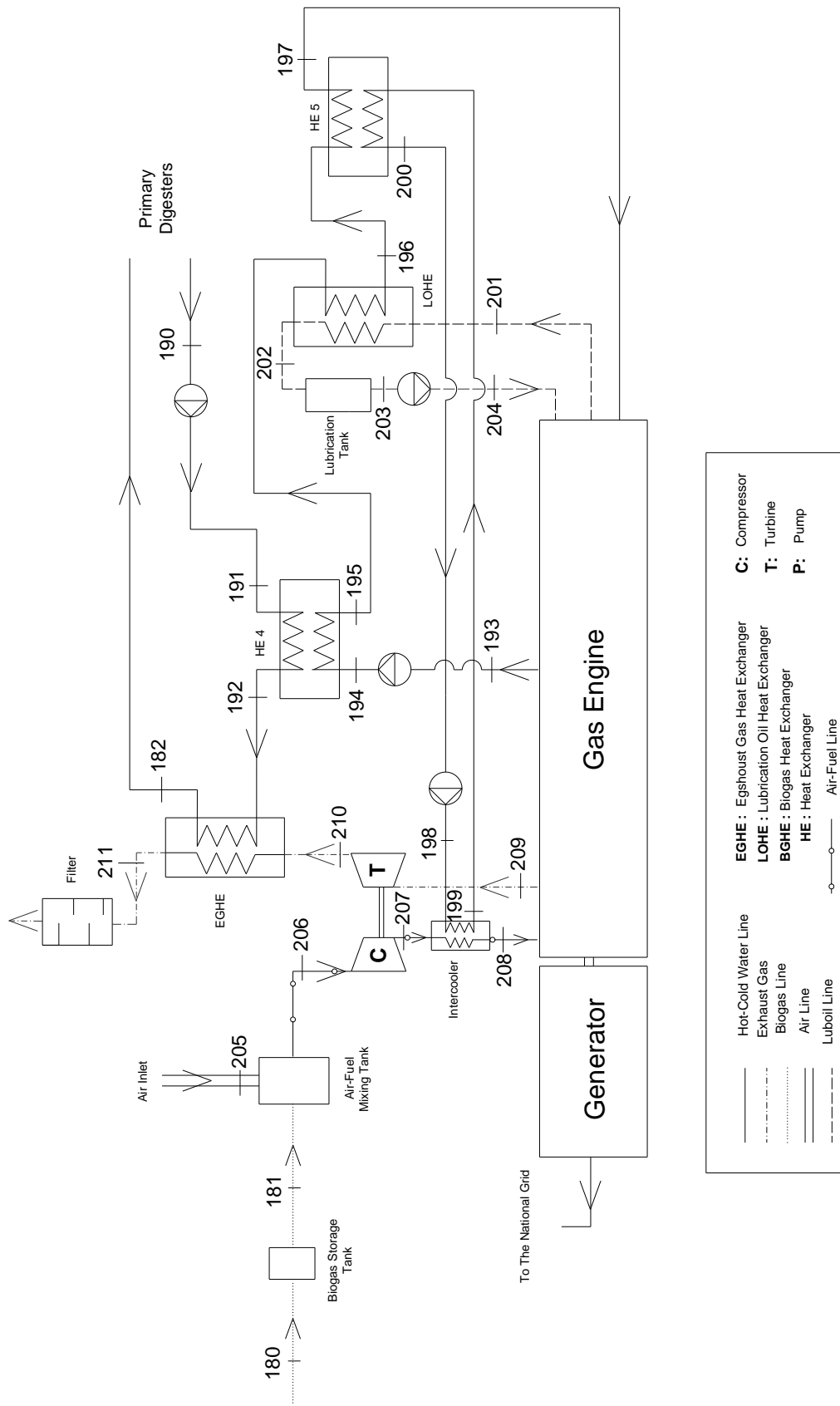


Figure 9.6: Biogas Engine Powered Cogeneration Unit of GASKI WWTP

Piston speed determines the instantaneous flow rate of air–fuel into the cylinder during intake and exhaust flow out of the cylinder during the exhaust stroke [165]. Displacement, or displacement volume V_d is the volume displaced by the piston as it travels from bottom dead center (BDC) to top dead center (TDC)

$$V_d = V_{\text{BDC}} - V_{\text{TDC}} \quad (9.3)$$

Displacement can be given for one cylinder or the entire engine. For one cylinder

$$V_d = \frac{\pi}{4} B^2 S \quad (9.4)$$

For an engine with N_c number of cylinders:

$$V_d = \frac{\pi}{4} B^2 S N_c \quad (9.5)$$

Typical values for engine displacement range from 0.1 cm³, for small model airplanes to about 8 L for large automobiles to much larger numbers for large ship engines. The displacement of a modern average automobile engine is about two to three liters [165].

For a given displacement volume a longer stroke allows for a smaller bore (under square), resulting less surface area in the combustion chamber and correspondingly less heat loss. This increases thermal efficiency within the combustion chamber. However, the longer stroke result in higher piston speed and higher friction losses that reduces the output power, which can be obtained off the crankshaft. If the stroke is shortened, the bore must be increased and the engine will be over square. This decreases friction losses but increases heat transfer losses [165]. Minimum cylinder volume occurs when the piston is at TDC and called the clearance volume V_C

$$V_C = V_{\text{TDC}} = V_d - V_{\text{BDC}} \quad (9.6)$$

The compression ratio is defined as

$$R_C = \frac{V_{\text{BDC}}}{V_{\text{TDC}}} = \frac{(V_C + V_d)}{V_C} \quad (9.7)$$

Modern spark ignition (SI) engines have compression ratios R_C of 6 to 11, while compression ignition (CI) engines have compression ratios in the range 12 to 24. Engines with superchargers or turbochargers usually have lower compression ratios than naturally aspirated engines [165].

Work is the output of any heat engine, and in a reciprocating I.C engine, this work is generated by the gases in the combustion chamber of the cylinder. Force due to gas pressure on the moving piston generates the work in an internal combustion engine cycle.

$$W = \int P dV \quad (9.8)$$

It is convenient to analyze engine cycles per unit mass of gas m within the cylinder. To do so, volume V is replaced with specific volume v and work is replaced with specific work:

$$w = \frac{W}{m}, \quad v = \frac{V}{m}, \quad w = \int P dv \quad (9.9)$$

Specific work is equal to the area under the process lines on the P- v coordinates of indicator diagram. The areas shown in the indicator diagram gives the work inside the combustion chamber and called as Indicated work W_i , but the work delivered by crankshaft is less than indicated one due to mechanical friction and parasitic loads of the engine W_f . Actual work available at the crankshaft is called brake work W_b .

$$W_b = W_i - W_f \quad (9.10)$$

The ratio of brake work to indicated work defines the mechanical efficiency of an engine. Mechanical efficiencies will be on the order of 75 % to 95 %,

$$\eta_m = \frac{W_b}{W_i} \quad (9.11)$$

An average or mean effective pressure (*mep*) is defined by:

$$mep = \frac{w}{\Delta v} = \frac{W}{V_d} \quad (9.12)$$

Mean effective pressure is a good parameter to compare engines for design or output because it is independent of engine size and /or speed. If torque is used for engine comparison, a larger will always look better. If power is used as the comparison speed becomes very important. Various *mep* can be defined by using different work terms. If brake work is used brake mean effective pressure is obtained:

$$bmep = \frac{W_b}{V_d} \quad (9.13)$$

Indicated work gives indicated mean effective pressure:

$$imep = \frac{W_i}{V_d} \quad (9.14)$$

Typical maximum values of *bmep* for naturally aspirated SI engines are in the range of 850 to 1050 kPa. For CI engines, they are 700 to 900 kPa for naturally aspirated engines and 1000 to 1200 kPa for turbocharger engines [165]. Torque is a good indicator of an engine's ability to do work. It is defined as force acting at a moment distance and has units of N-m. Torque is related to work by:

$$2\pi\tau = W_b = (bmep) \frac{V_d}{n} \quad (9.15)$$

$$\tau = (bmep) \frac{V_d}{4\pi} \quad \text{for four stroke cycle} \quad (9.16)$$

Power \dot{W} is defined as the rate of work of the engine. If n = number of revolutions per cycle and N = engine speed, then

$$\dot{W} = W \frac{N}{n} \quad (9.17)$$

Both torque and power are the functions of speed. At low speed torque increases as engine speed increases. As engine speed increases further torque reaches a maximum and then decreases because the engine is unable to ingest a full charge of air at higher speeds. Indicated power increases with speed, while brake power increases to a maximum and then decreases at higher speeds. This is because friction losses increase with speed and become the dominant factor at very high speeds [165].

Other characteristic parameters for an engine are given in equations below.

$$\text{Specific power } SP = \frac{\dot{W}_b}{A_p} \quad (9.18)$$

$$\text{Output per displacement } OPD = \frac{\dot{W}_b}{V_d} \quad (9.19)$$

$$\text{Specific volume } SV = \frac{V_d}{\dot{W}_b} \quad (9.20)$$

$$\text{Specific weight } SW = \frac{(\text{Weight}_{\text{engine}})}{\dot{W}_b} \quad (9.21)$$

Energy input to an engine Q_{in} comes from the combustion of a hydrocarbon fuel. Air is used to supply the oxygen needed for this chemical reaction. For combustion reaction to occur, the proper relative amounts of air (oxygen) and fuel must be present. Air-fuel ratio (AF) and fuel-air ratio (FA) are parameters used to describe the mixture ratio:

$$AF = \frac{m_a}{m_f} = \frac{\dot{m}_a}{\dot{m}_f} \quad (9.22)$$

$$FA = \frac{m_f}{m_a} = \frac{\dot{m}_f}{\dot{m}_a} \quad (9.23)$$

where m_a = mass of air, \dot{m}_a = mass flow rate air, m_f = mass of fuel, \dot{m}_f = mass fuel rate of fuel. Equivalence ratio is defined the actual ratio of fuel–air to ideal or stoichiometric fuel–air:

$$\Phi = \frac{(FA)_{act}}{(FA)_{stoich}} = \frac{(AF)_{stoich}}{(AF)_{act}} \quad (9.24)$$

Fuel consumption of an engine is calculated from the consumption per power generated; this is also called specific fuel consumption (*sfc*) and can be derived for all types of works. The specific fuel consumption equations for brake power and indicated power are given below:

$$bsfc = \frac{\dot{m}_f}{\dot{W}_b} \quad (9.25)$$

$$isfc = \frac{\dot{m}_f}{\dot{W}_i} \quad (9.26)$$

Brake specific fuel consumption decreases as engine speed increases, reaches a minimum and then increases at high speeds because of greater friction losses. It decreases with higher compression rate due to higher thermal efficiency [165]. In order to measure or comment on an engine performance, different types of efficiencies related with engine parameters must be known. These efficiencies are: Combustion efficiency η_c is defined as the fraction of fuel which burns. It has values in the range 0.95 to 0.98 and it is given as

$$\eta_c = \frac{\dot{Q}_{in}}{Q_{HV}\dot{m}_f} \quad (9.27)$$

where Q_{in} is the rate of net heat input to the engine and Q_{HV} is the lower heating value of the fuel. Thermal efficiency is defined as

$$\eta_{th} = \frac{W}{Q_{in}} = \frac{\dot{W}}{\dot{Q}_{in}} = \frac{\dot{W}}{\dot{m}_f \dot{Q}_{HV} \eta_c} = \frac{\eta_f}{\eta_c} \quad (9.28)$$

Thermal efficiency can be given as indicated or brake depending on whether indicated power or brake power is used. Fuel conversion efficiency is defined as

$$\eta_f = \frac{\dot{W}}{\dot{m}_f Q_{HV}} \quad (9.29)$$

Volumetric efficiency is defined as

$$\eta_v = \frac{n\dot{m}_a}{\rho_a V_d N} \quad (9.30)$$

where ρ_a is the density of atmospheric air. Volumetric efficiency is a measure of how much air is ingested into the engine and it could be greater than one for turbocharged engines.

Using the equations given in this section, various engine operating and performance characteristics are calculated and presented in Table 9.3.

9.5 Energy and Exergy Relations

The governing energy and exergy relations for subsystems and components of GASKI WWTP are presented in the Chapter 4. In this chapter, exergetic efficiency definitions related with the main subsystems of GASKI WWTP are improved.

9.5.1 GASKI Wastewater Treatment Plant

Since GASKI WWTP is subdivided to four main systems, the exergetic efficiency for each subsystem must be defined to exhibit its degree of thermodynamic perfection. The total input exergy rate flow of a subsystem is considered as the sum of the input exergy rate of fuel flow and total auxiliary power supply of the equipments in that subsystem. This approach is valuable from a scientific point of view since fuel exergy streams plus total power supply entering to a subsystem is accounted for to produce the main subsystem product output.

Table 9.3: Calculated engine operating and performance characteristics

Cylinder Diameter, D	170	mm
Cylinder Bore, B	170	mm
Stroke, S	195	mm
Crank Offset, a	97.5	mm
Number of Cylinders, N_c	12.0	-
Piston Area, A_p	0.023	m ²
Compression Ratio, r_c	13.5	-
Displacement Volume, V_d	4.425	dm ³
Clearance Volume, V_c	0.354	dm ³
Cylinder Volume, V	4.485	dm ³
Air Flow Rate, \dot{m}_a	1.387	kg/s
Fuel Flow Rate, \dot{m}_f	0.129	kg/s
Air-Fuel Ratio, AF	10.8	-
Lubrication Oil Flow Rate	20.0	kg/s
Exhaust Flow Rate	1.5	kg/s
Piston Mean Speed, U_p	9.8	m/s
Engine Speed, N	1500	rpm
Heating Value, Q_{HV}	17,892	kJ/kg
Break Power, \dot{W}_b	1000	kW
Break Power per Cylinder	50.0	kW
Brake Mean Effective Pressure, bmep	905.3	kPa
Torque, τ	3825	Nm
Brake Specific Fuel Consumption, $bsfc$	0.215	g/kWh
Specific Power, SP	2174	kW/m ²
Specific Volume, SV	0.089	L/kW
Output per Displacement, OPD	11.3	kW/L
Combustion Efficiency, η_c	1.0	-
Volumetric Efficiency, η_v	0.82	-
Thermal Efficiency, η_{th}	43.3	-

Following the assumption given above, the exergetic efficiencies for each subsystem in GASKI WWTP may be written as

1. *Primary Treatment System (PTS)*

$$\varepsilon_{PTS} = \frac{\dot{E}x_{P,PTS}}{\dot{E}x_{F,PTS}^2} = \frac{(\dot{m}_{\text{sewage}} \psi_{\text{sewage}}^T)_{\text{exit of PTS}}}{(\dot{m}_{\text{sewage}} \psi_{\text{sewage}}^T)_{\text{inlet of PTS}} + \dot{W}_{\text{input,PTS}}^T} \quad (9.31)$$

2. *Secondary Treatment System (STS)*

$$\varepsilon_{STS} = \frac{\dot{E}x_{P,STS}}{\dot{E}x_{F,STS}^2} = \frac{(\dot{m}_{\text{treated water}} \psi_{\text{treated water}}^T)_{\text{exit of STS}}}{(\dot{m}_{\text{sewage}} \psi_{\text{sewage}}^T)_{\text{inlet of STS}} + \dot{W}_{\text{input,STS}}^T} \quad (9.32)$$

3. *Flotation and Thickening System (FTS)*

$$\varepsilon_{FTS} = \frac{\dot{E}x_{P,FTS}}{\dot{E}x_{F,FTS}^2} = \frac{(\dot{m}_{\text{sludge}} \psi_{\text{sludge}}^T)_{\text{exit of FTS}}}{(\dot{m}_{\text{sludge}} \psi_{\text{sludge}}^T)_{\text{inlet of FTS}} + \dot{W}_{\text{input,FTS}}^T} \quad (9.33)$$

4. *Anaerobic Digestion System (ADS)*

$$\varepsilon_{ADS} = \frac{\dot{E}x_{P,ADS}}{\dot{E}x_{F,ADS}^2} = \frac{(\dot{m}_{\text{biogas}} \psi_{\text{biogas}}^T)_{\text{exit of ADS}}}{(\dot{m}_{\text{sludge}} \psi_{\text{sludge}}^T)_{\text{inlet of ADS}} + \dot{W}_{\text{input,ADS}}^T + \dot{E}x_{\text{heat input,ADS}}} \quad (9.34)$$

where ε_{PTS} , ε_{STS} , ε_{FTS} and ε_{ADS} are the exergetic efficiencies of primary treatment system, secondary treatment system, flotation and thickening system and anaerobic digestion system respectively; \dot{m}_{sewage} , $\dot{m}_{\text{treated water}}$, \dot{m}_{sludge} and \dot{m}_{biogas} are the mass flow rates of sewage, treated water, sludge and biogas at the given state, respectively; ψ_{sewage}^T , $\psi_{\text{treated water}}^T$, ψ_{sludge}^T and ψ_{biogas}^T are the total specific exergies of the sewage, treated water, sludge and biogas at the given state, respectively.

The overall exergetic efficiency of GASKI WWTP is defined according to the digested sludge output use at the end of the treatment process. In the actual case, at the end of the digestion process, sludge is dewatered and used for land applications

such as agricultural application. Thus this sludge is not considered as a useful plant output in exergetic point of view. In this case, the only useful outputs of GASKI WWTP are considered as the treated wastewater and biogas. Thus, the exergetic efficiency of GASKI WWTP may be defined as

$$\varepsilon_{\text{GASKI WWTP}}^1 = \frac{\sum_i \dot{E}x_{P,i}}{\sum_j \dot{E}x_{F,j}} = \frac{\left(\dot{m}_{\text{treated water}} \psi_{\text{treated water}}^T\right)_{\text{exit of STS}} + \left(\dot{m}_{\text{biogas}} \psi_{\text{biogas}}^T\right)_{\text{exit of ADS}}}{\left(\dot{m}_{\text{sewage}} \psi_{\text{sewage}}^T\right)_{\text{inlet of PTS}} + \dot{W}_{\text{GASKI WWTP}}^T} \quad (9.35)$$

However, instead of the elimination of this digested sludge in an incineration facility, it may be utilized as a valuable secondary fuel source for off-site applications such as a cement facility. Then it would become one of the useful product outputs of the treatment system. In this second case, the exergetic efficiency of GASKI WWTP may be defined as

$$\varepsilon_{\text{GASKI WWTP}}^2 = \frac{\sum_i \dot{E}x_{P,i}}{\sum_j \dot{E}x_{F,j}} = \frac{\left(\dot{m}_{\text{treated water}} \psi_{\text{treated water}}^T\right)_{\text{exit of STS}} + \left(\dot{m}_{\text{biogas}} \psi_{\text{biogas}}^T\right)_{\text{exit of ADS}} + \left(\dot{m}_{\text{sludge}} \psi_{\text{sludge}}^T\right)_{\text{exit of ADS}}}{\left(\dot{m}_{\text{sewage}} \psi_{\text{sewage}}^T\right)_{\text{inlet of PTS}} + \dot{W}_{\text{GASKI WWTP}}^T} \quad (9.36)$$

9.5.2 Biogas Engine Powered Cogeneration System

For the biogas engine in the cogeneration system, the thermal efficiency may be expressed as the ratio of net power produced to the fuel (biogas) energy input:

$$\eta_{\text{biogas engine}} = \frac{\dot{W}_{\text{net}}}{\dot{m}_{\text{biogas}} q_{\text{LHV, biogas}}} \quad (9.37)$$

The exergetic efficiency of the biogas engine may be defined by three approaches. In the first approach, the exergetic efficiency is defined as the net power divided by the rate of fuel exergy input:

$$\varepsilon_{\text{biogas engine}}^1 = \frac{\dot{W}_{\text{net}}}{\dot{m}_{\text{biogas}} \psi_{\text{biogas}}^T} \quad (9.38)$$

In the second approach, the process heat output due to using exhaust gases to heat water circulating through anaerobic digesters is also considered. The system in this case is a cogeneration system with work and process heat outputs. Then the exergetic efficiency may be written as (see Figure 9.6)

$$\varepsilon_{\text{biogas engine}}^2 = \frac{\dot{W}_{\text{net}} + \dot{E}x_{\text{process}}}{\dot{m}_{\text{biogas}} \psi_{\text{biogas}}^T} \quad (9.39)$$

In the third approach, we consider all fluid streams entering and leaving the biogas engine and express the exergy efficiency as the total exergy output from the engine divided by the total exergy input to the engine (see Figure 9.6):

$$\varepsilon_{\text{biogas engine}}^3 = \frac{\dot{W}_{\text{net}} + \dot{E}x_{193} + \dot{E}x_{201} + \dot{E}x_{209}}{\dot{m}_{\text{biogas}} \psi_{\text{biogas}}^T + \dot{E}x_{197} + \dot{E}x_{204}} \quad (9.40)$$

Expressing the exergy of process heat as the exergy change of water, this equation may be written for this biogas engine powered cogeneration (BEPC) system as

$$\varepsilon_{\text{BEPC}} = \frac{\dot{W}_{\text{net}} + \dot{E}x_{\text{process}}}{\dot{E}x_{\text{biogas}}^T} = \frac{\dot{W}_{\text{net}} + \dot{m}_{\text{water}} [h_e - h_i - T_0(s_e - s_i)]_{\text{water}}}{\dot{m}_{\text{biogas}} \psi_{\text{biogas}}^T} \quad (9.41)$$

The overall exergetic efficiency of GASKI WWTP including biogas engine powered cogeneration system (BEPC) may be defined as the total exergy rate of principal outputs (treated water, electricity produced, and digested sludge) divided by the total exergy rate of inputs (sewage and total electricity supply)

$$\begin{aligned}
\varepsilon_{\text{WWTP\&BEPC}}^{\text{GASKI}} &= \frac{\sum_i \dot{E}x_{P,i}}{\sum_j \dot{E}x_{F,j}} \\
&= \frac{\left(\dot{m}_{\text{treated water}} \psi_{\text{treated water}}^T\right)_{\text{exit of STS}} + \dot{W}_{\text{net}} + \left(\dot{m}_{\text{sludge}} \psi_{\text{sludge}}^T\right)_{\text{exit of ADS}}}{\left(\dot{m}_{\text{sewage}} \psi_{\text{sewage}}^T\right)_{\text{inlet of PTS}} + \left(\dot{W}_{\text{net}} + \dot{W}_{\text{from national grid}}\right)}
\end{aligned} \tag{9.42}$$

9.6 Results and Discussion for Energy and Exergy Analysis

The GASKI WWTP including biogas engine powered cogeneration system (BEPC) is divided into five subsystems and each subsystem is analyzed and evaluated by the thermodynamic relations developed in the first part of the study and using the data provided by GASKI WWTP and BEPC.

9.6.1 Energy and Exergy Analysis of Primary Treatment System (PTS)

The temperature, pressure, and mass flow rate data and the resulting energy and exergy rates in the plant are presented in Table 9.4 according to the nomenclature shown in Figure 9.2. The chemical oxygen demand (COD) value of the sewage at the inlet of the PTS is determined to be 661.32 mg/l (see Table 9.1). The specific chemical exergy of the sewage at the inlet of wastewater treatment system is calculated using Equation (4.22) given in the Chapter 4 as 9.0 kJ/kg. Since the total mass flow rate of sewage input to GASKI WWTP is 2566.23 kg/s, the total exergy rate of sewage at the PTS inlet is found to be 23,096 kW. This value is the total sum of the exergy rates of the sewage being treated through the PTS (2480 kg/s) and the non-treated part of the sewage being sent to the outlet chambers in the STP (86.23 kg/s). The non-treated part of the sewage is used to increase the bacterial content of the sludge as the seed for further treatment steps. At the exit of the PTS, assuming the COD value of the half-treated sewage reduces to 367.6 mg/l due to the decreasing BOD₅ value [3], the specific chemical exergy of the sewage is obtained as 5.0 kJ/kg and the corresponding total exergy rate of sewage becomes 11,420 kW. Note that the non-treated part of the sewage has a total exergy rate of 776.1 kW. Since the dry matter content of the activated sludge is less than 0.1% at the exit of the primary treatment process, it may be considered like sewage. Then, the total exergy rate of sludge at the PTS exit is calculated separately to be 1060.30 kW.

Table 9.4: Primary Treatment System data, thermodynamic properties, energy and exergy rates in the plant with respect to state points in Figure 9.2

State No	Fluid	Pressure P (bar)	Temperature T (°C)	Mass flowrate \dot{m} (kg/s)	Enthalpy h (kJ/kg)	Entropy s (kJ/kg°C)	Specific energy e (kJ/kg)	Total specific exergy ψ^T (kJ/kg)	Energy rate \dot{E} (kW)	Total exergy rate $\dot{E}x^T$ (kW)
0	Air	1.00	25.00	-	298.40	5.6990	0.000	0.000	0.00	0.00
0'	Water	1.00	25.00	-	104.20	0.3648	0.000	0.000	0.00	0.00
0''	Sewage	1.00	25.00	-	104.20	0.3648	---	---	---	---
0'''	Sludge	1.00	25.00	-	104.20	0.3648	---	---	---	---
1	Sewage	1.00	25.00	2566.23	104.20	0.3648	0.000	9.000	0.00	23,096.07
2	Sewage	1.00	25.00	86.23	104.20	0.3648	0.000	9.000	0.00	776.07
3	Sewage	1.00	25.00	2480.00	104.20	0.3648	0.000	9.000	0.00	22,320.00
4	Air	1.79	90.00	0.34	363.90	5.7300	65.430	56.010	22.25	19.04
5	Air	1.79	90.00	0.34	363.90	5.7300	65.430	56.010	22.25	19.04
6	Air	1.79	90.00	0.68	363.90	5.7300	65.430	56.010	44.49	38.09
7	Air	1.79	90.00	0.34	363.90	5.7300	65.430	56.010	22.25	19.04
8	Air	1.79	90.00	0.34	363.90	5.7300	65.430	56.010	22.25	19.04
9	Sewage	1.05	25.05	36.05	104.40	0.3655	0.2138	9.005	7.707	324.63
10	Sewage	1.05	25.05	12.02	104.40	0.3655	0.2138	9.005	2.57	108.24
11	Sewage	3.40	25.00	12.02	104.50	0.3651	0.321	9.241	3.86	111.08
12	Sewage	1.05	25.05	24.03	104.40	0.3655	0.2138	9.005	5.14	216.39
13	Sewage	4.30	25.00	24.03	104.70	0.3652	0.441	9.331	10.60	224.22
14	Sewage	1.17	25.60	66.67	106.70	0.3732	2.526	9.020	168.40	601.36
15	Sewage	2.17	25.60	66.67	106.90	0.3733	2.659	9.120	177.30	608.03
16	Sewage	1.17	25.60	66.67	106.70	0.3732	2.526	9.020	168.40	601.36
17	Sewage	2.17	25.60	66.67	106.90	0.3733	2.659	9.120	177.30	608.03
18	Sewage	2.17	25.60	133.3	106.90	0.3733	2.659	9.120	354.60	1215.70
19	Sewage	1.17	25.30	2.00	105.50	0.3690	1.271	9.018	2.54	18.04
20	Sewage	8.37	25.40	2.00	106.40	0.3698	2.234	9.740	4.47	19.48
21	Sewage	1.17	25.30	2.00	105.50	0.3690	1.271	9.018	2.54	18.04
22	Sewage	8.37	25.40	2.00	106.40	0.3698	2.234	9.740	4.47	19.48
23	Sewage	8.37	25.40	4.00	106.40	0.3698	2.234	9.740	8.93	38.96
24'	Sewage	1.10	25.50	2484	106.30	0.3718	2.101	9.012	5218.88	22,385.81
24''	Sewage	1.15	25.60	2480	106.70	0.3732	2.524	9.018	6259.5	22,364.64
24	Sludge	1.17	25.20	121.2	105.10	0.3676	0.852	5.017	103.26	608.06
24'''	Sewage	1.18	25.70	2274	107.20	0.3746	2.945	5.022	6693.93	11,420.03
25	Sludge	1.17	25.20	40.40	105.10	0.3676	0.852	5.017	34.43	202.69
26	Sludge	3.48	25.20	40.40	105.40	0.3679	1.161	5.249	46.91	212.06
27	Sludge	1.17	25.20	40.40	105.10	0.3676	0.852	5.017	34.43	202.69
28	Sludge	3.48	25.20	40.40	105.40	0.3679	1.161	5.249	46.91	212.06
29	Sludge	1.17	25.20	40.40	105.10	0.3676	0.852	5.017	34.43	202.69
30	Sludge	3.48	25.20	40.40	105.40	0.3679	1.161	5.249	46.91	212.06
31	Sludge	3.48	25.20	121.2	105.40	0.3679	1.161	5.249	140.70	636.18
32	Sludge	1.17	25.20	80.80	105.10	0.3676	0.852	5.017	68.84	405.37
33	Sludge	1.17	25.20	40.40	105.10	0.3676	0.852	5.017	34.43	202.69
34	Sludge	3.48	25.20	40.40	105.40	0.3679	1.161	5.249	46.91	212.06
35	Sludge	1.17	25.20	40.40	105.10	0.3676	0.852	5.017	34.43	202.69
36	Sludge	3.48	25.20	40.40	105.40	0.3679	1.161	5.249	46.91	212.06
37	Sludge	3.48	25.20	80.80	105.40	0.3679	1.161	5.249	93.83	424.12
38	Sludge	3.48	25.20	202.0	105.30	0.3676	1.066	5.249	215.30	1060.30

As explained, in defining the exergy flow through the subsystems, fuel and product terms must be identified for each subsystem. The product represents the desired

result produced by the component (i.e. subsystem) whereas the fuel represents the resources expended to generate this product. Both the product and the fuel are expressed in terms of exergy, and definitions of the exergies of the fuels $\dot{E}x_f$ and the exergies of products $\dot{E}x_p$ for the components of the subsystem should be provided. In Table 9.5, energy and exergy analyses results of the PTS are given. We note the followings from these results:

- The total exergy rate of sewage at the PTS inlet increases from 23,096 kW to 23,306 kW by adding the total power supply to the primary treatment process. The exergetic efficiency of the PTS is found to be 56.9% using Equation (9.31). The remaining 43.1% of the sewage exergy input to the PTS is destroyed. This corresponds to 10,048.96 kW, which is the total exergy destruction in the PTS.
- The total exergy destructions in the components of the PTS account for 0.151% of the total sewage exergy input and 0.351% of the total exergy destruction in the system. The remaining 99.65% of the total exergy destruction in the PTS is mostly due to the highly complex and irreversible characteristics of the primary treatment process.
- The exergetic efficiencies of the air blowers and pumps are determined to be 85.6% and 75.0%, respectively. These values may be viewed as the indication of satisfactory exergetic performance for these components.

9.6.2 Energy and Exergy Analysis of Secondary Treatment System (STS)

The temperature, pressure, and mass flow rate data and energy and exergy rates in the plant according to the nomenclature shown in Figure 9.3 are presented in Table 9.5. The total exergy rates of the half-treated and the non-treated sewages at the inlet of the STS are determined to be 12,196 kW. The COD value of the treated water at the exit of the STS is reduced to 64.37 mg/l (see Table 9.1). Then the specific chemical exergy of the treated water at the exit of wastewater treatment plant is calculated as 0.875 kJ/kg. Since the total mass flow rate of the treated water is 2000.0 kg/s, the total exergy rate of treated wastewater in the plant exit is found to be 3624.4 kW. The activated sludge processed through the STS is sent to the aeration

tanks installed in the flotation and thickening system (FTS) for further treatment to precipitate the biogas production. At the exit of the STS, the activated sludge has a dry matter content of 0.5% [37] and its specific chemical exergy becomes 66.87 kJ/kg based on the specific exergy value of the dry sludge, which is obtained as 13,373 kJ/kg by Equation (4.23) given in the Chapter 4 and the data given in Table 9.6 [166]. The lower heating value (LHV) of the digested dry sludge is taken as 12,000 kJ/kg [33].

Table 9.5: Energy and exergy analysis results for the components in the Primary Treatment System (PTS). State numbers refer to Figure 9.2 and Table 9.4.

P: Pump; DWRT: Dirty Water Recovery Tank; PSTSP: Primary Settling Tanks Sludge Pumps

Component	States	\dot{Q} (kW)	\dot{W} (kW)	$\dot{E}x_F$ (kW)	$\dot{E}x_P$ (kW)	$\dot{E}x_D$ (kW)	y_D^* (%)	y_D (%)	ϵ (%)
Air Blower									
AB-1	0-4	-	22.25	22.25	19.04	3.21	0.033	0.014	85.6
AB-2	0-5	-	22.25	22.25	19.04	3.21	0.033	0.014	85.6
Sand Pumps									
P1	10-11	-	3.86	3.86	2.89	0.967	0.010	0.004	75.0
P2	12-13	-	10.60	10.60	7.95	2.647	0.027	0.011	75.0
DWRT									
P3	14-15	-	8.92	8.92	6.692	2.228	0.023	0.010	75.05
P4	16-17	-	8.92	8.92	6.692	2.228	0.023	0.010	75.05
Water Pumps									
P5	19-20	-	1.93	1.93	1.45	0.485	0.005	0.002	75.02
P6	21-22	-	1.93	1.93	1.45	0.485	0.005	0.002	75.02
PSTSP									
P7	25-26	-	12.48	12.48	9.36	3.12	0.032	0.014	75.01
P8	27-28	-	12.48	12.48	9.36	3.12	0.032	0.014	75.01
P9	29-30	-	12.48	12.48	9.36	3.12	0.032	0.014	75.01
P10	33-34	-	12.48	12.48	9.36	3.12	0.032	0.014	75.01
P11	35-36	-	12.48	12.48	9.36	3.12	0.032	0.014	75.01
Electric Motors									
	-	-	66.23	-	-	-	-	-	-
PTS	-	-	209.29	23,305.36	13,256.4	10,048.96	100	43.10	56.90

Table 9.6: The digested dry sludge composition in a municipal wastewater treatment plant [166]

Content	Volumetric values (%)
Carbon (C)	50.0
Hydrogen (H)	2.5
Oxygen (O)	12.5
Nitrogen (N)	1.1
Sulfur (S)	0.4
Ash	10.0
Other	23.5

Table 9.7: Secondary Treatment System data, thermodynamic properties, energy and exergy rates in the plant with respect to state points in Figure 9.4.

State No	Fluid	Pressure P (bar)	Temperature T (°C)	Mass flowrate \dot{m} (kg/s)	Enthalpy h (kJ/kg)	Entropy s (kJ/kg°C)	Specific energy e (kJ/kg)	Total specific exergy ψ^T (kJ/kg)	Energy rate \dot{E} (kW)	Total exergy rate $\dot{E}x^T$ (kW)
0	Air	1.00	25.00	-	298.40	5.6990	0.000	0.000	0.00	0.00
0'	Water	1.00	25.00	-	104.20	0.3648	0.000	0.000	0.00	0.000
0''	Sewage	1.00	25.00	-	104.20	0.3648	---	---	---	---
0'''	Sludge	1.00	25.00	-	104.20	0.3648	---	---	---	---
39	Air	2.28	130.00	3.83	404.30	5.7660	105.900	85.700	405.50	328.20
40	Air	2.28	130.00	3.83	404.30	5.7660	105.900	85.700	405.50	328.20
41	Air	2.28	130.00	3.83	404.30	5.7660	105.900	85.700	405.50	328.20
42'	Sludge	1.71	25.30	277.32	105.50	0.3690	1.321	66.942	366.2	18,564.36
42	Sludge	1.71	25.30	46.22	105.50	0.3690	1.321	66.942	61.04	3094.06
43	Sludge	3.74	25.30	46.22	105.80	0.3692	1.591	67.146	73.52	3103.49
44	Sludge	1.71	25.30	46.22	105.50	0.3690	1.321	66.942	61.04	3094.06
45	Sludge	3.74	25.30	46.22	105.80	0.3692	1.591	67.146	73.52	3103.49
46	Sludge	1.71	25.30	46.22	105.50	0.3690	1.321	66.942	61.04	3094.06
47	Sludge	3.74	25.30	46.22	105.80	0.3692	1.591	67.146	73.52	3103.49
48	Sludge	1.71	25.30	46.22	105.50	0.3690	1.321	66.942	61.04	3094.06
49	Sludge	3.74	25.30	46.22	105.80	0.3692	1.591	67.146	73.52	3103.49
50	Sludge	1.71	25.30	46.22	105.50	0.3690	1.321	66.942	61.04	3094.06
51	Sludge	3.74	25.30	46.22	105.80	0.3692	1.591	67.146	73.52	3103.49
52	Sludge	1.71	25.30	46.22	105.50	0.3690	1.321	66.942	61.04	3094.06
53	Sludge	3.74	25.30	46.22	105.80	0.3692	1.591	67.146	73.52	3103.49
54	Sludge	3.74	25.30	277.32	105.80	0.3692	1.591	67.146	441.10	18,620.93
55	Sludge	3.74	25.30	220.0	105.80	0.3692	1.591	67.146	349.90	14,772.12
56	Sludge	3.74	25.30	57.32	105.80	0.3692	1.591	67.146	91.17	3848.81
57'	Sewage	1.71	25.30	1996.68	105.50	0.3690	1.321	3.072	2472	6133.80
57	Sewage	1.10	25.00	624.0	104.20	0.3648	0.0093	0.885	5.78	552.24
58	Sewage	1.10	25.00	312.0	104.20	0.3648	0.0093	0.885	2.902	276.12
59	Sewage	2.33	25.00	312.0	104.40	0.3650	0.178	1.008	55.49	314.50
60	Sewage	1.10	25.00	312.0	104.20	0.3648	0.0093	0.885	2.902	276.12
61	Sewage	2.33	25.00	312.0	104.40	0.3650	0.178	1.008	55.49	314.50
62	Sewage	2.33	25.00	624.0	104.40	0.3650	0.178	1.008	111.00	629.00
63	Sewage	1.10	25.00	624.0	104.20	0.3648	0.0093	0.885	5.78	552.24
64	Sewage	1.10	25.00	312.0	104.20	0.3648	0.0093	0.885	2.902	276.12
65	Sewage	2.33	25.00	312.0	104.40	0.3650	0.178	1.008	73.52	314.50
66	Sewage	1.10	25.00	312.0	104.20	0.3648	0.0093	0.885	2.902	276.12
67	Sewage	2.33	25.00	312.0	104.40	0.3650	0.178	1.008	73.52	314.50
68	Sewage	2.33	25.00	624.0	104.40	0.3650	0.178	1.008	111.00	629.00
69	Sewage	1.10	25.00	624.0	104.20	0.3648	0.0093	0.885	5.78	552.24
70	Sewage	1.10	25.00	312.0	104.20	0.3648	0.0093	0.885	2.902	276.12
71	Sewage	2.33	25.00	312.0	104.40	0.3650	0.178	1.008	73.52	314.50
72	Sewage	1.10	25.00	312.0	104.20	0.3648	0.0093	0.885	2.902	276.12
73	Sewage	2.33	25.00	312.0	104.40	0.3650	0.178	1.008	73.52	314.50
74	Sewage	2.33	25.00	624.0	104.40	0.3650	0.178	1.008	111.00	629.00
75	Sewage	1.15	25.05	25.0	104.40	0.3655	0.223	0.890	5.576	22.25
76	Sewage	9.90	25.10	25.0	105.40	0.3658	1.190	1.768	29.75	44.20
77	Sewage	1.15	25.05	25.0	104.40	0.3655	0.223	0.890	5.576	22.25
78	Sewage	9.90	25.10	25.0	105.40	0.3658	1.190	1.765	29.75	41.13
79	Water	9.90	25.10	50.0	105.40	0.3658	1.190	1.768	59.51	88.40
80	Water	9.90	25.10	2000	105.40	0.3658	1.190	1.768	2380	3536.0

In Table 9.8, energy and exergy analyses results of the STS are given. We note the followings from these results:

- The total exergy rate of the half-treated sewage at the STS inlet increases from 12,196 kW to 13,944 kW by adding the total power supply to the secondary treatment process. The exergetic efficiency of the STS is found to be 26.0% using Equation (9.32). The remaining 74.0% of the half-treated sewage exergy input to the STS is destroyed. This corresponds to 10,319.12 kW, which is the total exergy destruction in the STS.

Table 9.8: Energy and exergy analyses results for the components in the Secondary Treatment System (STS). State numbers refer to Figure 9.3 and Table 9.7.

P: Pump; ATSP: Aeration Tanks Sludge Pumps; ATSRP: Aeration Tanks Sludge Recirculation Pumps; OCP: Outlet Chamber Pumps

Component	States	\dot{Q} (kW)	\dot{W} (kW)	$\dot{E}x_F$ (kW)	$\dot{E}x_P$ (kW)	$\dot{E}x_D$ (kW)	y_D^* (%)	y_D (%)	ε (%)
Air Blower									
AB-3	0-39	-	405.5	405.5	328.2	77.3	0.902	0.634	80.94
AB-4	0-40	-	405.5	405.5	328.2	77.3	0.902	0.634	80.94
AB-5	0-41	-	405.5	405.5	328.2	77.3	0.902	0.634	80.94
ATSP									
P12	42-43	-	12.48	12.48	9.41	3.07	0.036	0.025	75.43
P13	44-45	-	12.48	12.48	9.41	3.07	0.036	0.025	75.43
P14	46-47	-	12.48	12.48	9.41	3.07	0.036	0.025	75.43
P15	48-49	-	12.48	12.48	9.41	3.07	0.036	0.025	75.43
P16	50-51	-	12.48	12.48	9.41	3.07	0.036	0.025	75.43
P17	52-53	-	12.48	12.48	9.41	3.07	0.036	0.025	75.43
ATSRP									
P18	58-59	-	55.49	55.49	41.62	13.87	0.162	0.114	75.0
P19	60-61	-	55.49	55.49	41.62	13.87	0.162	0.114	75.0
P20	64-65	-	55.49	55.49	41.62	13.87	0.162	0.114	75.0
P21	66-67	-	55.49	55.49	41.62	13.87	0.162	0.114	75.0
P22	70-71	-	55.49	55.49	41.62	13.87	0.162	0.114	75.0
P23	72-73	-	55.49	55.49	41.62	13.87	0.162	0.114	75.0
OCP									
P24	75-76	-	29.75	29.75	22.31	7.44	0.087	0.061	75.0
P25	77-78	-	29.75	29.75	22.31	7.44	0.087	0.061	75.0
Electric Motors	-	-	63.6	-	-	-	-	-	-
STS	-	-	1747.42	13,943.52	3624.4	10,319.12	100	74.0	26.0

- The total exergy destructions in the components of the STS accounts for 2.85% of the total half-treated sewage exergy input and 4.07% of the total exergy destruction in the system. The remaining 95.93% of the total exergy destruction in the STS is mostly due to the highly complex and irreversible characteristics of the secondary treatment process.

- The exergetic efficiencies of the air blowers and pumps are determined to be 80.9% and 75.4%, respectively.

9.6.3 Energy and Exergy Analysis of Flotation and Thickening System (FTS)

Sludge produced by municipal wastewater treatment plants is usually processed the water content of the sludge, its fermentation propensity and pathogens content. The water content of the sludge is mainly reduced by flotation and thickening process. In GASKI WWTP, dissolved-air flotation technique is used for sludge thickening process. However, while taking the power consumption for the FTS in GASKI WWTP as 135.6 kWh per ton dry matter content of the sludge into account, the energy cost for the FTS is also significant. The temperature, pressure, and mass flow rate data, and energy and exergy rates in the plant according to the nomenclature shown in Figure 9.4 are presented in Table 9.9.

Table 9.9: Flotation and Thickening System data, thermodynamic properties, energy and exergy rates in the plant with respect to state points in Figure 9. 4.

State No	Fluid	Pressure P (bar)	Temperature T (°C)	Mass flowrate \dot{m} (kg/s)	Enthalpy h (kJ/kg)	Entropy s (kJ/kg°C)	Specific energy e (kJ/kg)	Total specific exergy ψ^T (kJ/kg)	Energy rate \dot{E} (kW)	Total exergy rate $\dot{E}x^T$ (kW)
0	Air	1.00	25.00	-	298.40	5.6990	0.000	0.000	0.00	0.00
0'	Water	1.00	25.00	-	104.20	0.3648	0.000	0.000	0.00	0.000
0''	Sludge	1.00	25.00	-	104.20	0.3648	---	---	---	---
38'	Sludge	1.50	25.00	18.09	104.30	0.3648	0.0463	66.920	0.837	1210.58
38''	Sludge	1.10	27.00	18.09	112.6	0.3928	8.375	668.690	151.5	12,096.60
81	Sludge	1.10	25.05	6.03	104.40	0.3655	0.218	668.660	1.317	4032.02
82	Sludge	10.90	25.10	6.03	105.50	0.3659	1.324	669.643	7.98	4037.95
83	Sludge	1.10	25.05	6.03	104.40	0.3655	0.218	668.660	1.317	4032.02
84	Sludge	10.90	25.10	6.03	105.50	0.3659	1.324	669.643	7.98	4037.95
85	Sludge	1.10	25.05	6.03	104.40	0.3655	0.218	668.660	1.317	4032.02
86	Sludge	10.90	25.10	6.03	105.50	0.3659	1.324	669.643	7.98	4037.95
87	Sludge	10.90	25.10	18.09	105.50	0.3659	1.324	669.643	23.95	12,113.84
88	Sludge	1.10	25.05	93.48	104.40	0.3655	0.218	66.880	20.38	6251.94
89	Sludge	1.10	25.05	46.74	104.40	0.3655	0.218	66.880	10.79	3125.97
90	Sludge	13.77	25.10	46.74	105.90	0.3663	1.708	68.150	79.81	3185.33
91	Sludge	1.10	25.05	46.74	104.40	0.3655	0.218	66.880	10.79	3125.97
92	Sludge	13.77	25.10	46.74	105.90	0.3663	1.708	68.150	79.81	3185.33
93	Sludge	13.77	25.10	93.48	105.90	0.3663	1.708	68.150	159.60	6370.66
94	Sludge	1.10	25.05	93.48	104.40	0.3655	0.218	66.880	20.38	6251.94
95	Sludge	1.10	25.05	46.74	104.40	0.3655	0.218	66.880	10.79	3125.97
96	Sludge	13.77	25.10	46.74	105.90	0.3663	1.708	68.150	79.81	3185.33
97	Sludge	1.10	25.05	46.74	104.40	0.3655	0.218	66.880	10.79	3125.97
98	Sludge	13.77	25.10	46.74	105.90	0.3663	1.708	68.150	79.81	3185.33

99	Sludge	13.77	25.10	93.48	105.90	0.3663	1.708	68.150	159.60	6370.66
100	Air	5.77	333.30	0.07	613.90	5.9200	315.5	249.600	22.40	17.72
101	Air	5.77	333.30	0.036	613.90	5.9200	315.5	249.600	11.36	8.98
102	Air	5.77	333.30	0.035	613.90	5.9200	315.5	249.600	11.04	8.73
103	Sludge	1.32	25.40	9.05	105.90	0.3704	1.703	668.683	15.41	6051.58
104	Sludge	3.72	25.40	9.05	106.20	0.3707	2.024	668.924	18.32	6053.76
105	Sludge	1.32	25.40	9.05	105.90	0.3704	1.703	668.683	15.41	6051.58
106	Sludge	3.72	25.40	9.05	106.20	0.3707	2.024	668.924	18.32	6053.76
107	Sludge	3.72	25.40	18.10	106.20	0.3707	2.024	668.924	36.63	12,107.52
108	Sludge	1.10	25.05	6.04	104.40	0.3655	0.218	668.660	1.319	4038.71
109	Sludge	1.10	25.05	3.02	104.40	0.3655	0.218	668.660	0.66	2019.35
110	Sludge	6.40	25.10	3.02	104.90	0.3654	0.722	669.192	2.18	2020.96
111	Sludge	1.10	25.05	3.02	104.40	0.3655	0.218	668.660	0.66	2019.35
112	Sludge	6.40	25.10	3.02	104.90	0.3654	0.722	669.192	2.18	2020.96
113	Sludge	6.40	25.10	6.04	104.90	0.3654	0.722	669.192	4.36	4041.92
114	Sludge	1.10	25.05	12.06	104.40	0.3655	0.218	668.660	2.634	8064.04
115	Sludge	1.10	25.05	6.03	104.40	0.3655	0.218	668.660	1.317	4032.02
116	Sludge	8.20	25.10	6.03	105.20	0.3656	0.963	669.372	5.81	4036.31
117	Sludge	1.10	25.05	6.03	104.40	0.3655	0.218	668.660	1.317	4032.02
118	Sludge	8.20	25.10	6.03	105.20	0.3656	0.963	669.372	5.81	4036.31
119	Sludge	8.20	25.10	12.06	105.20	0.3656	0.963	669.372	11.61	8072.63
120	Sludge	1.10	25.05	15.08	104.40	0.3655	0.218	668.660	3.30	10083.39
121	Sludge	1.10	25.05	7.54	104.40	0.3655	0.218	668.660	1.65	5041.70
122	Sludge	9.00	25.10	7.54	105.30	0.3657	1.070	669.452	8.07	5047.67
123	Sludge	1.10	25.05	7.54	104.40	0.3655	0.218	668.660	1.65	5041.70
124	Sludge	9.00	25.10	7.54	105.30	0.3657	1.070	669.452	8.07	5047.67
125	Sludge	9.00	25.10	15.08	105.30	0.3657	1.070	669.452	16.13	10,095.34
126	Sludge	1.10	25.05	6.04	104.40	0.3655	0.218	668.660	1.319	4038.71
127	Sludge	1.10	25.05	3.02	104.40	0.3655	0.218	668.660	0.66	2019.35
128	Sludge	6.40	25.10	3.02	104.90	0.3654	0.722	669.192	2.18	2020.96
129	Sludge	1.10	25.05	3.02	104.40	0.3655	0.218	668.660	0.66	2019.35
130	Sludge	6.40	25.10	3.02	104.90	0.3654	0.722	669.192	2.18	2020.96
131	Sludge	6.40	25.10	6.04	104.90	0.3654	0.722	669.192	4.36	4041.92
132	Water	1.50	25.20	150.8	105.10	0.3676	0.883	0.925	133.10	139.49
133	Water	3.11	25.20	150.8	105.30	0.3678	1.098	1.087	165.60	163.92
134	Water	1.50	25.20	150.8	105.10	0.3676	0.883	0.925	133.10	139.49
135	Water	3.11	25.20	150.8	105.30	0.3678	1.098	1.087	165.60	163.92
136	Water	1.50	25.20	150.8	105.10	0.3676	0.883	0.925	133.10	139.49
137	Water	3.11	25.20	150.8	105.30	0.3678	1.098	1.087	165.60	163.92
138	Water	3.11	25.20	452.4	105.30	0.3678	1.098	1.087	496.80	491.76
139	Sludge	1.10	25.00	4.02	104.20	0.3648	0.0093	668.66	0.037	2688.01
139'	Sludge	1.10	25.00	21.11	104.20	0.3648	0.0093	668.66	0.195	14,115.41
140	Sludge	6.00	25.00	4.02	104.70	0.3647	0.4628	669.151	1.86	2689.99
141	Sludge	1.10	25.00	4.02	104.20	0.3648	0.0093	668.66	0.037	2688.01
142	Sludge	6.00	25.00	4.02	104.70	0.3647	0.4628	669.151	1.86	2689.99
143	Sludge	1.10	25.00	4.02	104.20	0.3648	0.0093	668.66	0.037	2688.01
144	Sludge	6.00	25.00	4.02	104.70	0.3647	0.4628	669.151	1.86	2689.99
145	Sludge	6.00	25.00	12.06	104.70	0.3647	0.4628	669.151	5.581	8069.96

The total exergy rate of the activated sludge at the inlet of the FTS is found to be 15,832 kW. This value is the total exergy rates of the activated sludge which has a dry matter content of 0.5% from the STS (14,772 kW) and of the sewage-like sludge which has a dry matter content of less than 0.1% (1060.3 kW) from PTS. At the exit state of FTS process, the mass flow rate of the sludge is reduced to 12.06 kg/s while

the dry matter content of the activated sludge increases up to 5.0% [37], which make the total exergy rate of the sludge at this state to be 8070 kW. In Table 9.10, energy and exergy analyses results of the STS are given.

Table 9.10: Energetic and exergetic analyses results for the subsystems in Flotation and Thickening System (FTS). State numbers refer to Figure 9.4 and Table 9.9.

P: Pump; STTP: Sludge Thickening Tanks Pumps; SSTP: Sludge Storage Tank Pumps; C1: Compressor ; BSPP: Bottom Sludge Pit Pumps; SSPP: Single Sludge Pit Pumps; DSPP: Double Sludge Pit Pumps; MSPP: Main Sludge Pit Pumps; SMTP: Sludge Mixing Tank Pumps

Component	States	\dot{Q} (kW)	\dot{W} (kW)	$\dot{E}x_F$ (kW)	$\dot{E}x_P$ (kW)	$\dot{E}x_D$ (kW)	y_D^* (%)	y_D (%)	ε (%)
STTP									
P26	81-82	-	7.983	7.983	5.986	1.997	0.026	0.013	75.0
P27	83-84	-	7.983	7.983	5.986	1.997	0.026	0.013	75.0
P28	85-86	-	7.983	7.983	5.986	1.997	0.026	0.013	75.0
SSTP									
P29	89-90	-	79.81	79.81	59.85	19.96	0.257	0.126	75.0
P30	91-92	-	79.81	79.81	59.85	19.96	0.257	0.126	75.0
P31	95-96	-	79.81	79.81	59.85	19.96	0.257	0.126	75.0
P32	97-98	-	79.81	79.81	59.85	19.96	0.257	0.126	75.0
C1	0-100	-	22.40	22.40	17.72	4.68	0.060	0.03	79.1
BSPP									
P33	103-104	-	2.905	2.905	2.180	0.725	0.009	0.005	75.03
P34	105-106	-	2.905	2.905	2.180	0.725	0.009	0.005	75.03
SSPP-1									
P35	109-110	-	2.181	2.181	1.635	0.546	0.007	0.003	75.0
P36	111-112	-	2.181	2.181	1.635	0.546	0.007	0.003	75.0
DSPP									
P37	115-116	-	5.806	5.806	4.354	1.452	0.019	0.009	75.0
P38	117-118	-	5.806	5.806	4.354	1.452	0.019	0.009	75.0
MSPP									
P39	121-122	-	8.066	8.066	6.049	2.017	0.026	0.013	75.0
P40	123-124	-	8.066	8.066	6.049	2.017	0.026	0.013	75.0
SSPP-2									
P41	127-128	-	2.181	2.181	1.635	0.546	0.007	0.003	75.0
P42	129-130	-	2.181	2.181	1.635	0.546	0.007	0.003	75.0
DDWTP									
P43	132-133	-	32.47	32.47	24.356	8.114	0.105	0.051	75.0
P44	134-135	-	32.47	32.47	24.356	8.114	0.105	0.051	75.0
P45	136-137	-	32.47	32.47	24.356	8.114	0.105	0.051	75.0
SMTP									
P46	139-140	-	2.688	2.688	2.016	0.672	0.009	0.042	75.0
P47	141-142	-	2.688	2.688	2.016	0.672	0.009	0.042	75.0
P48	143-144	-	2.688	2.688	2.016	0.672	0.009	0.042	75.0
Electric Motors	-	-	29.44*	-	-	-	-	-	-
FTS	-	-	542.78	16,375.2	8069.96	8305.24	100	50.7	49.3

* The power consumption for sludge thickening process is 135.6 kWh per ton of dry matter content of the activated sludge.

We note the followings from these results:

- The total exergy rate of the activated sludge at the FTS inlet increases from 15,832 kW to 16,375 kW by adding the total power supply to the flotation and thickening process. The exergetic efficiency of FTS is found to be 49.3% using Equation (9.33). The remaining 50.7% of the activated sludge exergy input to FTS is destroyed. This corresponds to 8305.24 kW, which is the total exergy destruction in FTS.
- The total exergy destructions in the components of FTS accounts for 0.91% of the total activated sludge exergy input and 1.65% of the total exergy destruction in the system. The remaining 98.35% of the total exergy destruction in the FTS is due to the reduction of mass flow rate of the activated sludge through thickening process and the complex mechanism of the FTS.
- The exergetic efficiencies of pumps are determined to be 75.0%.

9.6.4 Energy and Exergy Analysis of Anaerobic Digestion System (ADS)

The temperature, pressure, and mass flow rate data, and energy and exergy rates in the plant according to the nomenclature shown in Figure 9.5 are presented in Table 9.11.

The total exergy rate of the activated sludge at the inlet of ADS is 8070 kW. This sludge has the dry matter content of 5.0%. Through the anaerobic digestion process, the dry matter content of the sludge increases to 8.0% [37], which make the total exergy rate of the digested sludge at the exit of secondary digestion unit as 11,294 kW. This digested sludge is then sent to the de-watering facility for increasing the dry matter content of it to 22.0%. The mass flow rate of the digested sludge is reduced to 2.48 kg/s at the de-watering facility exit and the total exergy rate of the sludge cake is obtained as 7296.4 kW. Note that the power consumption for the de-watering process in GASKI WWTP is about 81 kWh per ton dry matter content of the digested sludge. This sludge cake is not used for any useful purpose for possible on-site or off-site applications, and thus is considered as waste and not taken into account for actual exergy analysis and assessment of ADS process. In this case, the

only useful output of ADS is the biogas. Biogas production strongly depends upon the type of the sludge and the operating conditions of the anaerobic digesters. For each 1 m³ biogas produced in GASKI WWTP, 68.26 kg of sludge with the dry matter content of 8.0% is digested (or degraded). Due to the mesophilic sludge digestion process in the anaerobic reactors, biogas is produced with the composition of which is listed in Table 9.2 given in the first part of the study. The lower heating value of the produced biogas is 21.47 MJ/Nm³ (17,892 kJ/kg). The specific chemical exergy of the biogas in this composition is calculated to be 31,168 kJ/kg by using Equation (4.25) given in the Chapter 4. Then the total exergy rate of the biogas produced with a mass flow rate of 0.212 kg/s is obtained as 6653.2 kW.

In Table 9.12, energy and exergy analyses results of the ADS are given. We note the followings from these results:

- The total exergy rate of the activated sludge at the ADS inlet increases from 8070 kW to 8268 kW by adding the total power supply to the anaerobic digestion system. The exergetic efficiency of ADS is found to be 80.5% using Equation (9.34). The remaining 19.5% of the activated sludge exergy input to ADS is destroyed. This corresponds to 1615.22 kW, which is the total exergy destruction in ADS. The high exergetic efficiency obtained for the ADS depends on high processing capacity of anaerobic reactors in which a sufficiently large bacterial mass is retained. For sludge digestion process in GASKI WWTP, high rate anaerobic reactors are used. In these reactors, a high concentration of anaerobic sludge is retained under high hydraulic loading conditions (12,000 m³ per day) for a 15-day period. This causes the maximum contact between the incoming feedstock and the bacterial mass, which increases the methane content in the produced biogas.
- The total exergy destructions in the components of ADS accounts for 1.811% of the total activated sludge exergy input and 9.95% of the total exergy destruction in the system. The remaining 90.05% of the total exergy destruction in the ADS is due to complex bacterial mechanisms occurred through the anaerobic digestion process at the mesophilic temperature conditions.

Table 9.11: Anaerobic Digestion System data, thermodynamic properties, and energy and exergy rates in the plant with respect to state points in Figure 9.5.

State No	Fluid	Pressure P (bar)	Temperature T (°C)	Mass flowrate \dot{m} (kg/s)	Enthalpy h (kJ/kg)	Entropy s (kJ/kg°C)	Specific energy e (kJ/kg)	Total specific exergy ψ^T (kJ/kg)	Energy rate \dot{E} (kW)	Total exergy rate $\dot{E}x^T$ (kW)
0	Air	1.00	25.00	-	298.40	5.6990	0.000	0.000	0.00	0.00
0'	Water	1.00	25.00	-	104.20	0.3648	0.000	0.000	0.00	0.000
0'''	Sludge	1.00	25.00	-	104.20	0.3648	---	---	---	---
0'''	Biogas	1.00	25.00	-	-4650	11.620	---	---	---	---
145	Sludge	6.00	25.00	12.06	104.70	0.3647	0.4628	669.151	5.581	8069.96
146	Sludge	6.00	25.00	4.02	104.70	0.3647	0.4628	669.151	1.860	2689.99
147	Sludge	6.00	25.00	4.02	104.70	0.3647	0.4628	669.151	1.860	2689.99
148	Sludge	6.00	25.00	4.02	104.70	0.3647	0.4628	669.151	1.860	2689.99
149	Sludge	1.10	30.00	12.00	125.10	0.4344	20.920	668.834	251.1	8026.01
150	Sludge	2.80	30.00	12.00	125.40	0.4346	21.150	669.005	253.8	8028.06
151	Sludge	2.80	37.00	12.00	154.60	0.5299	50.360	669.815	755.3	8037.78
152	Sludge	1.10	30.00	12.00	125.10	0.4344	20.920	668.834	251.1	8026.01
153	Sludge	2.80	30.00	12.00	125.40	0.4346	21.150	669.005	253.8	8028.06
154	Sludge	2.80	37.00	12.00	154.60	0.5299	50.360	669.815	755.3	8037.78
155	Sludge	1.10	30.00	12.00	125.10	0.4344	20.920	668.834	251.1	8026.01
156	Sludge	2.80	30.00	12.00	125.40	0.4346	21.150	669.005	253.8	8028.06
157	Sludge	2.80	37.00	12.00	154.60	0.5299	50.360	669.815	755.3	8037.78
158	Sludge	1.10	35.00	4.02	146.10	0.5029	41.840	936.807	168.2	3765.96
159	Sludge	1.10	35.00	4.02	146.10	0.5029	41.840	936.807	168.2	3765.96
160	Sludge	1.10	35.00	4.02	146.10	0.5029	41.840	936.807	168.2	3765.96
161	Sludge	1.10	35.00	12.06	146.10	0.5029	41.840	936.807	504.6	11,297.89
162	Sludge	1.05	32.00	12.06	133.50	0.4619	29.290	936.454	353.2	11,293.64
162''	Sludge	1.10	27.00	2.48	112.60	0.3928	8.375	2942.098	20.35	7296.40
163	Biogas	1.032	35.00	0.106	-4628.0	11.67	22.530	31372.665	2.388	3325.50
164	Biogas	1.30	57.00	0.106	-4577.0	11.71	73.110	31411.64	7.749	3329.63
165	Biogas	1.28	50.00	0.106	-4593.0	11.67	56.86	31407.83	6.027	3329.23
166	Biogas	1.032	35.00	0.106	-4628.0	11.67	22.530	31372.665	2.388	3325.50
167	Biogas	1.30	57.00	0.106	-4577.0	11.71	73.110	31411.64	7.749	3329.63
168	Biogas	1.28	50.00	0.106	-4593.0	11.67	56.86	31407.83	6.027	3329.23
169	Biogas	1.032	35.00	0.106	-4628.0	11.67	22.530	31372.665	2.388	3325.50
170	Biogas	1.30	57.00	0.106	-4577.0	11.71	73.110	31411.64	7.749	3329.63
171	Biogas	1.28	50.00	0.106	-4593.0	11.67	56.86	31407.83	6.027	3329.23
172	Biogas	1.032	35.00	0.106	-4628.0	11.67	22.530	31372.665	2.388	3325.50
173	Biogas	1.30	57.00	0.106	-4577.0	11.71	73.110	31411.64	7.749	3329.63
174	Biogas	1.28	50.00	0.106	-4593.0	11.67	56.86	31407.83	6.027	3329.23
175	Biogas	1.032	35.00	0.053	-4628.0	11.67	22.530	31372.665	1.194	1662.75
176	Biogas	1.032	35.00	0.053	-4628.0	11.67	22.530	31372.665	1.194	1662.75
177	Biogas	1.032	35.00	0.053	-4628.0	11.67	22.530	31372.665	1.194	1662.75
178	Biogas	1.032	35.00	0.053	-4628.0	11.67	22.530	31372.665	1.194	1662.75
179	Biogas	1.032	35.00	0.212	-4628.0	11.67	22.530	31372.665	4.775	6651.00
180	Biogas	1.10	42.00	0.212	-4612.0	11.69	38.460	31383.21	8.154	6653.24
182	Water	3.40	88.0	20.88	368.10	1.167	263.90	24.73	5510	516.4
183	Water	5.30	88.0	20.88	368.40	1.168	264.20	24.94	5516	520.7
184	Water	5.30	88.0	6.96	368.30	1.167	264.00	27.92	1838	173.4
185	Water	5.25	75.80	6.96	317.10	1.023	212.90	16.71	1481	116.3
186	Water	5.30	88.00	6.96	368.30	1.167	264.00	27.92	1838	173.4
187	Water	5.25	75.80	6.96	317.10	1.023	212.90	16.71	1481	116.3
188	Water	5.30	88.00	6.96	368.30	1.167	264.00	27.92	1838	173.4
189	Water	5.25	75.80	6.96	317.10	1.023	212.90	16.71	1481	116.3
190	Water	5.25	75.80	6.96	317.10	1.023	212.9	16.71	4444	349.0

- The exergetic efficiencies of pumps and compressors are determined to be 75.0% and 77.0% respectively. The most exergy destructive components of ADS are anaerobic digester recirculation heat exchangers (ADRHEs). Exergy destructions in these heat exchange units are mainly due to the high average temperature difference between the two unmixed fluid streams.

The exergy assessment of the four subsystems in GASKI WWTP is given schematically in Figure 9.7. According to this figure and developed exergy efficiency formulas in the first part of the study, the exergetic efficiency of the overall system may be defined due to the sludge output use at the end of the wastewater treatment and biogas production processes. In the actual case, the de-watered digested sludge output is sent to the city's incineration plant for elimination. Thus, it is considered as waste and the actual exergetic efficiency of the overall system using Equation (9.35) is obtained as

$$\varepsilon_{\text{GASKI WWTP}}^1 = \frac{3536 \text{ kW} + 6653 \text{ kW}}{23,097 \text{ kW} + 2698 \text{ kW}} = 0.395 \text{ or } 39.5\%$$

In the ideal case, the de-watered digested sludge would be used as a secondary energy and/or raw material source for off-site applications. In this case, the sludge output from the WWTP could be seen as a by-product and the exergetic efficiency of the overall system would become (Equation 9.36)

$$\varepsilon_{\text{GASKI WWTP}}^2 = \frac{3536 \text{ kW} + 6653 \text{ kW} + 7296}{23,096 \text{ kW} + 2698 \text{ kW}} = 0.678 \text{ or } 67.8\%$$

The usage of digested sludge output as a secondary valuable energy source clearly increases the exergetic efficiency of the overall system.

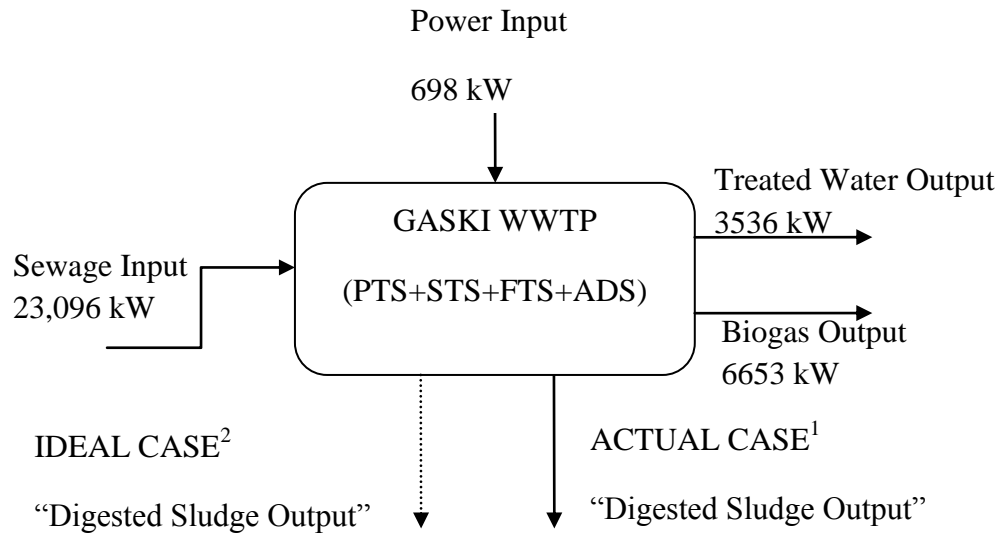


Figure 9.7: Exergy Assessment of the Four Subsystems in GASKI WWTP

Table 9.12: Energetic and exergetic analyses results for the subsystems in the Anaerobic Digestion System (ADS). State numbers refer to Figure 9.5 and Table 9.11

P: Pump; PADRP: Primary Anaerobic Digester Recirculation Pump; ADRHE: Anaerobic Digester Recirculation Heat Exchanger; BC: Biogas Compressor

Component	States	\dot{Q} (kW)	\dot{W} (kW)	$\dot{E}x_F$ (kW)	$\dot{E}x_P$ (kW)	$\dot{E}x_D$ (kW)	y_D^* (%)	y_D (%)	ε (%)
PADRP									
P49	149-150	-	2.732	2.732	2.06	0.672	0.047	0.008	75.4
P50	152-153	-	2.732	2.732	2.06	0.672	0.047	0.008	75.4
P51	155-156	-	2.732	2.732	2.06	0.672	0.047	0.008	75.4
ADRHE-1									
Water Line	184-185	-356.2	-	57.1	13.21	43.89	3.10	0.544	23.1
Sludge Line	150-151	350.5	-						
ADRHE-2									
Water Line	186-187	-356.2	-	57.1	13.21	43.89	3.10	0.544	23.1
Sludge Line	153-154	350.5	-						
ADRHE-3									
Water Line	188-189	-356.2	-	57.1	13.21	43.89	3.10	0.544	23.1
Sludge Line	156-157	350.5	-						
BC-1	163-164	-	5.362	5.362	4.131	1.231	0.087	0.015	77.0
BC-2	166-167	-	5.362	5.362	4.131	1.231	0.087	0.015	77.0
BC-3	169-170	-	5.362	5.362	4.131	1.231	0.087	0.015	77.0
BC-4	172-173	-	5.362	5.362	4.131	1.231	0.087	0.015	77.0
Booster	179-180	-	3.379	3.379	2.236	1.144	0.081	0.081	66.2
P52	182-183	-	5.471	5.471	4.342	1.129	0.080	0.014	79.4
Electric Motor	-	-	160.0*	-	-	-	-	-	-
ADS	-	-516.4 349.0	198.5	8268.46	6653.24	1615.22	100.0	19.50	80.50

* The power consumption for sludge de-watering process is nearly 81.0 kWh per ton of dry matter content of the digested sludge

9.6.5 Energy and Exergy Analysis of Biogas Engine Powered Cogeneration

The biogas engine powered cogeneration system (BEPC) installed in GASKI WWTP area is divided into subcomponents as shown schematically in Figure 9.6. The temperature, pressure, and mass flow rate data, and energy and exergy rates in the BEPC system according to the nomenclature shown in Figure 9.6 are presented in Table 9.13.

Table 9.13: Biogas Engine Powered Cogeneration data, thermodynamic properties, energy and exergy rates in the plant with respect to state points in Figure 9.6.

State No	Fluid	Pressure P (bar)	Temperature T (°C)	Mass flowrate \dot{m} (kg/s)	Enthalpy h (kJ/kg)	Entropy s (kJ/kg°C)	Specific energy e (kJ/kg)	Total specific exergy ψ^T (kJ/kg)	Energy rate \dot{E} (kW)	Total exergy rate $\dot{E}x^T$ (kW)
0	Air	1.00	25.00	-	298.40	5.6990	0.00	0.00	0.00	0.00
0'	Water	1.00	25.00	-	104.20	0.3648	0.00	0.00	0.00	0.00
0'''	Sludge	1.00	25.00	-	104.20	0.3648	---	---	---	---
0''''	Biogas	1.00	25.00	-	-4650	11.620	---	---	---	---
0'''''	Lub oil	1.00	25.00	-	-	-	-	0.00	-	0.00
181	Biogas	1.02	30.10	0.129	-4639.0	11.64	11.45	31370.585	1.477	4046.81
191	Water	6.20	75.80	20.88	317.20	1.023	213.0	16.81	4447	351.1
192	Water	6.10	82.80	20.88	346.40	1.106	242.2	21.31	5057	444.9
193	Water	2.80	88.40	15.61	369.70	1.172	265.5	24.97	4145	389.7
194	Water	7.60	88.50	15.61	370.40	1.173	266.2	25.49	4155	397.9
195	Water	7.50	72.40	15.61	302.90	0.9815	198.7	14.90	3101	232.7
196	Water	7.30	77.90	15.61	325.90	1.048	221.7	18.20	3461	284.2
197	Water	7.20	78.50	15.61	328.50	1.055	224.3	18.59	3502	290.2
198	Water	4.55	50.00	11.28	209.20	0.7021	105.0	4.523	1185	51.02
199	Water	4.50	52.10	11.28	218.10	0.7293	113.9	5.228	1284	58.97
200	Water	1.10	50.00	11.28	208.80	0.7017	104.6	4.165	1180	46.98
201	Lub oil	4.69	100.6	20.0	166.30	0.4974	166.3	18.09	3326	361.9
202	Lub oil	4.50	89.00	20.0	140.80	0.428	140.8	13.25	2816	265.1
203	Lub oil	1.00	85.00	20.0	132.00	0.4036	132.0	11.74	2640	234.7
204	Lub oil	6.90	87.00	20.0	132.90	0.4158	132.9	12.48	2659	249.7
205	Air	1.00	25.00	1.387	298.40	5.699	0.00	0.00	0.00	0.00
206	Air-fuel	1.00	25.00	1.50	298.40	5.699	0.00	31367.43	0.00	4046.40
207	Air-fuel	1.90	116.9	1.50	391.00	5.785	92.580	31434.21	138.9	4055.01
208	Air-fuel	1.90	51.00	1.50	324.60	5.599	26.140	31423.38	39.21	4053.62
209	Exhaust gas	2.40	460.0	1.50	749.20	6.374	450.80	249.4	676.1	374.1
210	Exhaust gas	1.17	360.6	1.50	642.70	6.424	344.30	128.1	516.5	192.1
211	Exhaust gas	1.00	65.00	1.50	353.80	5.869	55.340	4.518	60.34	3.661

The biogas used as the fuel in the gas engine of the BEPC system is nearly 61% (0.129 kg/s) of the total biogas produced in anaerobic digestion system, which is 0.212 kg/s. The remaining part (0.083 kg/s) is reserved in the biogas storage tank. For 1 kWh electricity produced in the gas engine, 0.387 m³ of biogas with 60% of methane content is consumed in the BEPC plant. The total exergy input of air and biogas (fuel) to the gas engine is 4054 kW.

In Table 9.14, energy and exergy analyses results of the BEPC system are given. We note the followings from these results:

- The total exergy rate of the air and fuel at the inlet of to the gas engine increases from 4054 kW to 4594 kW by adding lubrication oil and engine cooling water exergy rates at the inlet of the engine following the third approach developed by Equation (9.40). The exergetic efficiency of the gas engine is found to be 24.7% by using the first approach defined in Eq. (9.38), 26.4% by using the second approach defined in Equation (9.39), and 46.3% by using the third approach defined in Equation (9.40). Since the second approach is more appropriate for the cogeneration scheme, the assessments based on this approach are more meaningful from the exergy method point of view.
- 24.7% of exergy entering the BEPC plant is converted to electrical power (1000 kW). The net steam production of the BEPC plant represents only 1.8% (71.5 kW) of the total exergy input. The remaining 73.6% of the exergy input to the BEPC plant is destroyed. This corresponds to 2982 kW, which is the total exergy destruction in the plant.
- The exergetic efficiency of the BEPC plant is obtained to be 26.4%. The exergy destruction in the gas engine of the cogeneration plant accounts for 73.6% of the total exergy input and 89.4% of the total exergy destruction in the plant. The exergy destruction in the engine is mostly due to the highly irreversible combustion process, heat losses from the engine, and friction.
- The exergetic efficiencies of the compressor and turbine of the turbocharger are 72.1% and 87.7%, respectively. The exergetic efficiencies of pumps, P53, P54, P55 and P56, are 78.6%, 79.1%, 76.9%, and 80.6%, respectively.

- The exergetic efficiencies of exhaust gas heat exchanger and intercooler are calculated as 37.9% and 48.8%, respectively making them the least efficient components of the plant. Exergy destructions in these heat exchange units in the plant are mainly due to the high average temperature difference between the two unmixed fluid streams.
- The percentages of exergy losses associated with the other heat exchangers (HE-4 and HE-5) and lubrication oil cooler are not very high. This is due to the use of low-temperature water in these processes.
- The fuel utilization efficiency (FUE) of the BEPC system is determined to be 63.0% by Equation (4.40) developed in the Chapter 4. This value is high compared to the thermal efficiencies of power plants whose sole purpose is the production of electricity [167]. In BEPC, the main product is electricity and the hot water generated by exhaust gas heat exchanger may be called as “byproduct”. The thermal efficiency of the gas engine defined as the power output over the fuel energy input is calculated to be 43.3% by Equation (9.37) given in the first part of the study, which is consistent with the gas engine efficiency given by the manufacturer [150].

Power to heat ratio (PHR) of the BEPC plant is calculated to be 2.21 by Equation (4.41) given in the Chapter 4. This is a characteristic of internal combustion engine powered cogeneration systems for which the process heat output is typically small compared to electrical output [167].

The overall exergetic efficiency of GASKI WWTP including biogas engine powered cogeneration system (BEPC) is calculated using Equation (9.42) developed in the first part of the study as

$$\varepsilon_{\text{GASKI WWTP\&BEPC}} = \frac{3624 \text{ kW} + 1000 \text{ kW} + 7296 \text{ kW}}{23,096 \text{ kW} + 1000 \text{ kW} + 1698 \text{ kW}} = 0.462 \text{ or } 46.2\%$$

This value indicates that 46.2% of the total exergy input to the GASKI WWTP and BEPC is converted to the useful outputs, i.e., treated water, de-watered digested sludge, and power output. The total exergy destruction of the overall plant accounts about 53.9% of the total exergy input. This corresponds to 13,873 kW, which is the

total exergy destruction in the plant. The overall exergy assessment of the plant is summarized in Figure 9.8.

Table 9.14: Energy and exergy analyses results for the subsystems in the Biogas Engine Powered Cogeneration (BEPC). State numbers refer to Figure 9.6 schematized in the first part of the study and Table 9.13.

P: Pump; PADRP: Primary Anaerobic Digester Recirculation Pump; ADRHE: Anaerobic Digester Recirculation Heat Exchanger; BC: Biogas Compressor; BHE: Biogas Heat Exchanger; T: Turbocharger; EGHE: Exhaust Gas Heat Exchanger; HE: Heat Exchanger

Component	States	\dot{Q} (kW)	\dot{W} (kW)	$\dot{E}x_F$ (kW)	$\dot{E}x_P$ (kW)	$\dot{E}x_D$ (kW)	y_D^* (%)	y_D (%)	ε (%)
P53	190-191	-	2.714	2.714	2.134	0.580	0.019	0.014	78.6
P54	193-194	-	10.34	10.34	8.205	2.135	0.072	0.053	79.1
Turbine (T)	209-210	-	159.6	182.0	159.6	22.40	0.751	0.553	87.7
Compressor (T)	206-207	-	138.9	138.9	100.2	38.70	1.298	0.955	72.1
Intercooler Water Line	198-199	99.45	-	16.28	7.95	8.33	0.279	0.205	48.8
Air-Fuel Line	207-208	-99.66	-	-	-	-	-	-	-
P55	200-198	-	5.247	5.247	4.036	1.211	0.041	0.030	76.9
P56	203-204	-	18.55	18.55	14.95	3.597	0.121	0.089	80.6
EGHE Water Line	192-182	453.2	-	188.4	71.5	116.9	3.92	2.884	37.9
Exhaust Line	210-211	-456.1	-	-	-	-	-	-	-
HE-4 Cold Water	191-192	609.7	-	165.2	93.8	71.4	2.394	1.761	56.8
Hot Water	194-195	-1054	-	-	-	-	-	-	-
HE-5 Cold Water	196-197	41.09	-	12.00	6.0	6.0	0.201	0.148	50.0
Hot Water	199-200	-104.7	-	-	-	-	-	-	-
LOHE Lub Oil Line	201-202	510.4	-	96.8	51.5	45.3	1.519	1.519	53.2
Water Line	195-196	-359.4	-	-	-	-	-	-	-
Gas Engine	-	-	1000	4053.62 ¹ 4593.52 ³	1000 ¹ 1071.5 ² 2125.7 ³	3053.62 ¹ 2982.12 ² 1927.92 ³	89.38 ² 64.65 ³	75.33 ¹ 73.57 ² 53.72 ³	24.67 ¹ 26.43 ² 46.28 ³
BEPC (or CP)	-	1713.8 -2073.9	1000	4053.62	1071.5	2982.12	100.0	73.57	26.43

^{1,2,3} Values obtained by using Equations (9.38), (9.39), and (9.40), respectively.

9.7 Economic Analysis

The thermoeconomic (exergoeconomic analysis) of a municipal wastewater treatment system has some difficulties due to the huge amount of data presented. In order to accomplish this task in an effective manner, GASKI WWTP is simplified considering main subsystems, components and flows and it is named as *Primary Economic Control Volume*. By this approach, the biogas engine powered cogeneration system can be considered as *Secondary Economic Control Volume*.

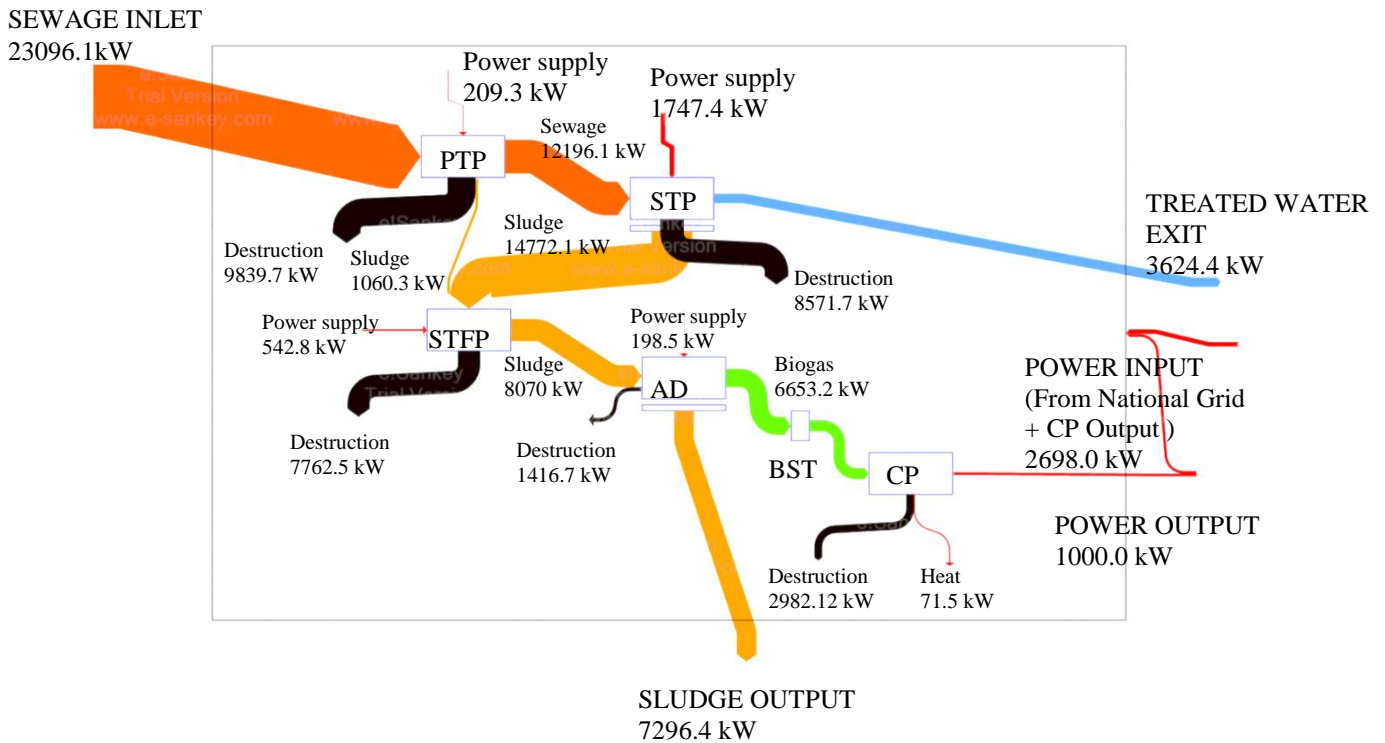
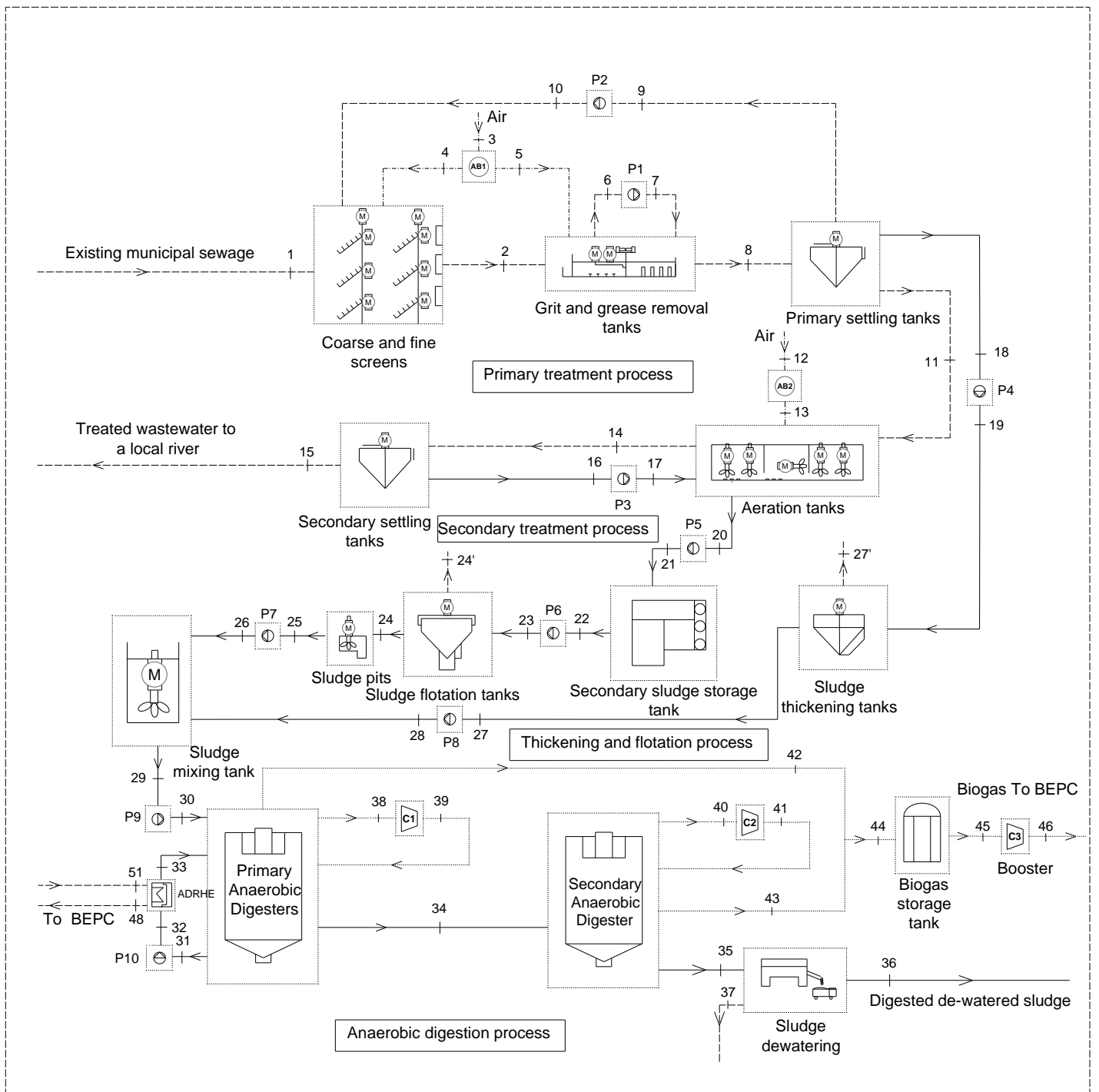


Figure 9.8: Overall Exergy Assessment of GASKI WWTP and BEPC (or CP)

9.7.1 GASKI WWTP: Primary Economic Control Volume

The simplified schematic of primary economic control volume of GASKI WWTP is shown in Fig. 9.9. The economic data including the first capital investments and the other expenditures of GASKI WWTP are obtained from the plant management. The operating and maintenance (OM) costs are obtained by considering WWTP's entire economic life (i.e., 25 years from January 1999 to December 2024). These costs are escalated by using average nominal escalation rate, which is 5% in US dollars. The average capacity factor (τ) for the entire WWTP is 91.7% which means that the system operates at full load 8030 h out of the total available 8760 h per year. The total capital investment of GASKI WWTP was 56.0 million US dollars. The purchased equipment costs, the hourly levelized costs of the capital investment, the OM costs, and the total costs of the components of the WWTP plant are given in Table 9.15.



-----	Sewage Line	ADRHE : Anaerobic Digester Re-circulation Heat Exchanger
————	Sludge Line	BEPC : Biogas Engine Power Cogeneration
.....	Biogas Line	AB : Air Blower
- - - -	Air Line	M : Electrical Motor
		P : Pump
		C : Compressor

Figure 9.9: A Simplified Schematic of GASKI WWTP: Primary Economic Control Volume

Table 9.15: The cost rates associated with first capital investment and OM costs for the subcomponents of the GASKI WWTP (Primary Economic Control Volume).

Component	PEC ($\times 10^3$ \$)	\dot{Z}_k^{CI} (\$/h)	\dot{Z}_k^{OM} (\$/h)	\dot{Z}_k^{TOTAL} (\$/h)
Coarse and fine screens	1200	3.97	0.04	4.01
Grit and grease removal tanks	2000	6.61	0.70	7.31
Primary sedimentation tanks	4000	13.23	1.32	14.55
Aeration tanks	6000	19.84	2.00	21.84
Secondary sedimentation tanks	4000	13.23	1.32	14.55
Sludge thickening tanks	4000	13.23	1.32	14.55
Sludge flotation tanks	4000	13.23	1.32	14.55
Sludge mixing tank	1000	3.31	0.03	3.34
Primary anaerobic sludge digestion tanks	4500	14.90	0.15	15.05
Secondary anaerobic sludge digestion tank	1500	4.96	0.05	5.01
Sludge dewatering unit	1000	3.31	0.03	3.34
Air blower - AB1	21.0	0.07	0.0014	0.071
Air blower - AB2	450.0	1.49	0.03	1.52
Pump-P1	15.12	0.05	0.001	0.051
Pump-P2	2.760	0.009	0.0002	0.009
Pump-P3	1380	4.56	0.09	4.65
Pump-P4	20.50	0.068	0.0014	0.069
Pump-P5	23.31	0.08	0.0016	0.082
Pump-P6	15.68	0.052	0.001	0.053
Pump-P7	7.60	0.03	0.005	0.035
Pump-P8	1.80	0.006	0.0001	0.006
Pump-P9	4.80	0.016	0.0032	0.017
Pump-P10	1.02	0.0034	0.0007	0.004
Sludge heat exchanger- ADRHE	225	0.744	0.015	0.758
Biogas compressors-C1	750	2.480	0.05	2.53
Biogas compressor-C2	250	0.827	0.017	0.844
Booster- C3	250	0.827	0.017	0.844
Other plant equipment	551	1.822	0.018	1.84
TOTAL PURCHASED-EQUIPMENT COSTS (PEC)	37,169.740	122.89	1.843	124.73
Purchased-equipment installation	3360	-	-	-
Piping	2000	-	-	-
Instrumentation and controls	1548	-	-	-
Electrical equipment and materials	2000	-	-	-
TOTAL ONSITE COSTS	46,077.7	-	-	-
Total offsite costs	3000	-	-	-
TOTAL DIRECT COSTS (DC)	49,077.7	-	-	-
TOTAL INDIRECT COSTS (IC)	3500	-	-	-
FIXED CAPITAL INVESTMENT	52,577.7	-	-	-
Other outlays	3422.3	-	-	-
TOTAL CAPITAL INVESTMENT	56,000.0	-	-	-

9.7.2 GASKI BEPC: Secondary Economic Control Volume

Since state numbers of BEPC system is changed according to the new simplified WWTP, i.e. primary economic control volume, schematic of BEPC system is presented in this section one more time with its changed state numbers (see Fig. 9.10).

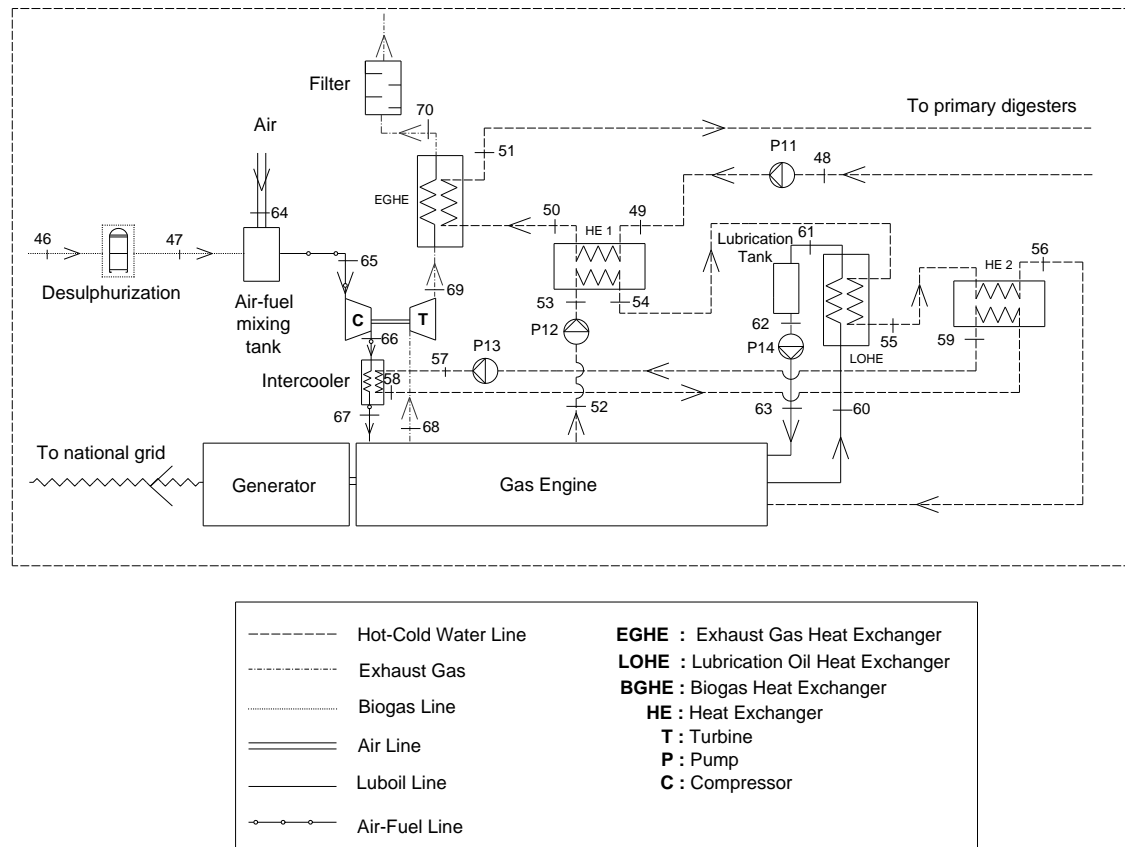


Figure 9.10: Schematic of GASKI BEPC: Secondary Economic Control Volume

In the actual case, the BEPC system is supplied as packaged system and cost allocation among its components is not separately quoted. However, to obtain more accurate results from thermoeconomic analysis, the subsystems are considered and cost allocation of subsystems and the other expenditures are obtained from the plant manager of GASKI WWTP and the contractor of the BEPC system. The operating and maintenance (OM) costs are obtained by considering BEPC's entire economic life, i.e. 25 years from 2006 to 2031. These costs are escalated by using average nominal escalation rate, which is 5% in US dollars. The average capacity factor (τ) for the entire WWTP is 91.7% which means that the system operates at full load

8030 h out of the total available 8760 h per year. The total capital investment of GASKI BEPC was 1.237 million US dollars. The purchased equipment costs, the hourly levelized costs of the capital investment, the OM costs, and the total costs of the components of the BEPC plant are given in Table 9.16.

Table 9.16: The cost rates associated with first capital investment and OM costs for the subcomponents of the Biogas Engine Powered Cogeneration (Second economic control volume).

Component	PEC ($\times 10^3$ \$)	\dot{Z}_k^{CI} (\$/h)	\dot{Z}_k^{OM} (\$/h)	\dot{Z}_k^{TOTAL} (\$/h)
Compressor (T)	38.461,5	0.09	0.005	0.095
Turbine (T)	38.461,5	0.09	0.005	0.095
P11	2.412,6	0.006	0.0002	0.0062
P12	1.853,1	0.0043	0.0009	0.0052
P13	1.573,4	0.0036	0.0007	0.0043
P14	2.237,81	0.005	0.0001	0.0051
Intercooler	17.482,5	0.04	0.008	0.048
EGHE	19.580,4	0.05	0.001	0.051
HE-1	8.898,6	0.02	0.0004	0.0204
HE-2	8.898,6	0.02	0.0004	0.0204
LOHE	6.993,0	0.02	0.0004	0.0204
Gas engine	419.580,4	0.96	0.1	1.06
Other plant equipment	3.496,5	0.0084	0.0006	0.0091
TOTAL PURCHASED-EQUIPMENT COSTS (PEC)	569.930,1			
Purchased-equipment installation	184.615,4	-	-	-
Piping	195.804,2	-	-	-
Instrumentation and controls	67.132,9	-	-	-
Electrical equipment and materials	72.727,3	-	-	-
TOTAL ONSITE COSTS	1.079.720,3	-	-	-
Total offsite costs	69.930,1	-	-	-
TOTAL DIRECT COSTS (DC)	1.149.650,4	-	-	-
TOTAL INDIRECT COSTS (IC)	69.930,1	-	-	-
FIXED CAPITAL INVESTMENT	1.219.580,5	-	-	-
Other outlays	17.482,5	-	-	-
TOTAL CAPITAL INVESTMENT	1.237.062,9	-	-	-

9.8 Thermoeconomic Analysis

Thermoeconomics assess the cost of consumed resources, money and system irreversibilities in terms of the overall production process. It helps to point out how resources are used more effectively in order to save them. Monetary costs express the economic effect of inefficiencies and are used to improve the cost effectiveness of production processes. Assessing the cost of the flow streams and processes in a plant helps to understand the process of cost formation, from the input resources to final products [168].

In this study, specific exergy costing (SPECOC) method is used to obtain and understand the cost formation structure of the plant. Exergetic cost rates balances and corresponding auxiliary equations of the plant are given in Chapter 5. Since the level at which the cost balances are formulated (i.e. aggregation level) affects the results of the thermoeconomic analysis, the lowest possible aggregation level is set. Exergetic cost rate balances and corresponding auxiliary equations are formulated for each subsystem of the first and second control volume. Auxiliary equations are found by applying \dot{F} and \dot{P} principles.

9.8.1 GASKI WWTP: Primary Economic Control Volume

Exergetic cost rate balances and corresponding auxiliary equations for each subsystem of GASKI WWTP are obtained by SPECOC method and are given in the Table 9.17.

Table 9.17: Exergetic cost rate balances and corresponding auxiliary equations for each subsystem of first economic control volume (GASKI WWTP). State numbers refer to Figure 9.9

(ADRHE: Anaerobic Digestion Recirculation Heat Exchanger)

Component	Exergetic cost rate balance equations	Auxiliary equations
Air blower AB-1	$c_3\dot{E}x_3 + c_e\dot{W}_{AB-1} + \dot{Z}_{AB-1} = c_4\dot{E}x_4 + c_5\dot{E}x_5$	$c_3 = 0 ; c_4 = c_5$ $\dot{E}x_3 = 0$
Coarse and fine screens	$c_1\dot{E}x_1 + c_4\dot{E}x_4 + c_e\dot{W}_{CFS} + \dot{Z}_{CFS} = c_2\dot{E}x_2$	$c_1 = 0$ $\dot{W}_{CFS} = 4.42 \text{ kW}$
Grit and grease removal tanks	$c_2\dot{E}x_2 + c_5\dot{E}x_5 + c_e\dot{W}_{GGRT} + \dot{Z}_{GGRT} = c_8\dot{E}x_8$	$\dot{W}_{GGRT} = 59.6 \text{ kW}$
Pump-P1	$c_e\dot{W}_{P1} + \dot{Z}_{P1} = c_7\dot{E}x_7 - c_6\dot{E}x_6$	$c_6 = c_2$
Primary settling tanks	$c_8\dot{E}x_8 + c_e\dot{W}_{PST} + \dot{Z}_{PST} = c_9\dot{E}x_9 + c_{11}\dot{E}x_{11} + c_{18}\dot{E}x_{18}$	$c_9 = c_{11} = c_{18}$ $\dot{W}_{PST} = 1.11 \text{ kW}$
Pump-P2	$c_e\dot{W}_{P2} + \dot{Z}_{P2} = c_{10}\dot{E}x_{10} - c_9\dot{E}x_9$	None
Air blower AB-2	$c_{12}\dot{E}x_{12} + c_e\dot{W}_{AB-2} + \dot{Z}_{AB-2} = c_{13}\dot{E}x_{13}$	$c_{12} = 0 ; \dot{E}x_{12} = 0$
Aeration tanks	$c_{11}\dot{E}x_{11} + c_{13}\dot{E}x_{13} + c_e\dot{W}_{AT} + \dot{Z}_{AT} = c_{14}\dot{E}x_{14} + c_{20}\dot{E}x_{20}$	$c_{14} = c_{20}$ $\dot{W}_{AT} = 57 \text{ kW}$
Secondary settling tanks	$c_{14}\dot{E}x_{14} + c_e\dot{W}_{SST} + \dot{Z}_{SST} = c_{15}\dot{E}x_{15} + c_{16}\dot{E}x_{16}$	$c_{15} = c_{16}$ $\dot{W}_{SST} = 6.6 \text{ kW}$
Pump-P3	$c_e\dot{W}_{P3} + \dot{Z}_{P3} = c_{17}\dot{E}x_{17} - c_{16}\dot{E}x_{16}$	None

Pump-P4	$c_e \dot{W}_{P4} + \dot{Z}_{P4} = c_{19} \dot{E}x_{19} - c_{18} \dot{E}x_{18}$	None
Pump-P5	$c_e \dot{W}_{P5} + \dot{Z}_{P5} = c_{21} \dot{E}x_{21} - c_{20} \dot{E}x_{20}$	None
Pump-P6	$c_e \dot{W}_{P6} + \dot{Z}_{P6} = c_{23} \dot{E}x_{23} - c_{22} \dot{E}x_{22}$	$c_{22} = c_{21}$
Sludge flotation tanks	$c_{23} \dot{E}x_{23} + c_e \dot{W}_{SFT} + \dot{Z}_{SFT} = c_{24} \dot{E}x_{24} + c_{24'} \dot{E}x_{24'}$	$c_{24} = c_{24'}$ $\dot{W}_{SFT-1} = 6.97 \text{ kW}$
Pump-P7	$c_e \dot{W}_{P7} + \dot{Z}_{P7} = c_{26} \dot{E}x_{26} - c_{25} \dot{E}x_{25}$	$c_{25} = c_{24}$
Sludge thickening tanks	$c_{19} \dot{E}x_{19} + c_e \dot{W}_{STT} + \dot{Z}_{STT} = c_{27} \dot{E}x_{27} + c_{27'} \dot{E}x_{27'}$	$c_{27} = c_{27'}$ $\dot{W}_{STT} = 4.5 \text{ kW}$
Pump-P8	$c_e \dot{W}_{P8} + \dot{Z}_{P8} = c_{28} \dot{E}x_{28} - c_{27} \dot{E}x_{27}$	None
Sludge mixing tanks	$c_{26} \dot{E}x_{26} + c_{28} \dot{E}x_{28} + c_e \dot{W}_{SMT} + \dot{Z}_{SMT} = c_{29} \dot{E}x_{29}$	$\dot{W}_{SMT} = 11.0 \text{ kW}$
Pump-P9	$c_e \dot{W}_{P9} + \dot{Z}_{P9} = c_{30} \dot{E}x_{30} - c_{29} \dot{E}x_{29}$	None
Pump-P10	$c_e \dot{W}_{P10} + \dot{Z}_{P10} = c_{32} \dot{E}x_{32} - c_{31} \dot{E}x_{31}$	$c_{31} = c_{30}$
ADRHE	$c_{32} \dot{E}x_{32} + c_{51} \dot{E}x_{51} + \dot{Z}_{ADRHE} = c_{33} \dot{E}x_{33} + c_{48} \dot{E}x_{48}$	$c_{48} = c_{51} = c_{15}$
Primary sludge digestion tanks (Sludge line)	$c_{30} \dot{E}x_{30} + c_{33} \dot{E}x_{33} + \dot{Z}_{PAD} = c_{31} \dot{E}x_{31} + c_{34} \dot{E}x_{34}$	None
Biogas compressor C-1	$c_e \dot{W}_{C-1} + \dot{Z}_{C-1} = c_{39} \dot{E}x_{39} - c_{38} \dot{E}x_{38}$	$c_{38} = c_{34}$
Primary sludge digestion tanks (Biogas line)	$c_{39} \dot{E}x_{39} + \dot{Z}_{PAD} = c_{42} \dot{E}x_{42}$	None
Secondary sludge digestion tank (Sludge line)	$c_{34} \dot{E}x_{34} + \dot{Z}_{SAD} = c_{35} \dot{E}x_{35}$	None
Biogas compressor C-2	$c_e \dot{W}_{C-2} + \dot{Z}_{C-2} = c_{41} \dot{E}x_{41} - c_{40} \dot{E}x_{40}$	$c_{40} = c_{35}$
Secondary sludge digestion tank (Biogas line)	$c_{41} \dot{E}x_{41} + \dot{Z}_{SAD} = c_{43} \dot{E}x_{43}$	None
Sludge dewatering	$c_{35} \dot{E}x_{35} + c_e \dot{W}_{DW} + \dot{Z}_{DW} = c_{36} \dot{E}x_{36} + c_{37} \dot{E}x_{37}$	$\dot{W}_{DW} = 160 \text{ kW}$ $c_{37} = 0$
Booster C-3	$c_{45} \dot{E}x_{45} + c_e \dot{W}_{C-3} + \dot{Z}_{C-3} = c_{46} \dot{E}x_{46}$	$c_{45} = c_{44}$ $c_{44} = (c_{42} + c_{43})/2.4$

The exergetic cost parameters of the WWTP subcomponents are given in Table 9.19. In this table, unit exergetic cost of fuel and products are obtained using the stream values listed in Table 9.18 and operation and maintenance cost rates are obtained from Table 9.16.

Table 9.18: Exergy flow rates, cost flow rates and the unit exergy costs associated with the main streams and components of the first economic control volume (GASKI WWTP). States are referred to Figure 9.9.

State	\dot{E}_x (kW)	c (¢/m ³)	\dot{C} (\$/h)
Sewage inlet	23,096.07	0.00	0.00
Treated wastewater exit	1894.0	3.804	62.047
Sludge exit (Primary treatment system)	1003.40	0.341	2.947
Sludge exit (Secondary Treatment system)	14,727.24	0.991	125.655
Sludge exit (Flotation unit)	16,716.50	0.277	152.572
Sludge exit (Thickening unit)	12,096.06	0.198	20.599
Sludge exit (Primary anaerobic digestion)	11,297.89	0.790	76.905
Sludge exit (Secondary anaerobic digestion and de-watering unit)	11,293.64	1.907	81.903
Biogas exit (Primary and secondary anaerobic digestion)	6651.0	13.478	175.985
Component	\dot{E}_x (kW)	c (\$/GJ)	\dot{C} (\$/h)
AB-1	44.54	27.0	4.329
AB-2	1216.79	27.0	118.272
Electric Motors	319.27	27.0	31.033
\dot{W}_{P1}	17.72	27.0	1.722
\dot{W}_{P2}	3.85	27.0	0.374
\dot{W}_{P3}	9.55	27.0	0.928
\dot{W}_{P4}	59.50	27.0	5.783
\dot{W}_{P5}	59.40	27.0	5.774
\dot{W}_{P6}	278.57	27.0	27.077
\dot{W}_{P7}	13.06	27.0	1.269
\dot{W}_{P8}	21.71	27.0	2.110
\dot{W}_{P9}	8.0	27.0	0.778
\dot{W}_{P10}	8.28	27.0	0.805
C-1	16.09	27.0	1.564
C-2	5.36	27.0	0.521
C-3	2.05	27.0	0.199

We note the followings from the exergoeconomic results of this wastewater treatment plant as listed in Table 9.18 and Table 9.19:

- Since wastewater treatment is one of the infrastructural services supplied by a local government, the exergetic cost rate and the specific unit exergetic cost of the sewage entering the WWTP are taken as zero. The corresponding values of these costs for the treated wastewater exit are 62.05 \$/h and 3.804 ¢/m³. The total amount of treated wastewater per day in the WWTP is 172,800 m³. This corresponds to the total treated wastewater cost of 6573.31 \$ per day. The treated

wastewater cost mainly includes the operation costs of the wastewater treatment processes.

- The exergetic cost rate and the specific unit exergetic cost of the activated sludge with a dry matter content of 0.5% at the exit of secondary treatment system are 125.65 \$/h and 0.991 ¢/m³, respectively. The corresponding costs for sludge at the thickening unit are 20.6 \$/h and 0.198 ¢/m³, respectively. This decrease is mainly due to the increased specific chemical exergy of the sludge at the end of the flotation and thickening processes. Note that, at the end of the thickening process, activated sludge has a dry matter content of 5.0%.
- The dry matter content of the sludge increases to 8.0% through the anaerobic digestion process and the specific unit exergetic cost of the digested sludge at the exit of primary anaerobic digestion unit is 0.790 ¢/m³. The corresponding value of the digested sludge at the exit of secondary digestion unit is 1.907 ¢/m³. The increase of unit cost in the primary digestion process is due to the high retention time which causes the maximum contact between the incoming activated sludge and the bacteria to increase the methane content in the produced biogas. The specific unit exergetic cost of the digested sludge at the exit of the secondary anaerobic digestion process is more than double the cost of the primary digestion. This is because, in addition to high retention time of sludge in reactor, the power consumption for the de-watering process in WWTP after secondary anaerobic digestion process is about 81 kW per ton dry matter content of the digested sludge. The exergetic cost rates of digested sludge at the exits of primary and secondary anaerobic digestion units are obtained as 76.91 \$/h and 81.90 \$/h, respectively.
- The daily biogas production of the GASKI WWTP is 18,300 m³. As stated, for each 1 m³ biogas produced in the plant, 68.26 kg of sludge with the dry matter content of 8.0% is digested in anaerobic reactors. The average exergetic cost rate and the average specific unit exergetic cost of the biogas at the exit of anaerobic digestion reactors are 175.9 \$/h and 13.48 ¢/m³, respectively. The daily biogas production cost in GASKI WWTP is obtained as \$2057.3. In the plant, this biogas is used as the fuel for gas engine powered cogeneration facility, which produces 24,000 kW net electricity output per day.

- The exergetic cost rates for the air-blower 2 (AB-2), electric motors and pump-6 (P6) are 118.27 \$/h, 31.03 \$/h and 27.07 \$/h, respectively. These costs are the highest exergy cost rates among the other plant components since the exergy flow rates of these components are notably high and all exergy available at the exit of these components is supplied by mechanical power which is the most expensive “fuel” in the plant. The exergoeconomic factor of the AB-2 is 0.13%, which is relatively low as compared with other components in the plant (see Table 9.21). This value depends on the dominant effect of the operation cost rate in the exergoeconomic factor definition given by Equation (5.38) in Chapter 5.

Table 9.19: The unit exergetic costs of fuels and products, cost rate of exergy destruction, operation and maintenance cost rate, and exergoeconomic factor for the first economic control volume (GASKI WWTP) components.

(ADRHE: Anaerobic Digestion Recirculation Heat Exchanger)

Component	$c_{f,k}$ (\$/GJ)	$c_{p,k}$ (\$/GJ)	$\dot{E}x_D$ (kW)	\dot{C}_D (\$/h)	\dot{Z}_k^{OM} (\$/h)	f (%)
Air blower-1	27.0	32.11	6.46	0.63	0.0014	0.22
Air blower-2	27.0	33.81	232.1	22.56	0.03	0.13
Pump-P1	27.0	34.82	4.39	0.43	0.001	0.23
Pump-P2	27.0	36.81	0.96	0.09	0.0002	0.22
Pump-P3	27.0	30.14	3.75	0.36	0.09	20.0
Pump-P4	27.0	36.00	13.10	1.27	0.0014	0.11
Pump-P5	27.0	33.15	14.52	1.41	0.0016	0.11
Pump-P6	27.0	32.04	41.13	4.00	0.001	0.02
Pump-P7	27.0	28.19	2.32	0.23	0.005	2.13
Pump-P8	27.0	34.16	3.93	0.38	0.0001	0.03
Pump-P9	27.0	42.21	2.08	0.20	0.0032	1.57
Pump-P10	27.0	42.03	2.12	0.21	0.0007	0.33
Biogas compressor - C1	27.0	39.32	3.70	0.36	0.05	12.20
Biogas compressor - C2	27.0	35.31	1.23	0.12	0.017	12.41
Booster-C3	27.0	42.71	0.69	0.07	0.017	19.50
ADRHE	9.10	51.79	138.24	13.44	0.015	0.11
Primary Treatment System	27.0	27.82	10,812.84	1051.0	2.064	0.20
Secondary Treatment System	27.0	34.33	10,875.37	1057.1	3.442	0.32
Thickening and Flotation System	27.0	28.85	7875.49	765.5	2.679	0.35
Anaerobic Digestion Process	27.0	34.35	1778.14	172.8	0.33	0.19

- The specific exergetic fuel and product costs for the anaerobic digestion reactor heat exchanger (ADRHE) unit are 9.1 \$/h and 51.8 \$/h, respectively. Note that ADRHE has the lowest exergetic efficiency of the WWTP (17.42%). This

difference between inlet and exit cost streams clearly indicates that the unit exergetic product cost is inversely proportional to the exergetic efficiency. Because of the low mass flow rate of hot water as compared to digested sludge in the ADRHE unit, exergetic destruction cost rate involve high weighing factor in the denominator of exergoeconomic factor relation. Cost effectiveness for this unit can be achieved by reducing both exergy destruction and operation cost.

- Pump-3 (P3) has the highest exergoeconomic factor (20.0%) among other pumps. It is due to high value of the operation and maintenance costs of this component compared with the exergetic destruction cost rate. On the other hand, pump-6 (P6) has the lowest exergoeconomic factor (0.02%) in the plant since the exergy destruction cost rate of this component is the highest among the other plant components.
- The exergoeconomic factor for biogas compressors (C1 and C2) and booster (C3) are 12.4% and 19.5%, respectively. Thermoeconomic improvement of these units can be achieved by a decrease of the total effect of the operation and destruction cost rates.
- Exergy destruction cost rates of the primary and secondary treatment systems are found to be 1051 \$/h and 1057 \$/h, respectively. These are the highest exergy destruction cost rates among other sub-systems. On the other hand, anaerobic digestion process has the lowest exergy destruction cost rate (172.8 \$/h). This is mainly due to the highly efficient process occurs in the digestion units.

In Figure 9.11, variation of exergoeconomic factors for subcomponents of WWTP with respect to corresponding cost rate of exergy destructions is given.

9.8.2 GASKI BEPC: Secondary Economic Control Volume

Exergetic cost rate balances and corresponding auxiliary equations for each subsystem of second economic control volume are obtained by SPECO method and are given in Table 9.20. Exergy based cost flow rates and unit exergy cost of main flows of the BEPC system is given in Table 9.21. The exergetic cost parameters of the BEPC system subcomponents are given in Table 9.22.

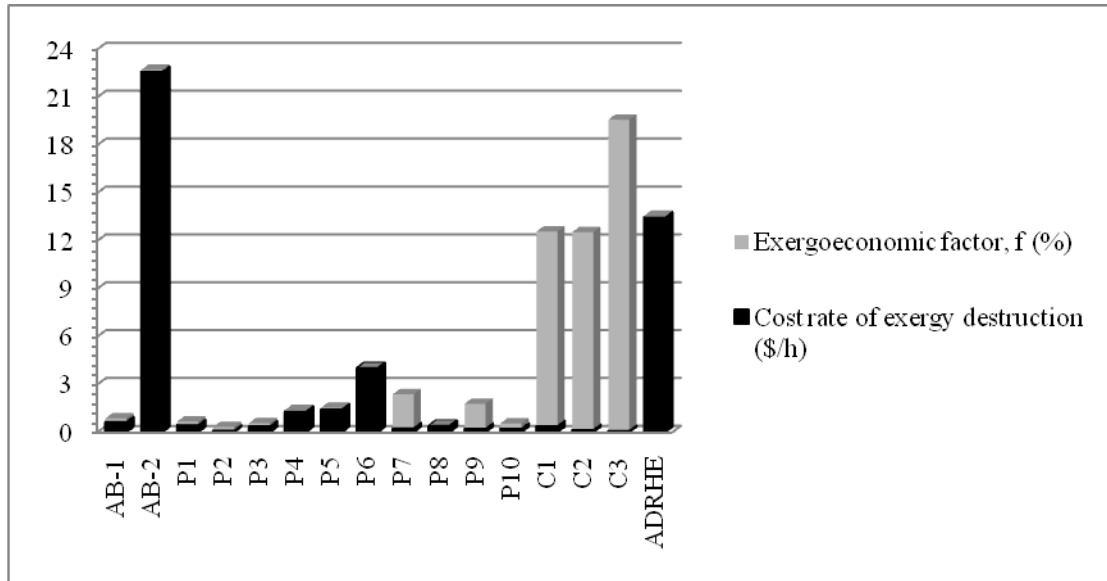


Figure 9.11: Variation of exergoeconomic factors for the subcomponents of WWTP with respect to corresponding cost rate of exergy destructions

Table 9.20: Exergetic cost rate balances and corresponding auxiliary equations for each subsystem of second economic control volume (BEPC). State numbers refer to Figure 9.10

Component	Exergetic cost rate balance equations	Auxiliary equations
Compressor	$c_e \dot{W}_{COMP} + \dot{Z}_{COMP} = c_{66} \dot{E}x_{66} - c_{65} \dot{E}x_{65}$	$c_{65} = c_{47}$
Turbine	$c_{68} \dot{E}x_{68} + \dot{Z}_{TURB} = c_e \dot{W}_{TURB} + c_{69} \dot{E}x_{69}$	$c_{68} = c_{69}$
EGHE	$c_{69} \dot{E}x_{69} + c_{50} \dot{E}x_{50} + \dot{Z}_{EGHE} = c_{70} \dot{E}x_{70} + c_{51} \dot{E}x_{51}$	$c_{69} = c_{70}$
Pump – P11	$c_e \dot{W}_{P11} + \dot{Z}_{P11} = c_{49} \dot{E}x_{49} - c_{48} \dot{E}x_{48}$	---
Pump – P13	$c_e \dot{W}_{P13} + \dot{Z}_{P13} = c_{57} \dot{E}x_{57} - c_{59} \dot{E}x_{59}$	$c_{59} = c_{15}$
BGHE	$c_{66} \dot{E}x_{66} + c_{57} \dot{E}x_{57} + \dot{Z}_{IC} = c_{67} \dot{E}x_{67} + c_{58} \dot{E}x_{58}$	$c_{57} = c_{58}$
HE-2	$c_{55} \dot{E}x_{55} + c_{58} \dot{E}x_{58} + \dot{Z}_{HE-2} = c_{56} \dot{E}x_{56} + c_{59} \dot{E}x_{59}$	$c_{55} = c_{56}$
Pump – P14	$c_e \dot{W}_{P14} + \dot{Z}_{P14} = c_{63} \dot{E}x_{63} - c_{62} \dot{E}x_{62}$	---
LOHE	$c_{60} \dot{E}x_{60} + c_{54} \dot{E}x_{54} + \dot{Z}_{LOHE} = c_{61} \dot{E}x_{61} + c_{55} \dot{E}x_{55}$	$c_{61} = c_{62}$ $c_{54} = c_{55}$
HE-1	$c_{53} \dot{E}x_{53} + c_{49} \dot{E}x_{49} + \dot{Z}_{HE-1} = c_{54} \dot{E}x_{54} + c_{50} \dot{E}x_{50}$	---
Pump – P12	$c_e \dot{W}_{P12} + \dot{Z}_{P12} = c_{53} \dot{E}x_{53} - c_{52} \dot{E}x_{52}$	---
Gas engine	$c_{67} \dot{E}x_{67} + c_{63} \dot{E}x_{63} + c_{56} \dot{E}x_{56} + \dot{Z}_{GE}$ $= c_{68} \dot{E}x_{68} + c_{60} \dot{E}x_{60} + c_{52} \dot{E}x_{52} + c_{GE} \dot{W}_{GE}$	$\dot{W}_{net} = 1000 \text{ kW}$

Table 9.21: Exergy flow rates, cost flow rates and the unit exergy costs associated with the main streams and components of the second economic control volume (BEPC). States are referred to Figure 9.10.

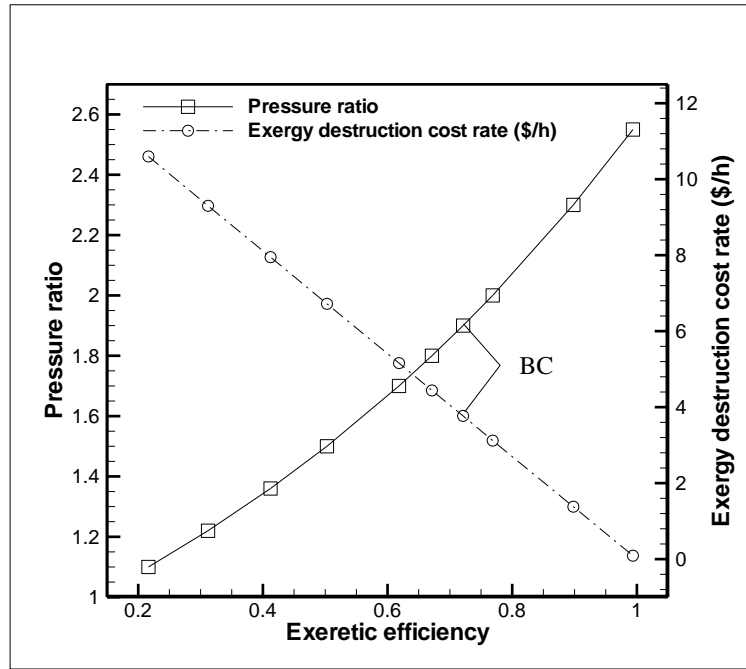
State	$\dot{E}x$ (kW)	c (¢/m ³)	\dot{C} (\$/h)
Biogas air mixing (Compressor inlet)	4046.40	13.627	92.451
Biogas air mixing (engine inlet)	4053.62	15.560	105.769
Hot water (EGHE exit)	516.40	3.804	16.917
Exhaust gas (Engine exit)	374.10	0.003	31.690
Exhaust gas (Turbine exit)	192.10	0.003	16.273
Component	$\dot{E}x$ (kW)	c (\$/GJ)	\dot{C} (\$/h)
Compressor (Turbocharger)	138.9	25.0	12.390
Turbine (Turbocharger)	159.6	23.53	14.236
Gas engine (Electricity)	1000.0	25.0	90.00
\dot{W}_{P11}	2.714	25.0	0.2443
\dot{W}_{P12}	10.34	25.0	0.9306
\dot{W}_{P13}	5.247	25.0	0.4722
\dot{W}_{P14}	18.55	25.0	1.6695

We note the followings from the exergoeconomic results of this cogeneration plant as listed in Table 9.21 and Table 9.22:

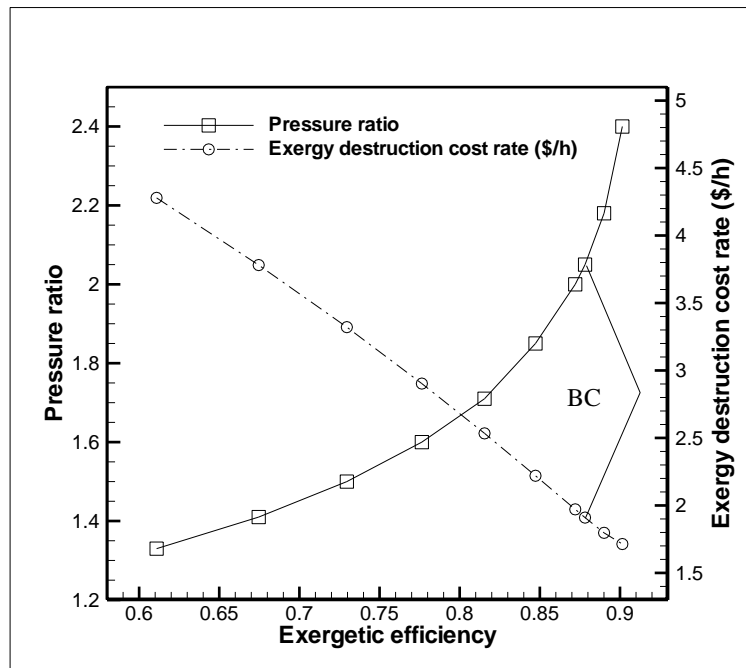
- The exergetic cost rate and the specific unit exergetic cost of the biogas entering the cogeneration system is 92.451 \$/h and 13.63 ¢/m³, respectively. The unit cost of the biogas is found to be 15.6 ¢/m³ at the engine inlet. Since for 1 kW electricity produced by the engine, 0.387 m³ of biogas with 60% methane content is consumed, the total consumption cost of the biogas for 1000 kWh electricity output is calculated to be 60.22 \$. Considering the unit cost of the natural gas for 1 kWh electricity production as 9.04¢ for Turkey [169], the total consumption cost of natural gas to be used for 1000 kWh electricity generation in a natural gas fuelled engine powered cogeneration system can be found as 90.40 \$ for comparison. Note that the consumption cost of the biogas used in the cogeneration system is, in fact, the stabilization cost of the sewage sludge by flotation, thickening, and anaerobic digestion systems in GASKI WWTP.
- The net electric output of the BEPC system is 1000 kWh. The exergetic cost rate and the specific unit exergetic cost of the power produced by the system are 12.4 \$/h and 25 \$/GJ (see Table 9.21), respectively. This means that the

unit cost of 1 kWh electricity produced in the cogeneration system is 9.0 ¢. Thus, the total cost the electricity produced in the system can be found as 90 \$. Note that the electricity price tariff adopted to industrial facilities by TEDAS [170] is 10.3 ¢/kWh.

- As indicated in Table 9.22, gas engine is the most exergy destructive component of the plant. The exergoeconomic factor of the gas engine is determined to be 1.34%. Depending on the total dominate effect of the highest investment and exergetic destruction cost rates of the engine itself, a decrease of the exergy destruction could be cost effective even if this would increase the investment cost for the gas engine.
- The exergoeconomic factor of the compressor is 2.46%. This value is 4.77% for the turbine. Thermoeconomic improvement of the turbocharger unit can be achieved by a decrease of the total effect of the initial investment and destruction cost rates (see Fig. 9.12 a, b).
- Exhaust gas heat exchanger unit (EGHE) involves an exergy destruction cost rate of 9.91 \$/h. The specific cost of this unit is due to considering the exhaust gas as fuel. The exergetic unit cost of hot water is inversely proportional to the exergetic efficiency of this unit. Because of the low mass flow rate of exhaust gas as compared to water in the exhaust gas heat exchanger, exergetic destruction cost rates involve high weighing factor in the denominator of exergoeconomic factor relation. Cost effectiveness for this unit can be achieved by reducing exergy destruction (see Fig. 9.13 a).
- The exergoeconomic factor for lubrication oil cooler is determined to be 0.33%, which is the lowest value of all components in the system. It may be suggested that a decrease in the investment cost may improve the cost effectiveness of component (see Fig. 9.13 b).

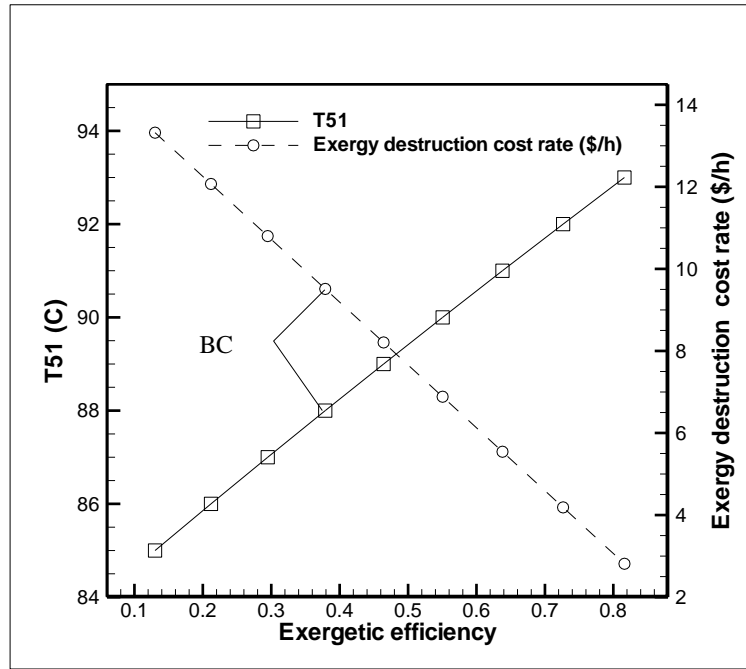


(a)

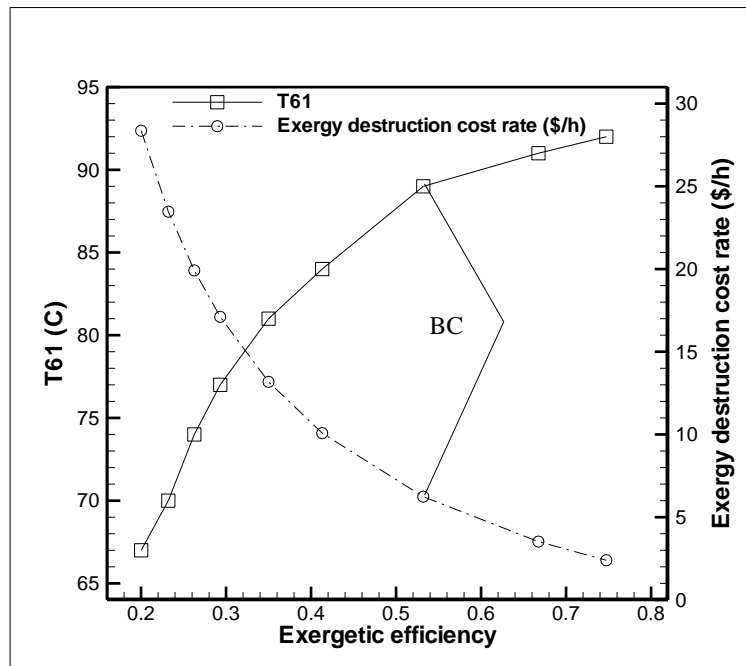


(b)

Figure 9.12: Variation of exergetic efficiency and exergy destruction cost rates with respect to (a) the pressure ratio of air-biogas mixture for the Compressor (b) the pressure ratio of exhaust gas for the Turbine



(a)



(b)

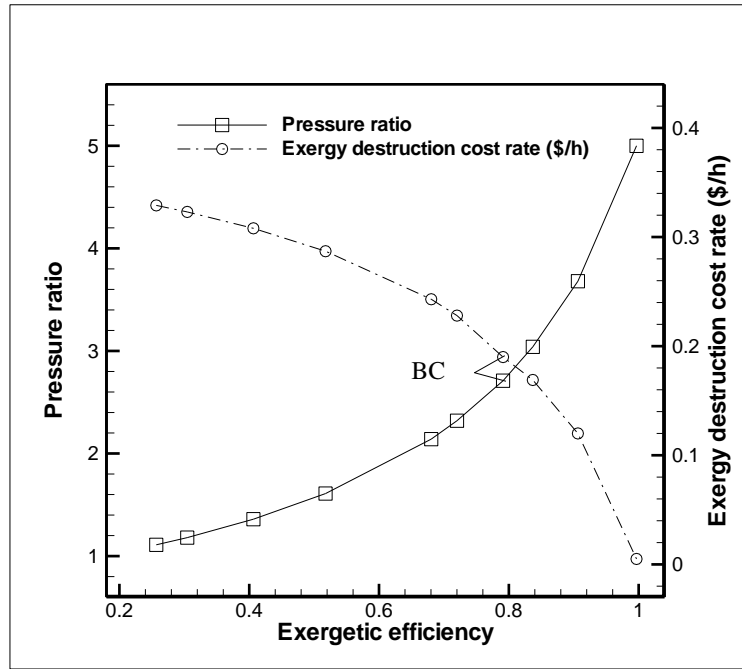
Figure 9.13: Variation of exergetic efficiency and exergy destruction cost rates with respect to (a) the exit temperature of hot (process) water for EGHE (b) the exit temperature of lubrication oil for LOHE

Table 9.22: The unit exergetic costs of fuels and products, cost rate of exergy destruction, operation and maintenance cost rate, and exergoeconomic factor for the second economic control volume (BEPC) components.

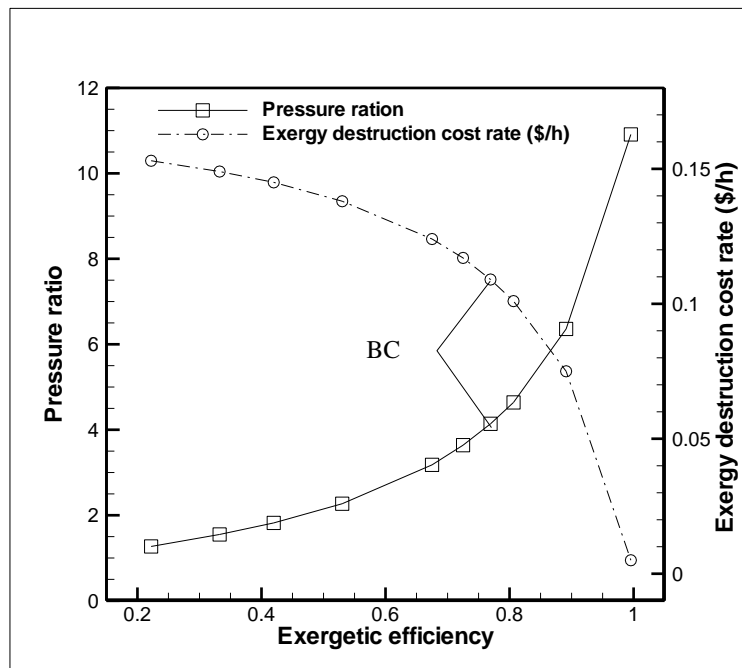
Component	$c_{f,k}$ (\$/GJ)	$c_{p,k}$ (\$/GJ)	$\dot{E}x_D$ (kW)	\dot{C}_D (\$/h)	\dot{Z}_k^T (\$/h)	f (%)
Compressor (T)	25.00	30.80	38.70	3.76	0.095	2.46
Turbine (T)	23.53	27.0	22.40	1.90	0.095	4.77
Intercooler	11.05	47.8	8.33	0.33	0.0062	1.43
EGHE	23.53	62.24	116.94	9.91	0.0052	0.51
LOHE	38.28	58.60	45.30	6.24	0.0043	0.33
HE-1	9.28	18.25	71.40	2.39	0.0051	0.85
HE-2	38.28	49.50	6.00	0.83	0.048	2.41
P11	25.00	39.19	0.58	0.05	0.051	10.70
P12	25.00	32.87	2.14	0.19	0.0204	2.65
P13	25.00	33.73	1.21	0.11	0.0204	3.83
P14	25.00	34.22	3.60	0.32	0.0204	1.56
Gas engine	7.25	25.00	2982.12	77.83	1.06	1.34

- The pumps, P12, P13, and P14 have the lowest exergy destruction cost rates of all system components. The exergoeconomic factors of these components are inversely proportional to the corresponding destruction cost rates (see Table 9.22). This is because the operation and maintenance costs of these components are high as compared to other components in the system. The variation of exergetic efficiency and exergy destruction cost rates of P12 and P13 with respect to their pressure ratios are shown in Fig. 9.14 a, b, respectively.

Thermoeconomic analyses of GASKI WWTP and BEPC system indicate that the cost flows of the existing systems are based on the two main factors: 1. Operation and maintenance costs, 2. Exergy destruction cost rates. Small improvements in the WWTP and BEPC design and operation can provide better enhancements in plants' performance compared to large improvements. In general, better exergetic performance and cost effectiveness can be achieved by reducing exergy destruction through better design and operation as well as by reducing investment and exergetic destruction costs.



(a)



(b)

Figure 9.14: Variation of exergetic efficiency and exergy destruction cost rates with respect to (a) the pressure ratio of P12 (b) the pressure ratio of P13

9.9 Thermo-economic Optimization of GASKI WWTP

The objective function expresses the optimization criterion as a function of dependent and independent variables. For the BEPC system, the objective function can be written as

$$\text{minimize } \dot{C}_{P,\text{total}} = \dot{C}_{F,\text{total}} + \dot{Z}_{\text{total}}^{\text{CI}} + \dot{Z}_{\text{total}}^{\text{OM}} \quad (9.43)$$

The variables, the total cost rate of fuel $\dot{C}_{F,\text{total}}$, the total cost rate of capital investment $\dot{Z}_{\text{total}}^{\text{CI}}$, and the total cost rate of O&M costs $\dot{Z}_{\text{total}}^{\text{OM}}$, are functions of decision variables. In this study, we minimize the total cost rate associated with the product $\dot{C}_{P,\text{total}}$ instead of the cost per unit of product exergy c_P .

The chemical oxygen demand (COD) value is taken as the decision variable in the optimization process of primary and secondary treatment systems. Since the chemical exergy of sewage decreases while its COD value is reduced through treatment processes, it becomes one of the major treatment process requirements. This decrease, which is accompanied by an excessive amount of operation costs, leads to an increase in cost level. The COD value for partially treated water is required to be given in the range between mg/l for the environmental operational restrictions of primary treatment system. The base case value (i.e. 367.65 mg/l) is the actual COD value of the partially treated water at the exit of primary treatment system. Figure 9.15 shows the variation of the exergetic product cost of the partially treated wastewater at the exit of primary treatment system with respect to different COD values and corresponding calculated exergetic efficiencies. The COD value for treated wastewater at the exit of secondary treatment system may be given in the range between mg/l. The base case COD value of the treated wastewater is given as 64.37 mg/l in Table 9.1. Figure 9.16 shows the variation of the exergetic product cost of the treated wastewater at the exit of secondary treatment system with respect to different COD values and corresponding calculated exergetic efficiencies.

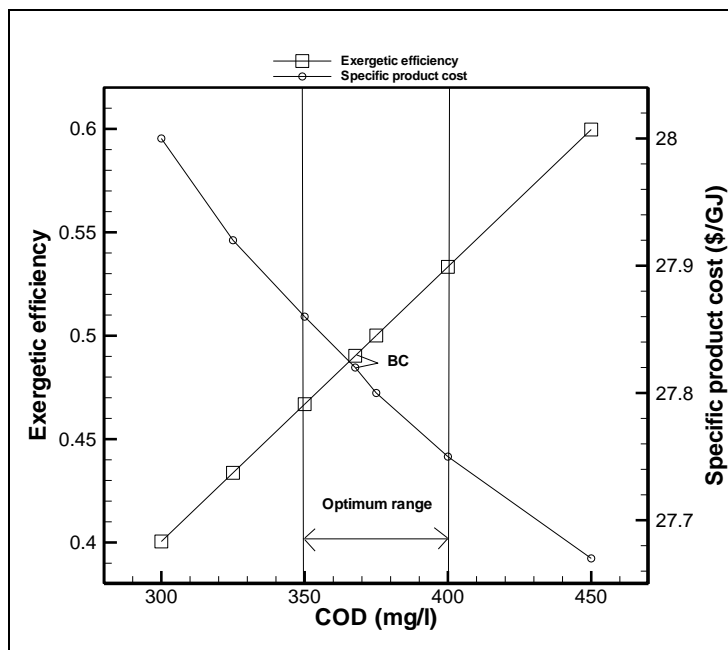


Figure 9.15: Variation of the product cost of the partially treated wastewater at the exit of primary treatment system with respect to different COD values and corresponding exergetic efficiencies

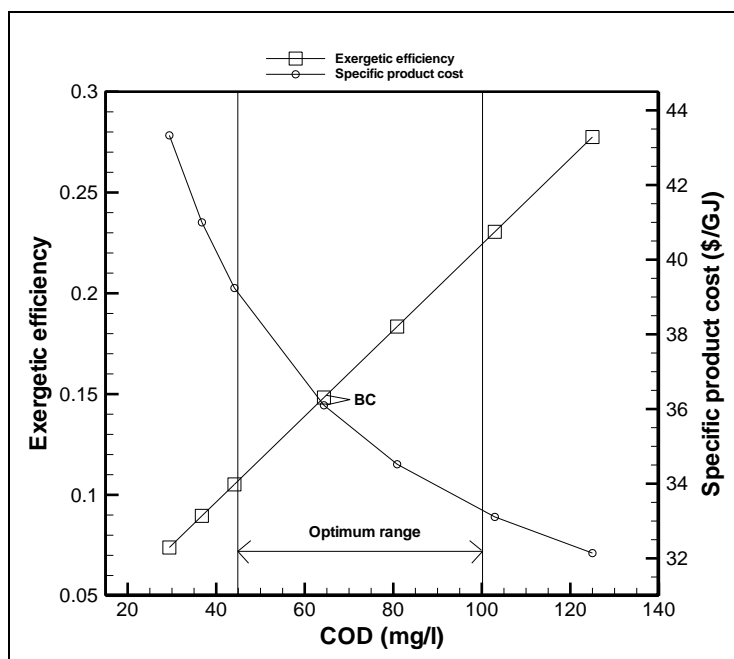


Figure 9.16: Variation of the product cost of the treated wastewater at the exit of secondary treatment system with respect to different COD values and corresponding exergetic efficiencies

The chemical exergy of sludge stream increases through sludge thickening process and the rate of exergy increase through processes in the sludge treatment subcomponents may cause a remarkable increase in cost level. The dry matter content (DMC) of sewage sludge at the inlet of thickening and flotation system is 0.5%. At the exit of this system, dryness of sludge increases to 5.0%, which is the actual base case value. The dry matter content of sewage sludge at the exit of thickening and flotation system may be given in the range between $4.0 \leq DMC \leq 5.5$. Figure 9.16 shows the variation of the exergetic product cost of the sewage sludge at the exit of thickening and flotation system with respect to different dry matter contents and corresponding exergetic efficiencies. Table 9.23 provides the costs obtained in the thermoeconomic optimization. The previously calculated base case costs through thermoeconomic analysis are also presented in this table.

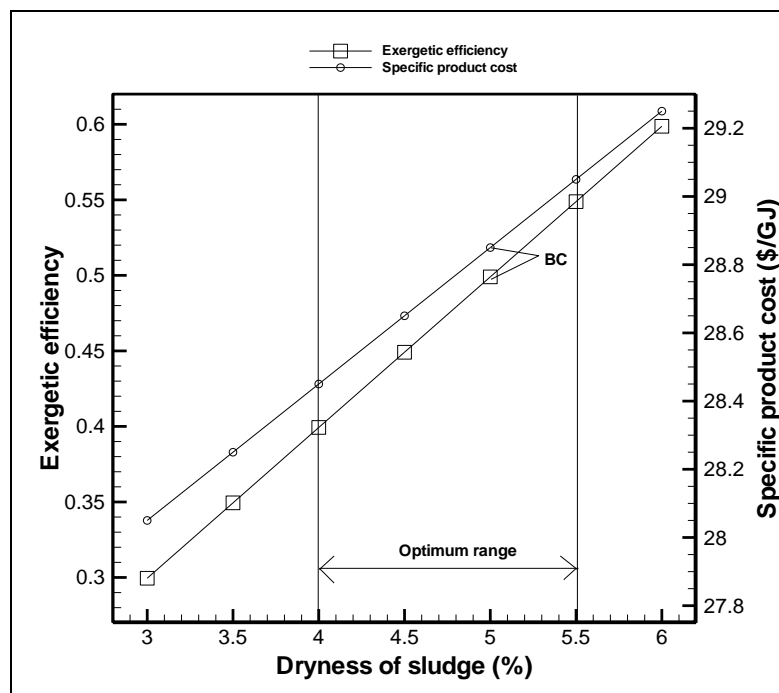


Figure 9.17: Variation of the product cost of the sewage sludge at the exit of thickening and flotation system with respect to different dry matter contents and corresponding exergetic efficiencies.

Table 9.23: The costs obtained through thermoeconomic analysis (base case) and thermoeconomic optimization (cost optimal case) for the municipal WWTP

Component	Base Case				Thermoeconomically Cost Optimal Case			
	COD (mg/l)	$c_{P,k}$ ($\text{¢}/\text{m}^3$)	ε	\dot{C}_D ($\text{\$/h}$)	COD (mg/l)	$c_{P,k}$ ($\text{¢}/\text{m}^3$)	ε	\dot{C}_D ($\text{\$/h}$)
PTS	367.65	0.34	0.4903	1154	400	0.31	0.5333	1056
STS	64.34	3.80	0.1483	1057.1	100	2.55	0.2305	955
	DMC (%)				DMC (%)			
TFS	5.0	0.79	0.4990	787.6	4.0	0.58	0.3993	709.2

As COD values increase at the exits of primary and secondary treatment systems, exergetic product costs of the partially and fully treated sewage streams decrease as compared to the actual base case values. In the thermoeconomic optimization of a WWTP, the objective is to minimize the destruction cost rate of the subsystems, by doing this we can optimize the product cost values of the subsystems. The optimum product cost for the partially treated wastewater at the exit of primary treatment system is found to be $0.31 \text{ ¢}/\text{m}^3$, whereas for the fully treated wastewater at the exit of secondary treatment system, it is found to be $2.55 \text{ ¢}/\text{m}^3$. The corresponding base case costs are obtained as $0.34 \text{ ¢}/\text{m}^3$ and $3.80 \text{ ¢}/\text{m}^3$, respectively. The exergetic efficiencies of the primary and secondary treatment systems increase in the optimum case as a result of the decreasing product cost values as shown in Table 9.23 and Figures 9.16 and 9.17. The thermoeconomically optimum product cost value of the sewage sludge at the exit of thickening and flotation system is found to be $0.58 \text{ ¢}/\text{m}^3$ whereas corresponding base case value is obtained as $0.79 \text{ ¢}/\text{m}^3$. The optimum exergetic efficiency of the thickening and flotation system is found to be 58%, which is lower than the corresponding base case efficiency value, 79%. This is due to the fact that while dry matter content of the sewage sludge increases, chemical exergy of it also increases. In cost optimal case of thickening and flotation system, dry matter content of the sludge is reduced to 4.0% , which decreases the chemical exergy of the sludge stream.

9.10 Accuracy of Measurements in GASKI WWTP and BEPC System

Measurements are done for each operating condition in GASKI WWTP and BEPC. Valid measurements are carried out at least two times. A measurement is considered to be valid if the variations of the engine brake torque and engine speed values in relation to the settings of the operating values do not exceed $\pm 2\%$. The variation of the power output during this period did not exceed $\pm 3\%$. The control system of the plant is calibrated due to the ISO-3046 standards. According to these standards there are some corrections factors which have to be used for calibrations and accuracy. The main aim is to keep the tolerance limit for the measurements at overall the plant within the $\pm 3\%$.

Table 9.24: Uncertainty of the measured quantities in GASKI WWTP

Measured Quantities in GASKI WWTP	Unit	Uncertainty (%)
Temperature	°C	± 2
Pressure	bar	± 2
Mass flow rate	kg/s	± 1
Power	kW	± 3

9.11 Thermodynamic and Economic Analyses of Developed Hydrogen Production Models for Wastewater Treatment Plants

In this chapter, thermodynamic and economic analyses of seven hydrogen production models developed for a municipal wastewater treatment plant are performed using the actual data obtained from GASKI WWTP and BEPC. The schematics and data provided for each model are also presented in Chapter 8. According to the price of electricity, the unit cost of hydrogen will be

$$Cost_{H_2} = C_{\text{electricity}} \times W_{\text{demand}} \quad (9.44)$$

where $C_{\text{electricity}}$ is the unit cost of electricity produced by cogeneration unit in WWTP and it is taken as 0.0893 \$/kWh, and W_{demand} is the electricity work needed for the hydrogen production in the developed models as kWh/kg H_2 .

Model 1:

For the model-1, the value of Gibbs free energy of water is 237,180 kJ/kmol at 25°C. Hydrogen produced by model-1 is calculated as 573 kg/day and the actual electricity cost of hydrogen production is found to be 3.74 \$/kg H₂. By using Equation (4.46) presented in Chapter 4, the thermal efficiency of electrolysis process for model-1 is found as 78%. The thermodynamic data, and the results of the energy and economic analyses for the model-1 according to the nomenclature shown in Figure 8.8 is given in Table 9.25.

Table 9.25: Thermodynamic data and results of the energy and economic analyses of model-1 with respect to the state points in Figure 8.8

State No	Property	Value
1	Biogas inlet	0.129 (kg/s)
2	Work	1000kWh
3	Water	0.06(kg/s) @25°C and 1bar
4	Pure water	0.06(kg/s) @25°C and 1bar
5	Hydrogen gas	573 kg/day
6	Oxygen gas	4584 kg/day
Type of electrolysis: Alkaline Efficiency of electrolysis: 78% Minimum Power consumption of electrolysis: 117,648.81 kJ/kg (32.68 kWh/kg H₂) Actual power consumption of electrolysis: 150,831.8 kJ/kg (41.9 kWh/kg H₂) Cost of electricity: 0.0893 \$/kWh Minimum electricity cost of hydrogen: 2.92 \$/kg H₂ Actual electricity cost of hydrogen: 3.74 \$/kg H₂		

Model 2:

For the model-2, water is heated up to 80°C and the value of Gibbs free energy of water at this temperature is 228,378 kJ/kmol. The heat requirement of the heating process of water is calculated to be 14.25 kW. Hydrogen produced by model-2 is calculated as 594 kg/day and the actual electricity cost of hydrogen production is found to be 3.60 \$/kg H₂. The thermodynamic data, and the results of the energy and economic analyses for the model-1 according to the nomenclature shown in Figure 8.9 is given in Table 9.26.

Table 9.26: Thermodynamic data and results of the energy and economic analyses of model-2 with respect to the state points in Figure 8.9

State No	Property	Value
1	Biogas inlet	0.129 (kg/s)
2	Work	1000kWh
3	Water	0.062(kg/s) @25°C and 1bar
4	Pure water	0.062(kg/s) @25°C and 1bar
5	Heated water	0.062(kg/s) @80°C and 1bar
6	Biogas	0.001 (kg/s)
7	Hydrogen gas	594 kg/day
8	Oxygen gas	4762.8 kg/day
Type of electrolysis: Alkaline Efficiency of electrolysis: 78% Minimum Power consumption of electrolysis: 113,282.7 kJ/kg (31.47 kWh/kg H₂) Actual power consumption of electrolysis: 145,234.23 kJ/kg (40.34 kWh/kg H₂) Cost of electricity: 0.0893 \$/kWh Minimum electricity cost of hydrogen: 2.81 \$/kg H₂ Actual electricity cost of hydrogen: 3.60 \$/kg H₂		

Model 3:

For the model-3, water is heated up to 80°C and the value of Gibbs free energy of water at this temperature is 228,378 kJ/kmol. The heat requirement of the heating process of water is calculated to be 15.0 kW. By using Equation (4.46) presented in Chapter 4, the thermal efficiency of electrolysis process for model-3 is found as 82%. Hydrogen produced by model-3 is calculated as 625.4 kg/day and the actual electricity cost of hydrogen production is found to be 3.43 \$/kg H₂. The thermodynamic data, and the results of the energy and economic analyses for the model-1 according to the nomenclature shown in Figure 8.10 is given in Table 9.27.

Table 9.27: Thermodynamic data and results of the energy and economic analyses of model-3 with respect to the state points in Figure 8.10

State No	Property	Value
1	Biogas inlet	0.129 (kg/s)
2	Work	1000kWh
3	Water	0.065(kg/s) @25°C and 1bar
4	Pure water	0.065(kg/s) @25°C and 1bar
5	Heated water	0.065(kg/s) @80°C and 1bar
6	Biogas	0.0011 (kg/s)
7	Hydrogen gas	625.4 kg/day
8	Oxygen gas	5003.2 kg/day

Type of electrolysis: PEM
Efficiency of electrolysis: 82%
Minimum Power consumption of electrolysis: 113,282.7 kJ/kg (31.47 kWh/kg H₂)
Actual power consumption of electrolysis: 138,149.6 kJ/kg (38.37 kWh/kg H₂)
Cost of electricity: 0.0893 \$/kWh
Minimum electricity cost of hydrogen: 2.81 \$/kg H₂
Actual electricity cost of hydrogen: 3.43 \$/kg H₂

Model 4:

For the model-4, the value of Gibbs free energy of steam is 18,519 kJ/kmol at 800°C. The heat requirement of the boiling process for steam production is calculated to be 363 kW. Hydrogen produced by model-4 is calculated as 868.6 kg/day and the actual electricity cost of hydrogen production is found to be 2.47 \$/kg H₂. By using Equation (4.46), the thermal efficiency of electrolysis process for model-4 is found as 94%. The thermodynamic data, and the results of the energy and economic analyses for the model-4 according to the nomenclature shown in Figure 8.11 is given in Table 9.28.

Table 9.28: Thermodynamic data and results of the energy and economic analyses of model-4 with respect to the state points in Figure 8.11

State No	Property	Value
1	Biogas inlet	0.129 (kg/s)
2	Work	1000 kWh
3	Water	0.09 (kg/s) @25°C and 1bar
4	Pure water	0.09 (kg/s) @25°C and 1bar
5	Steam	0.09 (kg/s) @800°C and 5bar
6	Biogas	0.025 (kg/s)
7	Hydrogen gas	868.6 kg/day
8	Oxygen gas	6,948.8 kg/day
Type of electrolysis: High temperature electrolysis Efficiency of electrolysis: 94% Minimum power consumption of electrolysis: 93,511.4 kJ/kg (25.98 kWh/kg H₂) Actual power consumption of electrolysis: 99,480.2 kJ/kg (27.63 kWh/kg H₂) Cost of electricity: 0.0893 \$/kWh Minimum electricity cost of hydrogen: 2.32 \$/kg H₂ Actual electricity cost of hydrogen: 2.47 \$/kg H₂		

Model 5:

For the model-5, the value of Gibbs free energy of the hydrogen sulfide is 73,289 kJ/kmol at 25°C while Gibbs free energy of water is 237,180 kJ/kmol at the same temperature for the comparison. As stated previously, the energy demand for the electrolysis process of H₂S is lower about 3.25 times than that of the water at the present temperature. Biogas produced in WWTP includes nearly 1% of H₂S and assuming that all of the hydrogen sulfide is collected through by separator, the mass flow rate of H₂S for the electrolysis process is found to be 7.63 kg/h. Hydrogen produced by model-5 is calculated as 10.8 kg/day and the actual electricity cost of hydrogen production is found to be 1.16 \$/kg H₂. By using Equation (4.46), the thermal efficiency of alkaline electrolysis process for model-5 is found as 78%. If hydrogen sulfide presence in the biogas was higher than that of the present case, it would be possible to produce 1901.5 kg/h of hydrogen in terms of 1000 kWh work input to the electrolysis system. The thermodynamic data, and the results of the energy and economic analyses for the model-5 according to the nomenclature shown in Figure 8.12 is given in Table 9.29.

Table 9.29: Thermodynamic data and results of the energy and economic analyses of model-5 with respect to the state points in Figure 8.12

State No	Property	Value
1	Biogas inlet	0.212 (kg/s)
2	Biogas	0.129 (kg/s)
3	H ₂ S	0.0021 (kg/s)
4	Work	5.83 kWh
5	Hydrogen gas	10.8 kg/day
6	Sulfur gas	170.6 kg/day
Type of electrolysis: Alkaline Efficiency of electrolysis: 78% Minimum power consumption of electrolysis: 36,353.7 kJ/kg (10.1 kWh/kg H₂) Actual power consumption of electrolysis: 46,607.3 kJ/kg (12.95 kWh/kg H₂) Cost of electricity: 0.0893 \$/kWh Minimum electricity cost of hydrogen: 0.90 \$/kg H₂ Actual electricity cost of hydrogen: 1.16 \$/kg H₂		

Model 6:

Wang et al. [171] demonstrate that hydrogen yield of original sewage sludge can be up to 0.9 mmol-H₂/g-DS (Dry solid content). Sludge content of GASKI WWTP is 2170.8 kg-DS/h. According to this value hydrogen production is hourly 3.94 kg. Equivalent of this value is 94.56 kg/day. The thermodynamic data, and the results of the energy and economic analyses for the model-6 according to the nomenclature shown in Figure 8.13 is given in Table 9.30.

Table 9.30: Thermodynamic data and results of the energy and economic analyses of model-6 with respect to the state points in Figure 8.13

State No	Property	Value
1	Sludge	12.06 (kg/s) @25°C
2	Sludge	12.06 (kg/s) @36°C
3	Hydrogen gas	94.56 kg/day @ 60% purity
4	Hydrogen gas	56.74 kg/day @ 100% purity
5	Carbon dioxide gas	37.82 kg/day
Type of hydrogen production: Dark fermentation (None pre-treatment) Power consumption of system: 176.4 kWh (74.7 kWh/ kg H₂)* Cost of electricity: 0.0893 \$/kWh Electricity cost of hydrogen: 6.7 \$/kg H₂		

*Power consumption of this process is taken by the assumption given in Ref [160].

Model 7:

Applying a pre-treatment process such like acidification before the dark fermentation process, hydrogen production may be increased up to 1.5-2.1 mmol-H₂/g on the chemical oxygen demand (COD) basis. Since the COD value of the sludge for GASKI WWTP is 65.28 g-COD/l, hydrogen production will be increased to 11.9 kg/h by a pre-treatment plus the dark fermentation processes. Hydrogen produced by model-3 is calculated to be 171.4 kg/day with 100% of H₂ by volume and the actual electricity cost of hydrogen production is found to be 2.2 \$/kg H₂. The thermodynamic data, and the results of the energy and economic analyses for the model-7 according to the nomenclature shown in Figure 9.14 is given in Table 9.31.

Table 9.31: Thermodynamic data and results of the energy and economic analyses of model-7 with respect to the state points in Figure 8.14

State No	Property	Value
1	Sludge	12.06 (kg/s) @25°C
2	Pre-treated sludge	12.06 (kg/s)
3	Hydrogen gas	285.6 kg/day with 60% of H ₂ by volume
4	Hydrogen gas	171.4 kg/day with 100% of H ₂ by volume
5	Carbon dioxide gas	114.2 kg/day
Type of hydrogen production: Dark fermentation + pre-treatment Power consumption of system: 176.4 kWh (24.8 kWh/ kg H₂) Cost of electricity: 0.0893 \$/kWh Electricity cost of hydrogen: 2.2 \$/kg H₂		

In Figure 9.18 hydrogen production rate of the models developed for an existing municipal WWTP are compared to each other:

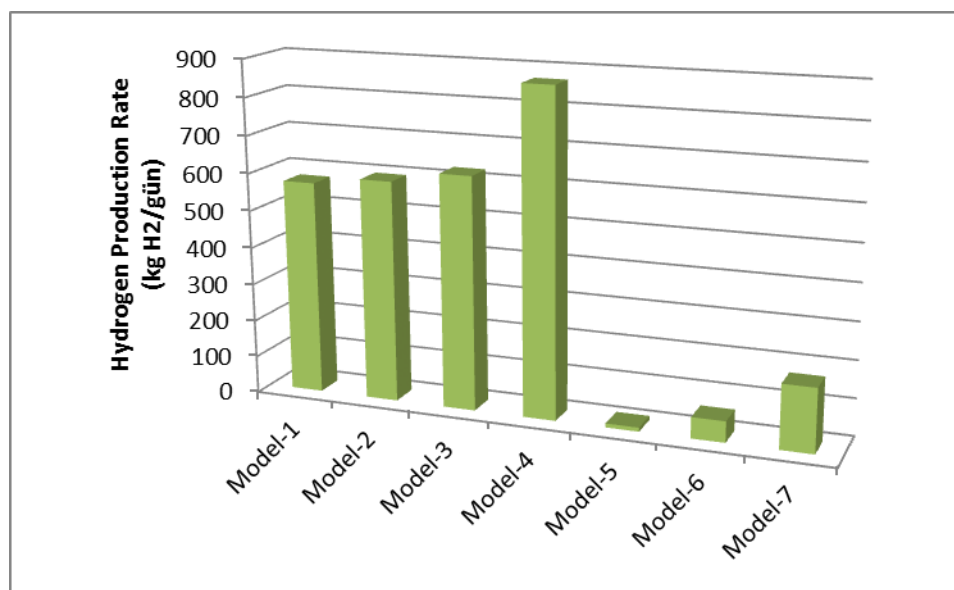


Figure 9.18: Comparison of hydrogen production rates of the models developed for GASKI WWTP

As can be seen, model-4 has a maximum hydrogen production rate than the other six models. Among seven models developed, model-5 has a minimum hydrogen production rate. The electricity produced by the biogas powered cogeneration system of WWTP is totally consumed by the electrolysis process for hydrogen production in the first four models developed. For the model-5, only a few amount of electricity produced by the cogeneration system is consumed due to the inadequate amount of H₂S presence in the biogas produced by anaerobic digestion system.

Although its biggest disadvantage is the low hydrogen production rate from sewage sludge, the performance of a dark fermentation process can be improved by a pre-treatment unit. Thus, model-6 is seen appropriate option for a municipal WWTP because of two important reasons: (1) Sludge utilized through model-6 is the digested sludge and it is the by-product of wastewater treatment application. This sludge, before the dark fermentation process for hydrogen production, is first used to produce biogas in the anaerobic digestion process. Thus, the biogas output is used for the power production, which provides the energy demand of the model-6. Note that the power demand of the model-6 is only the one-fourth of the total power produced by the cogeneration system (176.4 kWh). (2) After biogas production in the anaerobic digestion system, sludge is considered as a waste of the treatment facility and it must be eliminated. By model-3, this elimination process is replaced by a dark fermentation process with pre-treatment for hydrogen production. It means that digested sludge can be used further for another valuable system production, which is hydrogen. Fig. 9.19 shows the comparison of actual electricity consumptions of hydrogen production models developed.

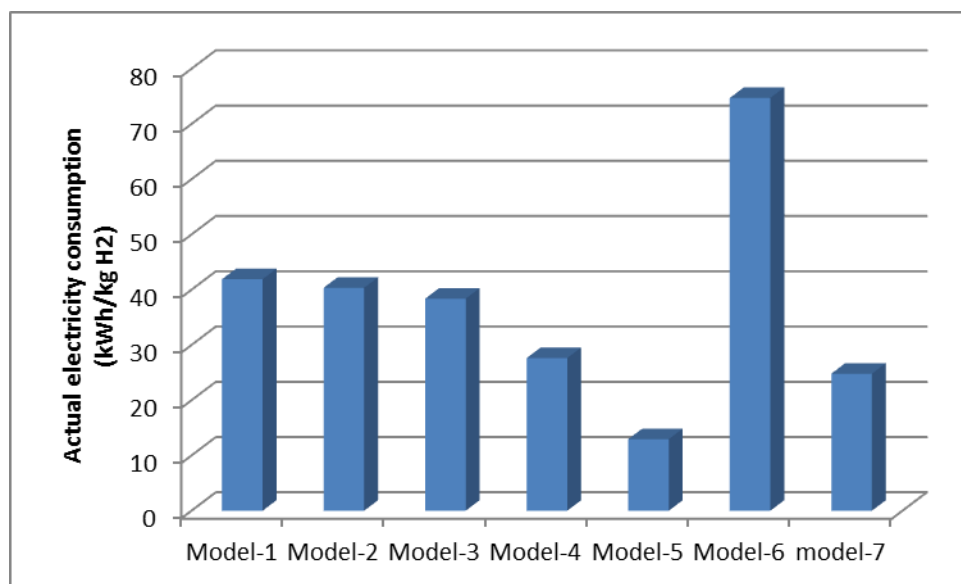


Figure 9.19: Comparison of electricity consumption rates of the models developed for GASKI WWTP

Table 9.32: Economic analysis results of hydrogen production models developed

Hydrogen Production Models	H ₂ production rate		H ₂ electricity cost		Capital investment cost		Operating and maintenance cost		Total H ₂ cost	
	kg/s	kg/year	\$/kg H ₂	\$/year	\$/kg H ₂	\$/year	\$/kg H ₂	\$/year	\$/kg H ₂	\$/year
Model-1	0.0066	200,550	3.74	750,050	5.88	1,123,080	1.07	204,370	10.69	2,077,500
Model-2	0.0069	207,900	3.60	748,440	5.66	1,120,680	1.03	203,940	10.29	2,037,420
Model-3	0.0072	218,890	3.43	750,792.7	5.39	1,123,635.3	0.98	204,297.3	9.8	2,042,973.3
Model-4	0.01	304,010	2.47	750,792.7	0.96	277,852	0.75	217,150	4.18	1,210,249
Model-5	0.00013	3600	1.16	4176	1.82	6552	0.33	1188	3.31	11,916
Model-6	0.00066	18,913.3	6.7	126,719.1	6.87	129,936.6	2.06	38,981	15.63	295,614.9
Model-7	0.00198	57,133.3	2.2	125,693.3	2.27	129,936.6	0.68	38,981	5.15	294,236.5

According to the economic analysis performed based on the electricity cost for the models developed, model-5 has the lowest hydrogen production cost (see Table 9.32). This is so because of low hydrogen production rate of the model due to the low value of hydrogen sulfide presence in the biogas. Model-6 involves the highest cost rate of all the models developed, due to the high investment and operation and maintenance costs of the dark fermentation process. However, considering the remarkable economical and environmental advantages of the direct usage of sludge in both for biogas and hydrogen productions, it can be considered as the most appropriate model for the municipal WWTPs. In Figure 9.20, the comparison of the hydrogen production costs for the models developed is presented.

One of the challenges in creating a hydrogen economy is the low efficiency of the current hydrogen liquefaction plant cycles [172]. In 1895, Carl von Linde and William Hampson invented a simple liquefaction cycle to liquefy air. This cycle is called the ‘Linde–Hampson cycle. However, according to what was explained by Barron [173], the systems that cannot be used to liquefy hydrogen are the Linde–Hampson, Linde dualpressure, Cascade, and Heylandt systems. A liquid nitrogen, pre-cooled Linde–Hampson system can be used to liquefy hydrogen. For a pre-cooled Linde–Hampson liquefaction system, minimum work input for liquefaction was calculated to be 11,963 kJ/kg H₂ (3.323 kWh/kg H₂) by the Yilmaz et al.[93]. Second law efficiency of the liquefaction cycle can be taken as 17% [174] and the actual work input of the liquefaction is 70,371 kJ/kg H₂ (19.5 kWh/kg H₂). Hydrogen liquefaction costs for models developed for GASKI WWTP is given in Table 9.33.

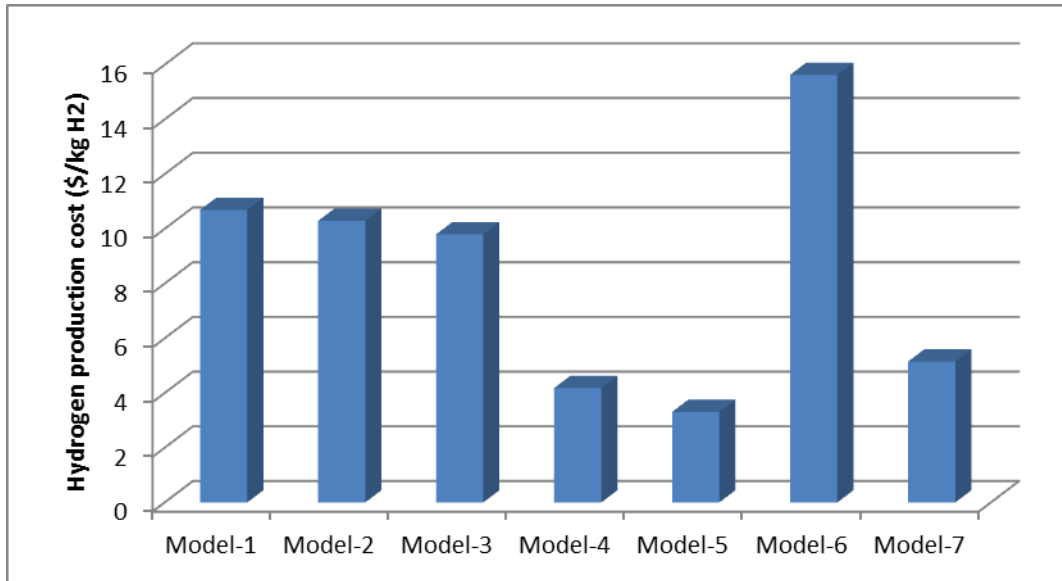


Figure 9.20: Comparison of hydrogen production costs of the models developed for GASKI WWTP

Table 9.33: Hydrogen liquefaction cost of models developed for GASKI WWTP

Model	Electricity Consumption (kWh)		Liquefaction Electricity Cost (\$/h)	
	Ideal	Actual	Ideal	Actual
Model-1	77.12	465.6	6.89	41.58
Model-2	79.94	482.6	7.14	43.10
Model-3	84.17	508.14	7.52	45.38
Model-4	116.9	705.74	10.44	63.02
Model-5	1.45	8.80	0.13	0.79
Model-6	7.64	46.10	0.68	4.12
Model-7	23.07	139.26	2.06	12.44

9.12 Conclusions

Energy, exergy, and thermoeconomic analysis and thermoeconomic optimization of GASKI WWTP and BEPC system are performed. The iterative methodology of exergy based economic optimization is used. In the iterative optimization procedure we use the variables exergetic efficiency ε , chemical oxygen demand (COD), dryness of sludge (DS) with the corresponding optimal values obtained through the optimization procedure. The effects of changes in the decision variables selected on exergetic efficiency and destruction cost rate can provide suggestions for the design changes that need to be considered in the next optimization step.

CHAPTER 10

CONCLUSIONS

This study is on thermodynamic and thermoeconomic analysis and optimization of biogas usage in electricity and hydrogen productions from wastewater treatment systems. The developed procedure and formulations are applied to an existing wastewater treatment plant in Gaziantep, Turkey using actual operational and cost data. The plant treats nearly 222,000 m³/day of domestic wastewater using primary, secondary (biological) and tertiary (anaerobic sludge digestion) treatments. At the end of the anaerobic sludge digestion process, 10,000-18,000 m³ biogas is generated daily which means approximately 60% of the organic fraction is converted to liquid and gaseous end products. The total electric produced by the biogas powered gas engine is 1000 kWh, which is used within the wastewater treatment facility.

Following conclusions can be drawn based on the analysis and the results obtained:

1. Thermodynamic relations of the plant and its subsystems/components are given in Chapter 9 based on the relations in Chapter 4. The temperature, pressure, and mass flow rate data and certain energy and exergy evaluations of the sub-processes and sub-components of the wastewater treatment plant and biogas engine powered cogeneration plant are presented in Tables 9.4, 9.5, 9.7, 9.8, 9.9, 9.10, 9.11, 9.12, 9.13 and 9.14. Energy and exergy calculations are done using commercial software with built-in thermodynamic property functions for a variety of substances.
2. The chemical oxygen demand (COD) value of the sewage at the inlet of the primary treatment system (PTS) is determined to be 661.32 mg/l (see Table 9.1). The specific chemical exergy of the sewage at the inlet of wastewater treatment system is calculated using Equation (4.22) given in the Chapter 4 as 9.0 kJ/kg. Since the total

mass flow rate of sewage input to GASKI WWTP is 2566.23 kg/s, the total exergy rate of sewage at the PTS inlet is found to be 23,096 kW. The total exergy rate of sewage at the PTS inlet increases from 23,096 kW to 23,306 kW by adding the total power supply to the primary treatment process. The exergetic efficiency of the PTS is found to be 56.9% using Equation (9.31). The remaining 43.1% of the sewage exergy input to the PTS is destroyed. This corresponds to 10,048.96 kW, which is the total exergy destruction in the PTS. The total exergy destructions in the components of the PTS account for 0.151% of the total sewage exergy input and 0.351% of the total exergy destruction in the system. The remaining 99.65% of the total exergy destruction in the PTS is mostly due to the highly complex and irreversible characteristics of the primary treatment process.

3. The total exergy rates of the half-treated and the non-treated sewages at the inlet of the secondary treatment system (STS) are determined to be 12,196 kW. The COD value of the treated water at the exit of the STS is reduced to 64.37 mg/l (see Table 9.1). Then the specific chemical exergy of the treated water at the exit of wastewater treatment plant is calculated as 0.875 kJ/kg. Since the total mass flow rate of the treated water is 2000.0 kg/s, the total exergy rate of treated wastewater in the plant exit is found to be 3624.4 kW. At the exit of the STS, the activated sludge has a dry matter content of 0.5% and its specific chemical exergy becomes 66.87 kJ/kg based on the specific exergy value of the dry sludge, which is obtained as 13,373 kJ/kg by Equation (4.23) given in the Chapter 4 and the data given in Table 9.6. The total exergy rate of the half-treated sewage at the STS inlet increases from 12,196 kW to 13,944 kW by adding the total power supply to the secondary treatment process. The exergetic efficiency of the STS is found to be 26.0% using Equation (9.32). The remaining 74.0% of the half-treated sewage exergy input to the STS is destroyed. This corresponds to 10,319.12 kW, which is the total exergy destruction in the STS. The total exergy destructions in the components of the STS accounts for 2.85% of the total half-treated sewage exergy input and 4.07% of the total exergy destruction in the system. The remaining 95.93% of the total exergy destruction in the STS is mostly due to the highly complex and irreversible characteristics of the secondary treatment process.

4. The total exergy rate of the activated sludge at the inlet of the flotation and thickening system (FTS) is found to be 15,832 kW. This value is the total exergy rates of the activated sludge which has a dry matter content of 0.5% from the STS (14,772 kW) and of the sewage-like sludge which has a dry matter content of less than 0.1% (1060.3 kW) from PTS. At the exit state of FTS process, the mass flow rate of the sludge is reduced to 12.06 kg/s while the dry matter content of the activated sludge increases up to 5.0%, which make the total exergy rate of the sludge at this state to be 8070 kW. The total exergy rate of the activated sludge at the FTS inlet increases from 15,832 kW to 16,375 kW by adding the total power supply to the flotation and thickening process. The exergetic efficiency of FTS is found to be 49.3% using Equation (9.33). The remaining 50.7% of the activated sludge exergy input to FTS is destroyed. This corresponds to 8305.24 kW, which is the total exergy destruction in FTS. The total exergy destructions in the components of FTS accounts for 0.91% of the total activated sludge exergy input and 1.65% of the total exergy destruction in the system. The remaining 98.35% of the total exergy destruction in the FTS is due to the reduction of mass flow rate of the activated sludge through thickening process and the complex mechanism of the FTS.

5. The total exergy rate of the activated sludge at the inlet of the anaerobic digestion system (ADS) is 8070 kW. This sludge has the dry matter content of 5.0%. Through the anaerobic digestion process, the dry matter content of the sludge increases to 8.0%, which make the total exergy rate of the digested sludge at the exit of secondary digestion unit as 11,294 kW. This digested sludge is then sent to the de-watering facility for increasing the dry matter content of it to 22.0%. The mass flow rate of the digested sludge is reduced to 2.48 kg/s at the de-watering facility exit and the total exergy rate of the sludge cake is obtained as 7296.4 kW. Biogas production strongly depends upon the type of the sludge and the operating conditions of the anaerobic digesters. For each 1 m³ biogas produced in GASKI WWTP, 68.26 kg of sludge with the dry matter content of 8.0% is digested. The lower heating value of the produced biogas is 21.47 MJ/Nm³ (17,892 kJ/kg). The specific chemical exergy of the biogas in this composition is calculated to be 31,168 kJ/kg by using Equation (4.25) given in the Chapter 4. Then the total exergy rate of the biogas produced with a mass flow rate of 0.212 kg/s is obtained as 6653.2 kW. The total exergy rate of the activated sludge at the ADS inlet increases from 8070 kW to 8268 kW by adding the total

power supply to the anaerobic digestion system. The exergetic efficiency of ADS is found to be 80.5% using Equation (9.34). The remaining 19.5% of the activated sludge exergy input to ADS is destroyed. This corresponds to 1615.22 kW, which is the total exergy destruction in ADS. The high exergetic efficiency obtained for the ADS depends on high processing capacity of anaerobic reactors in which a sufficiently large bacterial mass is retained. The total exergy destructions in the components of ADS accounts for 1.811% of the total activated sludge exergy input and 9.95% of the total exergy destruction in the system. The remaining 90.05% of the total exergy destruction in the ADS is due to complex bacterial mechanisms occurred through the anaerobic digestion process at the mesophilic temperature conditions.

6. The biogas used as the fuel in the gas engine of the biogas engine powered cogeneration system (BEPC) system is nearly 61% (0.129 kg/s) of the total biogas produced in anaerobic digestion system, which is 0.212 kg/s. The remaining part (0.083 kg/s) is reserved in the biogas storage tank. For 1 kWh electricity produced in the gas engine, 0.387 m³ of biogas with 60% of methane content is consumed in the BEPC plant. The total exergy input of air and biogas (fuel) to the gas engine is 4054 kW. The total exergy rate of the air and fuel at the inlet of to the gas engine increases from 4054 kW to 4594 kW by adding lubrication oil and engine cooling water exergy rates at the inlet of the engine following the third approach developed by Equation (9.40). The exergetic efficiency of the gas engine is found to be 24.7% by using the first approach defined in Eq. (9.38), 26.4% by using the second approach defined in Equation (9.39), and 46.3% by using the third approach defined in Equation (9.40). 24.7% of exergy entering the BEPC plant is converted to electrical power (1000 kW). The net steam production of the BEPC plant represents only 1.8% (71.5 kW) of the total exergy input. The remaining 73.6% of the exergy input to the BEPC plant is destroyed. This corresponds to 2982 kW, which is the total exergy destruction in the plant. The exergetic efficiency of the BEPC plant is obtained to be 26.4%. The exergy destruction in the gas engine of the cogeneration plant accounts for 73.6% of the total exergy input and 89.4% of the total exergy destruction in the plant. The exergy destruction in the engine is mostly due to the highly irreversible combustion process, heat losses from the engine, and friction. The exergetic efficiencies of the compressor and turbine of the turbocharger are 72.1% and 87.7% , respectively. The

exergetic efficiencies of pumps, P53, P54, P55 and P56, are 78.6%, 79.1%, 76.9%, and 80.6%, respectively. The exergetic efficiencies of exhaust gas heat exchanger and intercooler are calculated as 37.9% and 48.8%, respectively making them the least efficient components of the plant.

7. The fuel utilization efficiency (FUE) of the BEPC system is determined to be 63.0% by Equation (4.40) developed in the Chapter 4. This value is high compared to the thermal efficiencies of power plants whose sole purpose is the production of electricity. In BEPC, the main product is electricity and the hot water generated by exhaust gas heat exchanger may be called as “byproduct”. The thermal efficiency of the gas engine defined as the power output over the fuel energy input is calculated to be 43.3% by Equation (9.37) given in the first part of the study, which is consistent with the gas engine efficiency given by the manufacturer. Power to heat ratio (PHR) of the BEPC plant is calculated to be 2.21 by Equation (4.41) given in the Chapter 4. This is a characteristic of internal combustion engine powered cogeneration systems for which the process heat output is typically small compared to electrical output.

8. The overall exergetic efficiency of GASKI WWTP including biogas engine powered cogeneration system (BEPC) is calculated using Equation (9.42) as 46.2%. This value indicates that 46.2% of the total exergy input to the GASKI WWTP and BEPC is converted to the useful outputs, i.e., treated water, de-watered digested sludge, and power output. The total exergy destruction of the overall plant accounts about 53.9% of the total exergy input. This corresponds to 13,873 kW, which is the total exergy destruction in the plant.

9. The economic data including the first capital investments and the other expenditures of GASKI WWTP are obtained from the plant management. The operating and maintenance (OM) costs are obtained by considering WWTP’s entire economic life (i.e., 25 years from January 1999 to December 2024). These costs are escalated by using average nominal escalation rate, which is 5% in US dollars. The average capacity factor (τ) for the entire WWTP is 91.7% which means that the system operates at full load 8030 h out of the total available 8760 h per year. The total capital investment of GASKI WWTP was 56.0 million US dollars.

10. The BEPC system is supplied as packaged system and cost allocation among its components (i.e. subsystems) is not separately quoted. However, to obtain more accurate results from thermoeconomic analysis, the subsystems are considered as separate and cost allocation of subsystems and the other expenditures are obtained from the energy manager of the plant and the contractor of the BEPC system. The operating and maintenance (OM) costs are obtained by considering BEPC's entire economic life, i.e. 25 years from 2006 to 2031. These costs are escalated by using average nominal escalation rate, which is 5% in US dollars. The average capacity factor (τ) for the entire WWTP is 91.7% which means that the system operates at full load 8030 h out of the total available 8760 h per year. The total capital investment of GASKI BEPC was 1.237 million US dollars.

11. In this study, specific exergy costing (SPECOC) method is used to obtain and understand the cost formation structure of the plant. Exergetic cost rates balances and corresponding auxiliary equations of the plant are given in Chapter 5. Exergetic cost rate balances and corresponding auxiliary equations are formulated for each subsystem of the plant. Auxiliary equations are found by applying F and P principles and are given in Table 9.17 for GASKI primary economic control volume (WWTP), and in Table 9.20 for GASKI secondary economic control volume (BEPC). Results obtained are given in Tables 9.18 and 9.21 for WWTP and BEPC, respectively. The exergetic cost parameters of the plant components are given in Tables 9.19 and 9.22 for WWTP and BEPC, respectively.

12. Since wastewater treatment is one of the infrastructural services supplied by a local government, the exergetic cost rate and the specific unit exergetic cost of the sewage entering the WWTP are taken as zero. The corresponding values of these costs for the treated wastewater exit are 62.05 \$/h and 3.804 ¢/m³. The total amount of treated wastewater per day in the WWTP is 172,800 m³. This corresponds to the total treated wastewater cost of 6573.31 \$ per day. The treated wastewater cost mainly includes the operation costs of the wastewater treatment processes. The exergetic cost rate and the specific unit exergetic cost of the activated sludge with a dry matter content of 0.5% at the exit of secondary treatment system are 125.65 \$/h and 0.991 ¢/m³, respectively. The corresponding costs for sludge at the thickening unit are 20.6 \$/h and 0.198 ¢/m³, respectively. This decrease is mainly due to the

increased specific chemical exergy of the sludge at the end of the flotation and thickening processes. The specific unit exergetic cost of the digested sludge at the exit of primary anaerobic digestion unit is 0.790 ¢/m^3 . The corresponding value of the digested sludge at the exit of secondary digestion unit is 1.907 ¢/m^3 . The increase of unit cost in the primary digestion process is due to the high retention time which causes the maximum contact between the incoming activated sludge and the bacteria to increase the methane content in the produced biogas. The specific unit exergetic cost of the digested sludge at the exit of the secondary anaerobic digestion process is more than double the cost of the primary digestion. This is because, in addition to high retention time of sludge in reactor, the power consumption for the de-watering process in WWTP after secondary anaerobic digestion process is about 81 kW per ton dry matter content of the digested sludge. The exergetic cost rates of digested sludge at the exits of primary and secondary anaerobic digestion units are obtained as 76.91 \$/h and 81.90 \$/h, respectively.

13. The daily biogas production of the GASKI WWTP is $18,300 \text{ m}^3$. The average exergetic cost rate and the average specific unit exergetic cost of the biogas at the exit of anaerobic digestion reactors are 175.9 \$/h and 13.48 ¢/m^3 , respectively. The daily biogas production cost in GASKI WWTP is obtained as \$2057.3. In the plant, this biogas is used as the fuel for gas engine powered cogeneration facility, which produces 24,000 kW net electricity output per day.

14. The exergetic cost rates for the air-blower 2 (AB-2), electric motors and pump-6 (P6) are 118.27 \$/h, 31.03 \$/h and 27.07 \$/h, respectively. These costs are the highest exergy cost rates among the other plant components since the exergy flow rates of these components are notably high and all exergy available at the exit of these components is supplied by mechanical power which is the most expensive “fuel” in the plant. The exergoeconomic factor of the AB-2 is 0.13%, which is relatively low as compared with other components in the plant (see Table 9.21). This value depends on the dominant effect of the operation cost rate in the exergoeconomic factor definition given by Equation (5.38) in Chapter 5. The specific exergetic fuel and product costs for the anaerobic digestion reactor heat exchanger (ADRHE) unit are 9.1 \$/h and 51.8 \$/h, respectively. Exergy destruction cost rates of the primary and secondary treatment systems are found to be 1051 \$/h and 1057 \$/h,

respectively. These are the highest exergy destruction cost rates of all sub-systems. On the other hand, anaerobic digestion process has the lowest exergy destruction cost rate (172.8 \$/h).

15. The exergetic cost rate and the specific unit exergetic cost of the biogas entering the cogeneration system is 92.451 \$/h and 13.63 ¢/m³, respectively. The unit cost of the biogas is found to be 15.6 ¢/m³ at the engine inlet. Since for 1 kW electricity produced by the engine, 0.387 m³ of biogas with 60% methane content is consumed, the total consumption cost of the biogas for 1000 kWh electricity output is calculated to be 60.22 \$. The net electric output of the BEPC system is 1000 kWh. The exergetic cost rate and the specific unit exergetic cost of the power produced by the system are 12.4 \$/h and 25 \$/GJ, respectively. This means that the unit cost of 1 kWh electricity produced in the cogeneration system is 9.0 ¢. Thus, the total cost the electricity produced in the system can be found as 90 \$. Note that the electricity price tariff adopted to industrial facilities by TEDAS (2011) is 10.3 ¢/kWh. The biogas engine is the most exergy destructive component of the plant. The exergoeconomic factor of the gas engine is determined to be 1.34%. The exergoeconomic factor of the compressor is 2.46%. This value is 4.77% for the turbine. Exhaust gas heat exchanger unit (EGHE) involves an exergy destruction cost rate of 9.91 \$/h. The exergoeconomic factor for lubrication oil cooler is determined to be 0.33%, which is the lowest value of all components in the system.

16. For the existing systems such as the GASKI WWTP and BEPC system of this study, performance evaluation and optimization procedure may be considered as “performance improvement” and “searching a good solution” for the overall system rather than finding a global optimum. Since the optimal values of the decision variables given for thermodynamically and thermoeconomically optimal cases are not unique, the same values of the maximum exergetic efficiency and the minimum overall cost rate may be obtained through other combinations of the values of the decision variables. Besides, many different sets of the decision variables values may lead to nearly optimal values of the objective function. In the application of the iterative optimum procedure to the plant components, study presented follows the following procedure: (a) evaluation of detailed exergy analyses at the WWTP and BEPC system component level, (b) calculation of capital costs associated with each

plant component, (c) an exergoeconomic analysis using an exergy based costing method (SPECO method in this study), which is as detailed and objective as possible by keeping aggregation level is low, and (d) evaluation of the effects of decision variables on selected exergoeconomic variables.

17. The chemical oxygen demand (COD) value is taken as the decision variable in the optimization process of primary and secondary treatment systems. Since the chemical exergy of sewage decreases while its COD value is reduced through treatment processes, it becomes one of the major treatment process requirements. This decrease, which is accompanied by an excessive amount of operation costs, leads to an increase in cost level. The COD value for partially treated water is required to be given in the range between mg/l for the environmental operational restrictions of primary treatment system. The base case value (i.e. 367.65 mg/l) is the actual COD value of the partially treated water at the exit of primary treatment system. The COD value for treated wastewater at the exit of secondary treatment system may be given in the range between mg/l. The base case COD value of the treated wastewater is given as 64.37 mg/l in Table 9.1. As COD values increase at the exits of primary and secondary treatment systems, exergetic product costs of the partially and fully treated sewage streams decrease as compared to the actual base case values. In the thermoeconomic optimization of a WWTP, the objective is to minimize the destruction cost rate of the subsystems, by doing this we can optimize the product cost values of the subsystems. The optimum product cost for the partially treated wastewater at the exit of primary treatment system is found to be 0.31 ¢/m³, whereas for the fully treated wastewater at the exit of secondary treatment system, it is found to be 2.55 ¢/m³. The corresponding base case costs are obtained as 0.34 ¢/m³ and 3.80 ¢/m³, respectively.

18. The chemical exergy of sludge stream increases through sludge thickening process and the rate of exergy increase through processes in the sludge treatment subcomponents may cause a remarkable increase in cost level. The dry matter content (DMC) of sewage sludge at the inlet of thickening and flotation system is 0.5%. At the exit of this system, dryness of sludge increases to 5.0%, which is the actual base case value. The dry matter content of sewage sludge at the exit of thickening and flotation system may be given in the range between

$4.0 \leq DMC \leq 5.5$. The thermoeconomically optimum product cost value of the sewage sludge at the exit of thickening and flotation system is found to be 0.58 ¢/m^3 whereas corresponding base case value is obtained as 0.79 ¢/m^3 . The optimum exergetic efficiency of the thickening and flotation system is found to be 58%, which is lower than the corresponding base case efficiency value, 79%. This is due to the fact that while dry matter content of the sewage sludge increases, chemical exergy of it also increases. In cost optimal case of thickening and flotation system, dry matter content of the sludge is reduced to 4.0% , which decreases the chemical exergy of the sludge stream.

19. In this study, thermodynamic and economic analyses of seven hydrogen production models developed for a municipal wastewater treatment plant are performed using the actual data obtained from GASKI WWTP and BEPC. The schematics and data provided for each model are also presented in Chapter 8. For the model-1, the value of Gibbs free energy of water is 237,180 kJ/kmol at 25°C. Hydrogen produced by model-1 is calculated as 573 kg/day and the actual electricity cost of hydrogen production is found to be 3.74 \$/kg H₂. By using Equation (4.46) presented in Chapter 4, the thermal efficiency of electrolysis process for model-1 is found as 78%. The thermodynamic data, and the results of the energy and economic analyses for the model-1 according to the nomenclature shown in Figure 8.8 is given in Table 9.24. For the model-2, water is heated up to 80°C and the value of Gibbs free energy of water at this temperature is 228,378 kJ/kmol. The heat requirement of the heating process of water is calculated to be 14.25 kW. Hydrogen produced by model-2 is calculated as 594 kg/day and the actual electricity cost of hydrogen production is found to be 3.60 \$/kg H₂. The thermodynamic data, and the results of the energy and economic analyses for the model-1 according to the nomenclature shown in Figure 8.9 is given in Table 9.25. For the model-3, water is heated up to 80°C and the value of Gibbs free energy of water at this temperature is 228,378 kJ/kmol. The heat requirement of the heating process of water is calculated to be 15.0 kW. By using Equation (4.46) presented in Chapter 4, the thermal efficiency of electrolysis process for model-3 is found as 82%. Hydrogen produced by model-3 is calculated as 625.4 kg/day and the actual electricity cost of hydrogen production is found to be 3.43 \$/kg H₂. The thermodynamic data, and the results of the energy and

economic analyses for the model-1 according to the nomenclature shown in Figure 8.10 is given in Table 9.26.

20. For the model-4, the value of Gibbs free energy of steam is 18,519 kJ/kmol at 800°C. The heat requirement of the boiling process for steam production is calculated to be 363 kW. Hydrogen produced by model-4 is calculated as 868.6 kg/day and the actual electricity cost of hydrogen production is found to be 2.47 \$/kg H₂. By using Equation (4.46), the thermal efficiency of electrolysis process for model-4 is found as 94%. The thermodynamic data, and the results of the energy and economic analyses for the model-4 according to the nomenclature shown in Figure 8.11 is given in Table 9.27. For the model-5, the value of Gibbs free energy of the hydrogen sulfide is 73,289 kJ/kmol at 25°C while Gibbs free energy of water is 237,180 kJ/kmol at the same temperature for the comparison. Biogas produced in WWTP includes nearly 1% of H₂S and assuming that all of the hydrogen sulfide is collected through by separator, the mass flow rate of H₂S for the electrolysis process is found to be 7.63 kg/day. Hydrogen produced by model-5 is calculated as 10.8 kg/day and the actual electricity cost of hydrogen production is found to be 1.16 \$/kg H₂. By using Equation (4.46), the thermal efficiency of alkaline electrolysis process for model-5 is found as 78%. If hydrogen sulfide presence in the biogas was higher than that of the present case, it would be possible to produce 79.23 kg of hydrogen in terms of 1000 kWh work input to the electrolysis system. The thermodynamic data, and the results of the energy and economic analyses for the model-5 according to the nomenclature shown in Figure 8.12 is given in Table 9.28. The hydrogen yield of original sewage sludge can be up to 0.9 mmol-H₂/g-DS (Dry solid content). Sludge content of GASKI WWTP is 2170.8 kg-DS/h. According to this value hydrogen production is hourly 3.94 kg. Equivalent of this value is 94.56 kg/day. The thermodynamic data, and the results of the energy and economic analyses for the model-6 according to the nomenclature shown in Figure 8.13 is given in Table 9.29. Applying a pre-treatment process such like acidification before the dark fermentation process, hydrogen production may be increased up to 1.5-2.1 mmol-H₂/g on the chemical oxygen demand (COD) basis. Since the COD value of the sludge for GASKI WWTP is 65.28 g-COD/l, hydrogen production will be increased to 11.9 kg/h by a pre-treatment plus the dark fermentation processes. Hydrogen produced by model-3 is calculated to be 171.4 kg/day with 100% of H₂ by

volume and the actual electricity cost of hydrogen production is found to be 2.2 \$/kg H₂. The thermodynamic data, and the results of the energy and economic analyses for the model-7 according to the nomenclature shown in Figure 9.14 is given in Table 9.30.

21. Model-4 has a maximum hydrogen production rate than the other six models. Among seven models developed, model-5 has a minimum hydrogen production rate. The electricity produced by the biogas powered cogeneration system of WWTP is totally consumed by the electrolysis process for hydrogen production in the first four models developed. For the model-5, only a few amount of electricity produced by the cogeneration system is consumed due to the inadequate amount of H₂S presence in the biogas produced by anaerobic digestion system. Model-6 can be seen appropriate option for a municipal WWTP because of two important reasons: (1) Sludge utilized through model-6 is the digested sludge and it is the by-product of wastewater treatment application. This sludge, before the dark fermentation process for hydrogen production, is first used to produce biogas in the anaerobic digestion process. Thus, the biogas output is used for the power production, which provides the energy demand of the model-6. Note that the power demand of the model-6 is only the one-fourth of the total power produced by the cogeneration system (176.4 kWh). (2) After biogas production in the anaerobic digestion system, sludge is considered as a waste of the treatment facility and it must be eliminated. By model-3, this elimination process is replaced by a dark fermentation process with pre-treatment for hydrogen production. It means that digested sludge can be used further for another valuable system production, which is hydrogen. Fig. 9.19 shows the comparison of actual electricity consumptions of hydrogen production models developed.

22. According to the economic analysis performed based on the electricity cost for the models developed, model-5 has the lowest hydrogen production cost. This is so because of low hydrogen production rate of the model due to the low value of hydrogen sulfide presence in the biogas. Model-6 involves the highest cost rate of all the models developed, due to the high investment and operation and maintenance costs of the dark fermentation process. However, considering the remarkable economical and environmental advantages of the direct usage of sludge in both for biogas and hydrogen productions, it can be considered as the most appropriate model

for the municipal WWTPs. In Fig. 9.20, the comparison of the hydrogen production costs for the models developed is presented. Hydrogen liquefaction costs for models developed for GASKI WWTP is given in Table 9.32.

23. It may be concluded that the thermodynamic and thermoeconomic analyses and optimization of biogas usage in electricity and hydrogen productions from wastewater treatment systems can be used as a guide study to analyze and evaluate the thermodynamic and thermoeconomic analyses, assessments and optimizations of other municipal wastewater treatment and power plants. The results of the present thesis study are also expected to give a new and original direction to engineers, scientists and energy policy makers in implementing energy planning studies and dictating the energy strategies as a potential tool in the light of energy and exergy based economical methodologies.

24. The results of this thesis provides wastewater treatment plants and biogas powered cogeneration system investors, designers and engineers some key information: (i) In an effectively managed wastewater treatment plant, to develop an adequate cost model to be applied is extremely important because non-stop sewage flowing to the plant has a direct relation with the total value of energy resources to be consumed in the treatment process. Conventional energy and economic valuations of a wastewater treatment system may be used as the tools to understand the characteristics of the costs and benefits of internal flows. However, to understand the real causes and sources of costs which have undeniable impacts on cost structure of the system, we need to develop a more methodological approach that has a fundamental and direct correlation with inefficiencies appeared in the processes and devices of the system. Thermodynamic analysis, using exergy as a basis, can help determine the real costs of producing commodities and in pricing such products. Also, it can help evaluate economic viability and profitability. (ii) Biogas engine powered cogeneration applications are characterized with a high power to heat ratio, and thus they should be used when power demand is high and heat demand is low. (iii) Exergy methods can be effectively used to analyze municipal wastewater treatment plants and biogas powered cogeneration systems both thermodynamically and economically providing rational comparison to other wastewater treatment plant and cogeneration applications.

REFERENCES

- [1] Kothari, R., Tyagi, V. V., Pathak., A. (2010). Waste-to-energy: A way from renewable energy sources to sustainable development. *Renewable and Sustainable Energy Reviews*. **14**, 3164-3170.
- [2] Menegaki, A. (2008). Valuation for renewable energy: A comparative review. *Renewable and Sustainable Energy Reviews*. **12**, 2422-2437.
- [3] Muga, H. E., Mihelcic, J. R. (2008). Sustainability of wastewater treatment technologies. *Journal of Environmental Management*. **88**, 437-447.
- [4] Gallert C, Winter J. 2004. Environmental Biotechnology: Concepts and Applications. In: Jördening HJ, Winter J, editors. Bacterial metabolism in wastewater treatment systems, Wiley International.
- [5] Peavy HS, Rowe DR, Tchobanoglous G. 1985. Environmental Engineering. 1st edition. Singapore: McGraw-Hill.
- [6] Werther, J., Ogada, T. (1999). Sewage sludge combustion. *Progress in Energy and Combustion Science*. **25**, 55-116.
- [7] Balta, M. T., Dincer, I., Hepbasli, A. (2011). Exergoeconomic analysis of a hybrid copperechlorine cycle driven by geothermal energy for hydrogen production. *International Journal of Hydrogen Energy*. **36**, 11300 – 11308.
- [8] Coskun, C., Akyuz, E., Oktay, Z., Dincer, I. (2011). Energy analysis of hydrogen production using biogas-based electricity. *International Journal of Hydrogen Energy*. **36**, 11418–11424.

- [9] Maygarden, B. D., Yakubik, J. K., Weiss, E., Peyronnin, C., Jones, K. R. (1999). National Register Evaluation of New Orleans Drainage System, Orleans Parish, Louisiana. Final Report.
Available at: http://www.mvn.usace.army.mil/pdf/History/abt_nodrainreptdoc.pdf
- [10] Coelho, S. T. (2006). Biogas from sewage treatment used to electric energy generation, by a 30 kW (ISO) micro turbine. *World Bioenergy Conference & Exhibition, Jönköping, Sweden*.
- [11] Mukharje, P. K. (2007). Biogas an energy source for future. *Aavishkar Magazine*. 20-24.
- [12] Kalloum, S., Bouabdessalem, H., Touzi, A., Iddou, A., Ouali, M. S. (2011). Biogas production from the sludge of the municipal wastewater treatment plant of Adrar city (southwest of Algeria). *Biomass and Bioenergy Energy*. **35**, 2554-2560.
- [13] Bodik, I., Sedlacek, S., Kubaska, M., Hutnan, M. (2011). Biogas production in municipal wastewater treatment plants – Current status in EU with a focus on the Slovak Republic. *Chem. Biochem. Eng. Q.* **25 (3)**, 335–340.
- [14] Francioso, O., Estrada, M. T. R., Montecchio, D., Salomoni C., Caputo, A., Palenzona, D. (2010). Chemical characterization of municipal wastewater sludges produced by two-phase anaerobic digestion for biogas production. *Journal of Hazardous Material*. **175**, 740-746.
- [15] Yadvika, Santosh, S., Sreekrishnan, T. R., Kohli, S., Rana, V. (2004). Enhancement of biogas production from solid substrates using different techniques—a review. *Bioresource Technology*. **95**, 1-10.
- [16] Asam, Z. Z., Poulsen, T. G., Nizami, A. S., Rafique, R., Kiely, G., Murphy, J.D. (2011). How can we improve biomethane production per unit of feedstock in biogas plants? *Applied Energy*. **88**, 2013-2018.

- [17] Luostarinen, S., Luste, S., Sillanpaa, M. (2009). Increased biogas production at wastewater treatment plants through co-digestion of sewage sludge with grease trap sludge from a meat processing plant. *Bioresource Technology*. **100**, 79-85.
- [18] Tsagarakis, P. K. (2007). Optimal number of energy generators for biogas utilization in wastewater treatment facility. *Energy Conversion and Management*. **48**, 2694-2698.
- [19] Stern, S. A., Krishnakumar, B., Charati, S. G., Amato, W. S., Friedman, A. A., Fuess, D. J. (1998). Performance of a bench-scale membrane pilot plant for the upgrading of biogas in a wastewater treatment plant. *Journal of Membrane Science*. **15**, 63-74.
- [20] Tsagarakis, K. P., Papadogiannis, C. (2006). Technical and economic evaluation of the biogas utilization for energy production at Iraklio Municipality, Greece. *Energy Conversion and Management*. **47**, 844-857.
- [21] Solyom, K., Mato, R. B., Elvira, S. I. P., Cocero, M. J. (2011). The influence of the energy absorbed from microwave pretreatment on biogas production from secondary wastewater sludge. *Bioresource Technology*. **102**, 10849-10854.
- [22] Villela, I. A. C., Silveira, J. L. (2005). Thermoeconomic analysis applied in cold water production system using biogas combustion. *Applied Thermal Engineering*. **25**, 1141-1152.
- [23] Rasi, S., Veijanen, A., Rintala, J. (2007). Trace compounds of biogas from different biogas production plants. *Energy*. **32**, 1375–1380.
- [24] Tchobanoglous G, Burton FL, Stensel HD. 2003. Wastewater engineering: treatment and reuse. 4th edition. New York: McGraw-Hill.
- [25] EU. European Commission Directive (86/278/EEC). Available at: http://ec.europa.eu/environment/waste/sludge/pdf/organics_in_sludge.pdf

- [26] Paulsen, T. G., Hansen, J. A. (2003). Strategic environmental assessment of alternative sewage sludge management scenarios. *Waste Management & Research*. **21**, 19–28.
- [27] Andrews, R. J., Lloyd, J. W., Lerner, D. N. (1997). Modelling of nitrate leaching from arable land into unsaturated soil and chalk 1. Development of a management model for applications of sewage sludge and fertilizer. *Journal of Hydrology*. **200**, 179-197.
- [28] Wang, M. J. (1997). Land application of sewage sludge in China. *The Science of the Total Environment*. **197**, 149-160.
- [29] Wang, X., Chen, T., Ge, Y., Jia, Y. (2008). Studies on land application of sewage sludge and its limiting factors. *Journal of Hazardous Materials*. **160**, 554–558.
- [30] Bengtsson, M., Tillman, A. M. (2004). Actors and interpretations in an environmental controversy: the Swedish debate on sewage sludge use in agriculture. *Resources, Conservation and Recycling*. **42**, 65–82.
- [31] Ahmed, H. K., Fawy, E. A., Hady, E. S. A. (2010). Study of sewage sludge use in agriculture and its effect on plant and soil. *Agriculture and Biology Journal of North America*. **1(5)**, 1044-1049.
- [32] Murakami, T., Suzuki, Y., Nagasawa, H., Yamamoto, T., Koseki, T., Hirose, H., Okamoto, S. (2009). Combustion characteristics of sewage sludge in an incineration plant for energy recovery. *Fuel Processing Technology*. **90**, 778-783.
- [33] Stasta, P., Boran, J., Bebar, L., Stehlik, P., Oral, J., (2006). Thermal processing of sewage sludge. *Applied Thermal Engineering*. **26**, 1420-1426.

- [34] Houdkova, L., Boran, J., Ucekaj, V., Elsässer, T., Stehlik, P., (2008). Thermal processing of sewage sludge-II. *Applied Thermal Engineering*. **28**, 2083-2088.
- [35] Nadal, M., Schuhmacher, M., Domingo, J. L. (2009). Cost-benefit analysis of using sewage sludge as alternative fuel in a cement plant: a case study. *Environ Sci Pollut Res Int*. **16(3)**, 322-328.
- [36] Zabaniotou, A., Theofilou, C. (2008). Green energy at cement kiln in Cyprus—Use of sewage sludge as a conventional fuel substitute. *Renewable and Sustainable Energy Reviews*. **12**, 531-541.
- [37] Fytily, D., Zabaniotou, A. (2008). Utilization of sewage sludge in EU application of old and new methods—A review. *Renewable and Sustainable Energy Reviews*. **12**, 116-140.
- [38] Varga, T., Bokanyi, L. (2010). Energetic utilization of municipal sewage sludge and the applicable pre-treatments for the increased biogas yield. *1st Know Bridge Conference on Renewables, Miskolc, Hungary*.
- [39] Galvez, A., Conesa, J. A., Gullon, I. M., Font, R. (2007). Interaction between pollutants produced in sewage sludge combustion and cement raw material. *Chemosphere*. **69**, 387–394.
- [40] Nadziakiewicz, J., Koziol, M. (2003). Co-combustion of sludge with coal. *Applied Energy*. **75**, 239–248.
- [41] Kim, Y., Parker, W. (2008). A technical and economic evaluation of the pyrolysis of sewage sludge for the production of bio-oil. *Bioresource Technology*. **99**, 1409–1416.

- [42] Candel, M. B. A, Jordan, M. M., Pedreno, J. N., Solera, J. M., Lucas, I. G. (2007). Environmental evaluation of sewage sludge application to reclaim limestone quarries wastes as soil amendments. *Soil Biology & Biochemistry*. **39**, 1328–1332.
- [43] Kalderis, D., Aivalioti, M., Gidarakos, E. (2010). Options for sustainable sewage sludge management in small wastewater treatment plants on islands: The case of Crete. *Desalination*. **260**, 211–217.
- [44] Fontsa, I., Geab, G., Azuarab, M., Abregoc, J., Arauzo, J. (2012). Sewage sludge pyrolysis for liquid production: A review. *Renewable and Sustainable Energy Reviews*. **16**, 2781–2805.
- [45] Tanczuk, M., Ulbricht, R. (2009). Assessment of energy potential of biomass. *Proceedings of ECOpole*. **3(1)**, 23-26.
- [46] Ulleberg, Q. (2003). Modeling of advanced alkaline electrolyzers: a system simulation approach. *International Journal of Hydrogen Energy*. **28**, 21-23.
- [47] Shiga, H., Shinda, K., Hagiwara, K., Tsutsumi A., Sakurai, M., Yoshida, K., Bilgen, E. (1998). Large-scale hydrogen production from biogas. *International Journal of Hydrogen Energy*. **23**, 631-640.
- [48] Martini, A. M. (2007). Hydrogen production from biogas: A model for the H₂ SEED project. (M.Sc. Thesis), *University of Strathclyde, Glasgow, Scotland, United Kingdom*.

- [49] Pandu, K., Joseph, S. (2012). Comparisons and limitations of biohydrogen production processes: A review. *International Journal of Advances in Engineering & Technology*. **2**, 342-356.
- [50] Kapdan, I. K., Kargi, F. (2006). Bio-hydrogen production from waste materials. *Enzyme and Microbial Technology*. **38**, 569–582.
- [51] Genc, N. (2010). Biohydrogen production from waste sludge. *Journal of Engineering and Natural Sciences*. **28**, 235-248.
- [52] Ni, M., Leung, D. Y. C., Leung, M. K. H., Sumathy, K. (2006). An overview of hydrogen production from biomass. *Fuel Processing Technology*. **87**, 461 – 472.
- [53] Ntaikou, I., Antonopoulou, G., Lyberatos, G. (2010). Biohydrogen production from biomass and wastes via dark fermentation: A review. *Waste Biomass Valor*. **1**, 21–39.
- [54] Levin, B. D., Pitt, L., Love, M. (2004). Biohydrogen production: prospects and limitations to practical application. *International Journal of Hydrogen Energy*. **29**, 173 – 185.
- [55] Sen, U., Shakhwapee, M., Banerjee, R. (2008). Status of biological hydrogen production. *Journal of Scientific & Industrial Research*. **67**, 980-993.
- [56] Biagini, E., Masoni, L., Tognotti, L. (2010). Comparative study of thermochemical processes for hydrogen production from biomass fuels. *Bioresource Technology*. **101**, 6381–6388.

- [57] Gasafi, E., Reinecke, M. Y., Kruse, A., Schebek, L. (2008). Economic analysis of sewage sludge gasification in supercritical water for hydrogen production. *Biomass and Bioenergy*. **32**, 1085–1096.
- [58] Petrov, K., Baykara, S. Z., Ebrasu, D., Gulin, M., Veziroglu, A. (2011). An assessment of electrolytic hydrogen production from H₂S in Black Sea waters. *International Journal of Hydrogen Energy*. **36**, 8936 – 8942.
- [59] Mora, C. H., Oliveria, S. (2006). Environmental exergy analysis of wastewater treatment plants. *Thermal Engineering*. **5(2)**, 24-29.
- [60] Armando, G. M., Alejandro, Z. A., Barbara, G. R., Hugo, R. H. V. (2003). On an exergy efficiency definition of a wastewater treatment plant. *International Journal of Thermodynamics*. **6**, 169-176.
- [61] Ptasinski, K. J., Hamelinck, C., Kerkhof, P. J. A. M. (2002). Exergy analysis of methanol from the sewage sludge process. *Energy Conversion and Management*. **43**, 1445–1457.
- [62] Abusoglu, A., Demir, S., Kanoglu, M. (2011). Thermodynamic analysis and assessment of a wastewater treatment plant in scope of anaerobic sludge digestion and on-site electricity production from biogas. *2nd International Exergy, Life Cycle Assessment, and Sustainability Workshop & Symposium (ELCAS2), Nisyros – Greece*
- [63] Lamas, W. Q., Silveira, J. L., Giacaglia, G. E. O., Reis, L. O. M. (2009). Development of a methodology for cost determination of wastewater treatment based on functional diagram. *Applied Thermal Engineering*. **29**, 2061–2071.

- [64] Lamas, W. Q., Silveira, J. L., Giacaglia, G.E.O., Reis, L. O. M. (2010). Thermo-economic analysis applied to an alternative wastewater treatment. *Renewable Energy*. **35**, 2288-2296.
- [65] Kadar, Y., Siboni, G. (2006). Optimization of energy economy in the design and operation of wastewater treatment plants. Available at:
http://www.worldenergy.org/wecgeis/publications/default/tech_papers/17th_congress/2_3_09.asp?mode=print
- [66] Coble, J. J., Contreras, A. (2010). Energetic, exergetic, thermo-economic and environmental analysis of various systems for the cogeneration of biogas produced by an Urban Wastewater Treatment Plant UWTP. *18th World Hydrogen Energy Conference (WHEC), Essen-Germany*.
- [67] Hessami, M. A. (1994). Specific applications of bio/landfill gas produced from waste organic material. *Renewable Energy*. **5**, 832–834.
- [68] Dong, L., Liu, H., Riffat, S. (2009). Development of small-scale and micro-scale biomass fuelled CHP systems—a literature review. *Applied Thermal Engineering*. **29**, 2119–2126.
- [69] Pellegrini, L. F., Cano, A., Carpio, J. (2009). Supercritical steam cycles and biomass integrated gasification combined cycles for sugarcane mills. *Energy*. **35**, 1–9.
- [70] Raj, N. T., Iniyan, S., Goic, R. (2011). A review of renewable energy based cogeneration technologies. *Renewable and Sustainable Energy Reviews*. **15**, 3640–3648.

- [71] Basrawi, M. F. B., Yamada, T., Nakanishi, K., Katsumata, H. (2012). Analysis of the performances of biogas-fuelled micro gas turbine cogeneration systems (MGT-CGSs) in middle- and small-scale sewage treatment plants: Comparison of performances and optimization of MGTs with various electrical power outputs. *Energy*. **38**, 291–304.
- [72] Caceres, C. X., Caceres, R. E., Hein, D., Molina, M. G., Pia, J. M. (2012). Biogas production from grape pomace: Thermodynamic model of the process and dynamic model of the power generation system. *International Journal of Hydrogen Energy*. **XXX**, 1-7.
- [73] Bruno, J. C., Lopez, V. O., Coronas, A. (2009). Integration of absorption cooling systems into micro gas turbine trigeneration systems using biogas: Case study of a sewage treatment plant. *Applied Energy*. **86**, 837–847.
- [74] Farhad, S., Hamdullahpur, F., Yoo, Y. (2010). Performance evaluation of different configurations of biogas-fuelled SOFC micro-CHP systems for residential applications. *International Journal of Hydrogen Energy*. **35**, 3758-3768.
- [75] Kang, D. W., Kim, T. S., Hur, K. B., Park, J. K. (2012). The effect of firing biogas on the performance and operating characteristics of simple and recuperative cycle gas turbine combined heat and power systems. *Applied Energy*. **93**, 215–228.
- [76] Abosoglu, A., Demir, S., Kanoglu, M. (2012). Thermo-economic analysis of a biogas engine powered cogeneration system. *J. of Thermal Science and Technology*. **XXX**, 1-14.
- [77] Henham, A., Makkar, M. K. (1998). Combustion of simulated biogas in a dual-fuel diesel engine. *Energy Conversion and Management*. **39**, 2001-2009.

- [78] Santarelli, M., Cali, M., Macagno, S. (2004). Design and analysis of stand-alone hydrogen energy systems with different renewable sources. *International Journal of Hydrogen Energy*. **29**, 1571 – 1586.
- [79] Deshmukh, S., Boehm, R. F. (2007). Review of modeling details related to renewably powered hydrogen systems. *Renewable and Sustainable Energy Reviews*. **12**, 2301–2330.
- [80] Bartels, J. R., Pate, M. B., Olson, N. K. (2010). An economic survey of hydrogen production from conventional and alternative energy sources. . *International Journal of Hydrogen Energy*. **35**, 8371 – 8384.
- [81] Fabiano, B., Prego, P. (2002). Thermodynamic study and optimization of hydrogen production by *Enterobacter aerogenes*. *International Journal of Hydrogen Energy*. **27**, 149 – 156.
- [82] Burgess, G., Velasco, J. G. F. (2007). Materials, operational energy inputs, and net energy ratio for photobiological hydrogen production. *International Journal of Hydrogen Energy*. **32**, 1225 – 1234.
- [83] Kalinci, Y., Hepbasli, A., Dincer, I. (2009). Biomass-based hydrogen production: A review and analysis. *International Journal of Hydrogen Energy*. **34**, 8799 – 8817.
- [84] Modarresi, A., Wukovits, W., Friedl, A. (2010). Application of exergy balances for evaluation of process configurations for biological hydrogen production. *Applied Thermal Engineering*. **30**, 70–76.
- [85] Perera, K. R. J., Ketheesan, B., Gadhamshetty, V., Nirmalakhandan, N. (2010). *International Journal of Hydrogen Energy*. **35**, 12224–12233.

- [86] Cohce, M. K., Dincer, I., Rosen, M. A. (2011). Energy and exergy analyses of a biomass-based hydrogen production system. *Bioresource Technology*. **102**, 8466–8474.
- [87] Siddiqui, Z., Horan, N. J., Salter, M. (2011). Energy optimisation from co-digested waste using a two-phase process to generate hydrogen and methane. *International Journal of Hydrogen Energy*. **36**, 4792–4798.
- [88] Nath, K., Dast, D. (2011). Modeling and optimization of fermentative hydrogen production. *Bioresource Technology*. **102**, 8569–8581.
- [89] Tock, L., Marechal, F. (2012). Co-production of hydrogen and electricity from lignocellulosic biomass: Process design and thermo-economic optimization. *Energy*. **XXX**, 1–11.
- [90] Balta, M. T., Dincer, I., Hepbasli, A. (2009). Thermodynamic assessment of geothermal energy use in hydrogen production. *International Journal of Hydrogen Energy*. **34**, 2925 – 2939.
- [91] Kanoglu, M., Bolatturk, A., Yilmaz, C. (2010). Thermodynamic analysis of models used in hydrogen production by geothermal energy. *International Journal of Hydrogen Energy*. **35**, 8783 – 8791.
- [92] Ratlamwala, T. A. H., Dincer, I., Gadalla, M.A. (2012). Thermodynamic analysis of a novel integrated geothermal based power generation-quadruple effect absorption cooling-hydrogen liquefaction system. *International Journal of Hydrogen Energy*. **37**, 5840 – 5849.

- [93] Yilmaz, C., Kanoglu, M., Bolatturk, A., Gadalla, M. (2012). Economics of hydrogen production and liquefaction by geothermal energy. *International Journal of Hydrogen Energy*. **37**, 2058 – 2069.
- [94] Kanoglu, M., Ayanoglu, A., Abusoglu, A. (2011). Exergoeconomic assessment of a geothermal assisted high temperature steam electrolysis system. *Energy*. **36**, 4422 – 4433.
- [95] Joshi, A. S., Dincer, I., Reddy, B. V. (2010). Exergetic assessment of solar hydrogen production methods. *International Journal of Hydrogen Energy*. **35**, 4901 – 4908.
- [96] Zhang, X. R., Yamaguchi, H., Cao, Y. (2010). Hydrogen production from solar energy powered supercritical cycle using carbon dioxide. *International Journal of Hydrogen Energy*. **35**, 4925 – 4932.
- [97] Joshi, A. S., Dincer, I., Reddy, B. V. (2011). Solar hydrogen production: A comparative performance assessment. *International Journal of Hydrogen Energy*. **36**, 11246 – 11257.
- [98] Paola, A., Fabrizio, Z., Fabio, O. (2011). Techno-economic optimisation of hydrogen production by PV electrolysis: “RenHydrogen” simulation program. *International Journal of Hydrogen Energy*. **36**, 1371 – 1381.
- [99] Esmaili, P., Dincer, I., Naterer, G. F. (2012). Energy and exergy analyses of electrolytic hydrogen production with molybdenum-oxo catalysts. *International Journal of Hydrogen Energy*. **XXX**, 1 – 8.
- [100] Sherif, S. A., Barbir, F., Veziroglu, T. N. (2005). Wind energy and the hydrogen economy—review of the technology. *Solar Energy*. **78**, 647–660.

- [101] Bechrakis, D. A., McKeogh, E. J., Gallagher, P. D. (2006). Simulation and operational assessment for a small autonomous wind–hydrogen energy system. *Energy Conversion and Management*. **47**, 46–59.
- [102] Mathur, J., Agarwal, N., Swaroop, R., Shah, N. (2008). Economics of producing hydrogen as transportation fuel using offshore wind energy systems. *Energy Policy*. **36**, 1212–1222.
- [103] Khan, M. J., Iqbal, M.T. (2009). Analysis of a small wind-hydrogen stand-alone hybrid energy system. *Applied Energy*. **86**, 2429–2442.
- [104] Calderon, M., Calderon A. J., Ramiro, A., Gonzales, J. F., Gonzales, I. (2011). Evaluation of a hybrid photovoltaic-wind system with hydrogen storage performance using exergy analysis. *International Journal of Hydrogen Energy*. **36**, 5751 – 5762.
- [105] Kalinci, Y., Hepbasli, A., Dincer, I. (2011). Exergoeconomic analysis of hydrogen production from plasma gasification of sewage sludge using specific exergy cost method. *International Journal of Hydrogen Energy*. **36**, 11408 – 11417.
- [106] Stillwell, A. S., Hoppock, D. C., Webber, M. E. (2010). Energy recovery from wastewater treatment plants in the United States: A case study of the energy-water nexus. *Sustainability*. **2**, 945-962.
- [107] Antakyalı, R., Rölle, R. (2010). Energetic aspects regarding the sewage and sludge treatment process of WWTPs. *International Sustainable Water and Wastewater Management Symposium, Konya-Turkey*
- [108] Rulkens, W. (2008). Sewage sludge as a biomass resource for the production of energy: Overview and assessment of the various options. *Energy&Fuels*. **22**, 9-15.

- [109] IWA. International Water Association. 2011. Global Atlas of Excreta, Wastewater Sludge, and Biosolid Management: Turkey Overview.
Available at: <http://www.iwawaterwiki.org>
- [110] TSI. Turkish Statistical Institute. Available at: <http://www.turkstat.gov.tr>
- [111] Scott, K., Murano, C. (2007). A study of a microbial fuel cell battery using manure sludge waste. *Journal of Chemical Technology and Biotechnology*. **82**, 809-817.
- [112] Bejan A, Tsatsaronis G, Moran M. 1996. Thermal Design and Optimization. 1st edition. New York: Wiley.
- [113] Cengel YA, Boles MA. 2008. Thermodynamics: An Engineering Approach. 6th edition. New York: Mc-Graw Hill.
- [114] Van Wylen GJ, Sonntag RE. 1985. Fundamentals of Classical Thermodynamics. 3rd edition. New York: John Wiley & Sons.
- [115] Wark KJr. 1995. Advanced Thermodynamics for Engineers. 1st edition. New York: Mc-Graw Hill.
- [116] Ahern JE. 1980. The Exergy Method of Energy System Analysis. 1st edition. New York: John Wiley & Sons.
- [117] Tsatsaronis, G., Ho-Park, M. (2002). On avoidable and unavoidable exergy destructions and investment costs in thermal systems. *Energy Conversion and Management*. **43**, 1259-1270.
- [118] Tai, S., Matsushige, K., Goda, T. (1986). Chemical exergy of organic matter in wastewater. *International Journal of Environmental Studies*. **27(3-4)**, 301-15.

- [119] Szargut J, Morris DR, Steward FR. 1988. Exergy analyses of thermal, chemical and metallurgical processes. California: Hemisphere Publishing Co.
- [120] Xiang, J. Y., Cali, M., Santarelli, M. (2004). Calculation for physical and chemical exergy of flows in systems elaborating mixed-phase flows and a case study in an IRSOFC plant. *International Journal of Energy Research*. **28**, 101-15.
- [121] Wall, G. (1986). *Exergy – A useful concept*. A doctorate thesis, Physical Resource Theory Group, Chalmers University of Technology and University of Goteborg. Goteborg, Sweden.
- [122] Huang, F. F. (1996). Performance assessment parameters of a cogeneration system. *Proceedings of ECOS'96, Stockholm, Sweden*
- [123] Zeng, K., Zhang, D. (2010). Recent progress in alkaline water electrolysis for hydrogen production and applications. *Progress in Energy and Combustion Science*. **36**, 307-326.
- [124] Gaggioli, R. A., Wepfer, W. J. (1980). Exergy economics. *Energy, The International Journal*. **5**, 823-837.
- [125] Gaggioli, R. A., El-Sayed, Y. M. (1989). A critical review of Second Law costing methods -2: Calculus Procedures. *Journal of Energy Resources Technology*. **111**, 8-15.
- [126] Park CS. 1990. *Advanced Engineering Economics*. New York: John Wiley & Sons
- [127] Vajpayee SK. 2001. *Fundamentals of Economics for Engineering Technologists and Engineers*. London: Prentice Hall.
- [128] Gonen T. 1990. *Engineering Economy for Engineering Managers*. New York: John Wiley & Sons

- [129] Tsatsaronis, G., Moran, M. J. (1997). Exergy-aided cost minimization. *Energy Conversion and Management*. **38**, 1535-1542.
- [130] Grant EL. 1990. Principles of Engineering Economy. New York: John Wiley & Sons.
- [131] Lazzaretto, A., Tsatsaronis, G. (1997). On the quest for objective equations in exergy costing. *Proceedings of the ASME Advanced Energy Systems Division*, **37**, 197-209.
- [132] Lozano, M. A., Valero A. (1993). Theory of the exergetic cost. *Energy*. **18**, 939-960.
- [133] Reini, M., Lazzaretto A., Macor A. (1995). Average structural and marginal costs as a result of a unified formulation of the thermoeconomic problem. In *Proceedings of Second Law Analysis of Energy Systems: Towards the 21st Century, Rome*
- [134] Kwon, Y. H., Kwak, H. Y., Oh, S. D. (2001). Exergoeconomic analysis of gas turbine cogeneration systems. *Exergy, An International Journal*. **1**, 31-40.
- [135] Oh, S. D., Pang, H. S., Kim, S. M., Kwak, H. Y. (1996). Exergy analysis for a gas turbine cogeneration system. *Transactions of the ASME*. **118**, 782-791.
- [136] Lazzaretto, A., Tsatsaronis, G. (2001). Comparison Between SPECO-Based and Functional Exergoeconomic Approaches. In *Proceedings of the 2001 ASME International Mechanical Engineering Congress and Exposition in New York*, 1-16.
- [137] Frangopoulos, C. A. (1991). Intelligent Functional Approach: A method for analysis and optimal synthesis – design – operation of complex systems. *International Journal of Energy, Environment, Economics*. **1**, 267-274.

- [138] Frangopoulos, C. A. (1991). Optimization of synthesis – design – operation of a cogeneration system by The Intelligent Functional Approach. *International Journal of Energy, Environment, Economics*. **1**, 275-287.
- [139] Frangopoulos, C. A. (1987). Thermo-economic functional analysis and optimization. *Energy*. **12**, 563-571.
- [140] Manolas, D. A., Frangopoulos, C. A., Gialamas, T. P., Tsahalis, D. T. (1997). Operation optimization of an industrial cogeneration system by a genetic algorithm. *Energy Conversion and Management*. **38**, 1625-1636.
- [141] Von Spakovsky, M. R., Evans R. B. (1990). The design and performance optimization of thermal systems. *Journal of Engineering for Gas Turbines and Power*. **112**, 86-93.
- [142] Tsatsaronis, G., Pisa, J., Valero, A., Lozano, M. A., Serra, L., Frangopoulos, C., Von Spakovsky, M. (1994). CGAM problem: Definition and conventional solution. *Energy*. **19**, 279-286.
- [143] Tsatsaronis, G., Pisa, J. (1994). Exergoeconomic evaluation and optimization of energy systems – Application to the CGAM problem. *Energy*. **19**, 287-321.
- [144] Toffolo, A., Lazzaretto, A. (2002). Evolutionary algorithms for multi-objective energetic and economic optimization in thermal system design. *Energy*. **27**, 549-567.
- [145] Von Spakovsky, M. R. (1994). Application of engineering functional analysis to the analysis and optimization of the CGAM problem. *Energy*, **19**, 343-364.
- [146] El-Sayed, Y., , R. L. (1970). Thermo-economics and the design of heat systems. *Journal of Engineering and Power*, **92**, 27-35.
- [147] Frangopoulos, C. A. (1991). Comparison of thermo-economic and thermodynamic optimal designs of a combined-cycle plant. *International Conference on the Analysis of Thermal and Energy Systems, Athens, Greece*, 305-318.

- [148] Frangopoulos, C. A. (1994). Application of the thermoeconomic functional approach to the CGAM problem. *Energy*. **19**, 323-342.
- [149] M/J Industrial Solutions (2003). municipal wastewater treatment plant energy baseline study. Available at: <http://www.cee1.org/ind/mot-sys/ww/pge1.pdf>
- [150] TCG 2020 – The Gas Engine. Available at: www.deutz.de
- [151] PSO-F&U 2006-1-6287. 2008. Pre-investigation of water electrolysis. Available at: <http://www.risoe.dtu.dk/rispubl/NEI/NEI-DK-5057.pdf>
- [152] IEA. International Energy Agency. 2006. Hydrogen production and storage. Available at: <http://www.iea.org/papers/2006/hydrogen.pdf>
- [153] Midilli, A., Ay, M., Dincer, I., Rosen, M. A. (2005). On hydrogen and hydrogen energy strategies I: current status and needs. *Renewable and Sustainable Energy Reviews*. **9**, 255-271.
- [154] College of the desert, 2001. Module 2: Hydrogen use. Available at: http://www1.eere.energy.gov/hydrogenandfuelcells/tech_validation/pdfs/fcm02r0.pdf
- [155] Woodford, C. 2011. How does an electrolyzer work? Available at: <http://www.explainthatstuff.com/electrolyzers.html>
- [156] O'Brien, J. E. (2008). Thermodynamic considerations for thermal water splitting processes and high temperature electrolysis. *Proceedings of the 2008 International Mechanical Engineering Congress and Exposition, Boston, Massachusetts, USA*
- [157] Martini, A. M. (2007). Hydrogen production from biogas: A model for the H2 SEED project. A master thesis, Energy Systems and the Environment, University of Strathclyde, Glasgow, United Kingdom

- [158] Manish, S., Banerjee, R. (2007). Comparison of biohydrogen production processes. *International Journal of Hydrogen Energy*. **33(1)**, 279–286.
- [159] Demirbas A. 2009. Biohydrogen For Future Engine Fuel Demands. London: Springer
- [160] Reith JH., Wijffels RH., Barten H. 2003. The perspectives of biological methane and hydrogen production. In: Bio-methane & Bio-hydrogen
- [161] Dincer I, Kanoglu M. 2010. Refrigeration systems and applications. 2nd edition. Singapore: Wiley.
- [162] Rosen, M. A. 2002. Exergy and economics: Is exergy profitable? *International Journal of Exergy*. **2**, 218-20.
- [163] Kotas TJ. 1995. The Exergy Method in Thermal Plant Analysis. 2nd edition. Malabar: Krieger.
- [164] Wellinger A, Lindberg A. 1999. Biogas upgrading and utilization. Task 24: Energy from biological conversion of organic waste. IEA Bioenergy.
- [165] Pulkrabek WW. 1997. Engineering Fundamentals of The Internal Combustion Engines. New York: Prentice Hall.
- [166] Cartmell, E., Gostelow, P., Riddell-Black, D., Simms, N., Oakey, J., Morris, J. 2006. Biosolids – A fuel or a waste? An integrated appraisal of five co-combustion scenarios with policy analysis. *Environmental Science and Technology*.**40**, 649-658.

- [167] Abusoglu, A., Kanoglu, M. 2009. Exergetic and thermoeconomic analyses of diesel engine powered cogeneration: Part 2 – Applications. *Applied Thermal Engineering*. **29**, 242-249.
- [168] Valero, A., Lozano, M.A., Serra, L., Torres, C. (1994). Application of the exergetic cost theory to the CGAM problem. *Energy*. **19**, 365-381.
- [169] EE. 2011. Available at: <http://enerjiensitusu.com/s>
- [170] TEDAS. 2011. Available at: <http://www.tedas.gov.tr/1.html>
- [171] Wang, C. C., Chang, C. W., Chu, C. P., Lee, D. J., Chang, B. V., Liao, C. S. 2003. Producing hydrogen from wastewater sludge by *Clostridium bifermentans*. *Journal of Biotechnology*. **102**, 83-92.
- [172] Krasae-in, S., Stang, J. H., Neksa, P. (2010). Review: Development of large-scale hydrogen liquefaction processes from 1898 to 2009. *International Journal of Hydrogen Energy*. **35**, 4524–4533.
- [173] Barron RF. 1966. Cryogenic systems. Oxford, United Kingdom: Oxford University Press
- [174] Syed, M. T., Sherif, S. A., Veziroglu, T. N., Sheffield, J. W. 1998. An economic analysis of three hydrogen liquefaction systems. *International Journal of Hydrogen Energy*. **23**, 565-576.